الجـــــــــــــــــــــمـهـوريـــــة الجـــــــــــــــزائـريـة الديمـــــــقـراطيـة الـشـــــــــعبيـة

PEOPLE'S DEMOCRATIC REPUBLIC OF ALGERIA

وزارة التـــــــــــــــــــــــــــــعـليـم العـــــــالي و البـــــــــحث العـــــلـمـــي

Ministry of Higher Education and Scientific Research

جـــــــــــــــامعة أبي بكـــر بـلـقـايد – تـلمســـــــــــــــان –

Aboubakr Belkaïd University– Tlemcen –
Faculty of TECHNOLOGY

THESIS

Submitted for the **degree** of **DOCTORATE 3rd Cycle**
In : Biomedical Engineering

Speciality : Biomedical instrumentation

By : DEBBAL Imane

Subject

Synthesis and comparison of analysing techniques for cardiac pathologies

Publicly defended, on **29 / 04 / 2025** , before the jury composed of :

M BEREKSI-REGUIG Fethi	Professor	Univ. Tlemcen	Chair
M HAMZA CHERIF Lotfi	Professor	Univ. Tlemcen	Supervisor
Melle BAAKEK Yettou Nour El Houda	MCA	Univ. Tlemcen	Co- Supervisor
M MERAD Lotfi	Professor	ESSA- Tlemcen	Examiner 1
M DIB Nabil	MCA	Univ. Tlemcen	Examiner 2

Acknowledgements

الحمد لله الذي بنعمته تتم الصالحات

First of all, I would like to thank Almighty and Merciful **GOD**, who has given me the necessary strength and patience to complete this modest and humble work. Oh! **ALLAH**, all that I have, all that I am, and all that I do is because of and for you.

At the culmination of this academic endeavour, I am very thankful for my two supervisors, **Professor Hamza Cherif Lotfi** and **Dr Baakek Yettou Nour El Houda**, for their exemplary guidance, for their unfailing availability, for the time they gave me to complete and achieve the thesis objectives, for accompanying me throughout this project. They both provided a tremendous amount of help to make the content of this dissertation happen. For all this, and much more, I am very grateful.

I would like to express my sincere appreciation to my thesis committee. Their critical insights and thoughtful feedback have been invaluable to the refinement of this dissertation. **Professor Bereksi-Reguig Fethi,** the chair of this committee, whose expertise and guidance have greatly enhanced the quality of this research. **Dr Dib Nabil**, the internal examiner, his critical comments, suggestions, and encouraging words throughout this journey motivated me to improve this work. Special thanks to **Professor Merad Lotfi**, the external examiner, for his constructive feedback and for sharing his expertise, which has considerably enriched the quality of this dissertation.

Finally, I am profoundly grateful to the countless individuals who participated in reviewing articles, adding feedback on conferences, or contributing in any form.

Imane

Dedication

I dedicate this humble work:

To my dear father, who can be proud and find here the result of long years of sacrifice and privation to help me move forward in life. Thank you for the noble values, the education and the constant support that came from you. No dedication can fully express the deep love I have for you. Thank you for everything, PAPA.

To my mother, who has worked for my success, through her love, her support, all the sacrifices she has made and her invaluable advice, for all her assistance and her constant presence in my life. Through this work, however modest it may be, please accept the expression of my feelings and my eternal gratitude. Thank you for everything, MAMA.

Dear God! Have mercy on them, as they brought me up when I was little.

To my everything, my very dear elder sister Hadjer, who, through her tenderness, interest in this work, and advice, has been a great listener and supporter of all my endeavours. I wish her happiness and success and hope that ALLAH will always leave us in solidarity.

To my grandmothers, may they rest in peace, who have been a mental and spiritual support with their endless Douaa and Mounfarija throughout my studies; your memory has been my guiding light during this journey.

To all the members of my family, who have always made sure that I fought to take on this challenge and never let me down. Thank you for your endless motivation and fighting spirit.

To all my friends and colleagues at university with whom I shared my moments of joy and happiness.

To anyone who has helped me in any way, I would like to express my deepest gratitude and appreciation.

Finally, a special pat on the shoulder…to myself. Doing a PhD has been a personal challenge, since when I failed my first attempt in 2021. This time, I said challenge accepted and went for another go, and here I' am acknowledging the self-discovery and personal growth that this thesis has engendered. The journey of knowledge has been transformative, and I am grateful for the opportunities it has presented.

Imane

Abstract

Phonocardiogram (PCG) signal processing helped uncover many crucial parameters that reflect the presence of a specific pathology. Therefore, we conducted a synthesis and comparison study focusing on research using various spectral and spectro-temporal techniques on PCG signals, such as the Fast Fourier Transform (FFT), Short Time Fourier Transform (STFT), Discrete Wavelet Transform (DWT), and Bispectral analysis. We extracted several parameters, including the frequency band, spectral entropy, entropy of approximation coefficients, temporal and frequency extents, entropy of phase, third-order moment, and more. We achieved promising results and high accuracies using these parameters for discriminating, classifying, and assessing the severity of cardiac pathologies.

Finally, using complex feature-selection algorithms and machine learning/neural network classifiers, we compared the techniques and parameters to identify the optimal ones for cardiac severity assessment.

Keywords: Phonocardiogram signal, F.F.T, S.T.F.T, D.W.T, Bispectral, Feature selection, Severity-classification, Techniques comparison.

Résumé

De nombreux paramètres cruciaux qui reflètent la présence d'une pathologie spécifique ont pu être découverts grâce au traitement du signal phonocardiogramme (PCG). Notre étude de synthèse et comparaison utilise un certain nombre de techniques spectrales et spectro-temporelles sur les signaux PCG pour la discrimination, la classification et l'évaluation de la sévérité cardiaque. Dans ce but, diverses techniques telles que la transformée de Fourier rapide (FFT), la transformée de Fourier à court terme (STFT), la transformée en ondelettes discrètes (TOD) et l'analyse Bispectral ont été exploitées pour extraire plusieurs paramètres ; notamment la bande de fréquence, l'entropie spectrale, l'entropie des coefficients d'approximation, les étendues temporelles et fréquentielles, l'entropie de phase, le moment du troisième ordre, etc. Nous avons obtenu des résultats satisfaisants et des précisions élevées en utilisant ces paramètres pour atteindre nos objectifs.

Enfin, grâce à des algorithmes complexes de sélection des caractéristiques et à des classificateurs à apprentissage automatique/réseau neuronal, nous avons comparé les techniques et les paramètres pour identifier ceux qui sont optimaux pour l'évaluation de la sévérité cardiaque.

Mots clés : Phonocardiogramme, F.F.T, S.T.F.T, T.O.D, analyse Bispectral, classification de la sévérité, Comparaison des techniques.

ملخص

تم اكتشاف العديد من المعلمات الحاسمة التي تعكس وجود حالة مرضية معينة باستخدام معالجة إشارات مخطط تخطيط القلب الصوتي .(PCG) تهدف دراستنا التجميعية والمقارنة التي يقودها بحثنا باستخدام عدد من التقنيات الطيفية والزمانية الطيفية على إشارات مخطط تخطيط القلب PCGإلى استخدام بعض هذه المعلمات الحاسمة للتمييز والتصنيف وتقييم شدة المرض القلبي .

ولتحقيق هذا الهدف، تم استغلال تقنيات مختلفة مثل تحويل فورييه السري(FFT) ، وتحويل فورييه قصير الوقت(STFT) ، وتحويل المويجات المنفصلة(DWT) ، والتحليل الطيفي الثنائي لاستخراج العديد من المعلمات؛ لا سيما نطاق التردد، والإنتروبيا الطيفية، وإنتروبيا معاملات التقريب، والنطاقات الزمنية والترددية، وإنتروبيا الطور، وعزم الدرجة الثالثة، وما إلى ذلك. وقد تم الحصول على نتائج مرضية ودقة عالية باستخدام هذه المعلمات للأهداف المرجوة.

أخيرًا، باستخدام خوارزميات اختيار السمات المعقدة ومصنفات التعلم الآلي/الشبكة العصبية، قمنا بمقارنة التقنيات والمعلمات لتحديد الأفضل منها في تقييم شدة أمراض القلب.

الكلمات المفتاحية: مخطط صوتيات القلب، F.F.T، S.T.F.T، D.W.T، Bispectral، تصنيف شدة المرض، مقارنة بين التقنيات.

Table of contents

General introduction 2
CHAPTRE I: THEORITICAL NOTIONS ABOUT THE PHONOCARDIOGRAM . 7
I. Introduction 7
II. Heart Basics 7
II.1. Position of the heart in the thorax 7
II.2. Morphology of the Heart 8
II.2.1. The pericardium 8
II.3. Internal Anatomy of the Heart 8
II.3.1. Cardiac valves 9
II.4. Cardiac revolution 11
II.4.1. ventricular systole 11
II.4.2. Ventricular diastole 11
III. Theoretical notions about the phonocardiogram signal 13
III.1. Definition and description of the Phonocardiogram Signal 13
III.2. Heart Sounds 13
III.2.1. Heart sound S1 14
III.2.2. Heart sound S2 14
III.2.3. Heart sound S3 14
III.2.4. Heart sound S4 14
III.3. Additional abnormal heart sounds 14
III.3.1. Galloping rhythm 14
III.3.2. Mitral opening click 15
III.3.3. The click 15
Ejection Click 15
Open Snap 16
III.4. Heart murmurs 16
III.4.1. Systolic murmurs 17
Aortic stenosis (AS) 17
Mitral regurgitation (MR) 18
Systolic Pulmonary Stenosis (PS) 18
Tricuspid regurgitation (TR) 18
Mitral valve prolapse (MVP) 19

III.4.2. Diastolic murmurs 19
Mitral stenosis (MS) 19
Aortic regurgitation (AR) 19
Diastolic Atrial Septal Defect (DASD) 20
III.5. Temporal and frequency characteristics of the PCG signal 20
IV. PCG signals used 20
V. Conclusion 22
CHAPTER II: Cardiac severity study using basic phonocardiogram signal processing tools: The Fast Fourier Transform (FFT) and the Short Time Fourier Transform (STFT) 24
I. Introduction 24
II. Database pre-processing and ranking 25
II.1. Pre-processing 25
II.2. Database ranking 26
III. Fast Fourier Transform (FFT) analysis of the phonocardiogram signals (PCGs) 30
IV. Short-time Fourier transform (STFT) 31
V. Parameters study and analysing 32
V.1. Frequency Band 32
V.2. Spectral Entropy (SEnt) 32
V.3. Time-frequency features (ΔT, ΔF) 33
V.4. Energetic Ratio (ER) 33
VI. Results and Discussion 33
VII. Conclusion 47
CHAPTER III: Cardiac severity study using the Discrete Wavelet Transform (DWT) 50
I. Introduction 50
II. The discrete wavelet transform 51
III. Parameters study and analysis 53
III.1. The reconstruction error parameter 53
III.2. The entropy of approximation coefficients 53
III.3. The mean of detail coefficients 54
IV. Results and Discussion 54
IV.1. Three DWT-features efficiency testing 54
IV.2. The Entropy of Approximation Coefficients (EAC) efficiency testing 60

IV.2.1. Click/ Murmur discrimination 61
IV.2.2. Cardiac severity assessment 63
IV.3. Additional observation 66
IV.4. Accuracy testing using machine-learning classifiers 66
IV.4.1. Click/ Murmur discrimination 71
IV.4.2. Cardiac severity assessment 72
V. Conclusion 73
CHAPTER IV: Cardiac severity study using the High Order Spectra Analysis (HOSA) 76
I. Introduction 76
II. High Order Spectra: Bispectral Analysis 77
Before introducing the higher-order spectra and bispectral analysis, we need to define a few essential concepts. 77
II.1. Correlation function 77
II.2. Multicorrelation and multispectra 78
II.3. High order spectra 78
II.4. The bispectral analysis 78
III. Parameters study and analysis 79
IV. Feature selecting algorithms 81
IV.1. Random Forest Feature Importance (RFFI) 81
IV.2. SelectKBest feature selection approach 81
V. Results and discussion 82
VI. Conclusion 89
CHAPTER V: The optimal features for cardiac severity assessment using the Fast Fourier Transform (FFT), the Short Time Fourier Transform (STFT), the Discrete Wavelet Transform (DWT), and the HOSA-Bispectral technique. 91
I. Introduction 91
II. Materials and methods 92
II.1. Mutual Information (MI) 93
II.2. Variance Threshold (VT) 94
II.3. ReliefF 95
II.4. Recursive Feature Elimination (RFE) 95
II.5. Long Short Term Memory (LSTM) Classifier 96
III. Results and discussion 97

IV. Conclusion 104
References 106
General conclusion 117

List of figures

CHAPTRE I: THEORITICAL NOTIONS ABOUT THE PHONOCARDIOGRAM

Figure I-1 : Position of the heart in the thorax [4]. 8
Figure I-2: The anterior and posterior view of the heart [5]. 8
Figure I-3: Internal Anatomy of the Heart. [6] 9
Figure I-4: Illustration of the four cardiac valves 10
Figure I-5: Longitudinal and transverse sections of a heart valve in positions (a) open (b) close [7]. 10
Figure I-7: Cardiac cycle phases: Step 1, 2, and 5 represents the diastole; Step 3 and 4, illustrates the systole. 12
Figure I-8: Auscultation sites on the thorax [9]. 13
Figure I-9: Temporal representation of a PCG signal of a healthy patient. 13
Figure I-10 : Temporal representation of the Ejection Click signal. 15
Figure I-11: Temporal representation of the Open Snap 16
Figure I-12: Classification of heart murmurs [18]. 17
Figure I-13: Temporal representation of the aortic stenosis signal. 17
Figure I-14: Temporal representation of the mitral regurgitation signal. 18
Figure I-15: Temporal representation of the systolic pulmonary stenosis signal. 18
Figure I-16: Temporal representation of the tricuspid regurgitation signal. 18
Figure I-17: Temporal representation of the mitral valve prolapse signal. 19
Figure I-18: Temporal representation of the mitral stenosis signal. 19
Figure I-19: Temporal representation of the aortic regurgitation signal. 19
Figure I-20: Temporal representation of the diastolic atrial septal defect signal. 20

CHAPTER II: Cardiac severity study using basic phonocardiogram signal processing tools: The Fast Fourier Transform (FFT) and the Short Time Fourier Transform (STFT)

Figure II. 1 Cardiac severity analysing of the mitral stenosis according to the MSD manuals and Andrew JANGs' information (Light and moderate severity level). 29
Figure II. 2 Cardiac severity analysing of the mitral stenosis according to the MSD manuals and Andrew JANGs' information (severe level). 30
Figure II. 3 Illustrates the frequency band feature measurement for a healthy case on an FFT spectrum. 32

Figure II. 4 Time-frequency features representation on an STFT spectrum for a normal phonocardiogram case. 33
Figure II. 5 Obtained results of the frequency Band (FB) for group1-3 of phonocardiogram signals. 36
Figure II. 6 STFT representations for the three signals of the group 1 of PCG signals. 37
Figure II. 7 Obtained results of the spectral entropy (SEnt) for group1-3 of phonocardiogram signals. 38
Figure II. 8 Illustrates the non-linear to linear transformation when using support vector machine SVM technique [38]. 40
Figure II. 9 OVA-SVM classification results of group1-3 when implementing the frequency band (FB) and the spectral entropy (SEnt). 41
Figure II. 10 OVA-SVM classification results of group1-3 when implementing the STFT properties of (a) S1 or (b) S2 only. 42
Figure II. 11 OVA-SVM classification results of group1-3 when implementing the STFT properties of the click only. 43
Figure II. 12 OVA-SVM classification results of group1-3 when implementing the STFT features extracted from the murmur. 43
Figure II. 13 OVA-SVM severity classification results of the phonocardiogram signals present in the three groups using the frequency band (FB) feature. 44
Figure II. 14 OVA-SVM severity classification results of the phonocardiogram signals present in the three groups using STFT properties of (a) S1 or (b) S2. 45
Figure II. 15 OVA-SVM severity classification results of the phonocardiogram signals present in the three groups using STFT properties of the murmur. 46
Figure II. 16 OVA-SVM classification results when studying the severity through the spectral entropy feature. 47

CHAPTER III: Cardiac severity study using the Discrete Wavelet Transform (DWT)

Figure III. 1 Approximations and details representation of a Discrete Wavelet Transform. 52
Figure III. 2 The principle of Discrete Wavelet Transform: (a) DWT decomposition tree of the phonocardiogram signal, (b) Frequency domain representation of the DWT (Filter Banks) [13-14]. 52
Figure III. 3 histogram representation of the three studied features for Click PCG signals– (ER) Energetic Ratio, (ECA)1/ Entropy of Approximation Coefficients, (Ermoy) Reconstruction Error, (MD) 1/Mean Variance of Details [24]. 57
Figure III. 4 histogram representation of the three studied features for diastolic murmur PCG signals– (ER) Energetic Ratio, (ECA) 1/Entropy of Approximation Coefficients, (Ermoy) Reconstruction Error, (MD) 1/Mean Variance of Details [23]. 58
Figure III. 5 histogram representation of the three studied features for systolic murmur PCG signals– (ER) Energetic Ratio, (ECA) Entropy of Approximation Coefficients, (Ermoy) Reconstruction Error, (MD)1/ Mean Variance of Details [23]. 58
Figure III. 6 Boxplot representation of the EAC evolution for PCG signals with clicks and murmurs [23]. . 59
Figure III. 7 histograms of the DWT-EAC and the ER for click segments only: Click segment from : EAS, AG, EC, LS, OS, VG [24]. 61
Figure III. 8 Boxplot representation of the EAC variation between the studied PCG signals [24]. 62
Figure III. 10 histograms of the DWT-EAC and the ER for one PCG cycle: PCG cycle from : EAS, AG, EC, LS, OS, VG [24]. 62

Figure III. 11 histograms of the DWT-EAC and the ER for murmur segment only : (a) Murmur segments from four AS cases; (b) Murmur segments from four AR cases [24]. 64
Figure III. 12 Histograms of the DWT-EAC and the ER for one PCG cycle: (a) PCG cycle from four AS cases; (c) PCG cycle from four AR cases [24]. 65
Figure III. 13 Displays the difference values (EAC extracted from one PCG cycle - EAC from added sound segment) for the group 1 and group 2 signals [15]. 66
Figure III. 14 (a) Energetic Ratio (ER) evolution representation within the AS and the AR cases, (b) EAC (x10^4) evolution representation for the AS and the AR cases when using murmur segments only [14]. 68
Figure III. 15 (a) Energetic Ratio (ER) evolution representation within the AS and the AR cases, (b) EAC (x10^4) evolution representation for the AS and the AR cases when using one PCG cycle [14]. 69
Figure III. 16 (a) ER (%) evolution representation for the pathologies with click, (b) EAC (x10^4) evolution representation for the pathologies with click when using click segments only [14]. 70
Figure III. 17 ER (%) and EAC (x10^4) evolution representation for the pathologies with click when using one PCG cycle [14]. 71
Figure III. 18 A two-class classification (Click pathologies – Murmur pathologies) results using the One versus All Support Vector Machine (OVA-SVM): the pathologies with click are classified in the yellow zone and the 8 cases of the AS and the AR cases in the blue zone. 72
Figure III. 19 A three-class classification (Click pathologies – Aortic Stenosis – Aortic Regurgitation) results using the One versus All Support Vector Machine (OVA-SVM): the purple zone groups the pathologies with click, the blue one classifies the four cases of the AR and AS. 73

CHAPTER IV: Cardiac severity study using the High Order Spectra Analysis (HOSA)

Figure IV. 1 The non-redundant region in the bispectral analysis 79
Figure IV. 2 Bispectral extracted features. 81
Figure IV. 3 Variation of the average amplitude and the three entropies through the severity levels 82
Figure IV. 4 Variation of the five moments through the severity level. 83
Figure IV. 5 Variation of the weighted centre of the bi-spectral and its absolute through the severity levels 83
Figure IV. 6 illustrates the importance of all the features to the expected classification. 85
Figure IV. 7 The correlation between the six selected features: Ent3, AbsWcob2, Mo3, EntPh, Wcob2, Ent2. 87

CHAPTER V: The optimal features for cardiac severity assessment using the Fast Fourier Transform (FFT), the Short Time Fourier Transform (STFT), the Discrete Wavelet Transform (DWT), and the HOSA-Bispectral technique

Figure V. 1 Feature selection workflows 93
Figure V. 2 RNN architecture with its three gates [19]. 97

List of Tables

Table I. 1Temporal and frequency characteristics of the PCG signal 20
Table I. 2 List of the database sources..... 21

Table II. 1 Characteristics and origin of the studied pathologies in the three pre-established groups [16]..... 26
Table II. 2 Some of the MSD manuals and Andrew JANGs' information used for cardiac severity ranking. 27
Table II. 3 Obtained results for the spectral entropy when analysing the three pre-established groups. 35
Table II. 4 Obtained results for the spectral entropy when analysing different level of severity. 39

Table III. 1 Some of the MSD manuals and other references information used for cardiac severity ranking [16][13, 17-22]. 55
Table III. 2 displays the extracted features from the discrete wavelet transform (DWT) analysis on phonocardiogram signals [23]. 56
Table III. 3 List of the PCG signals studied in the EAC efficiency testing. 60

Table IV. 1 highlights the accuracies obtained when using all of the extracted features. 84
Table IV. 2 list of the six most important features between the 14 extracted ones. 86
Table IV. 3 Accuracies obtained when using the Random Forest Feature Importance (RFFI) selected features. 86
Table IV. 4 The correlation values between the six selected features: Ent3, AbsWcob2, Mo3, EntPh, Wcob2, Ent2. 87
Table IV. 5 The correlation values between the six selected features: Ent3, AbsWcob2, Mo3, EntPh, Wcob2, Ent2. 87
Table IV. 6 Accuracies obtained when using the Random Forest Feature Importance (RFFI) and SelectKbest selected features..... 88

Table V. 1 Feature Selection Methods. 92
Table V. 2 Features extracted from the Fast Fourier Transform (FFT), Short-Time Fourier Transform (STFT), Discrete Wavelet Transform (DWT), HOSA-Bispectral..... 98
Table V. 3 Selected features with the first workflow. 99
Table V. 4 Selected features using the second workflow. 100
Table V. 5 Accuracy results for the three final feature combinations using the One vs All Support Vector Machine (OVA-SVM), the K-Nearest Neighbor (KNN), and the Long Short Time Memory classifiers (LSTM)..... 102
Table V. 6 Comparison of our method with previous works. 103

Abbreviation Table:

PCG	Phonocardiogram
EEG	Electroencephalogram
EMG	Electromyogram
ECG	Electrocardiogram
G1	Group 1 of phonocardiogram signals
G2	Group 2 of phonocardiogram signals
G3	Group 3 of phonocardiogram signals
N	Normal (Healthy)
IM	Innocent murmur
COA	Coarctation of the Aorta
EAS	Early Aortic Stenosis
AG	Aortic gallop
VG	Ventricular Gallop
EC	Ejection click
OS	Opening Snap
LS	Later systolic
PS	Pulmonary Stenosis
AR	Aortic regurgitation
TR	Tricuspid regurgitation
AS	Aortic stenosis
MS	Mitral stenosis
MR	Mitral regurgitation
DAI	Diastolic Aortic Insufficiency
DASD	Diastolic Atrial Septal Defect
LAS	Late aortique systolique stenosis
S1	First heart sound
S2	Second heart sound
S3	Third heart sound

S4	Fourth heart sound
A2	Aortic component
P2	Pulmonic component
T1	Tricuspid component
M1	Mitral component
F.F.T	Fast Fourier Transform
ER	Energetic Ratio
FB	Frequency Band
SEnt	Spectral Entropy
AbsSEnt	Absolute Spectral Entropy
Δt	Temporal extent
Δf	Frequency extent
S.T.F.T	Short-Time Fourier Transform
W.T	Wavelet Transform
C.W.T	Continues Wavelet Transform
D.W.T	Discrete Wavelet Transform
T.O.D	Transformée en Ondelettes Discrètes
Db7	7^{th} order of the Daubechies wavelet
(a1,a2,....,a7)	The approximation levels of the discrete wavelet transform through the db7 wavelet
(d1,d2,...,d7)	The details levels of the discrete wavelet transform through the db7 wavelet
Ɛermoy	Reconstruction error
EAC	Entropy of approximation coefficients
Md	Mean of detail coefficients
HOSA	Higher order statistics Analysis
Var	Variance
Mean	Mean
f_1, f_2	Frequency 1 ,frequency 2
(Avgamp)	Average amplitude
(ent1)	Standard bi-spectral entropy

(ent2)	Standard bi-spectral square entropy
(ent3)	Standard bi-spectral cubic entropy
(entPh)	Entropy of Phase
(mo1)	Moment of 1st order
(mo2)	Moment of 2nd order
(mo3)	Moment of 3rd order
(mo4)	Moment of 4th order
(mo5)	Moment of 5th order
WCOB	Weighted Centre Of Bispectrum
$\boldsymbol{AbsWCOB}$	Absolute Weighted Centre Of Bispectrum
ER	Energetic Ratio
OVA-SVM	One-vs-All Support Vector Machine
KNN	K-Nearest Neighbor
LSTM	Long Short Time Memory
RFFI	Random Forest Feature Importance
RFE	Recursive Feature Elimination
MI	Mutual Information
VT	Variance Thresholding

General introduction

General introduction

During the Middle Ages, researchers vacillated between two main theories about the origins of feelings and voluntary movements, proposed by two prominent ancient scientists. Aristotle (4th century BC) attributed this role to the heart, while Galen (2nd century) placed these functions in the brain. Abd Allah Ibn Sîna 'Avicenna' (980-1037), while taking into account the importance of isolating the three main organs (Qanûn fi téb) for therapeutic purposes, considered that it would be difficult to remove the heart from its major function. Mohammed Ibn Rushd 'Averroes' (1126-1198), in the Colliget (colliyat in Arabic) approved Aristotle's hypothesis and made the heart the seat of general sensitivity.

It was not until the 17th century that William Harvey (1578-1658) definitively deprived the heart of its function as the seat of sensations, following many years of research and experimentation. This led Robert Hooke (1635-1703) to realise the importance of auscultating the heart for diagnosis.

The invention of the stethoscope by René Laennec in 1816 made cardiac auscultation an irreplaceable clinical tool up to the present day [1]. However, detecting the relevant symptoms that make up a diagnosis based on heart sounds recorded by a stethoscope is a complicated task for doctors that takes years of training to acquire and refine. Part of this difficulty stems from the fact that heart sounds are often separated from each other by less than 30 milliseconds. In addition, the heart sounds that characterise cardiac disorders are generally of low intensity compared with normal (non-pathological) heart sounds (or noises). This makes the task of acoustic detection more difficult for the doctor [2].

Phonocardiography, as a non-invasive method based on the recording of vibrations or oscillations of various frequencies corresponding to normal or pathological heart sounds [3], addresses this problem by providing clinicians with a graphic recording of heart sounds and murmurs. This recording is known as the phonocardiogram signal (PCG), and it translates the subject's cardiac activity much more accurately than the cardiologist's simple test, thus overcoming human hearing limitations [4].

Electrophysiological signals, such as the phonocardiogram (PCG) signals, conceal very valuable information for diagnosing cardiac pathologies. This thesis aims to find features capable of discriminating between normal and pathological cases, and more importantly, detecting the level of severity within the same pathology.

These features will help us follow the pathology evolution and establish, with the help of health professionals, an optimal treatment plan for the patients. Therefore, within this framework, we will carry out an in-depth study by applying a series of spectral and spectro_temporal analyses (FFT, STFT, TOD, HOS) to

PCG signals from various pathologies and of different degrees of severity listed in three levels (Light, Moderate, Severe).

To rank our database from the least to the most severe case, we referred to the online MSD manuals for professional valvular disorder diagnosis [21] and the online version of the <<valvular heart disease >> book by Andrew JANG [22]. Additionally, we employed the Energetic Ratio (ER) when the severity level was hard to identify.

As known phonocardiogram signal (PCG) has been the subject of several signal processing studies, where researchers applied various analysis techniques developed for sound and/or physiological signals and extracted countless features for different purposes. Hence, the automatic detection of numerous cardiac pathologies, discrimination between pathological and healthy cases, identification/ localisation of heart sounds - clicks and murmurs, and assessment of the cardiac severity. We would like to mention some of the research work carried out in the past, either by professors and doctoral students in our Biomedical Engineering department or by international researchers on phonocardiogram signals (PCG), which has led to significant results.

Previous studies such as Berraih, S. A., et al. and I. Debbal, et al., investigated HOS-based parameters extracted from three main PCG signal groups. Both concluded that the bispectrum graphic representation is a discriminative parameter; they then established a list of potential differentiation features [1-4]. D.S.B. Sundaram, et al., utilised the FFT power spectrum in a novel deep learning model as an image to discriminate normal from murmur heart sounds [5]. S.M. Debbal and Hamza Ch., found which of the heart sounds and their component are directly concerned by the pathology through FFT and STFT features [6]. In [7], Berraih, S. A., et al., assessed the cardiac severity in PCG signals through HOSA features. Later, P. Dhar et al. employed the Cross-wavelet spectrum as an image for a CNN (AlexNet) to classify PCG signals in healthy or pathologic classes [8]. Y. N. E. H. Baakek, et al., highlighted the influence of clicks and murmurs on heart sounds using an STFT analysis [9]. Followed by [10], who conducted a comparative study of window shapes and lengths in Short-Time feature extraction for the classification of heart sound signals, where various types of windows were applied on the PCG signals to conclude which of them gives the best accuracy results and affect less the signal.

A. Hussain et al., analysed PCG signals and extracted three discriminative features, the mean value, variance, and energy of DWT. The results proved that these features could differentiate between healthy/unhealthy phonocardiogram recordings [11]. A year later, J.A. Lee et al., improved the heart sound classification performance using methods like 1D-CNN and 2D-CNN, wavelet scattering transform (WST), and continuous wavelet transform (CWT) [12]. Lately, P. Careena et al., proposed a machine-learning technique for cardiac murmur detection and classification. The Peak Signal-to-Noise Ratio (PSNR) and Structural Similarity Index Matrix (SSIM) were extracted from comparing STFT spectrogram images of the

PCG signals and then fed into various decision trees to classify normal heart sound and murmurs like systolic, diastolic, and continuous [13].

All of these previous works inspired us to establish our research plan and since we are working on a synthesis and comparison study, we will test the chosen analysing techniques individually through different research purposes.

First, we will:

- Test the Fast Fourier Transform (FFT) and Short-Time Fourier Transform (STFT) features to classify cardiac pathologies in whether:
    - Group 1 (G1): Phonocardiogram signals with no clicks (reduced murmur) or murmurs.
    - Group 2 (G2): Phonocardiogram signals with clicks.
    - Group 3 (G3): Phonocardiogram signals with clicks or murmurs.
- Test the Discrete Wavelet Transform (DWT) features to discriminate between click and murmur segments.
- Select the optimal HOSA-Bispectral features for cardiac severity assessment and classification.

Secondly, we will retest all of these features for cardiac severity assessment through machine learning classifiers such as the One-vs-All Support Vector Machine (OVA-SVM) and the K-Nearest Neighbor (KNN).

Lastly, we will compare these techniques through a series of feature-selecting methods and machine-learning classifiers. Therefore, according to the feature selection results, the technique that delivers the most features of the final combination with the highest accuracy is the optimal one for cardiac severity assessment.

Our work is divided into five chapters. The first one [CHAPTER I] is dedicated to the anatomical study of the heart and its cardiac activity.

Each of the following three chapters will present the results and their interpretation obtained for each technique used:

CHAPTER II: Cardiac severity study using basic phonocardiogram signal processing tools: The Fast Fourier Transform (FFT) and the Short Time Fourier Transform (STFT).

CHAPTER III: Cardiac severity study using the Discrete Wavelet Transform (DWT).

CHAPTER IV: Cardiac severity study using the High Order Spectra Analysis (HOSA).

The fifth chapter [CHAPTER V] will discuss the comparison results and conclude which of the techniques or features are the optimal ones for cardiac severity assessment.

By analysing the obtained results, we expect the selected features to help us fulfil the set goals at the beginning by following the pathology evolution and then establishing, with the help of health professionals, an optimal treatment plan for the patients. The early identification of the pathology, the assessment of its severity, and the optimal treatment plans will allow us to stabilise the evolution of the pathology and reduce the rate of valvular implantation.

Finally, we will conclude with an overview of the work carried out and some perspectives for future work.

Chapter. I

CHAPTRE I: THEORITICAL NOTIONS ABOUT THE PHONOCARDIOGRAM

I. Introduction

A phonocardiogram (PCG) is a high precision copy of the heart sounds with the murmurs made during pumping blood [1]. Divers' pathological conditions of the cardiovascular system can be distinguish through the PCG recording. It is therefore imperative to understand the functioning of the heart and the genesis of this signal in order to facilitate the analysis and clarify the medical diagnosis with a view to prescribing adequate treatment to the patient. To meet the objectives set, we devote this chapter to necessary information on the anatomy of the heart and the genesis of this signal, followed by a brief description of some of the pathologies studied in this work.

II. Heart Basics

The heart is a hollow muscle whose function is to circulate blood throughout the body by acting like a pump through rhythmic contractions. It is capable of circulating 4 to 5 litres of blood, constantly, from birth until death.

II.1. Position of the heart in the thorax

The heart is a muscular organ weighing approximately 250 grams, lies in the protective thorax, posterior to the sternum and spine, and rests on the superior surface of the diaphragm. The heart assumes an oblique position in the middle part of the rib cage (the mediastinum) between the two lungs, surrounded by the pericardium (Figure I-1). [2][3]

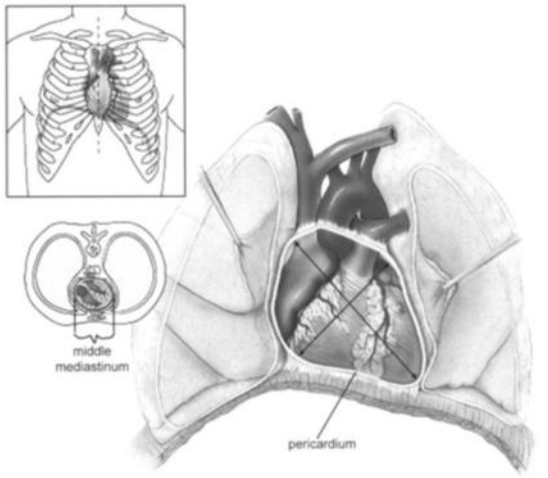

Figure I-1 : Position of the heart in the thorax [4].

II.2. Morphology of the Heart

Two atria (left and right) and two ventricles (left and right), four chambers in total (Figure I-2) compose the heart.[3]

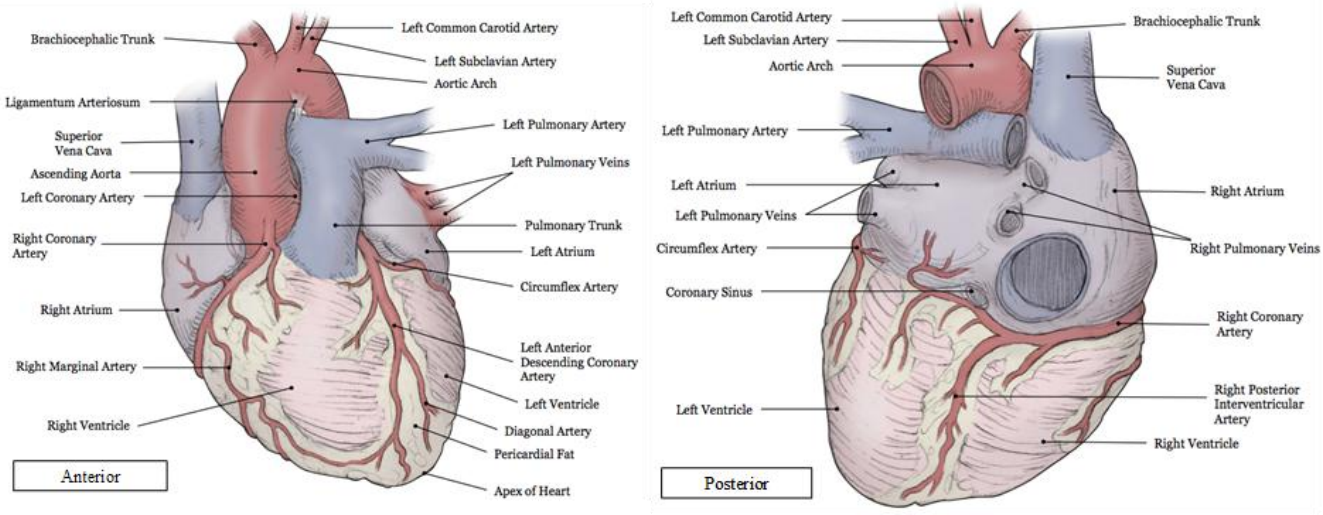

Figure I-2: The anterior and posterior view of the heart [5].

II.2.1. The pericardium

The pericardium is the coating that surrounds the heart (peri = "around" + cardia = "heart").It two distinct but continuous layers separate each other by a serous fluid. Furthermore, despite being one continuous layer, the pericardium is divided into two components [3].

II.3. Internal Anatomy of the Heart

The heart is composed of three distinctive layers (Figure I-3): (1) a superficial visceral pericardium; (2) a middle myocardium; and (3) the endocardium.

The myocardium is the heart wall layer that contracts. It pushes blood inferiorly through the atria and superiorly through the ventricles [3].

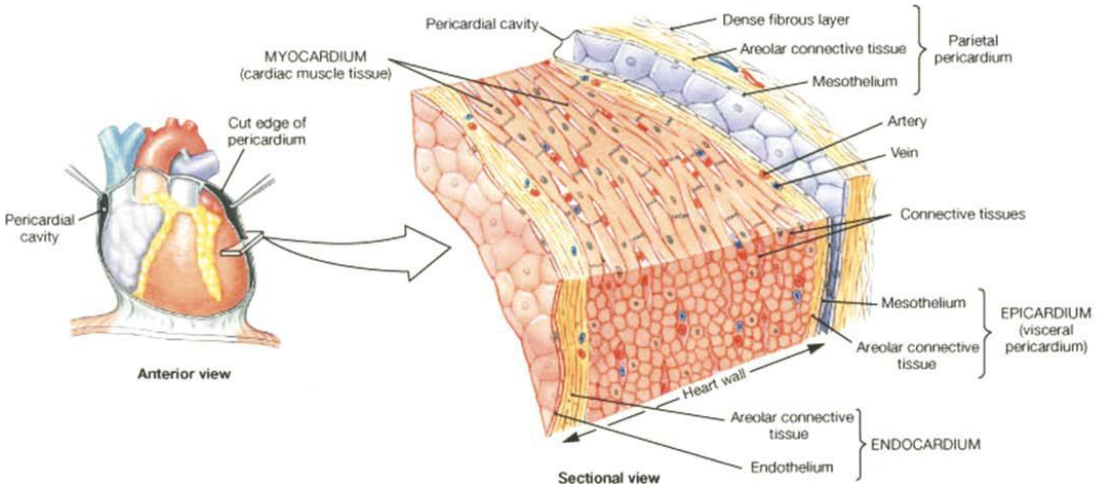

Figure I-3: Internal Anatomy of the Heart. [6]

II.3.1. Cardiac valves

In anatomy, heart valves are elastic, non-muscular structures of the heart, separating the different chambers and preventing blood from flowing backwards in the wrong direction. There are four of them (Figure I-4):

• The mitral valve between the left atrium and the left ventricle.

• The tricuspid valve between the right atrium and the right ventricle.

• The aortic valve between the left ventricle and the aorta.

• The pulmonary valve between the right ventricle and the pulmonary artery.

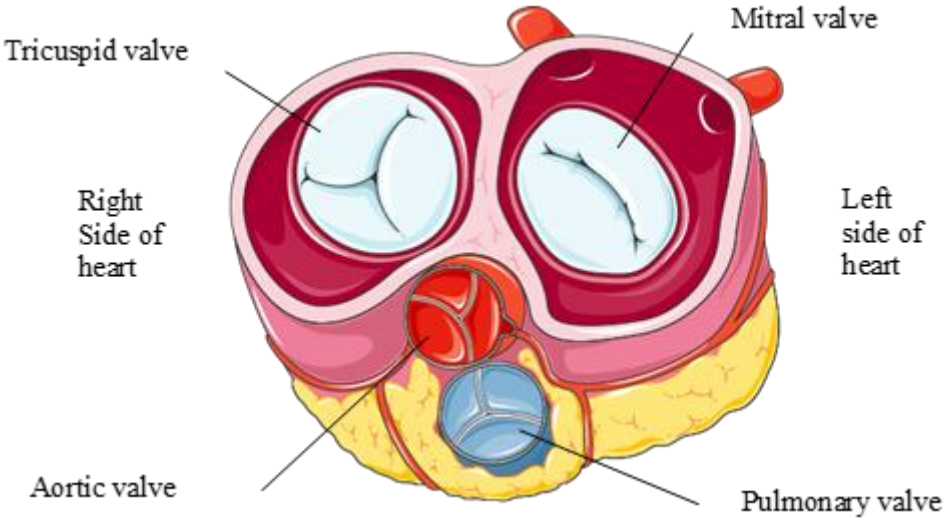

Figure I-4: Illustration of the four cardiac valves

Figure I-5 illustrates longitudinal and transverse sections of a heart valve in the open and closed positions (the physiology of valves in the heart):

• (a) open; the leaflets of the heart valve are moved apart to allow blood to pass, this opening causes blood turbulence which is part of heart sounds.

• (b) closed; the layers tighten so as not to allow the passage of blood; in the event of insufficiency, the valve does not close properly, which causes blood regurgitation [7].

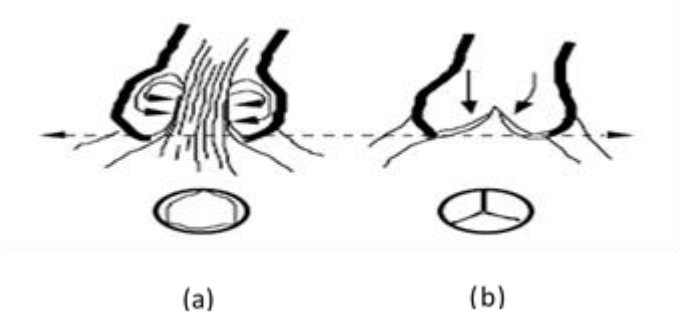

Figure I-5: Longitudinal and transverse sections of a heart valve in positions (a) open (b) close [7].

II.4. Cardiac revolution

The cardiac revolution takes place in two phases (Figure I-7):

• Phase 1, systole:

Consists of the contraction of the two ventricles, which causes the ejection of blood towards the periphery of the heart through the aorta, and towards the lungs via the pulmonary arteries.

• Phase 2, diastole:

Allows relaxation of both ventricles by filling with blood through the atrioventricular valves after accumulation in the atria.

PS; we can say that cardiac hemodynamics is divided into four essential phases: contraction and ventricular ejection constituting ventricular systole and isovolumetric relaxation then filling during ventricular diastole [8].

II.4.1. ventricular systole

Breaks down into 2 phases, a contraction phase and an ejection phase.

- **Ventricular contraction:** This phase is subdivided into two sub-phases;

1. Pre-isovolumetric contraction: the pressure in the ventricles increases rapidly and becomes greater than the pressure in the atria, which causes the atrioventricular valves to close [8].

2. Isovolumetric contraction: the atrioventricular and sigmoid valves (pulmonary and aortic valves) are closed. The two ventricles continue to contract, and the pressure becomes greater than the pressure in the arteries, causing the sigmoid valves to open.

This phase corresponds to the appearance of the first group of acoustic vibrations noted S1.

- **Ventricular ejection:** The ejection of ventricular blood towards the arteries occurs in three phases;

1. Rapid ejection phase: blood is propelled rapidly with a gradual increase in ventricular pressure.

2. Slow ejection phase: blood is ejected slightly according to the decrease in ventricular pressure.

3. Wiggers proto–diastole: ventricular pressure decreases too quickly but remains higher than the pressure in the arteries.

II.4.2. Ventricular diastole

It includes two phase, the isovolumetric relaxation and the filling phase.

- **Isovolumetric relaxation:** When the pressure in the ventricles becomes lower than the pressure in the arteries, the sigmoid valves close, which corresponds to the appearance of the second group of acoustic vibrations, denoted S2 [8].
- **Filling:** During this phase, the ventricles fill with blood from the atria through the atrioventricular valves. This phase is subdivided into four phases.

1. Rapid filling phase: ventricular pressure is very reduced compared to atrial pressure, which results in rapid filling of the ventricles.

2. Slow filling phase: the pressure in the atria begins to decrease, however the ventricular pressure continues to increase, ventricular filling is then less rapid.

3. Diastasis phase: when atrial and ventricular pressures are equal, the heart is in a resting phase. When there is an acceleration in heart rate, this phase disappears.

4. Active filling phase: the ventricles complete their filling with an increase in pressure due to atrial systole [8].

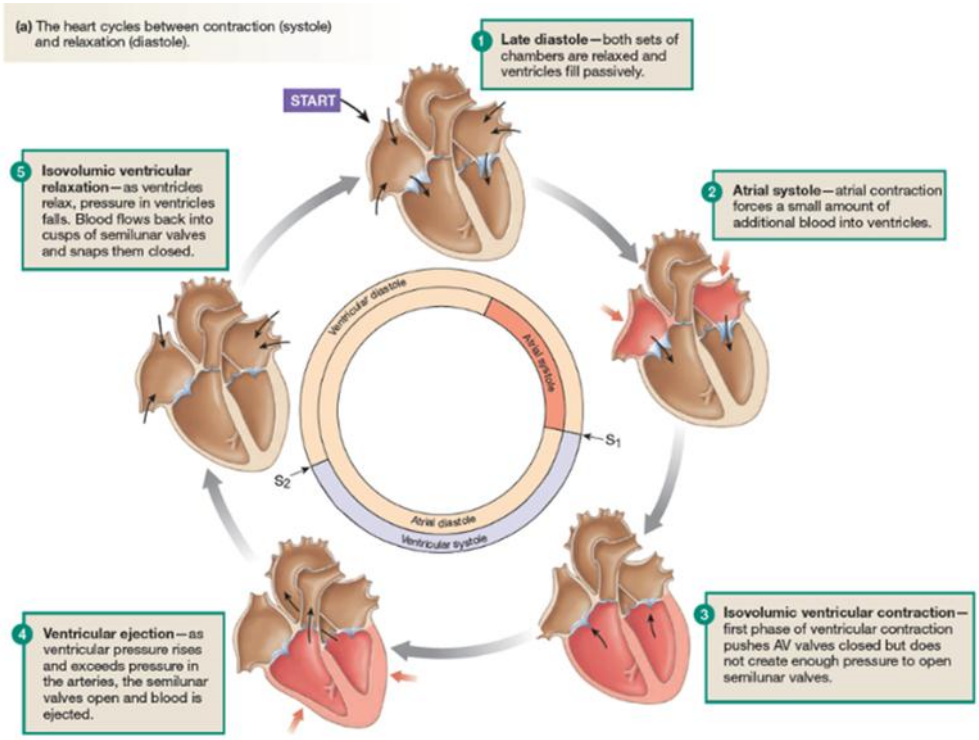

Figure I-6: Cardiac cycle phases: Step 1, 2, and 5 represents the diastole; Step 3 and 4, illustrates the systole.

III. Theoretical notions about the phonocardiogram signal

III.1. Definition and description of the Phonocardiogram Signal

A phonocardiogram signal illustrates the heart sounds and murmurs occurring during the procedure of pumping blood [1]. The signal is acquired through a microphone placed on one of the auscultation sites: aortic, tricuspid, mitral or pulmonary as illustrated in Figure I-8:

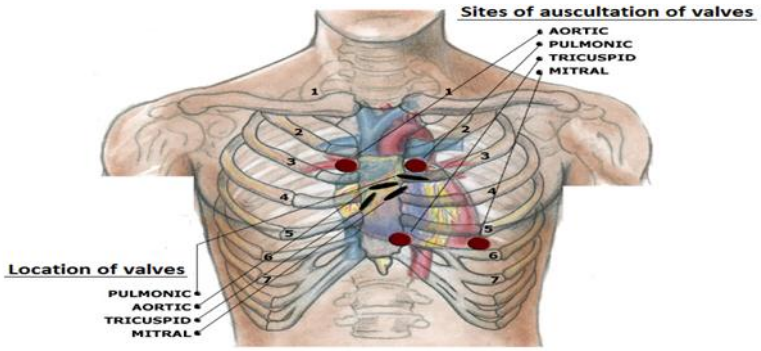

Figure I-7: Auscultation sites on the thorax [9].

III.2. Heart Sounds

Under normal conditions, we can distinguish two heart sounds on PCG recording.

- The first heart sound S1.
- The second heart sound S2.

When the heart beats normally, the two sounds follow each other quite quickly, and then there is a pause after the second sound: S1 S2 is shorter than S2 S1.

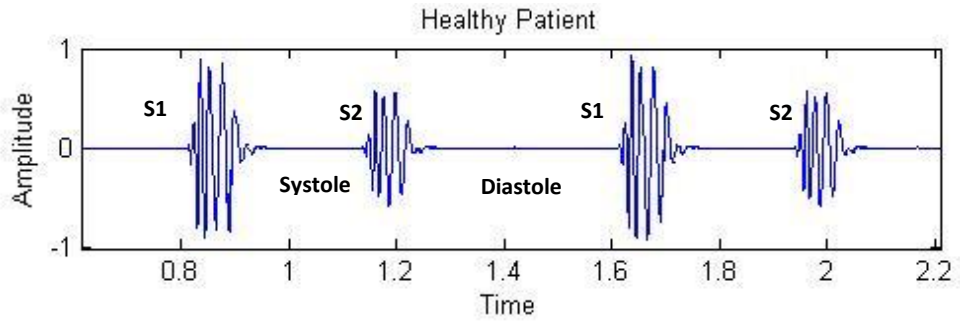

Figure I-8: Temporal representation of a PCG signal of a healthy patient.

III.2.1. Heart sound S1

The first heart sound, S1, emerges at the abrupt closure of the mitral and tricuspid valves, which leads to a blood and cardiac structure vibration in the ventricular chambers. It could be heard just after the QRS complex of the electrocardiogram (ECG) [10]. S1 presents two main components: the mitral component (M1) and the tricuspid component (T1); where M1 occurs before T1 [11], and the temporal delay between M1 and T1 for a healthy person, does not exceed 30ms [12].

III.2.2. Heart sound S2

The second heart sound, S2, manifests at the closure of the pulmonic and aortic valves referring to the beginning of the isovolumetric relaxation period. It could be heard toward the end of the T wave in the ECG [10]. S2 also contains two components A2 and P2 where the first one correspond to the closing of the aortic valve and the second one refers to the closing of the pulmonic valve. P2 is a little bit behind the A2 where this delay could indicate the presence of a specific disease if it is too important [13].

III.2.3. Heart sound S3

The third heart sound is a low frequency and low intensity signal that occurs 0.15 second after the aortic component (A2) of S2 during the period of rapid passive ventricular filling. S3 is considered normal for children and adults as it can be a sign of illness in the elderly[14][15].

III.2.4. Heart sound S4

The fourth heart sound, which normally inaudible low frequency and low intensity, is heard shortly before S1, is associated with atrial contraction and rapid active filling of the ventricle. S3 and S4 often accompany other congenital heart diseases [14][15].

III.3. Additional abnormal heart sounds

III.3.1. Galloping rhythm

It mainly the S3 and S4. These are low frequency sounds that become pathological after 30 years. This supernumerary sounds forms a 3-beat rhythm (hence the expression galloping rhythm), it is heard at the tip, in left lateral decubitus, or at the xiphoid. There are right and left gallop rhythms. Left gallop rhythms are more frequent. In fact there are three types of gallops:

- **Pro diastolic gallop:** this is S3; it corresponds to the rapid and powerful emptying of blood from the atrium towards the ventricle, at the beginning of diastole.
- **The pre-systolic gallop:** this is S4; just before S1. It corresponds to the arrival of the blood flow in the ventricle, during atrial systole, that is to say at the end of ventricular diastole.

- **The summons gallop**: it results from the addition of the two components S3 and S4, in the case of tachycardia [16].

III.3.2. Mitral opening click

It is a proto-diastolic sound (heard at the beginning of diastole), occurs after S2. This is a noise added to a normal S2 sound. It gives the impression of a duplication of S2 but in reality, it is clearly separated from it; this is a sign of mitral stenosis [16].

III.3.3. The click

Some clicks occur during systole; Unlike S1 and S2, the clicks are high pitched and present short duration. .Two types of clicks exist:

- The proto-systolic click is a dry, high-pitched noise, heard just after S1. It corresponds to the opening of the sigmoid muscles, marking the beginning of the systolic murmur of aortic valvular narrowing.
- The meso-systolic click is heard in the ballooning of the mitral valve and corresponds to the prolapse of the mitral valve within the left atrium, during contraction of the left ventricle [16].

Ejection Click

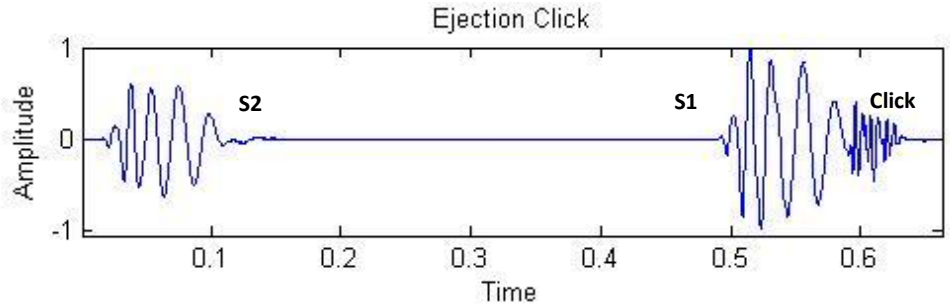

Figure I-9 : Temporal representation of the Ejection Click signal.

Open Snap

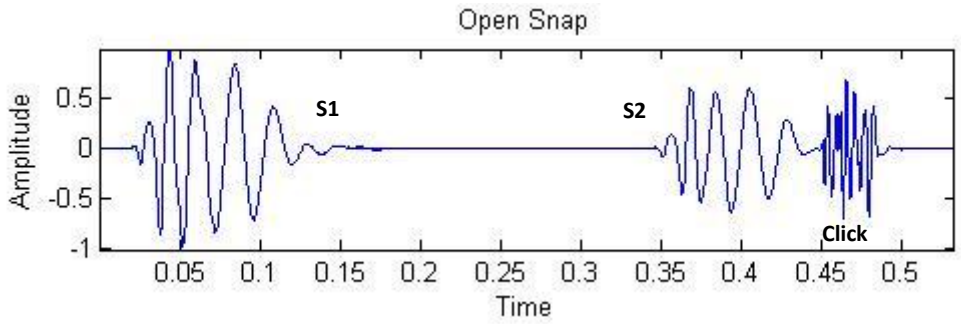

Figure I-10: Temporal representation of the Open Snap

III.4. Heart murmurs

Murmurs could be recorded in both systole or diastole and are usually due to abnormal pressure gradients and turbulent blood flow through cardiac valves that do not fully open or are completely closed.[17]

Classification of a heart murmur

We can classify murmurs according to several factors of their characteristics (Figure I-12), which are:

1. Their configuration: crescendo, decrescendo, crescendo-decrescendo or diamond-shaped, in a plateau.

2. Intensity: coded from 1/6 to 6/6. From 4/6 .

3. Timbre: it is the tone of the breath: raspy, inhaled, rumbling, soft, rolling, etc.

4. Time: proto/meso/tele/holo-systolic/diastolic, or continuous;

5. The seat: place where the murmur is perceived with maximum intensity (aortic, mitral, tricuspid, pulmonic).

6. Irradiation: direction in which the blast propagates (apex, carotids, tricuspid site) [13].

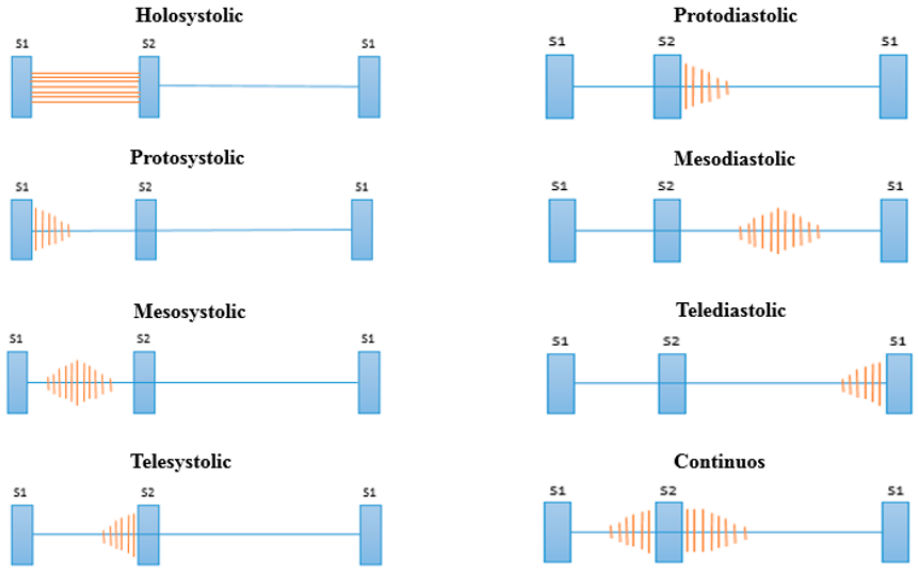

Figure I-11: Classification of heart murmurs [18]

III.4.1. Systolic murmurs

Systolic murmurs can be normal or abnormal and are always between S1 and S2. They can be proto, meso, tele or holo-systolic (pan systolic).

Aortic stenosis (AS)

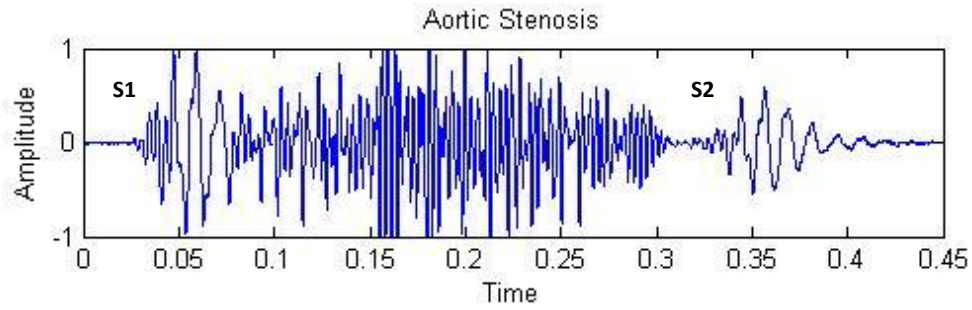

Figure I-12: Temporal representation of the aortic stenosis signal.

Mitral regurgitation (MR)

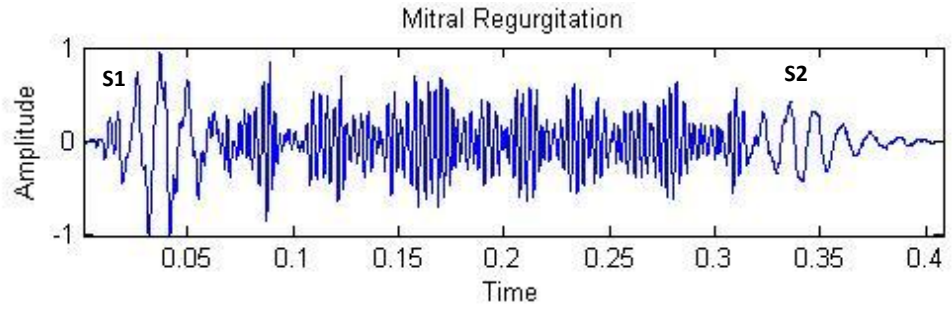

Figure I-13: Temporal representation of the mitral regurgitation signal.

Systolic Pulmonary Stenosis (PS)

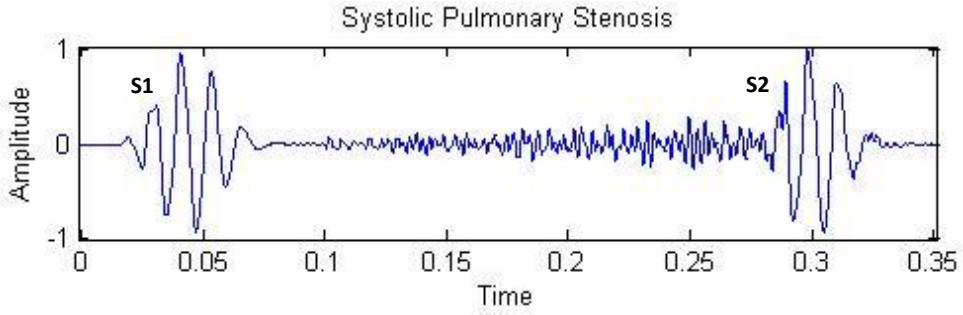

Figure I-14: Temporal representation of the systolic pulmonary stenosis signal.

Tricuspid regurgitation (TR)

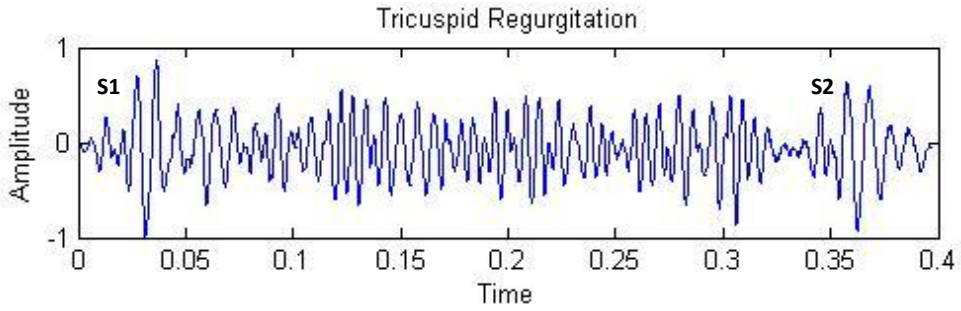

Figure I-15: Temporal representation of the tricuspid regurgitation signal.

Mitral valve prolapse (MVP)

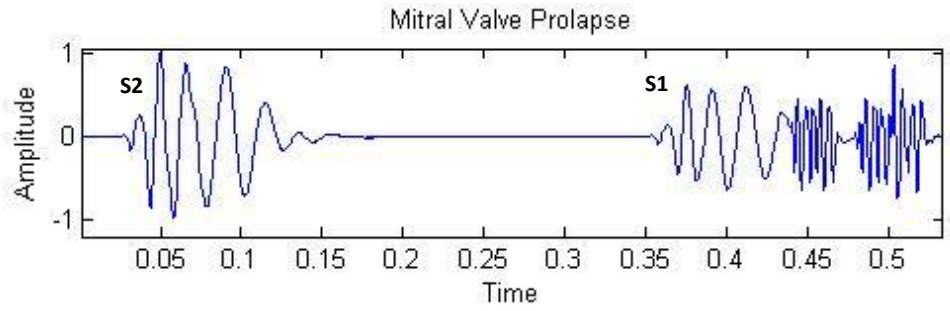

Figure I-16: Temporal representation of the mitral valve prolapse signal.

III.4.2. Diastolic murmurs

A diastolic murmur always occurs between S2 and S1. Unlike the systolic murmur, a diastolic murmur is always pathological and linked to an abnormality of cardiac anatomy or function.

Mitral stenosis (MS)

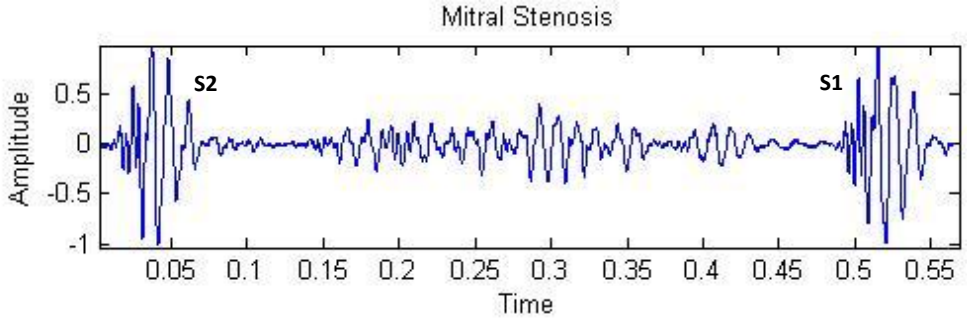

Figure I-17: Temporal representation of the mitral stenosis signal.

Aortic regurgitation (AR)

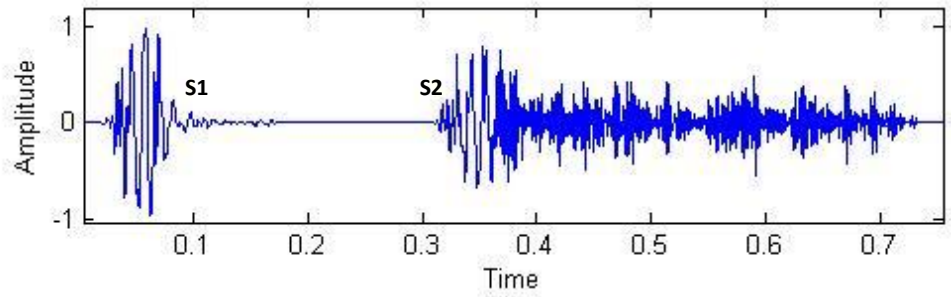

Figure I-18: Temporal representation of the aortic regurgitation signal.

Diastolic Atrial Septal Defect (DASD)

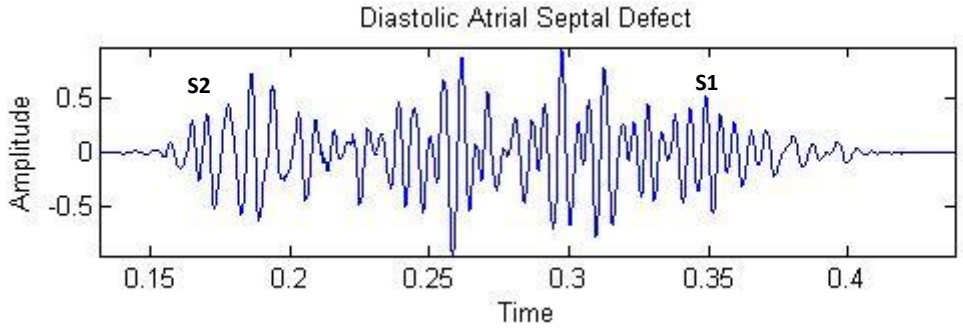

Figure I-19: Temporal representation of the diastolic atrial septal defect signal.

III.5. Temporal and frequency characteristics of the PCG signal

Table I. 1Temporal and frequency characteristics of the PCG signal

Heart sounds	Frequency Range (HZ)	Duration (Ms)	Main Components
Sound S1	91-179	100	M1-T1
Sound S2	145-200	70-100	A2-P2
Sound S3	<80	60-80	
Sound S4	80	60-80	
Murmur	<1000	>S1,S2	

IV. PCG signals used

The PCGs signals used in our study are real signals acquired from the four auscultation sites (aortic, tricuspid, mitral and pulmonary). They were taken from four internet addresses:

Table I. 2 List of the database sources.

Name	Site	Last Visit	Signals used from this site	Sample Frequency
American college of cardiology	http://www.egeneralmedical.com	2009	5 N, Im,Coa,Ec, Os,Ag,Eas, Tr,Ps,Ls, 5 Mvp, DASD,Dr, 4 Ar,7 As, 7 Mr,4 Ms, 7 AI	8000-11025
Heart Sounds and Murmurs	http://www.cardiosource.com/heartsounds			
/	http://www.dundee.ac.uk/medther/Cardiology/hsmur.html			
Yassen2018	https://github.com/yaseen21khan/Classification-of-Heart-Sound-Signal-Using-Multiple-Features-	2023	20 As 20 Ms 20 Mr 20 Mvp	1024

V. Conclusion

The study carried out in this chapter on intracardiac hemodynamics provides information on the nature of heart sounds as well as the origin of pathological cases often occurring in the form of valvular disease.

The phonocardiogram signal reflects the condition of the examined patient heart; it is a medical diagnosis aiding tool. The PCG signal confirms, refines the auscultation data and provides additional information from the sound activities regarding the chronology of pathological signs in the cardiac revolution, by situating them in relation to normal heart sounds.

PCG signal analysis helped uncover the relation between the valves' activities (opening/ closing) and some cardiac diseases like stenosis and regurgitation. Therefore, we mainly focus on algorithms with a quantitative, precise and objective interpretation of heart sounds to improve the process of cardiovascular diagnosis.

Computer-assisted auscultation helps identify cardiac pathologies that may be unrecognized through a conventional auscultation. Reason why the PCG signal is the subject for many research purposes, like denoising, segmentation, decomposition, parameter extraction, and classification. In the following chapters, we will first describe the different methods proposed for processing the PCG signal.

Chapter. II

CHAPTER II: Cardiac severity study using basic phonocardiogram signal processing tools: The Fast Fourier Transform (FFT) and the Short Time Fourier Transform (STFT)

I. Introduction

Phonocardiogram signal (PCG) has been the subject of several signal processing studies, where researchers applied various analysis techniques developed for sound and/or physiological signals and extracted countless features for different purposes. Hence, the automatic detection of numerous cardiac pathologies, discrimination between pathological and healthy cases, identification/ localisation of heart sounds - clicks and murmurs, and assessment of the cardiac severity.

The Fast Fourier Transform (FFT) and the Short Time Fourier Transform (STFT) are basics in phonocardiogram signal processing; their extracted features serve many purposes. Indeed, BF. Beritelli and S. Serrano found that by using a frequency representation based on FFT, we could easily identify different heart sounds [1]. S.M.Debbal and F.Bereksi-Reguig also analysed the PCG signals (cardiac noises, click, or murmur), and noticed that the FFT technique could provide frequency information on their evolution [2][3]. Later, A. K. Abbas and R. Bassam stated that spectral PCG signal analysis is an energetic tool for inspecting various cardiovascular disorders and their characteristics associated with variations in spectral attributes [4].

On another hand, the authors of [5] separated and measured heart sounds, once, time and frequency localisation was achieved. Then, M.S.Bendelhoum has shown in [6] that the STFT technique does have good temporal resolution for a small Δt and good frequency resolution for a small Δf and can overcome the FFT drawbacks.

Researchers kept using these two basic techniques for even more complex purposes. D.S.B. Sundaram et al., utilised the power spectrum in a novel deep learning model as an image to discriminate normal from murmur heart sounds [7]. S.M. Debbal and Hamza Ch., identified which of the heart sounds component is directly affected by the pathology using the FFT and STFT [8]. M. Atteeq, et al., worked on extracting the foetus's heartbeat from the mother's beat using a Blind source and separation technique like STFT to discriminate between the two heartbeats using the STFT spectrogram and the average frequencies of mother and foetus [9].

Recently, Y. N. E. H. Baakek et al., highlighted the effect of clicks and murmurs on heart sounds using an STFT analysis [10]. Followed by M. Fakhry, and A.F. Brery, who conducted a comparative study of window shapes and lengths for the classification of heart sound signals, where various types of windows were applied on the PCG signals to conclude which of them gives the best accuracy results and affect less the signal [11].

Most recently, P. Careena, et al., proposed a machine learning technique for cardiac murmurs detection and classification. The Peak Signal-to-Noise Ratio (PSNR) and Structural Similarity Index Matrix (SSIM) were extracted from comparing STFT spectrogram images of the PCG signals and then fed into various decision trees to classify normal heart sound and murmurs like systolic, diastolic, and continuous [12].

In this chapter, we will discuss the ability of the most basic phonocardiogram signal processing tools, the (FFT) and the (STFT), to discriminate cardiac pathologies and assess the severity evolution through the extracted features. First, we will start by dividing the collected database into three groups, namely:

- G1: phonocardiogram signals without clicks nor murmurs.
- G2: phonocardiogram signals with clicks.
- G2: phonocardiogram signals with clicks or murmurs.

These three groups will allow us to test the ability of our FFT and STFT features for cardiac pathologies discrimination and introduce the possibility of a severity assessment.

Secondly, we will create another group (G4) of phonocardiogram recordings at different severity levels. Aortic Stenosis (AS), Mitral Stenosis (MS), and Mitral Regurgitation (MR) will be the studied pathologies in this fourth group.

Lastly, we will implement our features into a K-Nearest Neighbor (KNN) and a One versus All Support Vector Machine (OVA-SVM) graphic classifier. This will provide us with accuracy percentages and a graphic representation of the classification results when using the FFT and STFT features extracted from the four pre-established groups.

II. Database pre-processing and ranking

II.1. Pre-processing

This study started by visualising the databases' phonocardiogram signals (PCGs), choosing a few cardiac pathologies, and selecting the PCG signals that require pre-processing. Some PCG signals were pre-processed before uploading to the online access platform.

For those that required pre-processing, a simple Butterworth second order band-pass filter with a cut-off frequency of 50Hz-2KHz as suggested by A. Djebbari in [13] was efficient for PCG signals denoising and

for more complicated cases we employed the Discrete Wavelet transform (DWT) with the seventh level DAUBECHIES (Db7) and a soft Stein's unbiased risk estimate (SURE) threshold.

II.2. Database ranking

To rank our database from the least to the most severe case, we referred to the online MSD manuals for professional valvular disorder diagnosis [14] and the online version of the <<valvular heart disease >> book by Andrew JANG [15]. We started by ranking the phonocardiogram signals of the three pre-established groups using Table II.1 references and the temporal representation of each signal then compared the obtained results with previous published works that employed the Energetic ratio (ER) as a severity ranking feature, where we obtained similar ranking order.

After establishing a similar severity ranking than published works, we decided to continue this study by referring to MSD manuals, Andrew JANG for database severity ranking and the Energetic Ratio in complex cases or if it is impossible to determine the level of severity through the previous references. Figure II.1-2 illustrates how we analyse each segment of the PCG cycle by referring to Table II.2 information for severity ranking.

Table II.1 below presents some information used for ranking the PCG database in one of the three groups.

Table II. 1 Characteristics and origin of the studied pathologies in the three pre-established groups [16]

PCG signals	**Origin**			
Innocent murmur	A common finding in infants and children. Originate through normal flow patterns with no structural or anatomic abnormalities of the heart or vessels [17].			
Aortic Coarctation	Abnormalities in the development of the aorta prior to birth (Congenital heart defects).			
PCG signals	**Click / Murmur characteristics**			
	Frequency Range	Duration / location in the cardiac cycle	Configuration	Timber
Group 2				
Early Aortic Stenosis	100-800Hz (High pitch)	≈10-20ms, early-systolic	/	Dry
Ejection Click		early-systolic	/	Sharp
Late Systole		Late-systolic	/	/

Atrial Gallop	15-50Hz (Low pitch, very low frequency, short and faint)	≈0.08-0.20s just before S1	/	Galloping rhythm, lilt or canter quality
Group 3				
Pulmonary Stenosis	Up to 600Hz (High pitch)	Holo-systolic	Crescendo–decrescendo	Harsh
Tricuspid Regurgitation	Up to 600Hz (High to medium pitch)			Blowing
Aortic Stenosis	Up to 600Hz (Medium to low pitch)	Mid-, late-, holo-systolic		Harsh, rasping, grunting or rough
Aortic Regurgitation	Up to 600Hz (High or low pitch)	Early-diastolic	Decrescendo	Blowing

*Information regarding frequency range and timings from [18-23]

Table II. 2 Some of the MSD manuals and Andrew JANGs' information used for cardiac severity ranking.

Pathology	**Severity levels**		
	Light	Moderate	Severe
Aortic Stenosis	Normal S1 Normal split of S2 Soft murmur	Normal S1 Normal split of S2 Louder murmur	A2 merges with P2 The murmur is longer and peaks in volume later in systole (ie, crescendo phase becomes longer and the decrescendo phase becomes shorter)

			The 4th heart sound (S4) is occasionally present
Aortic regurgitation	murmur may be short and occurs only in early diastole		The absence of the 1st heart sound (S1) The presence of the 3rd heart sound (S3) Austin Flint murmur (mid to late diastolic murmur)
Mitral stenosis	Loud S1 Early diastolic opening snap	Loud S1 Normal split S2 with an exaggerated P2 Early diastolic opening snap Low-pitched decrescendo-crescendo rumbling diastolic murmur	Increasing duration of the murmur The snap moves closer to S2 Opening snap may be soft or absent
Mitral regurgitation	S1 may be soft or occasionally loud The systolic murmur may be abbreviated or occur late in systole	S1 may be soft or occasionally loud The murmur begins after S1 and continues to S2	The presence of the 3rd heart sound (S3) A short rumbling mid-diastolic inflow murmur may be present following an S3 The murmur tends to crescendo in volume up to S2, if the intensity varies

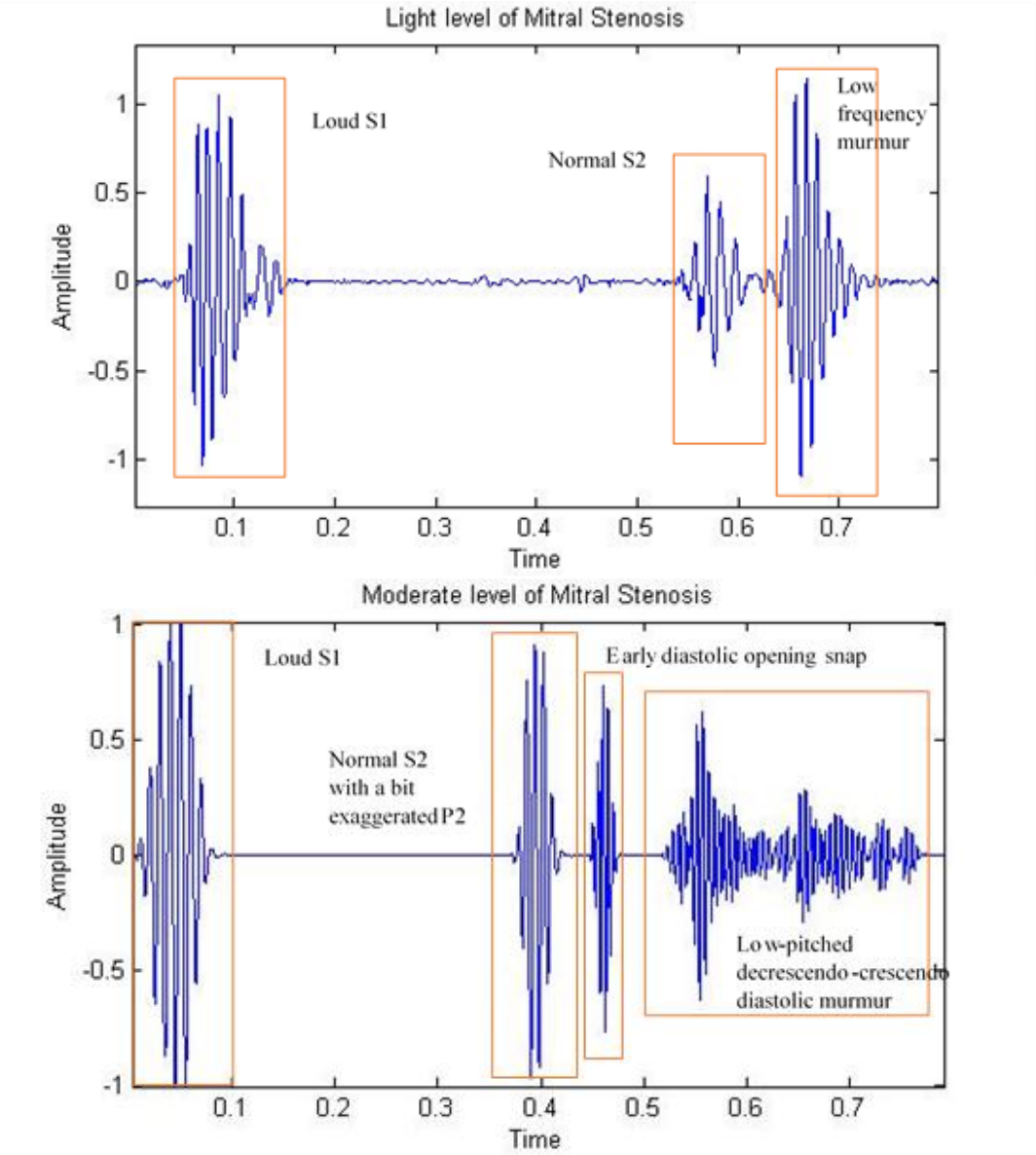

Figure II. 1 Cardiac severity analysing of the mitral stenosis according to the MSD manuals and Andrew JANGs' information (Light and moderate severity level).

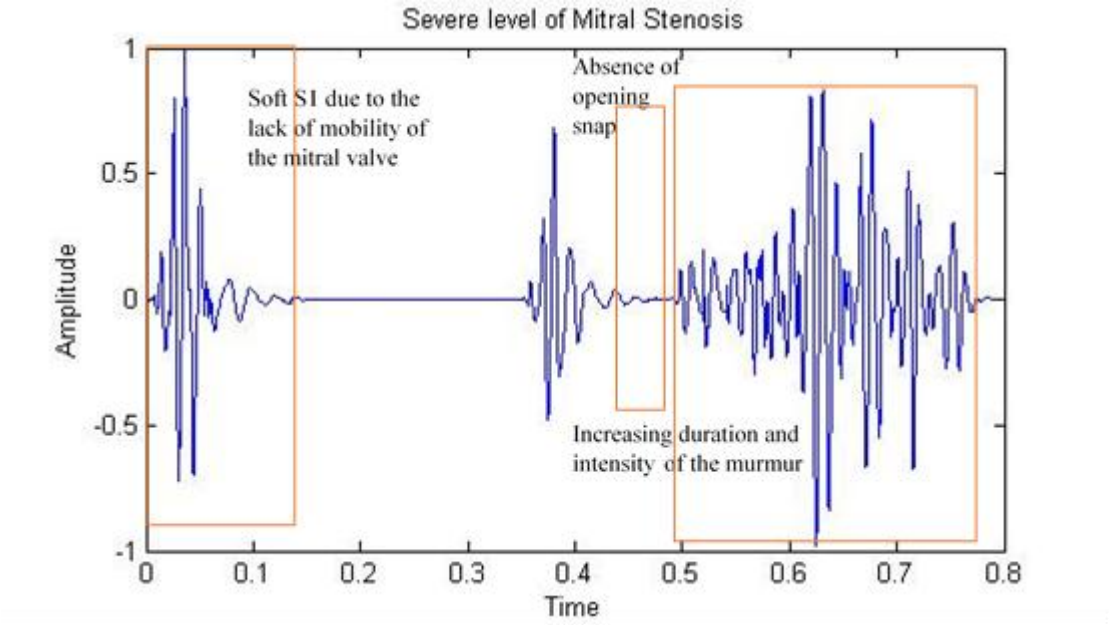

Figure II. 2 Cardiac severity analysing of the mitral stenosis according to the MSD manuals and Andrew JANGs' information (severe level).

III. Fast Fourier Transform (FFT) analysis of the phonocardiogram signals (PCGs)

The Fourier Transform (FT) is usually employed as an FFT algorithm (fast Fourier transform)[24].

Equation (II.1) give the mathematical definition of the FT:

$$X(f) = \int x(t) e^{-j2\Pi ft}\, dt \qquad \text{(II.1)}$$

Where t and f are respectively the time and frequency elements. $X(f)$ represents the spectrum of x(t) where its frequencies span the entire range in which it is non zero [25].

The Fourier Transform (FT) decomposes the signal into a set of cosine, sine, or imaginary exponential, which we call basic functions. We often employ temporal and frequency analysis together when processing a signal. Cause while the temporal representation highlights the duration and discontinuities of a signal, the frequency analysis presents it periodicity. Therefore, to transit from the time domain to the frequency domain we use the Fourier series, where it decomposes the signal into a sum of sinusoidal functions of different frequencies.

The most imperative rule of the Fourier transform is that the signal should be of finite energy, i.e. square summable. This may look problematic for real signals; however, this condition is satisfied for a finite time measurement.

Another property of the Fourier transform is the PARSEVAL identity (Eq.II.2), which consists of the independence of the energy conservation from any time or frequency variation [26].

$$\int_{-\infty}^{+\infty} \left|s(t)\right|^2 dt = \frac{1}{2\prod} \int_{-\infty}^{+\infty} \left|\hat{s}(w)\right|^2 dw \qquad \text{(II.2)}$$

The Fourier transform can also be in discrete time, as defined in equation II.3:

$$\hat{s}_n = \sum_{k=0}^{N-1} s(k) e^{-j2\prod kn/N} \qquad n \in \{0,....,N-1\} \qquad \text{(II.3)}$$

Where N is the minimum number of samples required to reconstruct the signal s(t).

The Discrete Fourier Transform (DFT) (Eq.II.4) estimates the Fourier transform of a function from a finite number of its sampled points [4].

$$s(k) = \frac{1}{N} \sum_{n=0}^{N-1} s_n e^{j2\prod kn/N}, k \in \{0,....,N-1\} \qquad \text{(II.4)}$$

P.S:

It is possible to calculate the DFT through the Fast Fourier Transform (FFT) algorithm. The DFT has the aptitude of determining the weighting between different discrete frequencies, hence its application in numerous signal processing studies. While the discrete data taken as input for the DFT is commonly known as a **signal**, and it is defined in the time domain, the **spectrum** is defined in the frequency domain and refers to the output values.

IV. Short-time Fourier transform (STFT)

The short-time Fourier transform STFT algorithm windows the signal and applies the Fourier Transform on it different segments. A time dimension is added through the location of the sliding window, which results in a time-varying frequency analysis.

We can mathematically represent the STFT as the following:

$$S(t, f) = \int_{-\infty}^{+\infty} s(\tau) w(\tau - t) e^{-j2\pi \ ft} d\tau \qquad \text{(II.5)}$$

Where $w(\tau - t)$ it is the sliding window, $s(t)$ is the signal, t is the time, f is the frequency.

We choose the length of the window in a way to maintain signal stationary to calculate the Fourier transform.

To reduce the effect of having finite duration (the effect of leakage), we multiply each sub-record by an appropriate window and then apply the Fourier transform. As long as the sub-records maintain steady variations, the spectrogram will provide an accurate idea of how the spectral composition of the signal has changed during the whole time record.[24]

V. Parameters study and analysing

V.1. Frequency Band

It refers to the frequency range occupied by one phonocardiogram cycle in a Fast Fourier Transform (FFT) spectrum (Figure II.3).

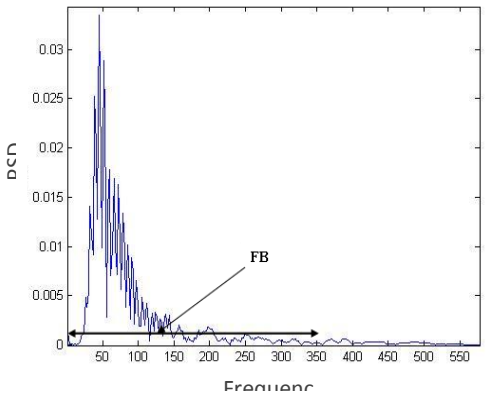

Figure II. 3 Illustrates the frequency band feature measurement for a healthy case on an FFT spectrum.

P.S: we start measuring the frequency band after the spectrum reaches 5% of its maximum height. This allows us to remove all the unnecessary information and values that are close to zero.

V.2. Spectral Entropy (SEnt)

The SEnt of a phonocardiogram signal is a measure of its power spectral distribution (PSD). It highlights the quantity of information present in a PCG spectrum.

$$SEnt[X] = -\int P(X) Log\, P(X) d(X) \qquad \text{(II.6)}$$

Where X is the selected part from the spectrum. P(X) : a probability density.

P.S: the spectral entropy will be extracted from the FFT spectrum.

V.3. Time-frequency features (ΔT, ΔF)

Figure II.4 displays graphically the definition of these two features.

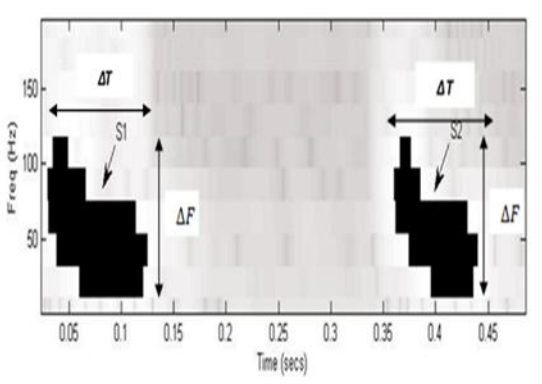

Figure II. 4 Time-frequency features representation on an STFT spectrum for a normal phonocardiogram case.

V.4. Energetic Ratio (ER)

The energy of a signal is one of the elements related to the severity evolution. The energy ratio refers to the energy of a murmur segment over the energy of one cardiac cycle [27].

$$\mathrm{ER} = \frac{\mathrm{E}_2}{\mathrm{E}_1 + \mathrm{E}_2} \times 100 \qquad \text{(II.7)}$$

Where E2 is the energy of the click or heart murmur, E1 is the energy of the two heart sounds S1 + S2; (E1 + E2) is the energy of one PCG cycle.

Energetic Ratio (%)	Severity Level
<30	Light
30-70	Moderate
>70	Severe

The equation II.8 varies from 0-100%. If it equals 100%, the murmurs dominate the cardiac cycle over cardiac sounds (S1, S2). Therefore, the efficiency of the ER in cardiac severity tracking [27]. This parameter served as a reference feature in divers studies [28-30].

VI. Results and Discussion

In this section, we'll display and discuss the Fast Fourier Transform (FFT) and the Short Time Fourier Transform (STFT) results.

We exploited the FFT and STFT features in two different ways:

- Groups discrimination
- Cardiac severity assessment

In this study, we compared and evaluated the obtained results with the Energetic Ratio (ER). However, we later employed machine-learning algorithms to confirm the accuracy of these features.

VI.1. Groups discrimination

Table 3-4 in [30] (see Appendix 1) displays the FFT and STFT obtained results for the three pre-established groups:

- Group 1 (G1): Phonocardiogram signals with no clicks or murmurs (N, IM, Coa).
- Group 2 (G2): Phonocardiogram signals with clicks (EAS, AG, EC, LS).
- Group 3 (G3): Phonocardiogram signals with murmurs (PS2, AR, TR, AS).

First, according to the results presented in Table 3 of [30] and Figure II.5, the frequency band (FB) of the three groups follows the ER evolution. In comparison to the healthy/normal case 'N', the innocent murmur and coarctation of the aorta cases presented a wider frequency band. On the other hand, the coarctation of the aorta frequency band was larger than the innocent murmur's. This refers to the severity importance of a COA compared to an innocent murmur, these results highlight the accuracy of the PCGs obtained ranking order by the medical bibliographic references.

G2 and G3 (PCG signals with clicks and murmurs) presented similar results of the FB feature (FB and the energetic ratio ER evolve proportionally).

Second, Figure II.6 represent the STFT spectrums obtained for group 1 signals. One can notice that ΔT of the two heart sounds is proportional to the energy of each studied signal. At the same time, ΔT of S2 is superior to that of S1 for the three pathologies of G1 (Table 4 in [30]), it is likely due to the semi-lunar shape of the aortic valves and rapidly closing lungs [31].

Contrarily to murmur segments in G3, the ΔT extracted from click segments of G2 presented a proportional evolution to that of the Energetic Ratio. Which is coherent, since murmurs of some cardiac pathologies tend to go shorter when the severity evolves.

Regarding the Frequency Extent ΔF, PCG signals of the second group (G2) presented a decrease in the ΔF of the two heart sounds and an increase in the ΔF of the clicks. In G3, the ΔF of both murmurs and heart sounds is proportionally correlated to the ER. (See Appendix 1)

According to these results, one can say that when the temporal extent presented an inverse correlation to the severity while the frequency extent proportionally followed the cardiac severity evolution.

Lastly, since frequency features (ΔF and FB) were found directly correlated to the cardiac severity, we decided to study the quantity of information present in a FFT spectrum. We extracted the entropy from the frequency bands of each signal.

Table II.3 and Figure II.7 illustrate the obtained results for these three groups. Spectral entropy is the definition of the intensity, complexity, irregularity, unpredictability characteristics present in a FFT spectrum. Therefore, it allowed discrimination between the three pre-established groups.

Table II. 3 Obtained results for the spectral entropy when analysing the three pre-established groups.

Features / **Signals**	**Severity Level**	**Spectral Entropy (SEnt)**
PCG signals without clicks nor murmurs		
N	healthy	1.6490
IM	Pathologic and morphologically similar to healthy signals	8.5120
Coa1	Pathologic and morphologically similar to healthy signals	11.4158
PCG signals with clicks		
EAS	Light	12.4002
AG	Light	17.2033
EC	Moderate	20.9964
LS	Moderate	24.6390
PCG signals with murmurs		
PS2	Light	6.7924
AR	Moderate	11.9424
TR	Moderate	14.1657
AS	Severe	46.3210

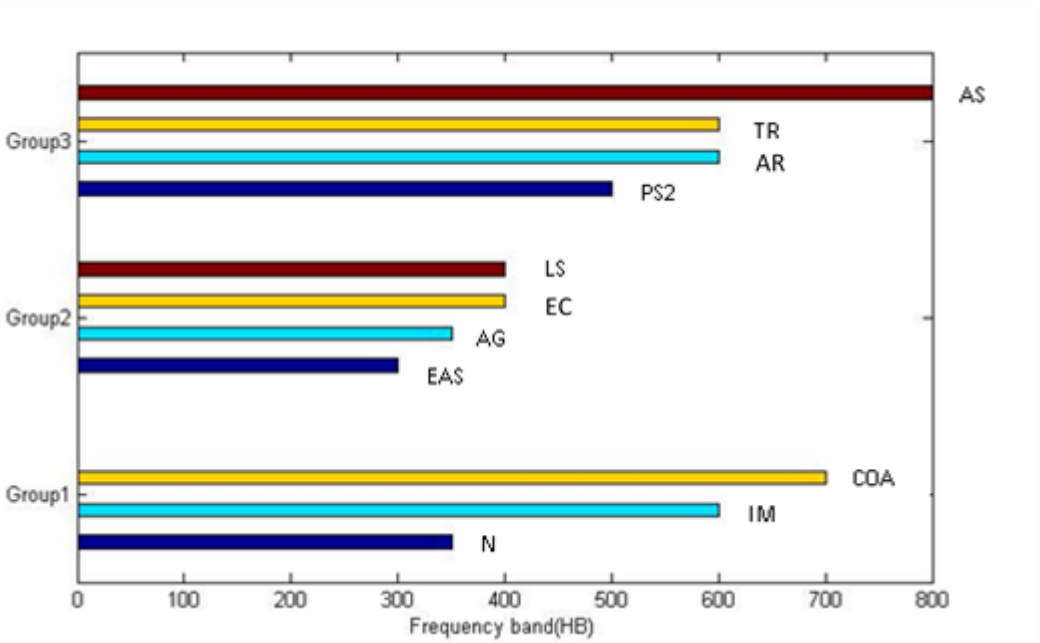

Figure II. 5 Obtained results of the frequency Band (FB) for group1-3 of phonocardiogram signals.

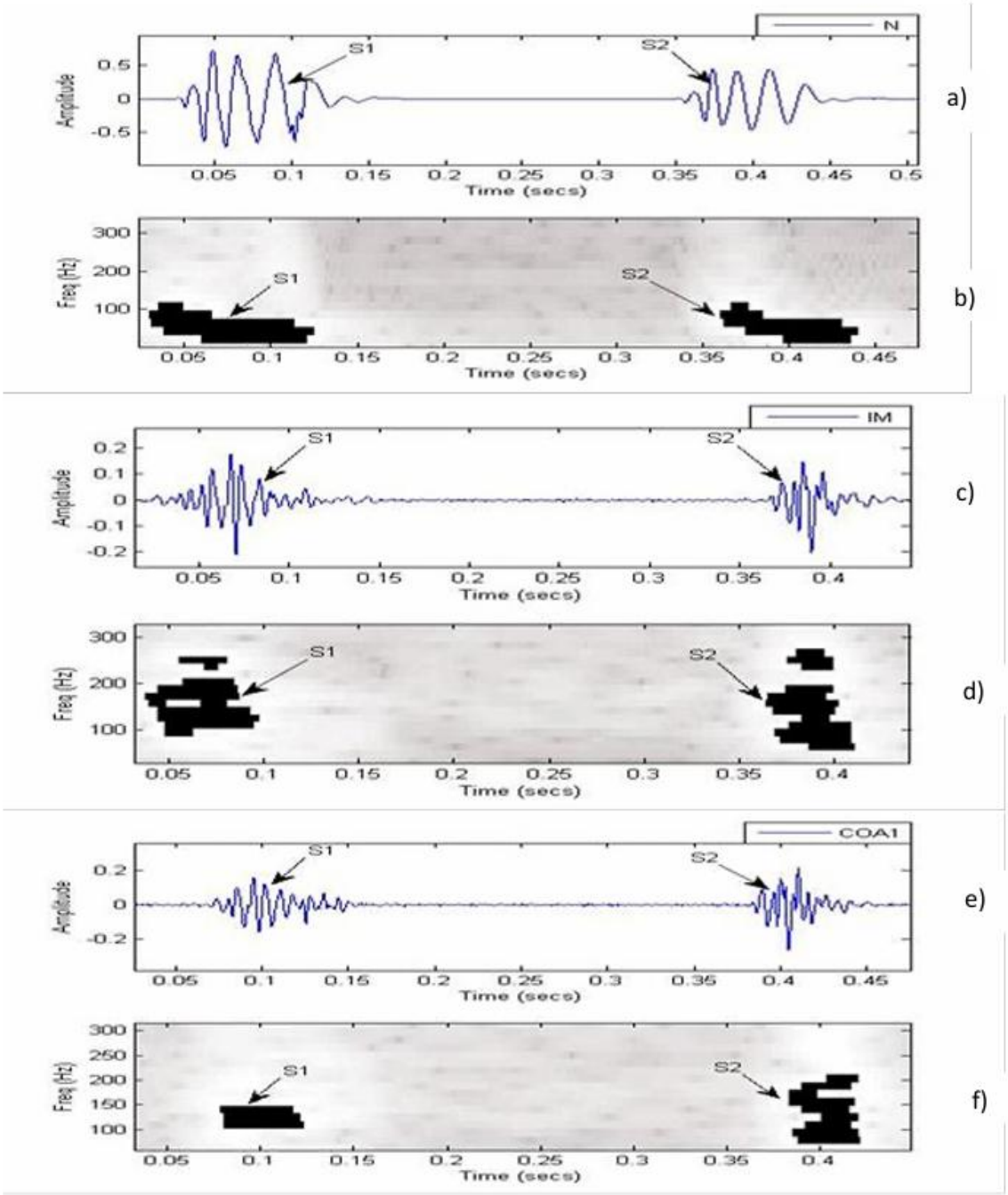

Figure II. 6 STFT representations for the three signals of the group 1 of PCG signals.

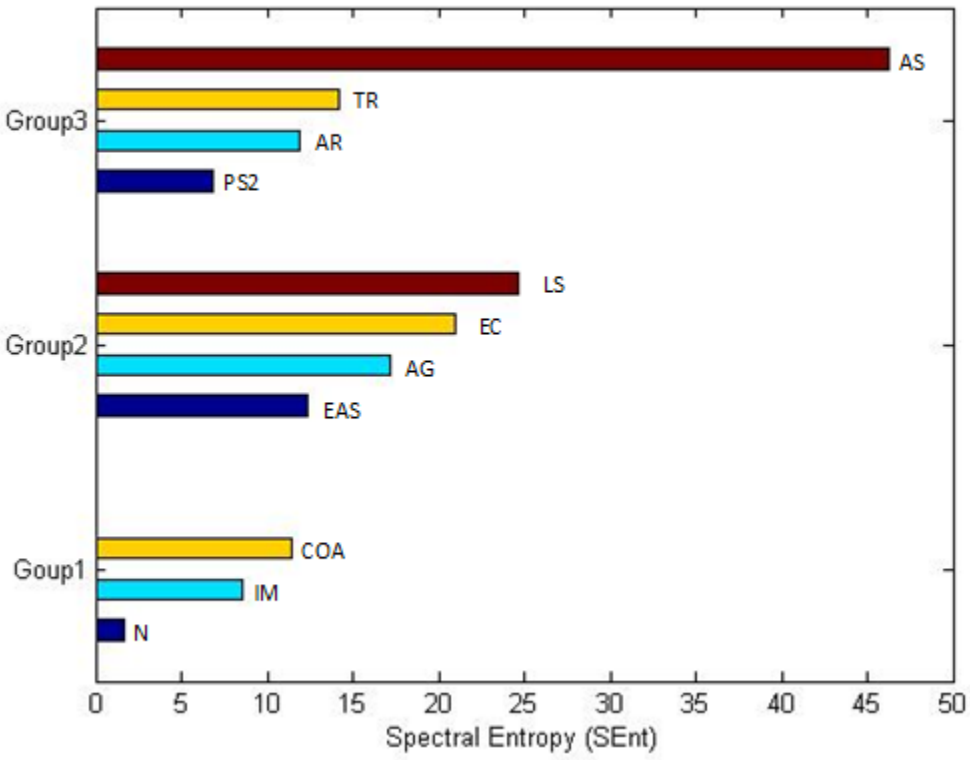

Figure II. 7 Obtained results of the spectral entropy (SEnt) for group1-3 of phonocardiogram signals.

VI.2. Cardiac severity assessment

Just like for group discrimination, we analysed the fourth group of phonocardiogram signals with the same algorithms, the same features, the ER as a comparison feature, and then implements the results into the KNN and OVA-SVM classifiers.

Figure 11 and table 5 in [30] highlighted the ability of the FB feature to assess cardiac severity. Where it presented an inverse correlation to the ER.

The temporal extent **ΔT** of the two heart sounds presented a correlation with the energetic ratio either directly as for the AS and MS signals, or inversely as for the MR signals. Similar results were obtained for the murmur segments, where **ΔT** presented a direct correlation to the ER for the aortic stenosis and an inverse one for the mitral stenosis and mitral regurgitation. (See Appendix 1)

Since the spectral entropy presented great discriminative results, we decided to test its ability in following the cardiac severity. However, instead of studying the three pathologies we limited ourselves to two (Mitral and Aortic Stenosis) but with different cardiac severity levels.

The spectrum in itself presented discriminative results between the different severity levels (figure 4 in [32]) (see Appendix 2) and the spectral entropy (SEnt) proved its ability with a proportional correlation to the cardiac severity evolution (Table II.4).

Table II. 4 Obtained results for the spectral entropy when analysing different level of severity.

signals	**Severity level**	**Spectral Entropy (SEnt)**
Signal 1	Light	45.5964
Signal 2	Light	20.1742
Signal 3	Light	20.1972
Signal 4	Light	21.5371
Signal 5	Light	10.7164
Signal 6	Light	29.9192
Signal 7	Moderate	31.9036
Signal 8	Moderate	31.8842
Signal 9	Moderate	22.5949
Signal 10	Moderate	10.4002
Signal 11	Moderate	17.8822
Signal 12	Severe	32.0659
Signal 13	Severe	44.7490
Signal 14	Severe	28.1976
Signal 15	Severe	43.7006
Signal 16	Severe	57.3391
Signal 17	Severe	47.1416
Signal 18	Severe	39.0744
Signal 19	Severe	40.0491
Signal 20	Severe	46.3008
Signal 21	Severe	49.3766
Signal 22	Severe	48.5661
Signal 23	Severe	50.7686

The high pressure gradient needed to propel the blood forward from the left atrium to the left ventricular in mitral stenosis or the augmentation of the left ventricular outflow and afterload due to the aortic valve dysfunctions in aortic stenosis [15] affects the PCG signals' intensity, complexity, irregularity, and unpredictability characteristics. Later, reflected in the entropy values extracted from these signals' frequency spectrum. Hence, the ascending variation obtained for the spectral entropy in the 23rd studied severity cases.

VI.3. Accuracy testing using machine-learning classifiers

As a last step for this chapter and after studying the FFT–STFT features ability to discriminate between group 1-3 and the different cardiac severity levels, we must check the accuracy of these results by using machine-learning classifiers like the K-Nearest Neighbor (KNN) and the One-vs-All Support Vector Machine (OVA-SVM).

VI.3.1. K-nearest neighbor (KNN)

This method is a nonparametric intuitive approach based on distance measurements. It states that patterns of the same class are close to each other in the feature space [4]. Therefore, the data class with the highest vote in nearest neighbors will be assigned to a query point, which results in a KNN classification. [33-35]

To use the KNN model we putted the number of epoch to 200, the learning rate to 1e-4, the neigbors number to 3, and chose the Euclidian distance.

VI.3.2. One-vs-All Support Vector Machine (OVA-SVM)

This machine learning classifier separates between different classes in a high dimensional feature space using hyper-planes (Figure II.8). Discriminating a set of linearly separable hyper-planes is possible when utilizing a Support Vector Machine, where hyper-planes must be placed in a way to maintain maximum distance from the both classes [36][37].

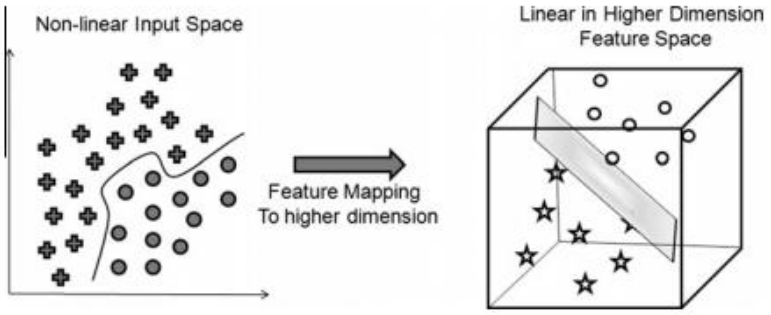

Figure II. 8 Illustrates the non-linear to linear transformation when using support vector machine SVM technique [38].

For multi-class problems, it is imperative to bring some modifications to the standard SVM algorithm. Generally, the one-versus-one method and one-versus-all method are the most common approaches to multiclass classification [39]. Where each class is studied separately in a binary way of classification, i.e. for an N-class classification, N binary SVM classifiers are required. In this chapter, we used a 3-class SVM binary classifiers following the one-versus-all approach.[40]

VI.3.3. Group discrimination

Through this classification, we will check the ability of the features to rank the phonocardiogram signals of the database into group1, 2, and 3 previously sorted according to MSD manuals, Andrew JANG and the Energetic Ratio.

Figures II.9-12 illustrates graphically the performance of the features when employing the OVA-SVM.

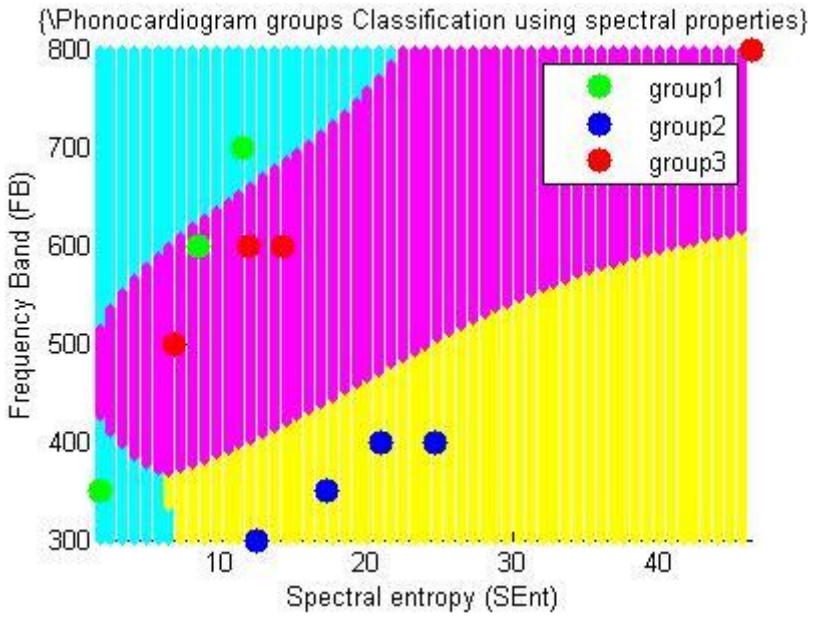

Figure II. 9 OVA-SVM classification results of group1-3 when implementing the frequency band (FB) and the spectral entropy (SEnt).

We can notice through the figure that one PCG signal of group 1 is classified in group 3. The mistaken signal is the innocent murmur (IM), which was previously discriminated as a pathological signal by the FFT and STFT features, but maintained a similar variation to that of group 1 (i.e. an FB and SEnt values that goes with the severity ascending evolution of the group 1) . Hence, for a machine learning algorithm, this similar variation is not enough for the (IM) to be classified into group 1.

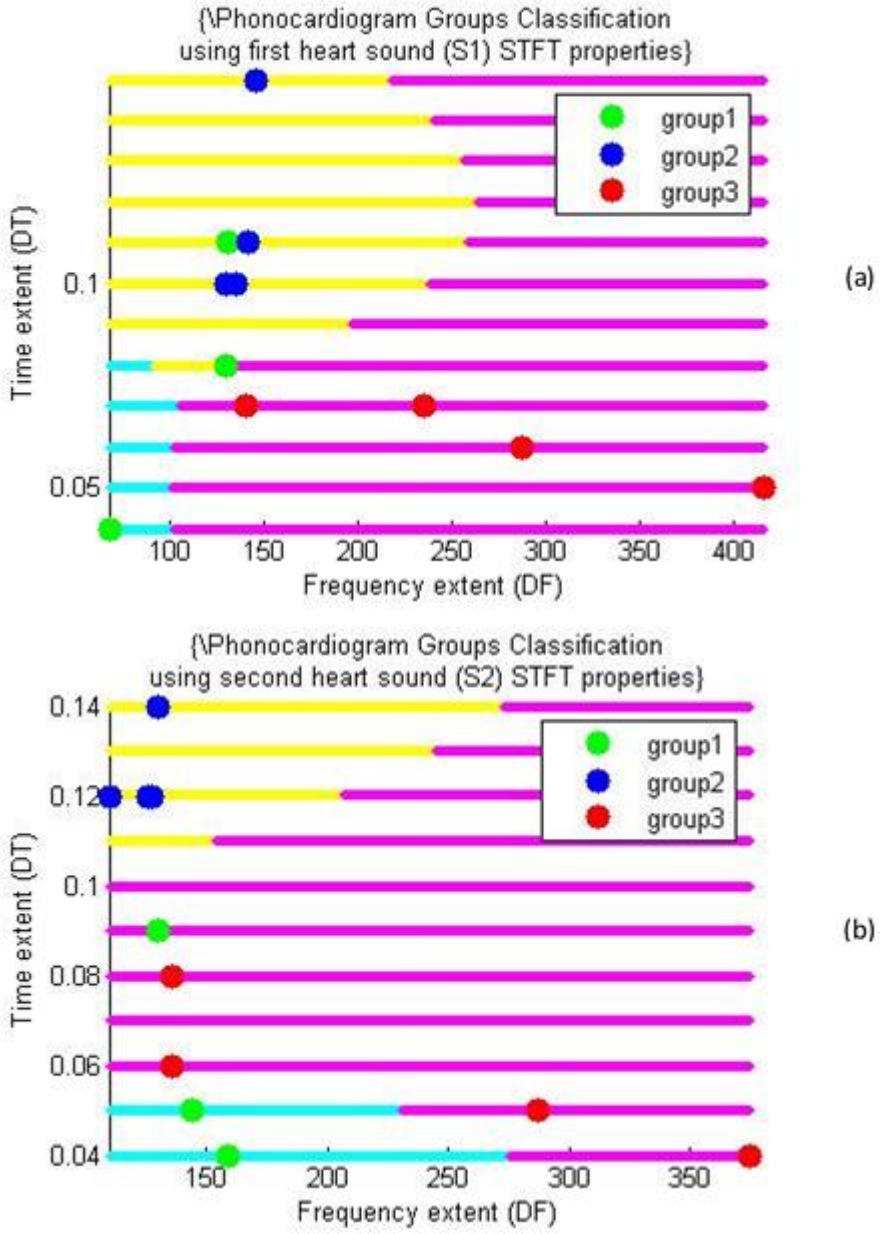

Figure II. 10 OVA-SVM classification results of group1-3 when implementing the STFT properties of (a) S1 or (b) S2 only.

As noticed in Figure II.10 (a) the OVA-SVM classified the IM and the Coa as pathological signals when using the first heart sound STFT features. However, the innocent murmur (IM) is correctly classified in figure II.10 (b) with the second heart sound STFT features.

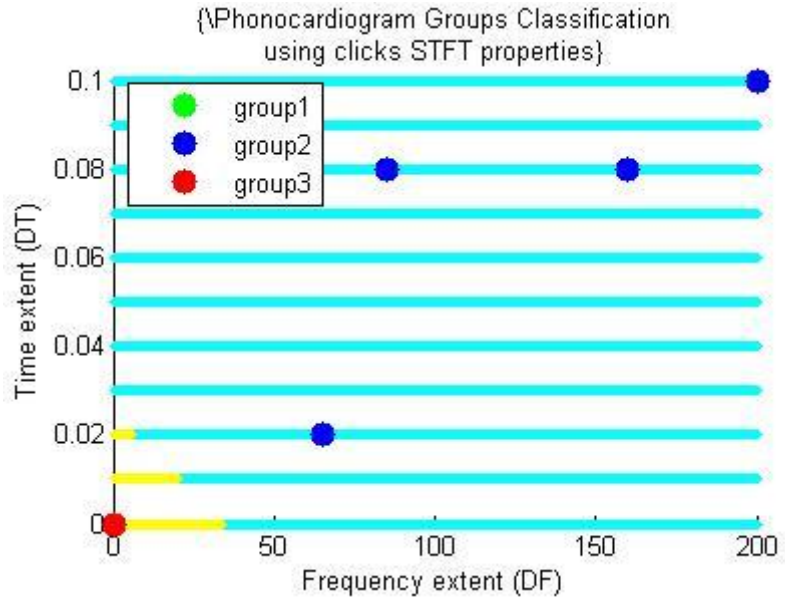

Figure II. 11 OVA-SVM classification results of group1-3 when implementing the STFT properties of the click only.

Group 2 of phonocardiogram signals contain pathologies with clicks as added sound, the remaining groups don't suffer from it. Therefore, when we studied the classification of these pathologies by using the STFT features extracted from the click, we obtained an accuracy of 100% since it is a binary classification, as you can see in figure II.11. The same observation is made when studying the classification of these pathologies by using the STFT features extracted from the murmur (figure II.12).

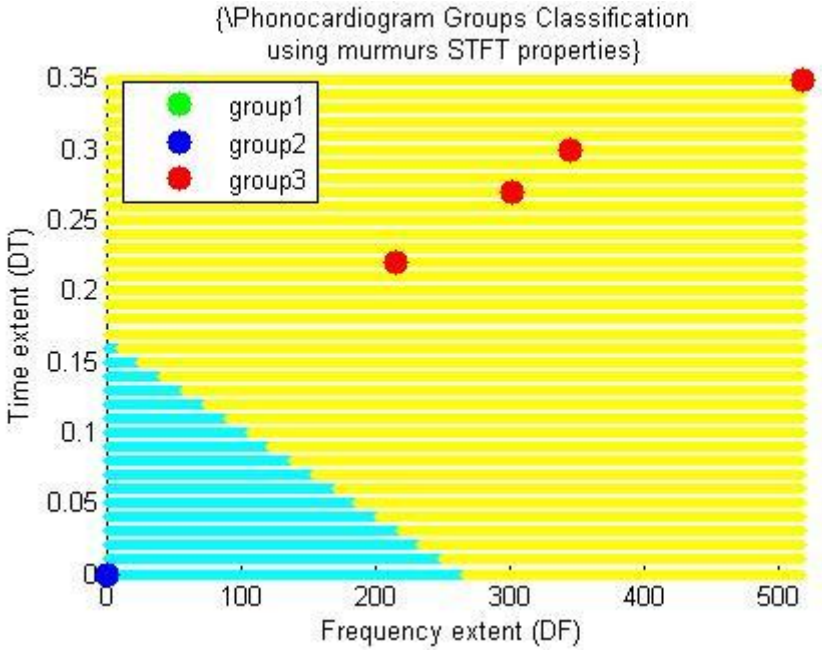

Figure II. 12 OVA-SVM classification results of group1-3 when implementing the STFT features extracted from the murmur.

Unlike the OVA-SVM classifier and even though the FFT and STFT features identified the IM and the Coa as pathological signals with similar values variation to that of group 1, the KNN correctly classified the three signals in group 1. An accuracy of 98.7% is then achieved when combining spectral and spectro-temporal features (FB, SEnt, ΔF, and ΔT) to rank the databases' signals in their respective groups (table of results present in appendix 1).

VI.3.4. Cardiac severity assessment

This part will test the ability of the extracted parameters to rank the fourth group of signals into three severity classes (light, moderate, and severe).

In order to rank our signals into the three severity classes (light, moderate, severe), we referred yet another time to the MSD manuals, Andrew JANG and the Energetic Ratio. The MSD manuals and Andrew JANG enlisted the different elements that may be present in the phonocardiogram recording at different severity levels. We used the energetic ratio to confirm our ranking or for the signals that were difficult to classify in one of the three classes.

Figures II.13-16 illustrate the efficiency of the features for the cardiac severity classification.

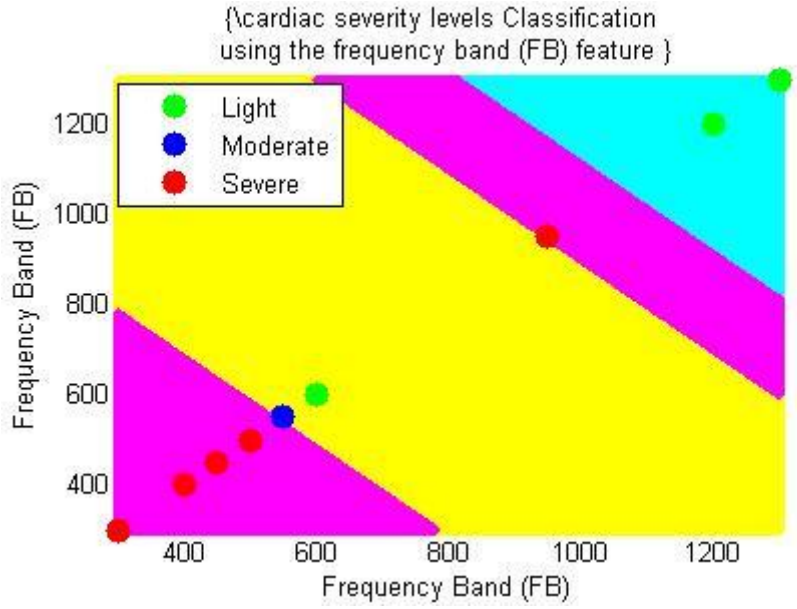

Figure II. 13 OVA-SVM severity classification results of the phonocardiogram signals present in the three groups using the frequency band (FB) feature.

This linear classification may appear incorrect or misleading; however, it is almost 100% correct. Four out of five severe signals, two out of three moderate signals and two out of three of light severity signals are correctly classified in their regions. We have two superposition and only one incorrect classification. The blue circle close to 1000Hz ranked as a severe signal is positioned in between the moderate and the severe region due to the similar variation between the two when the severity level is close to the next level. This same blue

circle is superposed to a moderate signal since both of them present close severity levels. Two other moderate signals are superposed and displayed as one green circle close to 600Hz. Lastly, one signal of light severity is falsely classified as a moderate signal since it present a variation that is close to the moderate severity.

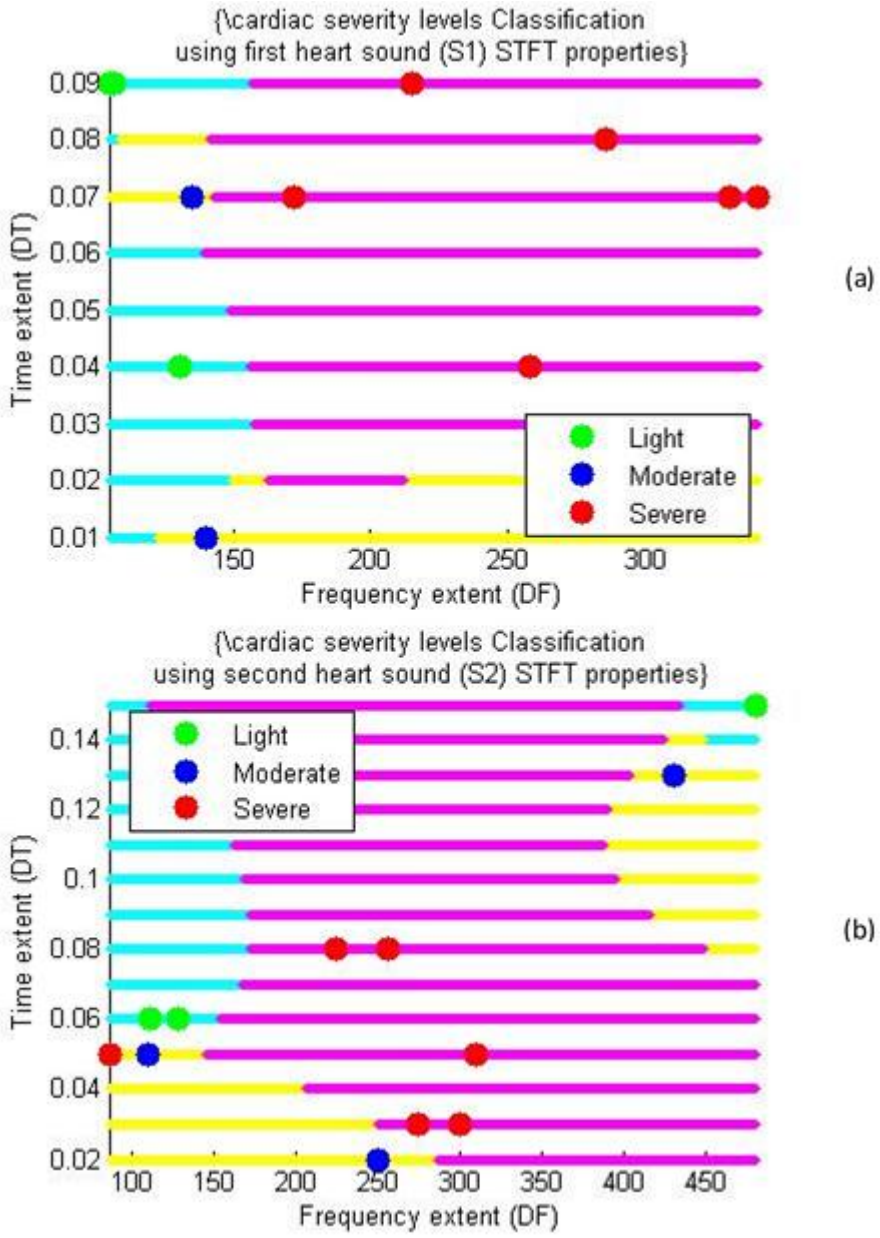

Figure II. 14 OVA-SVM severity classification results of the phonocardiogram signals present in the three groups using STFT properties of (a) S1 or (b) S2.

One can notice through Figure II.14 that the majority of the signals are correctly classified according to their severity level when using S1 or S2 STFT features. However, two PCG signals, one of moderate severity in Figure 14-(a) and another one of severe level in Figure 14-(b), are falsely classified due to their closeness with the next or previous severity level.

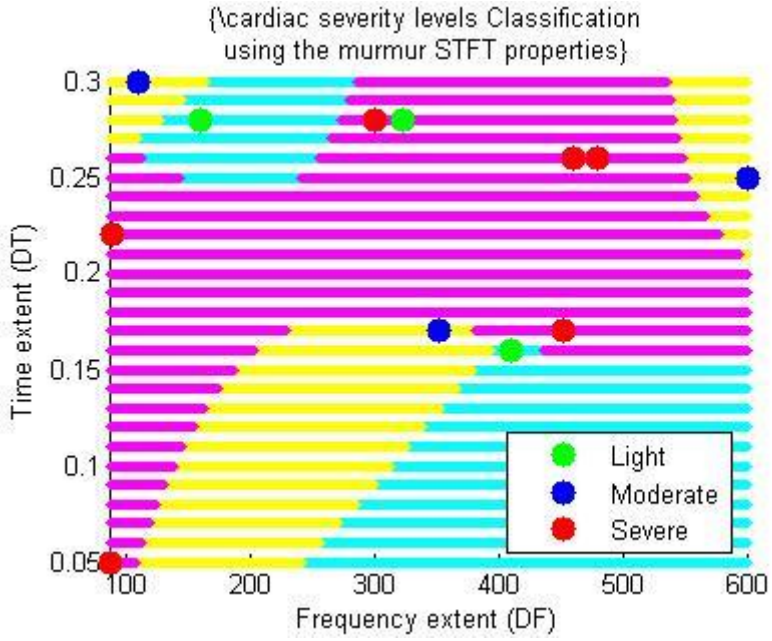

Figure II. 15 OVA-SVM severity classification results of the phonocardiogram signals present in the three groups using STFT properties of the murmur.

The STFT features extracted from the murmur correctly classified the majority of the PCG signals according to their severity level.

After classifying the fourth group of signals into three main classes using only the Frequency Band and STFT features, we obtained an accuracy of 98.9%, slightly higher than the one obtained for the three groups classification.

Since the spectral entropy presented great discriminative results, we tested its ability to follow the cardiac severity separately from the rest. Instead of studying the three pathologies with a limited number of severity levels we studied only two (Mitral and Aortic Stenosis) but with different cardiac severity levels. We implemented the Energetic ratio values along with the Spectral entropy since both features are related to the signals intensity and to not affect the spectral entropy values with an incompatible feature.

Figure II.16 illustrates the obtained OVA-SVM classification results when studying the severity through the spectral entropy feature.

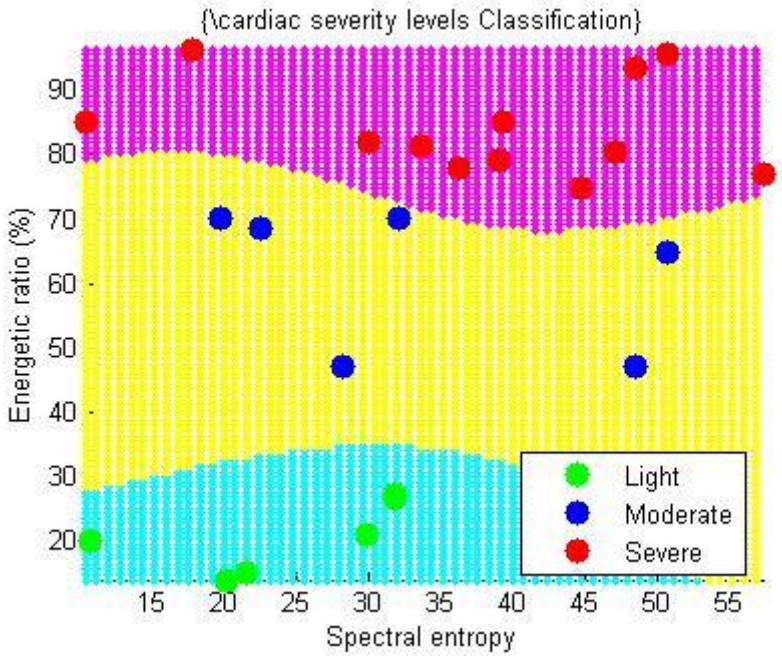

Figure II. 16 OVA-SVM classification results when studying the severity through the spectral entropy feature.

The twenty-three signals were correctly classified in their respective severity levels when using a combination of Energetic ratio and Spectral entropy.

An accuracy of 98.3% is achieved when studying different severity levels from the mitral and the aortic stenosis using the spectral entropy, a bit lower result than the one obtained when classifying the fourth group signals. Yet, it remains completely coherent since we studied a greater number of severity cases then the ones in Table 5 in [30] for this part of this chapter. Additionally, we should highlight the difficulty of the features to discriminate between the signals with close severity levels. It is likely that this difficulty negatively affected the accuracy result and prevented us from exceeding the 99% of accuracy.

Hence, the classification using either the KNN classifier or the OVA-SVM proved the ability of these two techniques (FFT and STFT) to classify phonocardiogram signals in healthy/clicks/murmurs classes and discriminate between the three cardiac severity levels.

VII. Conclusion

In this chapter, we tested the efficiency of the FFT and STFT to accomplish two main goals, namely the classification and discrimination of the three pre-mentioned groups and the identification of the cardiac severity level within the same pathology (aortic stenosis, mitral stenosis, and mitral regurgitation).

We employed two accuracy-checking approaches (One-vs-All Support Vector Machine and K-Nearest Neighbours classifier) to check the accuracy of our features (Frequency band, Spectral entropy, Time extent, Frequency extent) and appreciate the reliability of these two analysis techniques. An accuracy of 98.7% is scored in terms of the three main groups' discrimination and classification

These features also displayed an important accuracy of 98.9% and 98.3% for severity level identification and classification, which means that the majority of the database signals were successfully classified into three cardiac severity classes (light, moderate, and severe).

Through these results, we paved the way towards using basic, yet effective, techniques to assist clinicians in critical decision-making whether for cardiac pathologies discrimination and identification or severity level classification.

Chapter. III

CHAPTER III: Cardiac severity study using the Discrete Wavelet Transform (DWT)

I. Introduction

The Time-frequency analysis techniques, as mentioned in previous research, are suitable tools for biomedical signal processing. Their ability to compromise between time and frequency resolution helps them analyse the signals with good precision. The Wavelet Transform (WT) is one of the well-known time-frequency techniques; it was born from the convergence of already old theoretical works, in particular those of Haar (1910), Littlewood & Paley (1930), Zygmund (1930), Gabor (1940), then around 1960 by Calderon. Morlet was the first to propose the name wavelets in 1982 for the digital processing of particular signals or the development of mathematical tools used in theoretical physics by Grossmann (1983). Since then, several researchers have contributed solid mathematical foundations, introducing the notion of orthogonal basis (Meyer, 1985), multi-resolution analysis (Mallat, 1989), and compact wavelets (Daubechies, 1988) [1]. The WT gained popularity for its multiple applications, such as communication, signal processing, video and image compression, scientific visualization, and medical imaging.

We mentioned here some of the previous works that employed the WT in their research. Namely, V. Nivita et al. presented a noise-robust method for the detection and classification of heart murmurs using stationary wavelet transform (SWT) and Hilbert phase envelope, where it allowed the identification of the four heart sounds and heart murmur sub-bands [2]. Additionally, Cherif. L et al. The authors employed the PWT tree to separate between the pathological severities for different heart sound signals [3]. H. Li et al. followed and discriminated between diastolic murmurs in coronary heart disease and valvular disease by analysing their PCG database with the Empirical Wavelet Transform (EWT), where they stated that the essential difference between diastolic murmurs in valvular disease and coronary heart disease is the third mode's spectrum. Therefore, a feature using the spectral energy of the third diastolic modal spectrum was employed to directly distinguish diastolic murmurs in coronary heart disease and valvular disease [4]. Later on, P. Dhar et al. utilized the Cross-wavelet spectrum image as an input for a CNN (AlexNet) to classify PCG signals in healthy or pathologic classes by detecting abnormal heart sounds directly from the spectrum image without any manually selected feature [5].

On the other hand, the Discrete Wavelet Transform (DWT) is one of the many analyses provided by the Wavelet Transform (WT), the DWT proved it efficiency in many ways. For example, S.M. Debbal and F.

Bereksi-Reguig applied a wide range of orthogonal and bi-orthogonal wavelets over healthy phonocardiogram (PCG) signals. They concluded that the 7th level of the DAUBECHIES wavelet (db7) is the best option for PCG signal analysis since it delivers the lowest reconstruction error. Later, they proceeded with different PCG signals analyses at various severity levels and stated that the reconstruction error is a significant feature for cardiac pathologies discrimination and classification and the cardiac severity analysis [7].

Additionally, Meziani et al, could segment the different elements of a pathologic PCG signal (S1, S2, Murmur) using a DWT-based algorithm [8]. Followed by A. Hussain et. al. who analysed PCG signals and extract three discriminative features, the mean value, variance, and energy of DWT. The results proved that all of these features could differentiate between healthy/unhealthy phonocardiogram recordings [9]. Finally, yet importantly, Z. Hossein-Nejad and M. Nesri combined the Discrete Wavelet Transform (DWT) and group-based sparse features to distinguish the main and abnormal heart sounds of a PCG recording [10].

In this chapter, we will focus on studying the cardiac severity using the DWT features. First, we will start by testing three features over two distinct groups of cardiac pathologies:

- Pathologies with clicks (Minor murmurs).
- Pathologies with significant murmurs.

Second, due to the first feature testing and the satisfying performances of a specific feature in Chapter I, we will investigate the performances of a particular time-frequency parameter more deeply. Reference features and accuracy testing algorithms such as the (ER) and the (OVA-SVM) will be employed for this chapter's purposes.

II. The discrete wavelet transform

On the one hand, the continuous wavelet transform is characterised by redundancy [8] since it consists of determining the correlation between continuous scale functions that were continuously shifted over a signal that makes the obtained wavelet coefficients highly redundant because these scaled functions are near an orthonormal basis [11]. Conversely, we can reduce this redundancy by replacing the continuous wavelet family with a discrete one since they are not continuously scalable and translatable. Still, they can only be scaled and translated in discrete steps. Therefore, we will switch regular coefficients with discrete coefficients (time and scale) and the integrals with discrete sums, which will give us the discrete wavelet transform equation (the sampled version of the continuous wavelet transform):

$$C_s(2^{-j}, k2^{-j}) = 2^{j/2} \sum s(n)\psi(2^j n - k) \qquad \text{(III.1)}$$

The DWT analyses the input signal at different scales by passing it through a set of filters with different cut-off frequencies [6]. The high-pass filters extract the high frequencies, known as the 'approximations', and the low-pass filters extract the low frequencies, known as the 'details' [12] (Figure III.1). In our case, the approximations are our filtered signal and the details the filtered noises from the input PCG signal after decomposition. We can then define the DWT as a process of filtering the analysed signal by a band-pass filter of variable bandwidth.

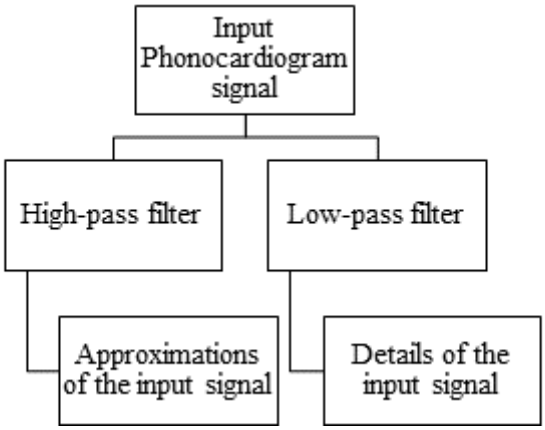

Figure III. 1 Approximations and details representation of a Discrete Wavelet Transform.

Figure III.2. (a) Displays the DWT functioning principle. The phonocardiogram signal is decomposed in width varying filter banks where the decomposition level defines the width of these band-pass filter banks (Figure III.2. (b)).

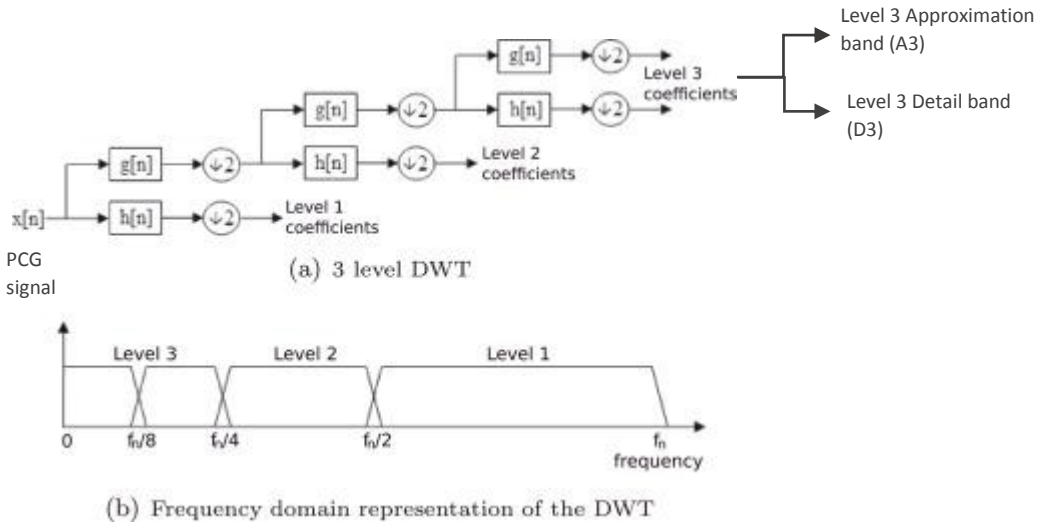

Figure III. 2 The principle of Discrete Wavelet Transform: (a) DWT decomposition tree of the phonocardiogram signal, (b) Frequency domain representation of the DWT (Filter Banks) [13-14].

Known through its ability to compensate for missed coefficients in the final decomposition paradigm [11] and the shape similarities with the heart sounds. The seventh level of the DAUBECHIES wavelet (db7) is one of the robust mother wavelets in the analysis of linear time-varying biomedical signals and the one we used for this chapter. A sampling frequency of 8 kHz was sufficient and very recommended by previous researchers for PCG signal processing and filtering. The DAUBECHIES scaling function (φ_3^D) is defined as the following [11]:

$$\varphi_3^D = \sum_{k=0}^{3} p_k \varphi(2t-k) \qquad \text{(III.2)}$$

III. Parameters study and analysis

When talking about the DWT features, a significant number of features can be discussed, for example, the approximation-signal ratio, correlation coefficient, the DWT variance, mean, standard deviation, and others. However, in this chapter, we decided to study only three distinct features extracted from the same origin namely:

- The reconstruction error (Ɛermoy).
- The mean of detail coefficients (Md).
- The entropy of approximation coefficients (EAC).

III.1. The reconstruction error parameter

$$\varepsilon_{ermoy} = \frac{\sum_{i=1}^{N} |S_0(i) - S_r(i)|}{N} \qquad \text{(III.3)}$$

With: N: equals Samples number, So: is the Original signal, and Sr: the Synthesis signal: the approximation signal. [15]

III.2. The entropy of approximation coefficients

In our framework, entropy defines a measure of information quantity contained in the murmur and click segments [1]. It also defines the complexity, irregularity, and unpredictability characteristics present in the phonocardiogram signal.

$$E[X] = -\int P(X) Log\, P(X) d(X) \qquad \text{(III.4)}$$

Where: X represents the approximation signal; P(X) is a probability density.

III.3. The mean of detail coefficients

We calculate the mean of detail coefficients from the sixth level of details (d6) for the two groups of the studied PCG signals.

$$Md = \frac{\sum_1^N d_j}{N} \qquad \text{(III.5)}$$

With dj Detail coefficient among N of level "j".

All of these features are extracted from the 6th level of DWT decomposition (Approximations 6 and Details 6) due to the minimal reconstruction error of the original signal presented by A6. Both EAC and MD are calculated for murmurs and clicks only, while the reconstruction error is for one PCG cycle.

IV. Results and Discussion

In this section, we will discuss the results of the cardiac severity study using the DWT features:

- Click/ Murmur discrimination
- Cardiac severity assessment

We started this study by testing three features over two distinct groups of cardiac pathologies:

- Pathologies with clicks (Minor murmurs).
- Pathologies with significant murmurs.

The purpose of studying these three features is to test their ability to discriminate between pathologies with click and murmur and identify each pathology as a separate severity level. These results will help us confirm that the 6th level of decomposition is optimal for extracting features since it presents minimal reconstruction error and relevant severity information reflected through extracted features. The features presented above were extracted before the resampling of the PCG signals at 8 kHz, yet they gave satisfactory results for pathological severity tracking and discriminating. The Energetic Ratio (ER) is used here to evaluate the three features evolution (See Appendix 3).

IV.1. Three DWT-features efficiency testing

First, we used Table III.1 information to segment manually the clicks and murmurs of the PCG recordings. We then analysed the segments with the (DWT), extracted the three features and compared it to the (ER) results. Table III.1 lists all the PCG signals studied in this chapter.

Table III. 1 Some of the MSD manuals and other references information used for cardiac severity ranking [16][13, 17-22].

PCG signals	**Click / Murmur characteristics**			
	Frequency Range	Duration / location in the cardiac cycle	Configuration	Timber
Group 1				
Early Aortic Stenosis (EAS)	100-800Hz (High pitch)	≈10-20ms, early-systolic	/	Dry
Ejection Click (EC)		early-systolic	/	Sharp
Late Systole (LS)		Late-systolic	/	/
Opening Snap (OS)		Early-diastolic	/	Sharp
Atrial Gallop (AG)	15-50Hz (Low pitch, very low frequency, short and faint)	≈0.08-0.20s just before S1	/	Galloping rhythm, lilt or canter quality
Ventricular Gallop (VG)		≈0.15s after S2, early-diastolic	/	
Group 2				
Aortic Stenosis (AS)	Up to 600Hz (Medium to low pitch)	Mid-, late-, holo-systolic	Crescendo–decrescendo	Harsh, rasping, grunting or rough

Aortic Regurgitation (AR) / **Diastolic Aortic Insufficiency (DAI)**	Up to 600Hz (High or low pitch)	Early-diastolic	Decrescendo	Blowing
Systolic Pulmonary Stenosis (PS2)	Up to 600Hz (High pitch)	Holo-systolic	Crescendo–decrescendo	Harsh
Mitral Regurgitation (MR)		Early, Mid-, late-, holo-systolic	Decrescendo	Blowing
Diastolic Atrial Septal Defect (DASD)	Up to 600Hz (High or low pitch)	Early-diastolic	Crescendo	Rumbling

It is recommended to always test the reconstruction error when selecting which wavelet type is perfect for the PCG database and it is also known that the one with the least reconstruction error value is the optimal one for your signals. Therefore, when going through this process we noticed that the reconstruction error is proportionally correlated to the cardiac severity and can follow the evolution of the energetic ratio parameter (ER) from the least to the most severe case, which adds this feature to the list of valuable parameters for pathological severity tracking (Figure III. 3-5 and Table III.2).

Table III. 2 displays the extracted features from the discrete wavelet transform (DWT) analysis on phonocardiogram signals [23].

PCG Signals	**Extracted features**			
	Energetic Ratio (ER)	***Reconstruction Error (Ɛermoy)***	***Entropy of approximation coefficients (EAC)***	***Mean of details (MD)***

PCG signals with minor murmurs (CLICKS)				
EAS	0.02	6.07e-07	5.48e-05	4.09e-04
AG	0.03	3.32e-06	4.93e-05	4.98e-05
EC	0.04	4.67e-06	7.13e-06	3.61e-05
LS	0.05	7.77e-06	9.51e-07	2.37e-05
OS	0.10	7.08e-05	5.26e-08	2.29e-05
PCG signals with significant murmurs				
Systolic murmurs				
PS	0.05	2.06e-07	4.45e+04	2.91e-05
MR	0.10	2.43e-06	1.19e+05	4.44e-05
AS	0.73	5.91e-06	1.23e+05	5.25e-05
Diastolic murmurs				
AR	0.38	2.44e-06	2.07e+05	1.11e-04
DASD	0.70	5.19e-06	1.75e+04	1.74e-05
DAI	0.84	8.24e-06	1.58e+04	1.60e-05

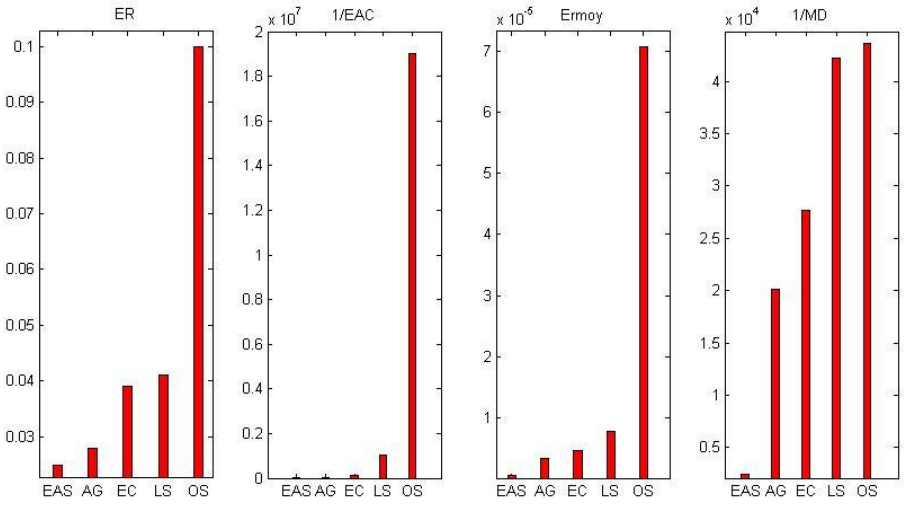

Figure III. 3 histogram representation of the three studied features for Click PCG signals– (ER) Energetic Ratio, (ECA)1/ Entropy of Approximation Coefficients, (Ermoy) Reconstruction Error, (MD) 1/Mean Variance of Details [24].

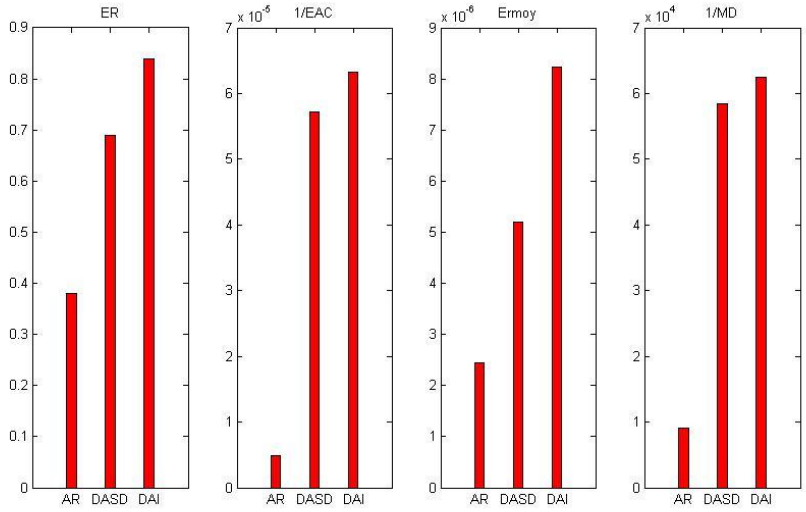

Figure III. 4 histogram representation of the three studied features for diastolic murmur PCG signals– (ER) Energetic Ratio, (ECA) 1/Entropy of Approximation Coefficients, (Ermoy) Reconstruction Error, (MD) 1/Mean Variance of Details [23].

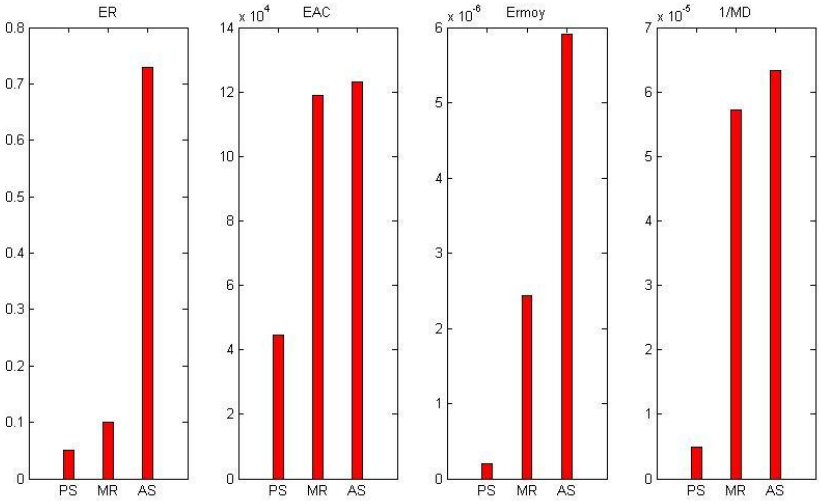

Figure III. 5 histogram representation of the three studied features for systolic murmur PCG signals– (ER) Energetic Ratio, (ECA) Entropy of Approximation Coefficients, (Ermoy) Reconstruction Error, (MD)1/ Mean Variance of Details [23].

The entropy of approximation coefficients (EAC) as listed in Table III.2 displayed an inverse correlation to the energetic ratio (ER) yet it discriminated between PCG signals with clicks and those with murmurs. While Figure III.3 illustrates this inverse correlation of the EAC when studying the pathologies with clicks, Figure III.4-5 shows the impact of the murmur's complexity on the pathology's severity due to the difference in quantity of information between the murmur and click. In addition, the boxplot in Figure III.6 displays the variation range of the EAC between these two added sounds, where we can clearly differentiate the clicks from the murmurs.

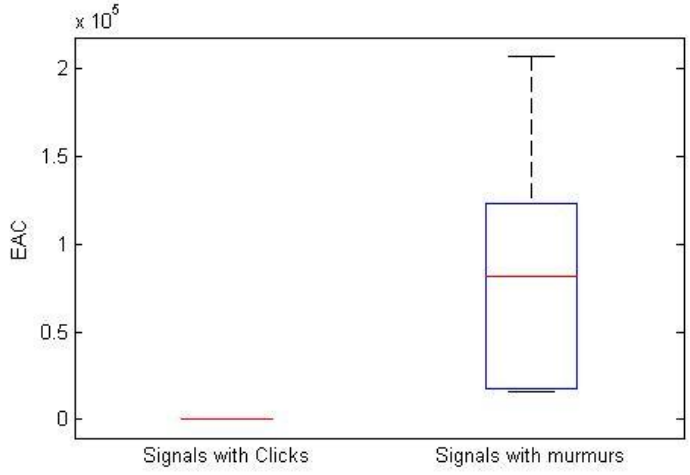

Figure III. 6 Boxplot representation of the EAC evolution for PCG signals with clicks and murmurs [23].

After a DWT decomposition and signal reconstruction, some valuable information remains in the detailed subbands. Therefore, to quantify it, we extracted the mean of details (MD) as a feature from these bands. Hence, we choose the sixth level of details (d6) that corresponds to the sixth level of approximation (a6) to calculate MD. This feature displayed a minimal variation compared to the EAC, which refers to the minimum amounts of valuable information remaining in the detail bands after a DWT analysis. Still, these minimum amounts of information follow the evolution of the cardiac severity for both clicks and murmurs (Figure III.3-5 and Table III.2).

Lastly, the three features displayed good performances for click/ murmur discrimination and cardiac severity assessment, where each pathology was identified as a separate severity level. However, out of these three features, the Entropy of Approximation Coefficients (EAC) had the best performance. Therefore, as a result of this first features testing part and the satisfying performances of the spectral entropy in Chapter I, we have decided to investigate the performances of the time-frequency entropy (EAC) more deeply through click/ murmur discrimination and cardiac severity assessment within the same pathology.

IV.2. The Entropy of Approximation Coefficients (EAC) efficiency testing

To highlight the importance of the EAC in differentiating between the pathological cardiac severities levels, we studied the PCG signals of Table III.3 in two ways:

Table III. 3 List of the PCG signals studied in the EAC efficiency testing.

Phonocardiogram signals	**Name Abbreviation**
Group 1	
EAS	Early Aortic Stenosis
EC	Ejection Click
LS	Late Systole
OS	Open Snap
AG	Atrial Gallop
VG	Ventricular Gallop
Group 2	
AS1/AS2/AS3/AS4	Aortic Stenosis
AR1/AR2/AR3/AR4	Aortic Regurgitation

First, we extracted the (EAC) from the click, and murmur segments, then compared it to the (ER) results for these two purposes:

- Click/ Murmur discrimination
- Cardiac severity assessment

Second, we processed one PCG cycle which allowed us to highlight the presence of severity information in the two heart sounds (S1+S2) and always for:

- Click/ Murmur discrimination
- Cardiac severity assessment

We choose the ER as a reference feature since the energy / intensity of the signal is one of the features related to the severity evolution. We adopted the sampling frequency of 8 kHz for this part of the chapter.

Lastly, to test the accuracy and efficiency of the Entropy of Approximation Coefficients (EAC) for click/ murmur discrimination and severity assessment, we introduced the obtained values from the two study ways into a One-vs-All Support Vector Machine (OVA-SVM) classifier (See Appendix 4-5).

IV.2.1. Click/ Murmur discrimination

The entropy of approximation coefficients (EAC) proved its ability to identify each studied pathology with minor murmurs (click) as a separate cardiac severity level by displaying a correlated evolution with the cardiac severity represented by the Energetic Ratio (ER). Figure III.8 illustrates the proportional correlation between the irregularity, complexity, unpredictability characteristics, and the intensity/ energy of the murmur/ click segments through the EAC and the ER for the six studied pathologies of group 1.

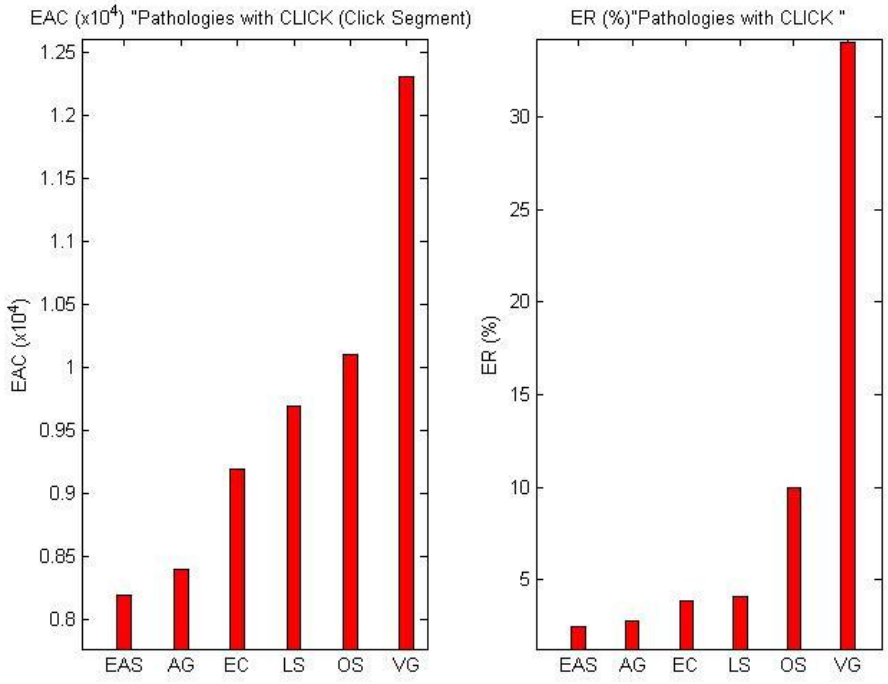

Figure III. 7 histograms of the DWT-EAC and the ER for click segments only: Click segment from : EAS, AG, EC, LS, OS, VG [24].

When boxploting the EAC values, three variation extents are identifiable. Each extent (boxplot) refers to a category. The first one presents a minimal variation compared to the second and third extent, since it represents the click pathologies while the two others express the murmur pathologies (Figure III.9). For more information and interpretation read [24] or appendix 4.

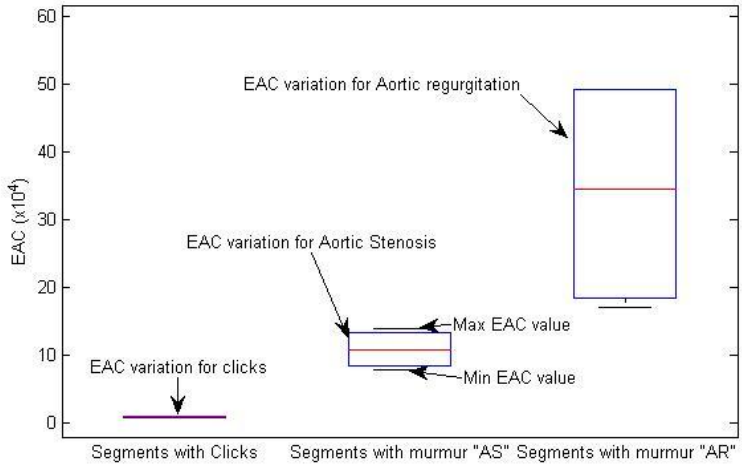

Figure III. 8 Boxplot representation of the EAC variation between the studied PCG signals [24].

Previous research on Phonocardiogram (PCG) signals stated that cardiac pathologies could affect heart sounds as well. Therefore, we processed one PCG cycle instead of CLICK or MURMUR segments. This allowed us to discriminate between the cycles with clicks from those with murmurs using the entropy of approximation coefficients values (Figure III.11).

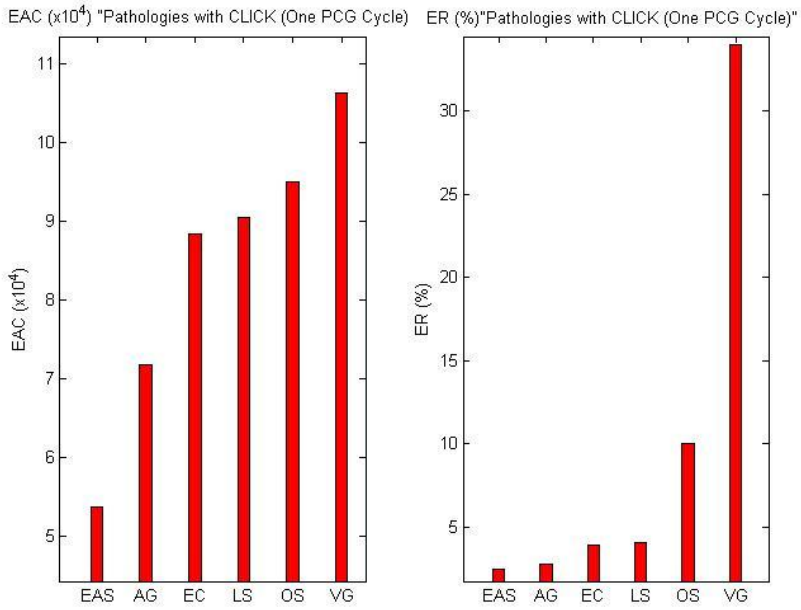

Figure III. 9 histograms of the DWT-EAC and the ER for one PCG cycle: PCG cycle from : EAS, AG, EC, LS, OS, VG [24].

IV.2.2. Cardiac severity assessment

This section presents the obtained results when testing the efficiency of the EAC in assessing the cardiac severity within the same pathology. We processed four signals, each with a different severity level, from the aortic regurgitation (AR1, AR2, AR3, and AR4) and the aortic stenosis (AS1, AS2, AS3, and AS4). After isolating the murmur segments, we applied the DWT algorithm and extracted the EAC.

The ascending evolution displayed by the EAC for the four cases of AS and AR reflects both the increase of the left ventricular outflow tract obstruction in the aortic stenosis [25] [26] and the increase of the stroke volume corresponding to the severity of the aortic regurgitation [25] (Figure III.12). In the other hand, the second and third extent in Figure III.9 illustrates the variation of the aortic stenosis and aortic regurgitation respectively between the least and the most severe case. Here, the aortic stenosis presents a more significant severity evolution rate than the aortic regurgitation, leading us to discriminate easily between these two cardiac pathologies using the entropy of approximation coefficients (EAC).

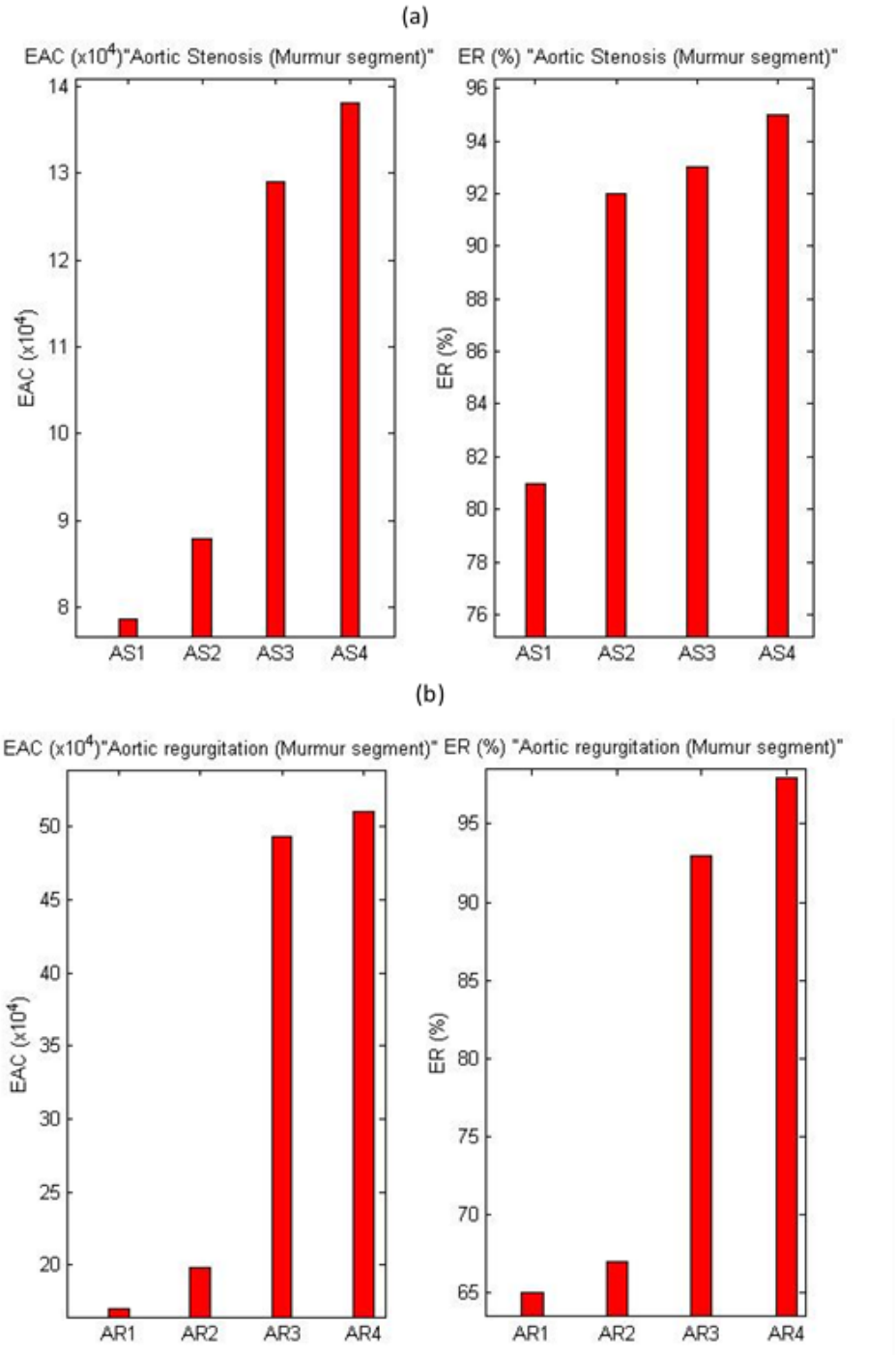

Figure III. 10 histograms of the DWT-EAC and the ER for murmur segment only : (a) Murmur segments from four AS cases; (b) Murmur segments from four AR cases [24].

Even after processing a complete PCG cycle, the EAC maintains a correlated evolution with the cardiac severity and the Energetic Ratio (ER), confirming that the probability of heart sounds retaining severity information evolving proportionally with the cardiac severity even within the same pathology [14]. Figures III.11 and 13 highlight this proportional evolution when studying the cardiac severity for groups 1 and 2.

Lastly, one can state through these results that adding heart sounds to the analysis algorithm will not negatively affect the EAC in the severity assessment.

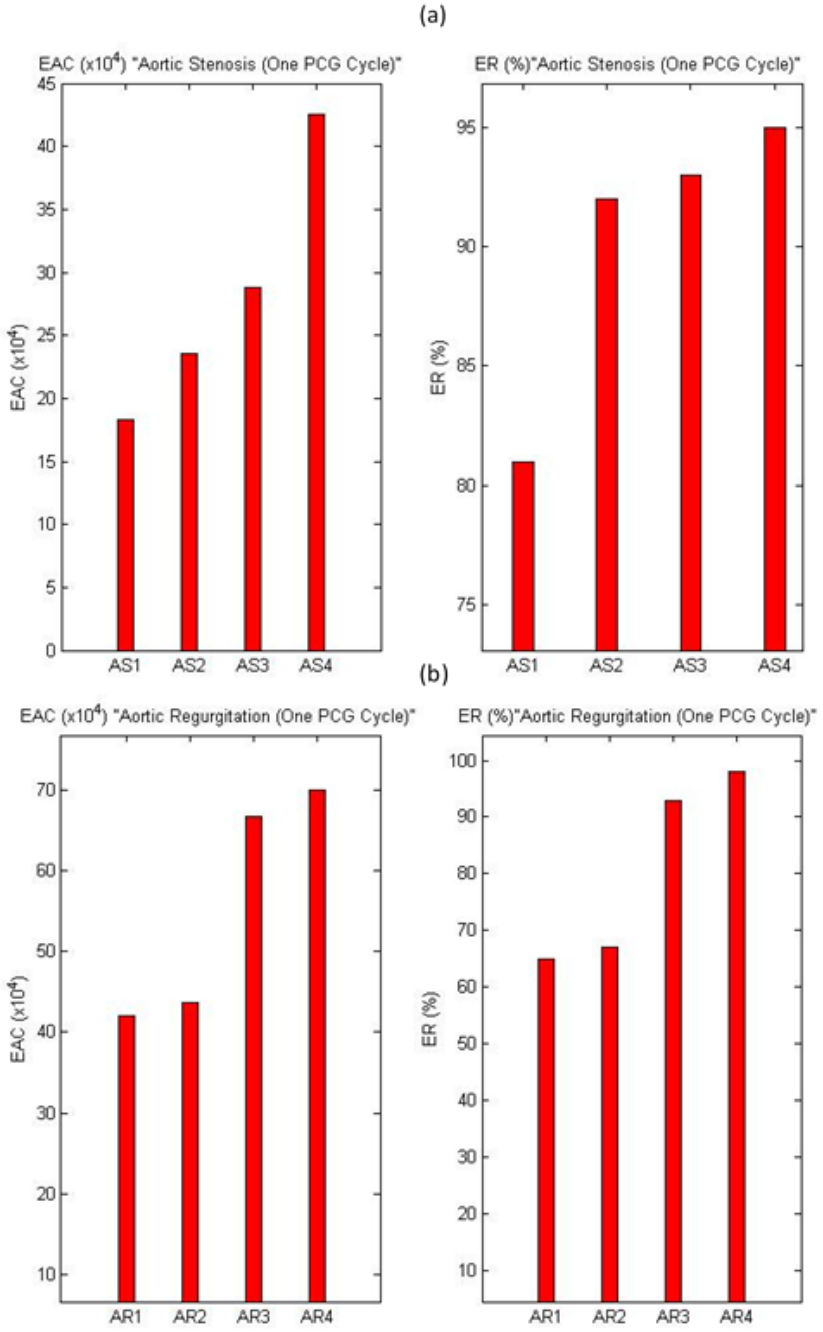

Figure III. 11 Histograms of the DWT-EAC and the ER for one PCG cycle: (a) PCG cycle from four AS cases; (c) PCG cycle from four AR cases [24].

IV.3. Additional observation

As mentioned above, we studied section III in two different ways, and after the comparison of the results, we noticed that the entropy (EAC) values when using a complete PCG cycle are superior to those when using added sound segments (Table II, Table III in Appendix 3). Therefore, to see if this augmentation in values is proportional to the pathological cardiac severity evolution, we calculated the difference between the two study ways for both groups 1 and 2, then plotted the results into a graph to appreciate its evolution (Figure III.14). Figure III.14 displays the proportional evolution obtained for the group 1 of PCG signals and the four Aortic Stenosis cases, which confirms again the probability of heart sounds retaining severity information that affects the cardiac cycle accordingly to the severity level evolution even within the same pathology. However, the inverse proportionality of the Aortic Regurgitation cases leads to a new probability that the heart sounds in some pathologies are not as affected by the pathology's severity evolution as in other cardiac diseases.

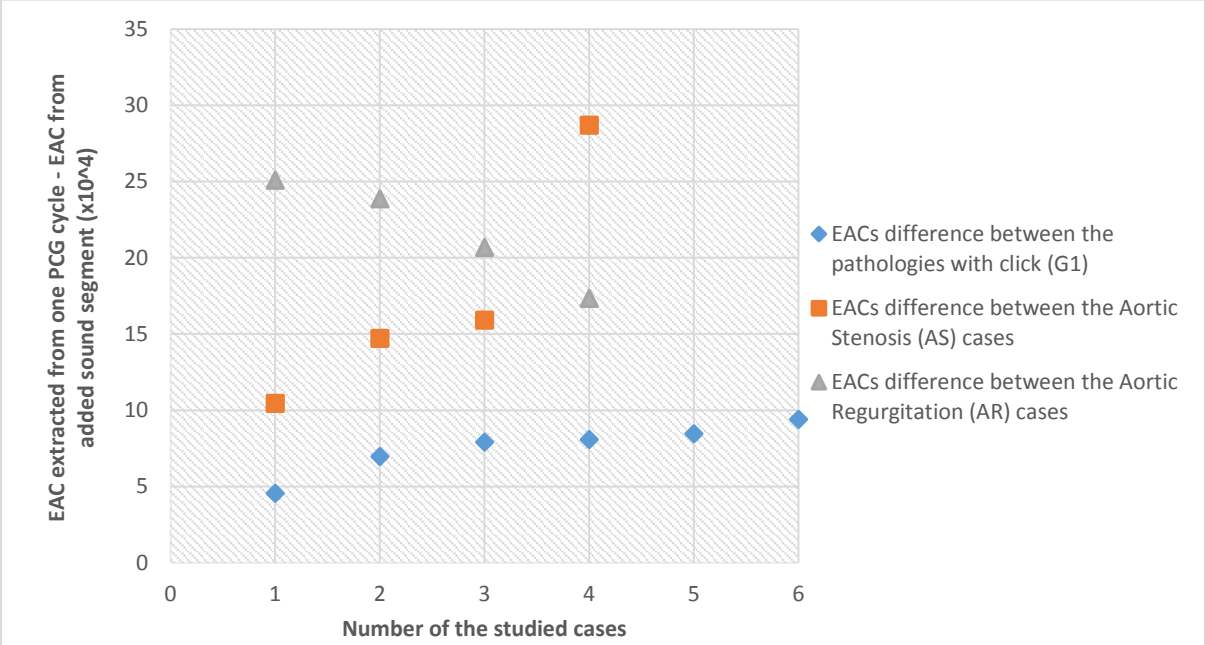

Figure III. 12 Displays the difference values (EAC extracted from one PCG cycle - EAC from added sound segment) for the group 1 and group 2 signals [15].

IV.4. Accuracy testing using machine-learning classifiers

In this chapter, we used the ER as a reference feature to compare our results to before introducing them into a One-vs-All Support Vector Machine classifier. Therefore, when going through this comparison process between the EAC results and the ER values, we noticed that the EAC displayed better results in discriminating and identifying the different severity levels of the studied cardiac pathologies when using the click and murmur segments and a complete PCG cycle (heart sound + added sound) (Figure III.3-13).

Relying only on the signal's Energy/ intensity when studying the cardiac severity may be misleading in some circumstances. Since, medical experts stated before that some cardiac pathologies tend to lose their murmur intensity at severe levels, like aortic stenosis that presents a short and soft murmur for extreme severity levels [26]. Thus, the necessity to use features like the Entropy of Approximation Coefficients (EAC) that quantify both the intensity and other characteristics of the studied signals makes it possible to establish a better discrimination between the severity levels than the energetic ratio ER. Therefore, it is logical to normalise the use of the EAC for severity level identification and assessment as a new approach to phonocardiogram severity analysis [14].

The entropy (EAC) in Figure III.15.(b) and 16.(b) not only discriminated between Aortic Stenosis and Regurgitation when the Energetic Ratio (ER) lacked precision and placed them together in high severities (Figure III.15.(a), Figure III.16.(a)) but also ranked them differently in terms of values importance compared to the ER. In addition, the aortic regurgitation displayed important EAC values compared to the aortic stenosis. This supports this chapter's theory that signal intensity is not the only element directly linked to cardiac severity, but by adding information such as the complexity, irregularity, and unpredictability characteristics of the signal, we can achieve better discrimination between cardiac pathologies whether by using click and murmur segments or one PCG cycle.

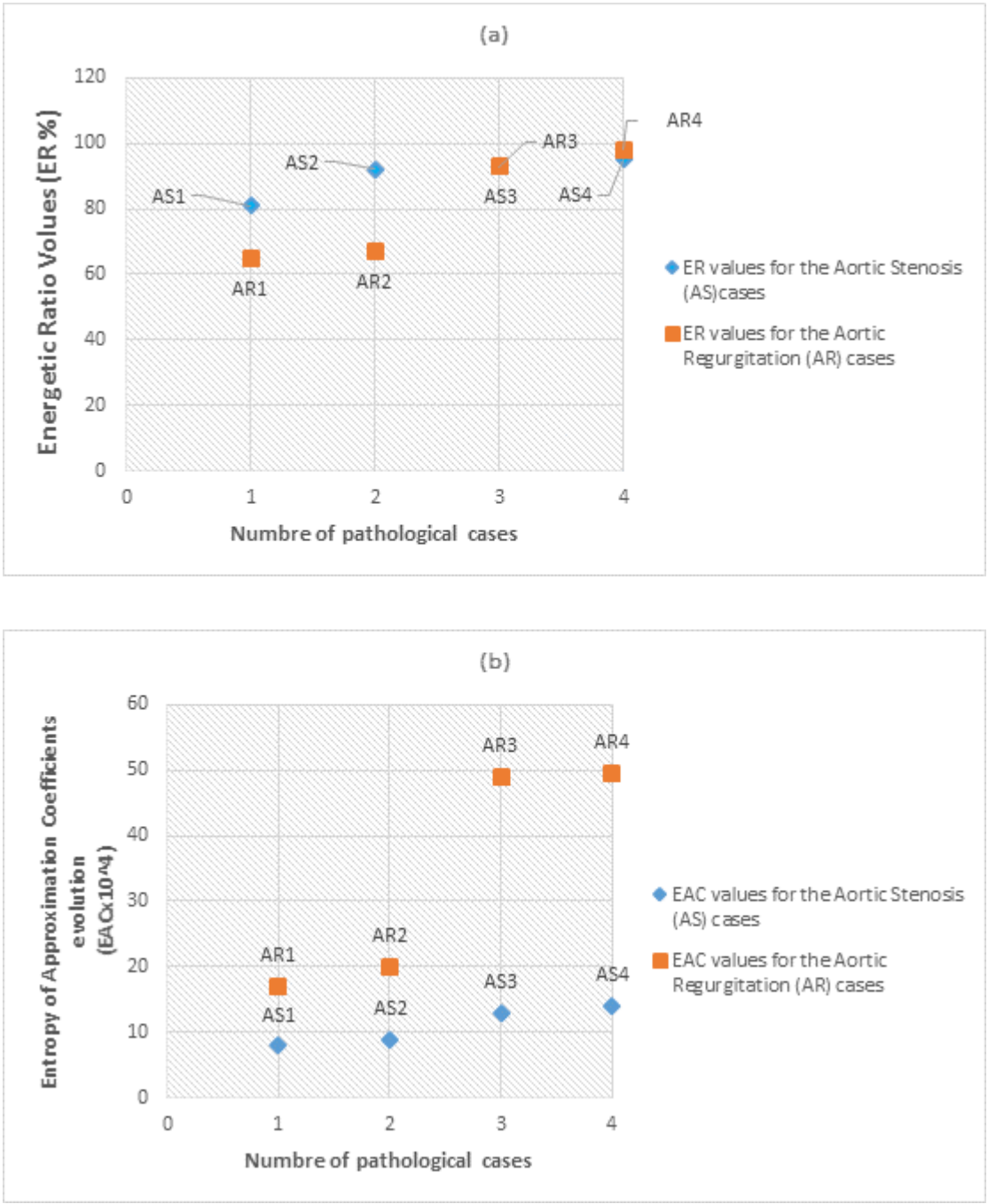

Figure III. 13 (a) Energetic Ratio (ER) evolution representation within the AS and the AR cases, (b) EAC (x10^4) evolution representation for the AS and the AR cases when using murmur segments only [14].

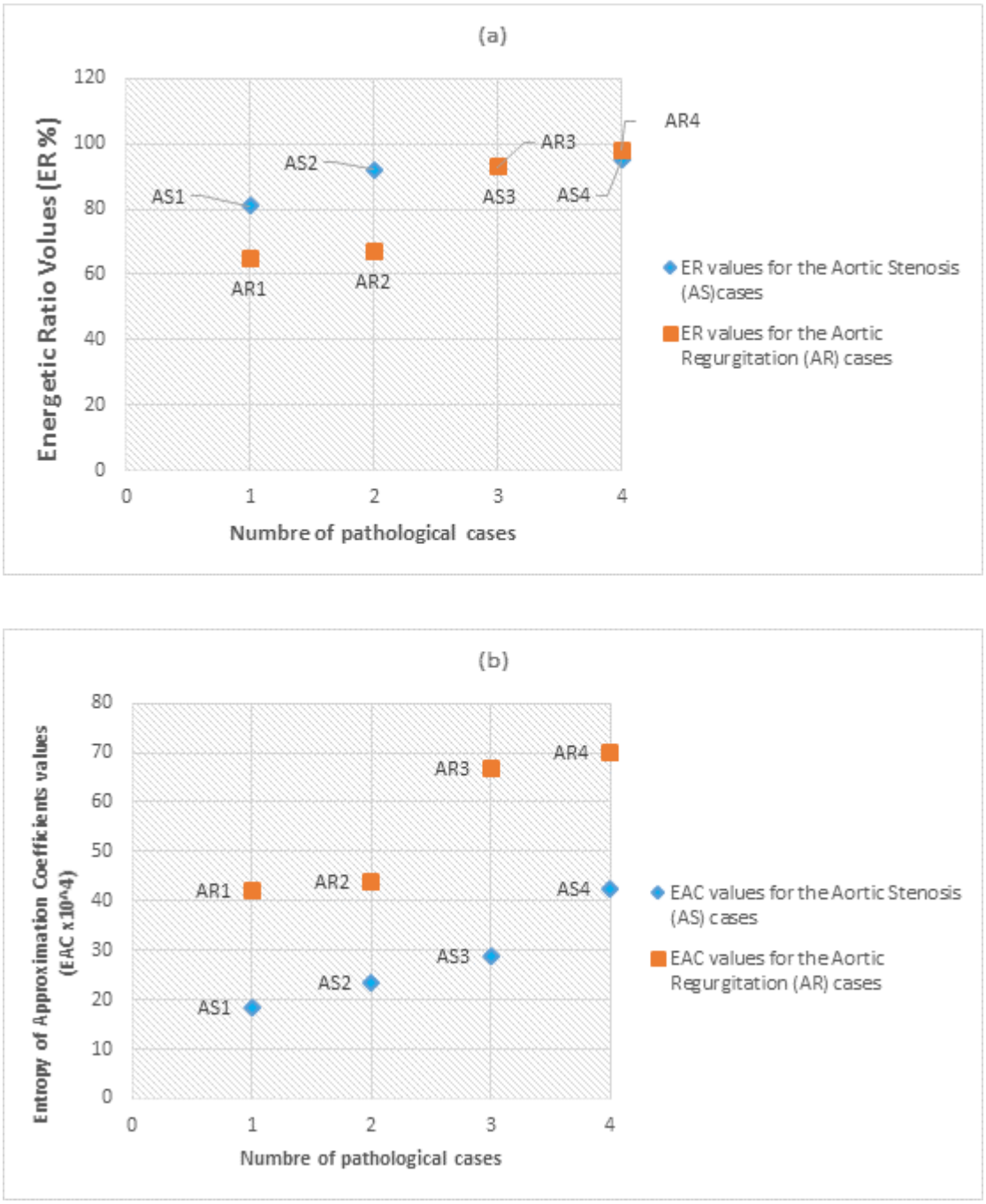

Figure III. 14 (a) Energetic Ratio (ER) evolution representation within the AS and the AR cases, (b) EAC (x10^4) evolution representation for the AS and the AR cases when using one PCG cycle [14].

The same applies to pathologies with minor murmur. When using the ER, only pathologies with high energy can be discriminated clearly as the Ventricular Gallop (VG) and Opening Snap (OS). However, low energy ones display a non-discriminative steady evolution (Figure III.17.(a), Figure III.18). The EAC, on the

other hand, discriminated and separated clearly between all the studied pathologies (Figure III.17.(b), Figure III.18).

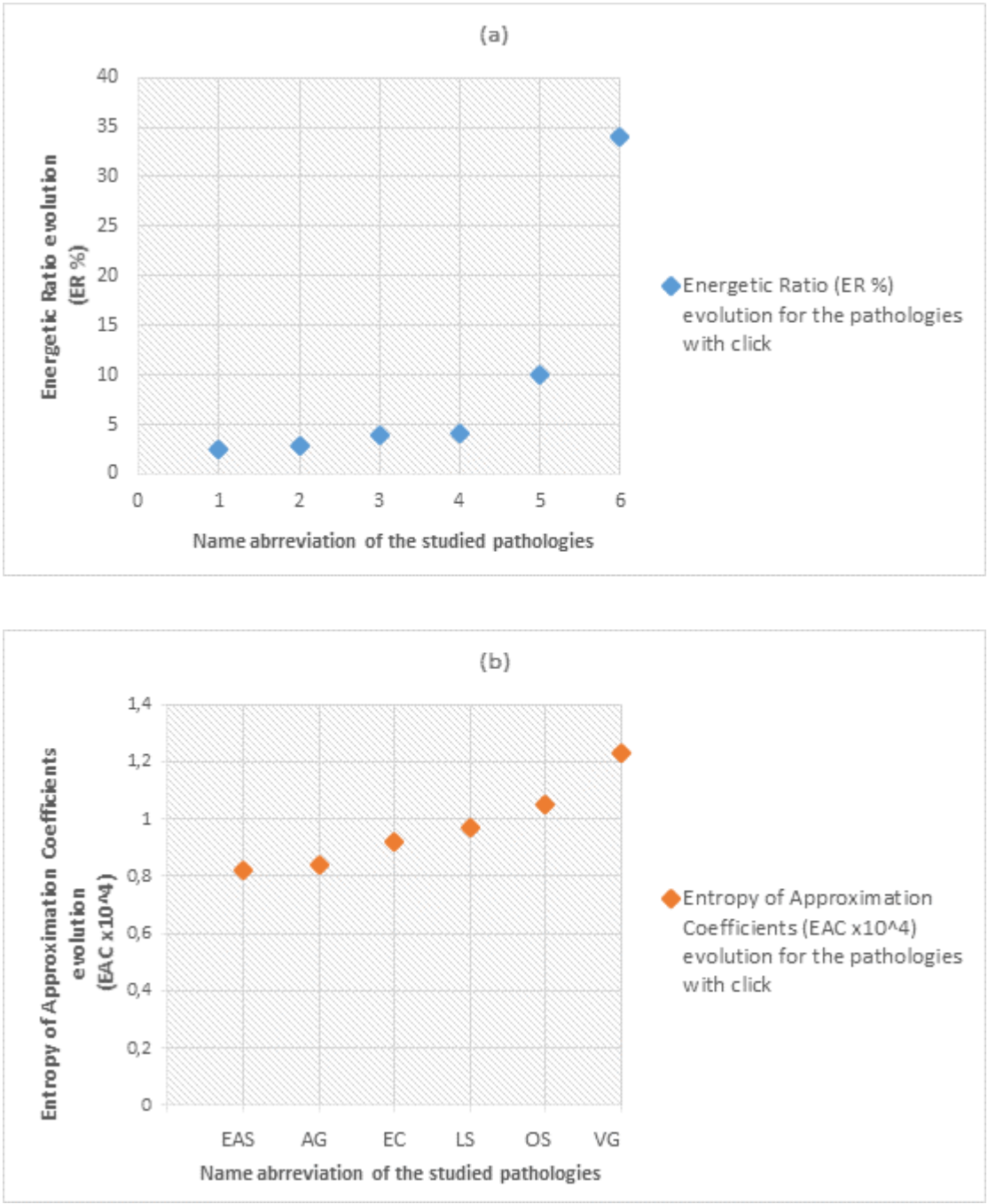

Figure III. 15 (a) ER (%) evolution representation for the pathologies with click, (b) EAC (x10^4) evolution representation for the pathologies with click when using click segments only [14].

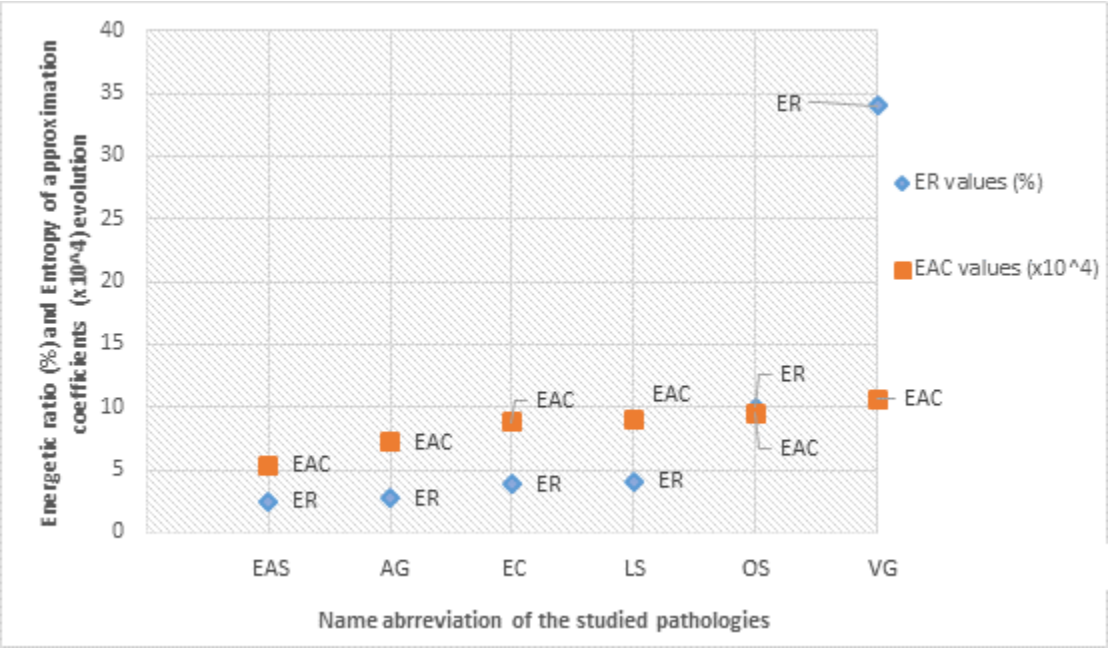

Figure III. 16 ER (%) and EAC (x10^4) evolution representation for the pathologies with click when using one PCG cycle [14].

Therefore, it seemed important to test the EAC values obtained from the two work axes through a machine learning classifier, we chose the One-vs-All SVM classifier with a graphic performance representation due to our limited database, to test the accuracy of these features for:

- Click/ Murmur discrimination
- Cardiac severity assessment

IV.4.1. Click/ Murmur discrimination

To test the ability of the EACs to discriminate between group 1 of cardiac pathologies with clicks and group 2 of those with murmur (G1 and G2), we used both the EAC extracted from added sound segment + EAC from one PCG cycle as two different features and divided the database into two distinct classes:

- Class 1 for the pathologies with minor murmurs (G1: EAS, AG, LS, EC, OS, VG).
- Class 2 for the pathologies with murmurs (G2: AS1, AS2, AS3, AS4, AR1, AR2, AR3, AR4).

One can notice through figure III.19 the successful classification of the database in the two distinct classes by using the Entropy of Approximation Coefficients (EAC). Even the AS and the AR cases hold different emplacements in the blue zone that refers to the PCG signals with murmurs, as discussed above when comparing our results with the ER.

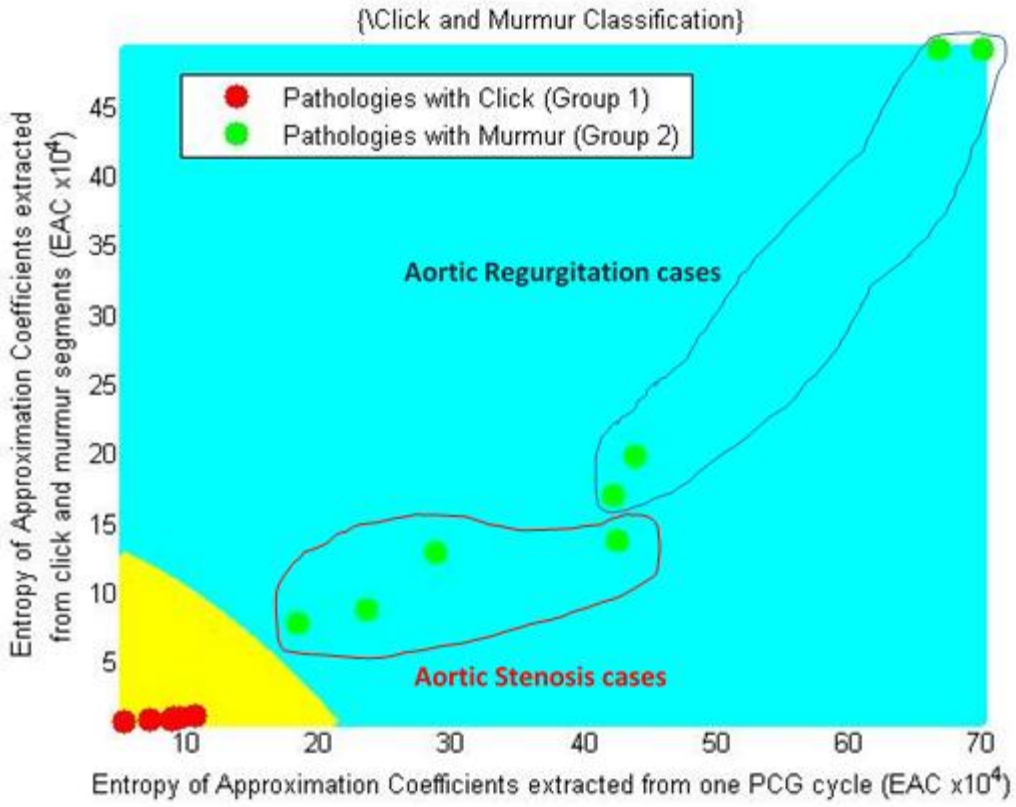

Figure III. 17 A two-class classification (Click pathologies – Murmur pathologies) results using the One versus All Support Vector Machine (OVA-SVM): the pathologies with click are classified in the yellow zone and the 8 cases of the AS and the AR cases in the blue zone.

IV.4.2. Cardiac severity assessment

To test the ability of the EACs to discriminate between the different severities levels of the studied cardiac pathologies whether for the group 1 or 2 of PCG signals, we used both the EAC extracted from added sound segment + EAC from one PCG cycle and divided the database into three classes:

- Class 1 EAS, AG, LS, EC, OS, VG.
- Class 2 AS1, AS2, AS3, and AS4.
- Class 3 AR1, AR2, AR3, and AR4.

One of the advantages of using a graphic performance representation is the aptitude to attest visually to the feature performance. Figure III.20 illustrates the OVA-SVM classifier results, where each of the three colourful zones represents a particular class. One can notice from these three colourful zones that the OVA-SVM using the EAC, not only correctly placed each signal in its respective class according to its severity level but also in a specific emplacement the way it displays a similar evolution to the ones obtained in figures III.15-18. This result affirms the efficiency of the Entropy of Approximation Coefficients (EAC) as a new feature for cardiac severity discrimination and assessment and graphically proves its high accuracy.

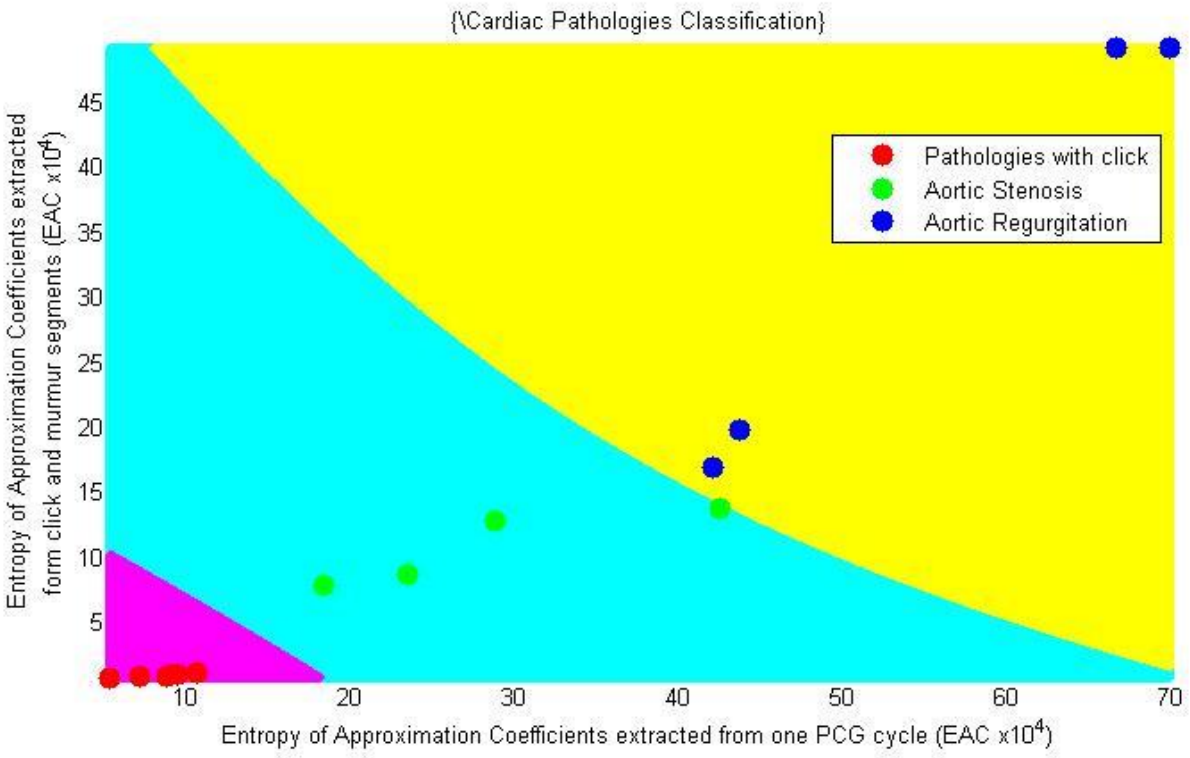

Figure III. 18 A three-class classification (Click pathologies – Aortic Stenosis – Aortic Regurgitation) results using the One versus All Support Vector Machine (OVA-SVM): the purple zone groups the pathologies with click, the blue one classifies the four cases of the AR and AS.

V. Conclusion

In conclusion, we managed through this chapter to prove yet another time that the discrete wavelet transform (DWT) features, like the reconstruction error ($\varepsilon_{\text{ermoy}}$), the mean of detail coefficients (MD), the entropy of approximation coefficients (EAC), are valuable tools for pathological phonocardiogram signals discrimination and cardiac severity assessment.

We begin this chapter by studying three different features extracted from the same DWT decomposition level, where all assessed the cardiac severity. This result confirms that the sixth level of decomposition is optimal for feature extraction when studying cardiac severity through phonocardiogram signals. Additionally, the Entropy of Approximation Coefficients (EAC) up-performed the two other features,

just as the spectral entropy in Chapter I. Therefore, we analysed it more deeply through click and murmur segments as a first step, then a whole PCG cycle. We compared the obtained results to the energetic ratio (ER), which was later found less efficient than the EAC. Lastly, we tested the accuracy of the EAC extracted from the added sound segment and the EAC from one PCG cycle for click/ murmur discrimination and cardiac severity assessment through a One-vs-All Support Vector Machine (OVA-SVM) classifier.

The classifier illustrated the high performances of the EAC and its accuracy when separating clicks from murmurs and assessing the cardiac severity by identifying each severity level as an independent level.

In the end, we successfully achieved the two main aims of this chapter. We demonstrated through three DWT features that the sixth level of decomposition is an excellent level for feature extraction and that the cardiac severity could be referred to by other elements then the energy.

Chapter. IV

CHAPTER IV: Cardiac severity study using the High Order Spectra Analysis (HOSA)

I. Introduction

Several types of analysis techniques have processed phonocardiogram signals. Whether it is of a spectral type, spectro-temporal, audio, or high order analysis, this leads to an unlimited list of features that could be employed for diverse purposes.

High order spectra hold different analysis techniques. The bispectral is one of them and the one employed in this chapter. B. Ergen and Y. Tatar studied the bispectrum of PCG signals early in 2005 for cardiac abnormalities characterisation. They concluded that the peaks and the diagonal slice of the bispectrum efficiently determine the cardiac dysfunctions affecting the heart sounds [1]. K.C. Chua, V. Chandran, et al. followed with a review article and reported that pathological signals have unique 2D plots of bispectrum and bicoherence. The review also mentioned the different HOS parameters used to differentiate and classify pathological bio-signals [2]. Later, A.M Amiri and G. Armano analysed PCG recordings with audio and speech processing techniques focusing on high-resolution methods, such as the Bispectrum and the Wigner Bispectrum. The study showed clear discrimination between pathological and normal (innocent) murmurs in newborns [3].

HOS also found application in other bio-signals like the electrocardiogram (ECG), electroencephalogram (EEG), electromyogram (EMG), and many more. For example, the work published by R. G. Garcia, G. Valenza, et al. where they assessed major depression through an instantaneous bispectral analysis of ECG signals [4]. The S. ABDELOUAHED and F. BOURDJI graduation project [5] supports the K. Chua, V. Chandran, et al. article and other works mentioned in this section by mentioning the first application of HOS in signal processing in the 1970s and its development in different areas. They then added that the estimation of the power spectrum of deterministic or stochastic signals is one of the most fundamental and useful tools in digital signal processing [2]. Particularly in biomedical signals, which are generally non-linear, non-stationary, and non-Gaussian in nature. On one hand, LJ. Hadjileontiadis offered new meaning for signal processing in 2018 by combining the continuous wavelet transform (CWT) with the third-order spectra and then extracting a time-bifrequency representation for two biomedical signals: ECG and EEG [6]. On the

other hand, N. Mahmoodian, A. Boese, et al. employed the HOS technique to detect epileptic seizures using cross-bispectrum on EEG signals [7].

Lastly, many researchers processed the phonocardiogram signal (PCG) with the HOSA for cardiac pathologies discrimination and severity assessment. Berraih, S. A., Debbal, S. M. E. A., and I. Debbal, H. Boudis et al. investigated a set of HOS-based parameters extracted from three main PCG signal groups. Both of them concluded that the bispectrum graphic representation is in itself a discriminative parameter; they then established a list of potential differentiation features [8-11]. In [12], Berraih, S. A., Baakek, Y. N. E. et al. assessed the pathological cardiac severity in PCG signals through a higher order spectra analysis. The study showed the presence of phase coupling in the PCG signals and displayed different signatures for each heart sound signal. The suggested parameters can also be considered for cardiac severity monitoring. Finally, Baakek, Y. N. E. H., Debbal, I. et al. processed these signals and concluded that the frequencies of the heart sound S1, S2, clicks, and murmurs extracted from the bispectrum have the same generator system and are far from being accidentally generated. Moreover, the research revealed that whatever the degree of pathological severity, the heart functions in perfect harmony [13].

Some of the mentioned articles employed bispectral features to achieve their research goals; some were effective, and others were less effective. Therefore, in this chapter, we will study these features' efficiency and select the ones with the best performances for cardiac severity level classification.

II. High Order Spectra: Bispectral Analysis

Before introducing the higher-order spectra and bispectral analysis, we need to define a few essential concepts.

II.1. Correlation function

A correlation function is a function that measures the degree of dependence or independence between two different signals as a function of delay time (τ), since the latter reflects the causal relationship between the two signals.

A correlation function is given by the following relationship [15]:

$$C_{xy}(\tau) = \lim_{T\to\infty} \frac{1}{T} \int_0^T x(t)y^*(t+\tau)dt. \qquad \text{(IV.1)}$$

If **x(t)=y(t)** (i.e. correlation in the same signal) the correlation function becomes an **autocorrelation** function and the equation will then be as the following :

$$C_{xx}(\tau) = \lim_{T\to\infty} \frac{1}{T} \int_0^T x(t)x^*(t+\tau)dt. \qquad \text{(IV.2)}$$

II.2. Multicorrelation and multispectra

Multicorrelations are defined by cumulants of order greater than 2 (note that classical correlation is defined from the cumulant of order 2 [5]).

For a random signal x(t) with real values, the (p-1)-order multicorrelation of x(t) is the p-order cumulant of the values (random variables) of the signal x(t) at instants [14] :

$$C_{p-1}(\tau_1, \tau_2, \ldots \tau_{p-1}) = \mathrm{cum}_p[x(t), x(t+\tau_1), x(t+\tau_3), \ldots, x(t+\tau_{p-1})]. \qquad \text{(IV.3)}$$

II.3. High order spectra

Higher-order spectra (polyspectra) are spectral representations of higher-order statistics, i.e. moments and cumulants of third order and above [15] (or, as already mentioned, are the Fourier transform of multicorrelation functions). They provide information about random processes mainly not existing in the ordinary power spectrum, such as the degree of non-linearity and deviations from normality [3]. HOS consists of averaging over the products of three or more samples of the processed signal, which allows us to assess the non-linear dependencies between several components of the spectrum.

II.4. The bispectral analysis

Since the polyspectra are Fourier transforms of the cumulants, the bispectrum is the Fourier transform of the third cumulant. It is a singular example of the higher-order spectra (HOS) technique and considered as an advanced signal processing tool that allows the exploring of quadratic (and cubic) non-linearities existence [16]. Whereas, the Fourier transform of the second-order cumulant is the power spectral density (PSD).[17-20]

It is possible to quantify the oscillatory relationships between basic frequencies *f*1, *f*2, and their harmonic component "*f*1 + *f*2" through the Fourier transform of the third-order correlation (Eq. IV.14) [16].

$$\mathrm{Bis}(f1,f2)=\lim T\to\infty(1T)E[X(f1+f2)X*(f1)X*(f2)] \qquad \text{(IV.4)}$$

Where X(f) is the Fourier transform of a time series x(nT). $X^*(f)$ is the complex conjugate of X(f) . E[ ] is the arithmetic average estimator.

According to equation (IV.14), the bispectrum is a function with two variable frequencies, unlike the power spectrum, which is a function with a single variable frequency [21]. It also represents the product of three frequency components, where one frequency is equal to the sum of the other two frequencies [15].

Here are a few characteristics and properties of bispectral analysis:

- Because of the symmetry properties of the bispectrum (the correlation function is an even function, so its FT gives spectrum symmetry (the spectrum repeats twice) and given that the bispectrum represents the FT of the tricorrelation function, so it will repeat four times [5] periodically beyond the Nyquist frequency), only a triangular region of bispectral space (around $\mathbf{f_2 \geq 0, f_1 \geq f_2}$ **et** $\mathbf{f_2 + f_1 = 0.5}$) [22], needs to be analysed (called the non-redundant region (Figure IV.1)) [23]. For the bispectrum we have:

$$S_3(f_1, f_2) = S_3(f_1, f_2) = S_3^*(-f_2, f_1) = S_3^*(-f_1, -f_2) = \\ = S_3(-f_1 - f_2, f_1) = S_3(f_2, -f_1 - f_2). \quad \text{(IV.5)}$$

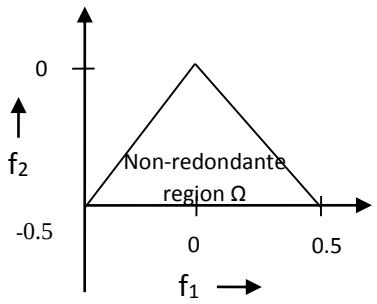

Figure IV. 1 The non-redundant region in the bispectral analysis

III. Parameters study and analysis

In this chapter, we studied a set of 14 different HOSA features and selected the ones with the best performances for cardiac severity classification.

The extracted features are the following:

Name	Equation
The average amplitude (avgamp)	$\text{avgamp} = \frac{1}{L}\sum_{\Omega} \lvert B(f_1, f_2)\rvert$
The standard bi-spectral entropy (ent1)	$P_1 = -\sum_n p_n \log p_n$ Where: $P_n = \frac{\lvert B(f_1,f_2)\rvert}{\sum_\Omega \lvert B(f_1,f_2)\rvert}$
The standard bi-spectral square entropy (ent2)	$P_2 = -\sum_n p_n \log p_n$ Where: $P_n = \frac{\lvert B(f_1,f_2)\rvert^2}{\sum_\Omega \lvert B(f_1,f_2)\rvert^2}$
The standard bi-spectral cubic entropy (ent3)	$P_3 = -\sum_n p_n \log p_n$ Where: $P_n = \frac{\lvert B(f_1,f_2)\rvert^3}{\sum_\Omega \lvert B(f_1,f_2)\rvert^3}$
The entropy of phase (entph)	$P_e = \sum_n p(\Psi_n)\ \log p(\Psi_n)$ Where: $\Omega =$ $\{(f_1, f_2) \lvert f_1, f_2, \text{in the non redundant region}\}$ $\Psi_n = \left\{\phi \middle\lvert -\pi + \frac{2\pi n}{N} \le \phi < -\pi + \frac{2\pi(n+1)}{N}, \quad n = 0,1,..,N-1\right\}$ $p(\Psi_n) = \frac{1}{L}\sum_\Omega 1(\varphi(B(f_1, f_2)) \in \Psi_n)$
Moment of 1st order	$mo1 = \sum_\Omega \log(\lvert B(f1, f2)\rvert)$,
Moment of 2nd order	$mo2 = \sum_\Omega \log(\lvert B(f_k, f_k)\rvert)$,
Moment of 3rd order	$mo3 = \sum_{k=1}^{N} k \log(\lvert B(f_k, f_k)\rvert)$,
Moment of 4th order	$mo4 = \sum_{k=1}^{N} (k - H3)^2 \log(\lvert B(f_k, f_k)\rvert)$,

Moment of 5th order	$mo5 = \sum_{\Omega} \sqrt{i^2+j^2} \log(\lvert B(f_i, f_j) \rvert)$
Weighted centre of the bi-spectral (WCOB)	$wcob_1 = \frac{\sum_{\Omega} iB(i,j)}{\sum_{\Omega} B(i,j)}$ $wcob_2 = \frac{\sum_{\Omega} jB(i,j)}{\sum_{\Omega} B(i,j)}$
The absolute of WCOB (AbsWCOB) are considered two other different features.	AbsWCOB

Figure IV. 2 Bispectral extracted features.

IV. Feature selecting algorithms

IV.1. Random Forest Feature Importance (RFFI)

Random forest (RF) algorithm is a well-known machine learning approach for analysing high-dimensional data and building models. The availability of feature selection or variable importance measures makes it popular [24] [25]. The algorithm assigns a score to input features based on how important and useful they are for predicting a target variable of the dataset [26] [27]. RF algorithm is a nonparametric technique based on decision trees integrated with bagging in the training process that introduces random feature selection. The process of a random forest for feature importance (RFFI) is the following: First, build a classification and regression tree to generate out-of-bag (OOB) sample data. Second, based on the OOB data, the random forest verifies the importance of the input data and assigns an importance score to each feature using the mean decrease accuracy (MDA). Third, RF turns the value of a feature parameter into a random number, then calculates its impact on the models' accuracy and measures the importance of this parameter based on the mean decrease accuracy value obtained from multiple calculations. The higher the value, the higher the importance of the variable [28].

IV.2. SelectKBest feature selection approach

The SelectKBest is an approach that consists on picking the K-best features from a dataset by referring to univariate statistical tests results. The feature-target variable relationship is evaluated, and a specific score is assigned to every feature [29] [30].

V. Results and discussion

After ranking our Phonocardiogram signals into four classes (healthy, light severity, moderate severity, and severe level) through the Energetic ratio and the information listed in Table II.2 of Chapter II, we applied our algorithm using a direct fast FOURIER transform-based HOSA and extracted the above pre-mentioned features. We then introduced the results in the KNN classifier for a multiclass severity classification.

Figures below (Figure IV.2-IV.4), displays the features variation for the four severity classes.

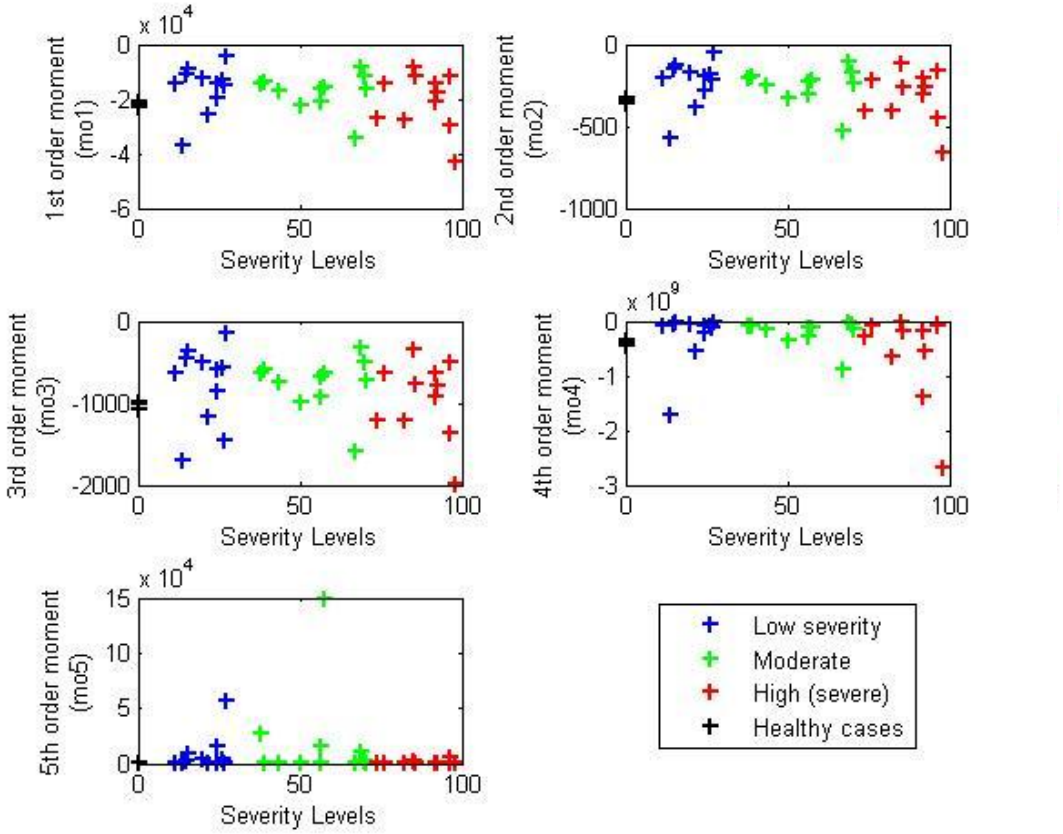

Figure IV. 3 Variation of the average amplitude and the three entropies through the severity levels

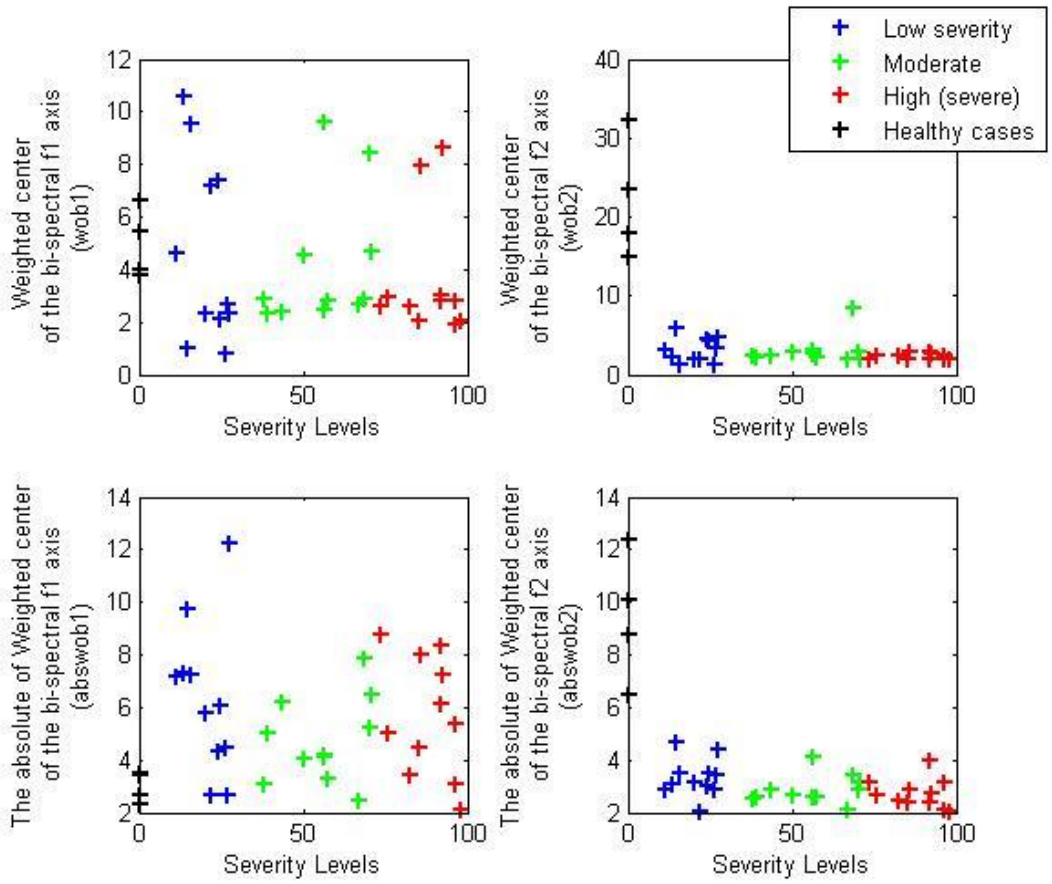

Figure IV. 4 Variation of the five moments through the severity level.

Figure IV. 5 Variation of the weighted centre of the bi-spectral and its absolute through the severity levels

After introducing the 14 features in the KNN classifier, we obtained an accuracy of 83% (Table IV.1). Unfortunately, features with an accuracy lower than 95% are considered insufficient for an effective cardiac severity classification.

Although some features numerically follow the cardiac severity evolution, it could negatively affect the machine learning classification process and results since it present a weak ability of severity levels discrimination. Therefore, to uncover which of these parameters are more discriminative and related to the cardiac severity level, we focused on selecting the features based on their importance to the severity level.

For this purpose, we used a Random Forest Feature Importance (RFFI) to calculate the features importance and then select the six features with the highest accuracy for cardiac severity classification.

Table IV. 1 highlights the accuracies obtained when using all of the extracted features.

Performance	Accuracy	Sensitivity	specificity
All HOSA-features	83%	82%	83.2%

We calculated the importance of the extracted features using an ensemble model of 40 decision trees for predicting response (Classification Labels) as a function of predictors (Matrix of Features). One can see through Figure IV.5 the importance of each feature to the expected classification. At the end, through the first feature selection step, six features out of fourteen presented high importance (Table IV.2). These features resulted in an accuracy of 98% when implemented into a KNN classifier (Table IV.3).

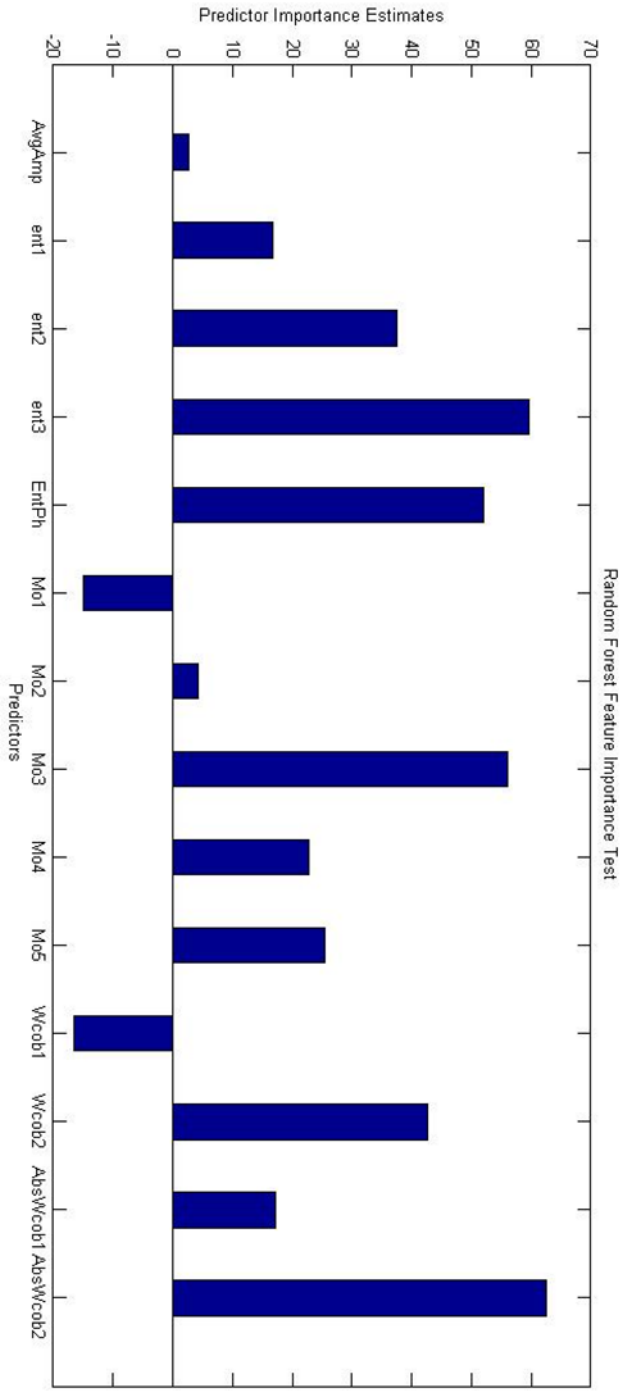

Figure IV. 6 illustrates the importance of all the features to the expected classification.

Table IV. 2 list of the six most important features between the 14 extracted ones.

Selected Features	**Abbreviations**
Absolute weighted centre of the bi-spectral	AbsWCOB2
Weighted centre of the bi-spectral 2	WCOB2
The standard bi-spectral cubic entropy	Ent3
The entropy of phase	EntPh
Moment of 3rd order	Mo3
The standard bi-spectral square entropy	Ent2

Table IV. 3 Accuracies obtained when using the Random Forest Feature Importance (RFFI) selected features.

Performance	**Accuracy**	**Sensitivity**	**specificity**
RFFI selected features	98%	97%	98.2%

An accuracy of 98% is sufficient for cardiac severity classification. However, some researchers recommend avoiding highly correlated features since they cause a loss of accuracy. Therefore, according to the correlation plot in (Figure IV.6), we removed one of the features that are more than 80% correlated (Table IV.4).

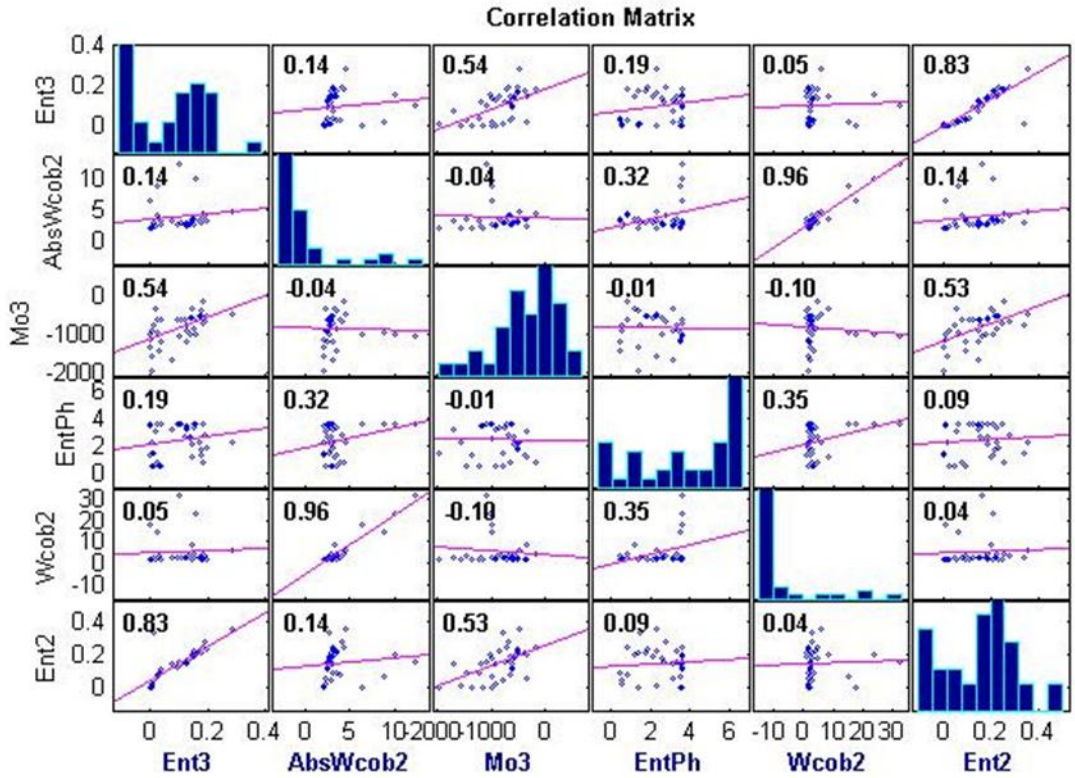

Figure IV. 7 The correlation between the six selected features: Ent3, AbsWcob2, Mo3, EntPh, Wcob2, Ent2.

Table IV. 4 The correlation values between the six selected features: Ent3, AbsWcob2, Mo3, EntPh, Wcob2, Ent2.

Correlation values (%)						
Features	**AbsWcob2**	**Wcob2**	**Ent3**	**EntPh**	**Ent2**	**Mo3**
AbsWcob2	100	**96**	14	32	14	-4
Wcob2	**96**	100	5	35	4	-10
Ent3	14	5	100	19	**83**	54
EntPh	32	35	19	100	9	-1
Ent2	14	4	**83**	9	100	53
Mo3	-4	-10	54	-1	53	100

Table IV. 5 The correlation values between the six selected features: Ent3, AbsWcob2, Mo3, EntPh, Wcob2, Ent2.

By referring to Table IV.4 and Figure IV.5 of the importance values, we removed Ent2 and WCOB2. Both respectively present an 83% and 96% correlation with less importance values than Ent3 and AbsWcob2. In this case, only four HOSA features were found to be relevant for cardiac severity classification using phonocardiogram signals.

To validate the RFFI results and since the HOSA features have, somehow, a statistical background, we thought of applying a second feature selection step using a statistical feature selection algorithm. The SelectKbest, with the percentile of the highest scores as a score function, it selects the top 'K' features based on their statistical scores. In our case, the feature with the highest score is the most important.

With K=4 (i.e. selecting the best four features), the same RFFI selected features were selected another time through the SelectKbest and ranked according to their importance with respect to the classification labels. Once the features were selected, we tested the accuracy through the KNN classifier. An accuracy of 99.7% is scored (Table IV.5), which refers to the ability of these latter to correctly classify almost all of our test database into the four pre-established classes (healthy, light severity, moderate severity, and severe level).

Table IV. 6 Accuracies obtained when using the Random Forest Feature Importance (RFFI) and SelectKbest selected features.

Performance	**Accuracy**	**Sensitivity**	**specificity**
After RFFI and SelectKbest features selection	99.7%	98.7%	99.9%

Thus, the most effective bispectral features for cardiac severity classification when using the phonocardiogram signals, are the:

- **Absolute weighted centre of the bi-spectral (AbsWCOB2)**
- **The standard bi-spectral cubic entropy (Ent3)**
- **The entropy of phase (EntPh)**
- **Moment of 3rd order (Mo3)**

Here we listed the four features accordingly to their importance results.

One can notice through this list and the definition of the HOS features that the obtained results are coherent. Since the absolute weighted centre displays information on the distribution and the number of leaks in the i^{th} line or in the j^{th} column of the bispectrum, the moments describe the highest frequencies weight and characterize the energy turbulence. As for the HOS-entropy, it refers to the complexity, regularity or irregularity, unpredictability characteristics, or the phasic information for the entropy of phase of a bio-signal from a bispectrum plot. Therefore, we can conclude that the selected features represent elements highly variable with the severity evolution.

Lastly, through this chapter, we established two kinds of classifications a: Healthy / Pathological classification and a cardiac severity level classification. Since the database contained PCG signals of different cardiac severity levels along with healthy records as well. Hence, the 4^{th} selected features are eligible for the two kinds of classifications.

VI. Conclusion

In closure, this chapter allowed us to test the efficiency of the HOS features for the cardiac severity assessment when using phonocardiogram signals (PCG). The study consisted of applying the bispectral algorithm on our test database, extracting fourteen different parameters from the bispectrum, and then employing them as features for the K-Nearest Neighbor (KNN) classifier. An average accuracy of 83% is achieved when employing the fourteen parameters as a set of discriminative features for the KNN classifier. Therefore, the study contained two feature-selecting steps with two different feature-selecting algorithms, mainly focusing on the importance of each feature to the severity levels (i.e. target class), the Random Forest Feature Importance (RFFI), and the SelectKBest algorithm.

Thus, out of fourteen extracted features, only the combination of the absolute weighted centre of the bi-spectral (AbsWCOB2), the standard bi-spectral cubic entropy (Ent3), the entropy of phase (EntPh), and the moment of 3rd order (Mo3); allowed us to reach a high accuracy of 99.7% for cardiac severity classification.

Therefore, even though the numerical variation of some HOS features can follow the cardiac severity evolution as displayed in previous similar research. Yet, they are not discriminative enough to classify the PCG signals into the four cardiac severity classes (healthy, light severity, moderate severity, and severe level).

Finally, one can recommend through this chapter's results to consider these four selected features when processing the phonocardiogram signals with the Bispectral analysis for maximum efficiency.

Chapter. V

CHAPTER V: The optimal features for cardiac severity assessment using the Fast Fourier Transform (FFT), the Short Time Fourier Transform (STFT), the Discrete Wavelet Transform (DWT), and the HOSA-Bispectral technique.

I. Introduction

Some pathologies are undetectable for multiple reasons, such as the medical staff's incapacity, the complexity of the pathology, or technical issues. Therefore, researchers applied various analysis techniques developed for sound and/or physiological signals, extracting numerous features to explore PCG aspects in both time and frequency domains. This allows them to highlight the main features used to discriminate cardiac pathologies and view the efficiency of each technique in assessing the cardiac severity evolution.

As mentioned in previous chapters, numerous techniques and features were studied throughout the years for different research purposes, where some were effective and others unfortunately not when introduced into machine learning classifiers. Therefore, the need for feature-selecting algorithms.

Algorithms such as the SelectKBest, Random Forest Feature Importance (RFFI), Recursive Feature Elimination (RFE), Relief-F, Mutual Information (MI), Variance-Thresholding, Principal Component Analysis (PCA), Genetic Algorithm, and many more propose feature selection or dimensionality reduction. Thus, their employment in diverse research fields. H. Jeon and S. Oh., recommended the use of a SVM-Recursive Feature Elimination for large database efficient feature selection, which performs better than regular RFE algorithms [1]. M.M.R. Khan Mamoun and T. Elfouly, combined RFE with ensemble method for the detection of cardiovascular disease using Clinical Parameters [2]. E.A. Algehyne, et al., combined Fuzzy Neural Network Expert System with an Improved Gini Index Random Forest-Based Feature Importance Measure Algorithm for Early Diagnosis of Breast Cancer [3]. A. Almadhor, et al., utilised the SelectKBest algorithm to select the most efficient features for stress detection based on chest electrodermal activity [4]. J.

Liang, et al., demonstrated that the conditional Mutual Information-based Feature Selection considering Interaction detects feature interactions and eliminates redundancies [CMIFSI] [5].

N. Pudjihartono, et al., discussed in a review article how the Relief-based algorithm (RBA) is another popular family of filter algorithms. It scores the importance of a feature according to how well it can distinguish between samples that are similar to each other but belong to different classes. [6].

In this thesis, we studied cardiac severity through a chain of frequency and time-frequency techniques like the Fast Fourier Transform (FFT), the Short Time Fourier Transform (STFT), the Discrete Wavelet Transform (DWT), and the HOSA-Bispectral technique. We extracted different relevant features and tested their efficiency independently in each chapter of this thesis.

In this chapter, we will combine all of the studied techniques and features for a larger database and then introduce them into two feature selection workflows. This will allow us to select the most efficient and important features for the cardiac severity assessment and compare the different techniques to see which of them delivers relevant features for our research purpose.

II. Materials and methods

Each technique studied in previous chapters delivered several features; some were efficient for discriminating cardiac pathologies and assessing severity, while others were less so.

The main aim of these features is to identify each severity level individually, helping us classify our PCG recordings in their proper severity classes. Since this thesis is a synthesis and comparison study, there exist plenty of ways to compare the different techniques. Yet, we decided to compare them according to the efficiency of their respective features. To do so, feature selection methods are required to eliminate irrelevant or redundant features.

Feature selection methods could be divided into three to four methodological categories (Table V. 1):

Table V. 1 Feature Selection Methods.

Methods	**Examples**
Embedded Methods	- LASSO or Elastic Net. - Tree-Based Methods (e.g., Random Forest, Gradient Boosting).
Wrapper Methods	- Recursive Feature Elimination (RFE). - Genetic Algorithms.

Filter Methods	- Mutual Information. - Correlation-Based Feature Selection (CFS).
Specialized Techniques for biomedical data	- ReliefF Algorithm. - Boruta Algorithm.

After referring to previous works and nature of our features, we established two workflows (Figure V.1) for the feature selection manoeuver to retain the most relevant components. The main workflow is as follow:

- **Initial Screening** through filter methods as Variance Thresholding or Mutual Information to remove non-informative features.
- **Feature Refinement** through applying Embedded (e.g., Random Forest Feature Importance (RFFI)) or Wrapper methods (e.g., Recursive Feature Elimination (RFE)).
- **Validate** the selected features using cross-validation to ensure robustness

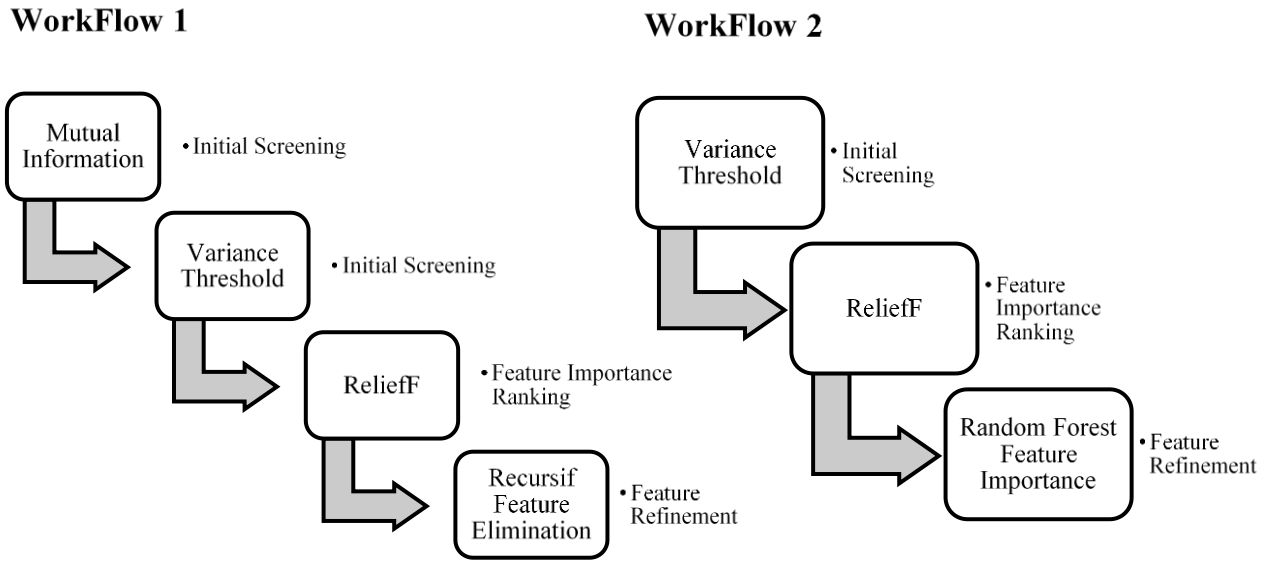

Figure V. 1 Feature selection workflows

First, let's describe and understand each of the used algorithms.

II.1. Mutual Information (MI)

Developed within Information Theory [7]. It measures the independence between two variables to determine the degree to which two sources of information (variables) share information. The entropy measures

how uncertain the possible outcomes of measurement of a variable are, which makes it the elementary measure of information within Information Theory. Equation V.1 defines the Shannon entropy:

$$H(X) = -\sum_{i=1}^{n} p(x_i) log_2 p(x_i) \quad \text{(V.1)}$$

Where H is the entropy, X is the random variable, and p (xi) is the probability of the occurrence of measurement xi for variable X. Two scenarios are possible using this equation:

- A uniform probability distribution results in maximal entropy, indicating that a variable that can take any possible value.
- Entropy equals zero when a variable can take only one value.

In probability theory, MI quantifies the independence through a comparison of the two probability distributions. We can measure the joint probability of two independent events through this equation:

$$\text{MI(X, Y)} = \sum_{x \in X} \sum_{y \in Y} p(x, y) log_2 \frac{p(x, y)}{p(x) p(y)} \quad \text{(V.2)}$$

Where MI(X, Y) is the mutual information of the variables X and Y; p(x, y) is the measured joint distribution of the variables, and p(x)p(y) is the joint probability distribution assuming that X and Y are independent.

Shared information between two variables could be measured by quantifying the degree to which knowledge of the outcome of one variable limits the possibilities of the other variable [8].

In this paper, MI of the extracted features is calculated by choosing each time one feature column, e.g. /Variance/, and the target severity class.

II.2. Variance Threshold (VT)

In this case, a selection of the most relevant features is conducted by referring to the variance value of each feature plus a variance threshold. We experimentally determine the threshold value (T=0.01). Equation V.3 defines the variance score [9]:

$$\text{Variance score (fi)} = p(1 - p) \quad \text{(V.3)}$$

Where p is the percentage of instances taking the feature value 1. The aim of this method is to filter all features with little variation or those that consist only of noise [26].

II.3. ReliefF

Relief-F is an extension of the Relief-based algorithm (RBA) family. In general, RELIEF algorithm searches for the two nearest neighbours for a given instance:

- One from the same class (called nearest hit)
- Another from different class (called nearest miss).

Thus, RELIEF algorithm estimates W[A] of attribute A through the following difference of probabilities:

$$\begin{aligned} &W[A] \\ &= P(\text{different value of AInearest instance from different class}) \\ &- P(\text{different value of Alnearest instance from same class}) \end{aligned} \quad \text{(V.4)}$$

A good attribute differentiate between instances from different classes and have the same value for instances from the same class.

RELIEF-F: is a filter method solution for multiclass problems. Hence, replaces the one near miss M from different class by a one near miss M(C) for each different class then averages their contribution for updating estimates W[A]. The average is weighted with the prior probability of each class:

$$W[A] = W[A] - \frac{diff(A,R,H)}{m} + \sum_{C \neq Class(R)} \frac{[P(C) \times diff(A,R,M(C)]}{m} \quad \text{(V.5)}$$

Where W[A] represents all weights, R is the randomly selected instance, H is the nearest hit , M is the nearest miss.

The idea is that the algorithm should estimate the ability of attributes to separate each pair of classes regardless of which two classes are closest to each other [11].

II.4. Recursive Feature Elimination (RFE)

After building a classification model, traditional RFE consist on sequentially removing features that causes a drop in "classification accuracy". However, the new RFE approach evaluates the importance instead of the accuracy of the feature based on an SVM model, and eliminates the least important features [12].

For this new approach, we segment our database features into training and testing datasets. After training the SVM classifier, each feature receives a weight value reflecting it importance in this model. The features are then ranked decreasingly according to their weight and the one with the lowest value is removed. This process repeats itself across all the remaining features [12]. Lastly, we obtain the ranking of our features using the feature-importance-based RFE method. This method compensate for the weaknesses of the filter [13][1]. It is a wrapper feature selection method.

To ensure robustness of the selected features, a **cross-validation** code is inserted at the end of both workflows.

Cross-validation is a statistical technique that evaluate and compare different learning algorithms by partitioning data into two sets:

- A set for model training
- Another set for model validation.

We applied this method for performance comparison between the many used predictive modeling procedures [14], as well as for variable selection [15]. In this study, we divided the database into 5 subsets or folds, trained the model on a combination of these folds, and then tested the remaining fold. We repeated this processes multiple times where each fold served at least once as a test set. This approach provides a more reliable estimate on the model's performances on unseen data [16].

Since we planned to test the efficiency of the selected features through three different classifiers, the One vs All Support Vector Machine (OVA-SVM), the K-Nearest Neighbor (KNN), and the Long Short Term Memory (LSTM). We modified the cross-validation code each time to estimate the performances of each classifier on unseen data.

II.5. Long Short Term Memory (LSTM) Classifier

LSTM is one of the variants of Recurrent Neural Network (RNN) widely used for sequential data analysis. Unlike other neural networks, LSTM remembers previous input along with recent input to current output during prediction through feedback connections and not feed-forward connections [17]. To decide what to forget and memorise for the long term, LSTM employs "memory cell" and multiple repeating sigmoid and tanh as activation layers [18]. In terms of memory, the LSTM surpasses RNN, which makes it suitable for learning long-duration inputs. The RNN's layers are built using LSTM's units as building blocks (LSTM Networks). We can define three gates in LSTM: input, forget, and output gate, as illustrated in Figure V.2.

The analogue nature of gates allows execution of back-propagation mechanism [19].

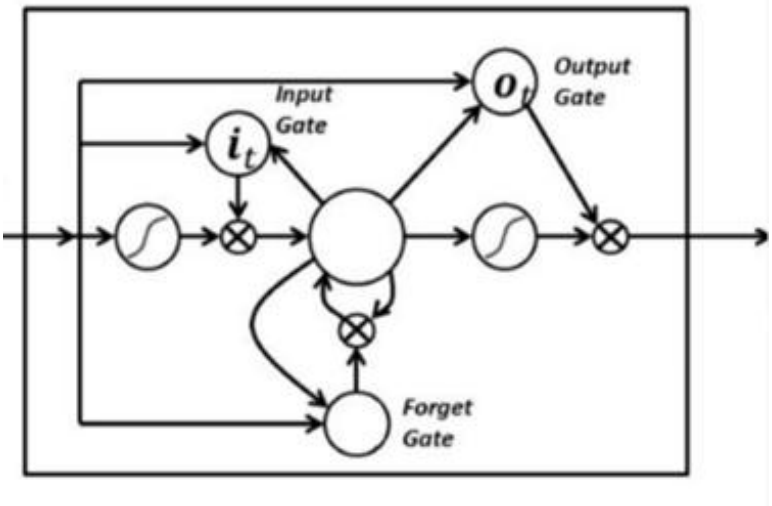

Figure V. 2 RNN architecture with its three gates [19].

III. Results and discussion

For this last chapter, we increased the number of analysed signals to 70 PCG recordings and extracted 18 features out of the four studied techniques. Since this is a comparison thesis, we decided to compare the four techniques based on their ability to deliver delivers the most relevant features for cardiac severity assessment. To achieve this, we implemented several feature selection algorithms to identify the most important ones and then then tested their efficiency using machine learning and neural network classifiers. Thus, the technique that delivers the most features in the final combination with the highest accuracy, according to the feature selection results, is considered the optimal one for cardiac severity assessment.

Table V.2 lists the features for each technique. Specifically, there are four features for bispectral analysis, five for DWT, three for FFT, and six for STFT.

Table V. 2 Features extracted from the Fast Fourier Transform (FFT), Short-Time Fourier Transform (STFT), Discrete Wavelet Transform (DWT), HOSA-Bispectral.

Analysing techniques	**Fast Fourier Transform (FFT)**	**Short Time Fourier Transform (STFT)**	**Discrete Wavelet Transform (DWT)**	**High Order Spectra Analysis: Bispectral**
Extracted Features	-Frequency Band **(FB)** -Spectral Entropy **(SEnt)** -Absolute Spectral Entropy **(AbsSEnt)**	-S1 Time extent **(S1ΔT)** -S1 Frequency extent **(S1ΔF)** -S2 Time extent **(S2ΔT)** -S2 Frequency extent **(S2ΔF)** -Murmur Time extent **(ΔTMurmur)** -Murmur Frequency extent **(ΔFMurmur)**	-Variance **(Var)** -Mean **(Mean)** -Mean of detail coefficients **(Md)** -Entropy of Approximation Coefficients **(EAC)** -Reconstruction error **(ε_{moy})**	-Bispectral cubic entropy **(ent3)** -Entropy of phase **(Entph)** -Absolute weighted centre of the bispectral2 **(AbsWCOB2)** -Moment of 3rd order **(Mo3)**

As mentioned in the previous section, we adopted two workflows to select the optimal features for cardiac severity assessment.

Workflow1:

- **MI:** Measures the dependencies between the frequency and time-frequency component and identifies highly informative features.
- **VT:** Removes redundant non-informative features.
- **ReliefF:** Suitable for feature selection in small to medium sized datasets and captures non-linear dependencies and high-order interactions.

- **RFE:** Possibility to select features using the chosen classifier

Workflow2:

- **VT - ReliefF**
- **RFFI:** Detect hierarchical relationships and non-linear interactions. Selects the most predictive feature through importance measurement.

After setting the variance and RFFI importance thresholds, number of nearest neighbors for ReliefF, and number of RFFI tree bagger, we proceeded with feature selection for a dataset of 30 signals. Table V.3 shows how we obtained the final features combination using the first workflow.

Table V. 3 Selected features with the first workflow.

Methods	**Selected features**
Mutual Information (MI>0.14)	Var-Mean-EAC-$\mathcal{E}_{moy}$-AbsSEnt-SEnt-ΔTMurmur-ΔFMurmur
Variance Threshold (VT>0.01)	EAC-$\mathcal{E}_{moy}$-AbsSEnt-SEnt-ΔTMurmur-ΔFMurmur
ReliefF features ranking order (number of nearest neighbors=5)	ΔFMurmur-ΔTMurmur-EAC-AbsSEnt-$\mathcal{E}_{moy}$-SEnt
Recursive Feature Elimination (SVM-RFE)	ΔFMurmur- EAC- AbsSEnt-$\mathcal{E}_{moy}$- SEnt

First, we noticed from Table V.3 results that MI and VT reduced the feature number from 18 to six relevant features. Then, ReliefF ranked those features decreasingly according to their importance, making the ΔFMurmur the most relevant one for cardiac severity assessment. Later approved through SVM-RFE final selection.

Second, we observed that the spectral entropy was selected twice in SVM-RFE through AbsSEnt and SEnt, Even though it did not score high in the ReliefF ranking order. Thus, the quantity of information present in the FFT spectrum is an important parameter that could translate the cardiac pathologies and severities efficiently. Hence, the use of FFT spectrums in [20] as a feature to classify and discriminate the PCG signals database.

The final combination contained three other time-frequency features (ΔFMurmur- EAC- $\mathcal{E}_{moy}$). The entropy of approximation coefficients (EAC) and reconstruction error ($\mathcal{E}_{moy}$) were both extracted from the DWT and proved their efficiency in separate works [19][21-24]. Their presence in the final combination through a chain of strict feature selection algorithms demonstrates another time their robustness. Especially, for the EAC that ranked second after the SVM-RFE selection. On the other hand, only one feature from the STFT made it to the end. However, it scored the highest value and ranked first in the final selection.

Lastly, to conclude this first workflow selection, time-frequency features slightly outperformed frequency features. As a result, three out of five features are directly related to the PCG signal's frequencies. This leads to the conclusion that cardiac severity indications are highly present in frequency information.

Table V.4 displays the selected features using the second workflow. In this workflow, we approved two final feature combination since they both displayed high scores in cross-validation.

Table V. 4 Selected features using the second workflow.

Methods	**Selected features**	**Methods**	**Selected features**
Variance Threshold (VT>0.01)	Entph-AbsWCOB2-Mo3-EAC-$\mathcal{E}_{moy}$-AbsSEnt-SEnt-ΔTMurmur-ΔFMurmur-FB	**Variance Threshold (VT>0.01)**	Entph-AbsWCOB2-Mo3-EAC-$\mathcal{E}_{moy}$-AbsSEnt-SEnt-ΔTMurmur-ΔFMurmur-FB
ReliefF features ranking order (number of nearest neighbors=10)	ΔFMurmur-ΔTMurmur-$\mathcal{E}_{moy}$-FB-AbsWCOB2-Mo3-Entph-EAC-SEnt- AbsSEnt	**ReliefF features ranking order (number of nearest neighbors=10)**	ΔFMurmur-ΔTMurmur-$\mathcal{E}_{moy}$-FB-AbsWCOB2-Mo3-Entph-EAC-SEnt- AbsSEnt
Random Forest Feature Importance (RFFI): Tree bagger=150 , Importance threshold=0.09	ΔFMurmur-ΔTMurmur-$\mathcal{E}_{moy}$-FB-Entph-EAC-SEnt- AbsSEnt	**Random Forest Feature Importance (RFFI): Tree bagger=100 , Importance threshold=0.1**	ΔFMurmur-FB-EAC- AbsSEnt

Firstly and contrarily to the first workflow, the bispectral features were present in VT and ReliefF selection and in one of the final combinations. This means that bispectral features' mutual information was inferior to the MI threshold in the first workflow. This led them out of the initial screening selection. We also discerned three additional features to the first workflow when using RFFI (Tree bagger=150, Importance threshold=0.09), namely ΔTMurmur-FB-Entph.

Secondly, the entropy of phase is an emblematic feature and the reason behind employing the bispectral technique in our studies. Its presence in the final combination although its exclusion in the first workflow, proves that features with low MI or variance could also hold importance in a particular way.

Thirdly, the workflow selected the Frequency Band feature, which supports the previous idea and results that the FFT spectrum is an important feature in all of its aspects. On the other hand, the selection of the ΔTMurmur feature indicates that severity information is highly present in murmurs and can be represented in the frequency or time domain through STFT features.

Afterward, upgrading the importance to 0.1, the ΔTMurmur and Entph were removed from the RFFI final selection. However, both RFFI final combinations showed equal accuracies in cross-validation. This may insinuate that these two features don’t hold any weight since their presence or absence won’t impact the obtained accuracy. Despite this, their initial selection proves their importance, which might be better appreciated in high-dimensional feature sets.

Lastly, as in the first workflow, time-frequency features outperformed frequency features, with a unique high-order parameter present in the first final combination. Yet, in the second combination, the equation changed, and the two types of features became equal. Whereas, for both combinations and as the first workflow, the features related to the PCG signal’s frequencies represent the majority.

Now that we have our feature combinations, efficiency testing on unseen data is primordial. For that, we upgraded our dataset to 70 signals and went with three different classifiers: KNN, OVA-SVM, and LSTM.

Table V.5 displays the obtained accuracies for the three features combination through the different classifiers.

Table V. 5 Accuracy results for the three final feature combinations using the One vs All Support Vector Machine (OVA-SVM), the K-Nearest Neighbor (KNN), and the Long Short Time Memory classifiers (LSTM).

Features combinations	**Accuracies**		
	KNN	**OVA-SVM**	**LSTM**
Workflow 1	88%	98%	75%
Workflow 2 (Tree bagger=150, Importance threshold=0.09)	97%	95%	85%
Workflow 2 (Tree bagger=100, Importance threshold=0.1)	97%	98%	85%

One can notice from Table V.5 that regular machine learning classifiers such as KNN and OVA-SVM displayed quite high accuracies (95%-98%) for cardiac severity classification, which was not the case for neuronal network variant (LSTM) that scored 75% and 85%.

Table V.6 compares our accuracy results with previous works. Although results comparison should be made between studies with the same datasets and since it was impossible for us to find such kind of studies due to the diverse nature of our dataset, we proceeded with this comparison to see the tendency variation of accuracy for similar research axes and works using similar feature selection methods. We discerned from this table that the obtained accuracies are closer to ours, if not a bit lower in some cases.

Table V. 6 Comparison of our method with previous works.

Authors	**datasets**	**Extracted Features**	**classifier**	**Accuracy (%)**
Yasseen and Kwon (2018)	Own dataset	MFCCs and DWT features	SVM KNN	97.9 91.6
Raza et al. (2019)	Pascal	Signal frames	LSTM-RNN	80.45
Aziz et al. (2020)	Own dataset	MFCCs and 1D-LTPs	SVM	95.24
Ahmed et al. (2021)	PhysioNet/CinC	MFCCs and DWT features	LSTM	90.04
Ozkan and Mustafa (2022)	Yasseen and Kwon (2018) dataset	MFCCs based on EMD	SVM	96.2
Khan Mamoun and Elfouly (2023)	NHANES survey dataset	Clinical parameters	SVM	72.43
This study	-American college of cardiology -Cardiosource Heart Sounds and Murmurs -Dundee -Yasseen and Kwon (2018) dataset	FFT-STFT-DWT-Bispectral features	OVA-SVM KNN	FC1: 98 FC2: 95 FC3: 98 FC1: 88 FC2: 97 FC3: 97

			LSTM	FC1: 75 FC2: 85 FC3: 85

*FC: Final Combination. *Works mentioned in this table are from [25-29]

The main aim of this chapter was to find which technique is the optimal one for cardiac severity assessment. On one hand, the bispectral features displayed poor performances for this specific purpose. On the other hand, it was hard to distinguish that one of the STFT, FFT, or DWT is better when comparing the three final feature combinations. Since, in the first final combination, we had one STFT feature, two DWT features, and two FFT features. In the second one, two STFT features, Two DWT features, Three FFT features, and one Bispectral feature. Lastly, the third one contained two FFT features and one from both STFT and DWT.

Thus, although the STFT features remain minimal in the final combinations, they ranked first and second, followed by the DWT features in the three final selections, which proves their importance for our research purpose. The FFT features ranked behind but always up-numbered the STFT features.

Lastly, the spectral, time-frequency, or high-order entropy are all selected in final combinations. This confirms the results obtained in the three previous chapters. Especially the ones in Chapter III, since the EAC ranked respectively second and third in the two final combinations with the highest accuracy. Another important point is, as mentioned before, in the three final combinations, the features related to the frequencies of the signals are dominant.

IV. Conclusion

In conclusion, this chapter grouped all the extracted features from the four studied techniques, we increased the number of PCG signals in the dataset, introduced a part of it in two workflows of feature selection methods, and then tested the efficiency of the three final feature combinations through OVA-SVM, KNN, and LSTM classifiers for unseen data of different severity levels.

We obtained an accuracy of 98% for two final feature combinations. This indicates the ability of these selected features to classify the majority of the dataset into light, moderate, or severe levels. Accordingly, the One vs All Support Vector Machine (OVA-SVM) was found to be the optimal classifier for our multiclass severity classification.

The main aim of this chapter was to find which technique is optimal for cardiac severity assessment. However, the results showed that bispectral features are not very important for this purpose, and none of the other techniques fully stood out in the two final combinations with the highest accuracy either. Instead, we

arrived at an unexpected conclusion: in both combinations, the number of features related to the frequencies of the PCG recordings was higher than the rest, and both contained spectral and time-frequency entropies.

Finally, when studying cardiac severity assessment, it is better to prioritise features that quantify information, such as entropy, and are related to the signals' frequencies. Therefore, we recommend choosing techniques that could deliver such features as the FFT, STFT, and DWT.

References

Intro:

[1] : O. Tahar, Etude du degré de sévérité pathologique des sténoses aortiques, Graduation Project, Abou Bekr Belkaid University Tlemcen, Algeria, pp. 40,2009.

[2] : M. HAMZA, S. ZIANI CHERIF, Etude et réalisation d'un stéthoscope électronique, Graduation Project, Abou Bekr Belkaid University Tlemcen, Algeria, pp. 10-11, 2013

[3] : F. Meziani, Analyse du degré de sévérité pathologique des signaux phono cardiogrammes (PCGs) par application des transformées d'ondelettes, PhD thesis, Abou Bekr Belkaid University Tlemcen, Algeria, pp. 64-67, 2013.

[4] : B. Zineb, Classification des Signaux Phonocardiogrammes sur la Base de L'étude du Rapport SNR, Graduation Project, A bou Bekr Belkaid University Tlemcen, Algeria, pp. 2-4, 2012.

[5] : GP. Armstrong. MD [Internet], Waitemata Cardiology, Auckland Valvular Disorders, MSD Manuals [updated 2023 April; cited 2024 January 03], Available from: https://www.msdmanuals.com/professional/cardiovascular-disorders/valvular-disorders

[6] : A. Wang, T.M. Bashore, editors. Valvular heart disease, 1st ed. New York: Humana press; 2009.

[7] : I. Debbal, H. Boudis, Y.N.E.H. Baakek, & S.M. Debbal, Phonocardiograms Signals Analysis using the Graphical Bispectral Technique. Ann. Clin. Cases, Vol. 1, No. 2, pp. 1009, 2020.

[8] : S.A. Berraih, S.M.E.A. Debbal, Pathological discrimination of the phonocardiogram signal using the bispectral technique. Physical and Engineering Sciences in Medicine, Vol. 43, No. 4, pp. 1371-1385, 2020.

[9] : S.A. Berraih, S.M.E.A. Debbal, Severity cardiac analysis using the Higher-order spectra. Applied Mathematics and Computation, Vol. 409, pp. 126389, 2021.

[10] : I. Debbal, H. Boudis, Y.N.E.H. Baakek, & S.M. Debbal, Cardiac Pathologies Analysis on the Phonocardiogram Signals Using the Bispectral Technic, International Journal of Advanced Science and Technology, Vol. 29, No. 3, pp. 6764 – 6784, 2020.

[11] : D. S. B. Sundaram, D. N. Damani, A. Kapoor, et al., Deep learning based discrimination of phonocardiogram signal with normal heart sounds and murmur: Feasiblity study. Biomedical Sciences Instrumentation, vol.57, no.2, 2021.

[12] : S.M. Debbal, L. Hamza Cherif, Pathologies cardiac discrimination using the Fast Fourir Transform (FFT) The short time Fourier transforms (STFT) and the Wigner distribution, J Cardiology Interventions, vol.1, no.1, 2021.

[13] : S.A. Berraih, Y.N.E.H. Baakek, & S.M.E.A. Debbal, Preliminary study in the analysis of the severity of cardiac pathologies using the higher-order spectra on the heart-beats signals. Polish Journal of Medical Physics and Engineering, Vol. 27, No. 1, pp. 73-85, 2021.

[14] : P. Dhar, S. Dutta, & V. Mukherjee, Cross-wavelet assisted convolution neural network (AlexNet) approach for phonocardiogram signals classification. Biomedical Signal Processing and Control, Vol. 63, pp.102142, 2021.

[15] : Y. N. E. H. Baakek, I. Debbal, H. Boudis, & S. M. E. A. Debbal, Study of the impact of clicks and murmurs on cardiac sounds S1 and S2 through bispectral analysis, Polish Journal of Medical Physics and Engineering, vol.27, no.1, pp. 63-72, 2021

[16] : M. Fakhry, A.F. Brery, Comparison of Window Shapes and Lengths in Short-Time Feature Extraction for Classification of Heart Sound Signals, International Journal of Electrical and Computer Engineering (IJECE), vol. 12, no 6, pp. 6090-6102. 2022.

[17] : A. Hossain, S. Uddin, P. Rahman, et al., Wavelet and Spectral Analysis of Normal and Abnormal Heart Sound for Diagnosing Cardiac Disorders. BioMed Research International, vol. 2022, Article ID 9092346, 2022.

[18] : J. A. Lee, K. C. Kwak, Heart Sound Classification Using Wavelet Analysis Approaches and Ensemble of Deep Learning Models. Applied Sciences, Vol. 13, No. 21, pp.11942, 2023.

[19] : P. Careena, M. Mary Synthuja Jain Preetha & P. Arun, Statistically significant feature-based heart murmur detection and classification using spectrogram image comparison of phonocardiogram records with machine learning techniques, Australian Journal of Electrical and Electronics Engineering, pp.1-15, 2024.

Chap I:

[1]: Varshney S, Singh S, Computation of Biological Murmurs In Phonocardiogram Signals Using Fast Fourier & Discrete Wavelet Transform, International Conference on Computation, Automation and Knowledge Management (ICCAKM) Amity University, 2020

[2] : Boudghene Stambouli Z, Classification of Phonocardiogram Signals Based on the Study of the SNR Ratio, Magister's thesis, Abou Bekr Belkaid University, Tlemcen, 2012.

[3] : Weinhaus, A.J., Roberts, K.P., Anatomy of the Human Heart, In: Iaizzo, P.A. (eds) Handbook of Cardiac Anatomy, Physiology, and Devices, Humana Press, pp51-79, 2005.

[4] : Elaine N. Marieb, Jon Mallatt, Human Anatomy, 3rd Ed. by Benjamin Cummings, p523, 2001.*(p. 523 from Human Anatomy, 3rd Ed. by Elaine N. Marieb and Jon Mallatt. © 2001 by Benjamin Cummings.)*

[5] : Anthony J. Busti, MD, PharmD, FNLA, FAHA Karolina DeAugustinis, MD [Internet]. EBM Consult, LLC [updated 2015 Jul; cited 2023 Oct 31]. Available from: https://www.ebmconsult.com/articles/anatomy-heart-external

[6] : Frederic H. Martini, Michael J. Timmons, Robert B. Tallitsch, Human Anatomy, 4th Ed.by by Frederic H. Martini, Inc. and Michael J. Timmons, pp553, 2003(p. 553 from Human Anatomy, 4th Ed.by Frederic H.

Martini, Michael J. Timmons, and Robert B. Tallitsch. © 2003 by Frederic H. Martini, Inc. and Michael J. Timmons.)

[7] : Hamza and Ziani Chrif Selmen, study and creation of an electronic stethoscope, Abou-bekr Belkaid University, Tlemcen, Master's thesis, 2013.

[8] : Djebbari A., Synthesis of time frequency analysis methods applied of phonocardiogram signal, Abou Bekr Belkaid University, Tlemcen, PhD. thesis, September 2014.

[9] : Li X et al , Synchronization control of pulsatile ventricular assist devices by combination usage of different physiological signals, Comput Assist Surg 24(sup1):105–112. 2019.

[10] : Mohrman DE, Heller L. eds. Cardiovascular Physiology, 8e. McGraw Hill; 2014.

[11] : A.G.Tilkian,M.B.Conover. Understanding heart sounds and murmurs with an introduction to lung sounds. Curr, probl.cardiol. 10,1985.

[12] : F.long. Common Heart Sounds.LandonPediatric Foundation.

[13] : MEZIANI Fadia, Analysis of the degree of pathological severity of phonocardiogram signals (PCGs) by application of wavelet transforms, Abou-bekr Belkaid University, Tlemcen, PhD. Thesis, 2013.

[14] : A.K.Abbas, R.Bassam, phonocardiography Signal Processing, Morgan and claypool,2009

[15] : S.Lukkarinen, A.Nopanen, K.Sikio,A.Angerla, A New Phonocardiographic recording System, Comput cardiol,pp.117-120,1997.

[16] : BELGRABI Faiza, Segmentation of a PCG Phonocardiogram signal, Master's Thesis, 2015.

[17] : Choi S., Jiang Z., Cardiac sound murmurs classification with autoregressive spectral analysis and multi-support vector machine technique, Computers in Biology and Medicine, Volume 40, Issue 1, pages 8-20, January 2010.

[18] : Narváez, P.; Gutierrez, S.; Percybrooks, W.S. Automatic Segmentation and Classification of Heart Sounds Using Modified Empirical Wavelet Transform and Power Features. Appl. Sci. 2020, 10, 4791.

Chap II:

[1] : BF. Beritelli, S. Serrano, Biometric Identification Based on Frequency Analysis of Cardiac Sounds, IEEE Transactions on Information Forensics and Security, vol.2, no.3, pp. 596- 604, Sept. 2007.

[2] : S.M.Debbal, F.Bereksi-Reguig, Features for Heartbeat Sound Signal Normal and Pathological, Recent Patents on Computer Science, vol.1, pp. 1-8, 2008.

[3] : S.M.Debbal, F.Bereksi-Reguig, Frequency analysis of the heartbeat sounds, Biomedical Soft Computing and Human Sciences, vol.13, no.1, pp. 85-90, 2008.

[4] : A. K. Abbas, R. Bassam, Phonocardiography Signal Processing, in Synthesis Lectures on Biomedical Engineering, edited by J. D. Enderle (Morgan & Claypool Publisher, New York, 2009).

[5] : A. Djebbari, F.Bereksi-Reguig, Short-time Fourier transform analysis of the phonocardiogram signal. In: The 7th IEEE international conference on electronics, circuits and systems, pp. 844–847, 2002.

[6] : M.S. Bendelhoum, Study of phonocardiogram signal discrimination parameters, pp.58, PhD thesis, Sidi- Bel-Abbes University, 2008.

[7] : D. S. B. Sundaram, D. N. Damani, A. Kapoor, S. Shivaram, & S.P. Arunachalam, Deep learning based discrimination of phonocardiogram signal with normal heart sounds and murmur: Feasiblity study. Biomedical Sciences Instrumentation, vol.57, no.2, 2021.

[8] : S.M. Debbal, L. Hamza Cherif, Pathologies cardiac discrimination using the Fast Fourir Transform (FFT) The short time Fourier transforms (STFT) and the Wigner distribution, J Cardiology Interventions, vol.1, no.1, 2021.

[9] : M. Atteeq, M. F. Khan, & A. N. Qureshi, Fetus Heart Beat Extraction from Mother's PCG Using Blind Source Separation, In Proceedings of the 2019 11th International Conference on Bioinformatics and Biomedical Technology, pp. 100-104, May 2019.

[10] : Y. N. E. H. Baakek, I. Debbal, H. Boudis, & S. M. E. A. Debbal, Study of the impact of clicks and murmurs on cardiac sounds S1 and S2 through bispectral analysis, Polish Journal of Medical Physics and Engineering, vol.27, no.1, pp. 63-72, 2021

[11] : M. Fakhry, A.F. Brery, Comparison of Window Shapes and Lengths in Short-Time Feature Extraction for Classification of Heart Sound Signals, International Journal of Electrical and Computer Engineering (IJECE), vol. 12, no 6, pp. 6090-6102. 2022.

[12] : P. Careena, M. Mary Synthuja Jain Preetha & P. Arun, Statistically significant feature-based heart murmur detection and classification using spectrogram image comparison of phonocardiogram records with machine learning techniques, Australian Journal of Electrical and Electronics Engineering, pp.1-15, 2024.

[13] : A. Djebbari, Synthesis of time-frequency analysis methods applied to phonocardiogram signal, PhD thesis, University of Abou Bekr Belkaid, Algeria, 2013.

[14] : GP. Armstrong. MD [Internet], Waitemata Cardiology, Auckland Valvular Disorders, MSD Manuals [updated 2023 April; cited 2024 January 03], Available from: https://www.msdmanuals.com/professional/cardiovascular-disorders/valvular-disorders/aortic-stenosis.

[15] : A. Wang, Bashore TM, editors. Valvular heart disease, 1st ed. New York: Humana press; 2009.

[16] : A. Dwivedi, A. Imtiaz, & E. Rodriguez-Villegas, Algorithms for automatic analysis and classification of heart sounds–a systematic review, IEEE Access, vol. 7, pp. 8316-8345, 2018.

[17] : T. Biancaniello, Innocent murmurs. Circulation, vol. 111, no 3, p. e20-e22, 2005.

[18] : C. Liu et al., An open access database for the evaluation of heart sound algorithms, Physiol. Meas., vol. 37, no. 12, pp. 2181–2213, 2016.

[19] : D. Mason, Listening to the heart: A comprehensive collection of heart sounds and murmurs, 2nd ed. Philadelphia, Hahnemann University, School of Medicine, 2000.

[20] : L. Thoms, G. Colicchia, & R. Girwidz, Phonocardiography with a smartphone, Phys. Educ., vol. 52, no. 023004, pp. 1–4, 2017.

[21] : H. Naseri, M.R. Homaeinezhad, Detection and boundary identification of phonocardiogram sounds using an expert frequency-energy based metric, Ann. Biomed. Eng., vol. 41, no. 2, pp. 279–292, 2013.

[22] : A.L. Noponen, S. Lukkarinen, A. Angerla, & R. Sepponen, Phono-spectrographic analysis of heart murmur in children, BMC Pediatr., vol. 7, no. 1, pp. 23, 2007.

[23] : J. Grayzel, Gallop rhythm of the heart, Am. J. Med., vol. 28, no. 4, pp. 578–592, 1960.

[24] : S.M. Debbal, F Bereksi-Reguig, Spectral analysis of the PCG signals, The Internet Journal of Medical Technology. Vol.4, no.1, 2006.

[25] : S.M. Debbal, F. Bereksi-Reguig, Cardiac Murmur Analysis Using The Short-Time Fourier Transform, Journal of Mechanics in Medicine and Biology, vol.6, no.3, pp. 273–284, 2006.

[26] : S. M. Debbal, F. Bereksi Reguig, The fast Fourier transform and the continuous wavelet transform analysis of the normal and the pathological phonocardiogram, Sciences et Technologies, vol. 17, pp. 81-86, 2002.

[27] : Abrams,J, Current Concepts of the genesis of heart sounds.I.First and second sounds.JAMA, 239-2787. 1978.

[28] : I. Debbal, L. Hamza Cherif & Y.N.E.H. Baakek, A new approach to phonocardiogram severity analysis, Journal of Medical Engineering & Technology, vol. 47, no 5, pp. 265-276, 2023.

[29] : F. Meziani, Phonocardiogram signal severity level analysis using wavelet transform (WT), PhD Thesis, Abou Bekr Belkaid University, Tlemcen, pp 64-67, 2013.

[30] : T.J. Ahmad, H. Ali, S.A. Khan, Classification of Phonocardiogram using an Adaptive Fuzzy Inference System, Proc. Int. Conf. Image Process. Comput Vis Pattern Recognit. Proceedings of the 2009 International Conference on Image Processing, Computer Vision, & Pattern Recognition, IPCV 2009, Las Vegas, Nevada, USA, July 13-16, 2009.

[31] : I. Debbal, L. Hamza Cherif, & Y.N.E.H. Baakek, Pathology cardiac monitoring study of the phonocardiogram signal, Journal of Theoretical and Applied Information Technology, vol.101, no.10, pp.3–18, 2023.

[32] : H. Lamraoui, Characterisation of the phonocardiogram signal. Hadj Lakhdar University. Batna 2. Algeria. 2016.

[33] : I. Debbal, L. Hamza Cherif, & Y.N.E.H. Baakek, Pathological cardiac severity discrimination using a spectral entropy. In: Proceedings of the 1st International Conference on Scientific and Academic Research (ICSAR2022), Konya, Turkey, pp. 323-328, December10-13 2022.

[34] : J. Laaksonen, E. Oja, Classification with learning k-nearest neighbors, in: Proceedings of International Conference on Neural Networks (ICNN'96), IEEE, pp.1480–1483, 1996.

[35] : Ö. Kramer, K-nearest neighbors, pp.13–23, 2013.

[36] : Ö. ARSLAN, M. KARHAN, Effect of Hilbert-Huang transform on classification of PCG signals using machine learning, Journal of King Saud University-Computer and Information Sciences, vol. 34, no 10, pp. 9915-9925, 2022.

[37] : V. Vapnik. The nature of statistical learning theory, Springer Verlag: New York, 1995.

[38] : C. Nello, S.T. John, An introduction to support vector machines and other kernel-based learning methods. Cambridge: Cambridge University Press, pp. 173–186, 2000.

[39] : J. Manikandan, B. Venkataramani, Design of a real time automatic speech recognition system using modified one against all SVM classifier, Microprocess Microsyst Vol.35, no.6, pp.568–578, 2011.

[40] : A. Rocha, S.K. Goldenstein, Multiclass from binary: expanding one-versus-all, one-versus-one and ECOC-based approaches. IEEE Trans Neural Netw Learn Syst. Vol.25, no.2, pp.289–302, 2013.

[41] : Deepak S, Ameer PM. Automated categorization of brain tumor from MRI using CNN features and SVM. J Ambient Intell Human Comput, vol.12, no.8, pp.8357–8369, 2020.

Chap III:

[1] : F. Meziani, Analyse du degré de sévérité pathologique des signaux phono cardiogrammes (PCGs) par application des transformées d'ondelettes, PhD thesis, Abou Bekr Belkaid University Tlemcen, Algeria, pp 64-67, 2013.

[2] : V. Nivitha Varghees & K. I. Ramachandran, Heart murmur detection and classification using wavelet transform and Hilbert phase envelope, 2015 Twenty First National Conference on Communications (NCC), Mumbai, India, pp. 1-6, 2015.

[3] : L. H. Cherif, S. M. Debbal, Adaptive filtering algorithm based on a wavelet packet tree for heart sound signal analysis. Int. J.Med. Eng. Inform. Vol. 10, No. 2, pp. 150–163, 2018

[4] : H. Li, G. Ren, X. Yu, et al., Discrimination of the diastolic murmurs in coronary heart disease and in valvular disease, IEEE Access, vol. 8, pp. 160407–160413, 2020.

[5] : P. Dhar, S. Dutta, & V. Mukherjee, Cross-wavelet assisted convolution neural network (AlexNet) approach for phonocardiogram signals classification. Biomedical Signal Processing and Control, Vol. 63, pp.102142, 2021.

[6] : S.M Debbal, F. Bereksi-Reguig, Second cardiac sound : analysis techniques and performance comparison, Journal of Mechanics in Medicine and Biology (JMMB), Vol. 5, No. 3, September2005.

[7] : S.M Debbal, F. Bereksi-Reguig, Filtering and classification of phonocardiogram signals using wavelet transform. Journal of Medical Engineering & Technology, Vol. 32, No. 1, pp. 53–65, 2008.

[8] : F. Meziani, S.M. Debbal, & A. Atbi, Analysis of phonocardiogram signals using wavelet transform. Journal of Medical Engineering & Technology, Vol. 36, No. 6, pp.283–302, 2012.

[9] : A. Hossain, S. Uddin, P. Rahman, et al., Wavelet and Spectral Analysis of Normal and Abnormal Heart Sound for Diagnosing Cardiac Disorders. BioMed Research International, vol. 2022, Article ID 9092346, 16 pages, 2022.

[10] : Z. Hossein-Nejad, M. Nasri, Heart Sound Classification based on Discrete Wavelet Transform and Group-based Sparse Features of PCG Signal, 2023 14th International Conference on Information and Knowledge Technology (IKT), Isfahan, Iran, Islamic Republic of Iran, pp. 218-222, 2023.

[11] : K. Abbas, R. Bassam, Phonocardiography Signal Processing, in Synthesis Lectures on Biomedical Engineering, edited by J. D. Enderle (Morgan & Claypool Publisher, New York, 2009).

[12] : F. Meziani, S. M. Debbal, &A. Atbi. Analyse du Degré de Sévérité Pathologique de La sténose aortiques(AS) par Application de La transformée en Ondelettes Continue (T.O.C), a l'occasion de : International Conférence on Multi Media Information Processing : CMIP'2012, Mascara, Algeria, 09-10 April 2012.

[13] : C. Liu, D. Springer, Q. Li, et al., An open access database for the evaluation of heart sound algorithms. Physiological measurement, vol. 37, no. 12, pp. 2181–2213, 2016.

[14] : I. Debbal, L. Hamza Cherif, & Y.N.E.H. Baakek, A new approach to phonocardiogram severity analysis, Journal of Medical Engineering & Technology, vol. 47, no 5, pp. 265-276, 2023.

[15] : I. Debbal, H. Boudis, Paramètres de discrimination pathologique des bruits cardiaques, Graduation project, Abou Bekr Belkaid University, Tlemcen, Algeria, 2020

[16] : GP. Armstrong. MD [Internet], Waitemata Cardiology, Auckland Valvular Disorders, MSD Manuals [updated 2023 April; cited 2024 January 03], Available from: https://www.msdmanuals.com/professional/cardiovascular-disorders/valvular-disorders

[17] : A. K. Dwivedi, S. A. Imtiaz, & E. Rodriguez-Villegas, Algorithms for automatic analysis and classification of heart sounds–a systematic review. IEEE Access, vol. 7, pp. 8316-8345, 2018.

[18] : D. Mason, Listening to the heart: A comprehensive collection of heart sounds and murmurs, 2nd ed. Philadelphia, Hahnemann University, School of Medicine, 2000.

[19] : L. Thoms, G. Colicchia, & R. Girwidz, Phonocardiography with a smartphone, Phys. Educ., vol. 52, no. 023004, pp. 1–4, 2017.

[20] : H. Naseri, M. R. Homaeinezhad, Detection and boundary identification of phonocardiogram sounds using an expert frequency-energy based metric, Ann. Biomed. Eng., vol. 41, no. 2, pp. 279–292, 2013.

[21] : A. L. Noponen, S. Lukkarinen, A. Angerla, et al., Phono-spectrographic analysis of heart murmur in children, BMC Pediatrics, vol. 7, no. 1, p. 23, 2007.

[22] : J. Grayzel, Gallop rhythm of the heart, Am. J. Med., vol. 28, no. 4, pp. 578–592, 1960.

[23] : I. Debbal, L. Hamza Cherif, & Y.N.E.H. Baakek, Pathological cardiac discrimination and severity monitoring of the phonocardiogram signal using the Discrete Wavelet Transform. In: Proceedings of the Conférence Nationale sur les Télécommunications et ses Applications (CNTA'22)., Ain-Temouchent University, pp. 387-390, December20-21 2022.

[24] : D. Imane, H.C. Lotfi, & B. Y. N. El Houda, Entropy parameter of cardiac degree severity analysis. Journal of Mechanics in Medicine and Biology, Vol. 24, No. 3 (2024), pp. 2350046, 2023.

[25] : A. Wang, T. M. Bashore, (Eds.), Valvular heart disease, Springer Science & Business Media. 2010.
[26] : G. P. Armstrong, MD [Internet]. Waitemata Cardiology, Auckland Valvular Disorders, MSDManuals [updated 2023 Apr; cited 2024 Jan 03]. Available from: https://www.msdmanuals.com/professional/cardiovascular-disorders/valvular-disorders/aortic-stenosis

Chap IV:

[1] : B. Ergen, Y. Tatar, Characterization of phonocardiogram signals using bispectral estimation, In Proceedings of the Eighth International Symposium on Signal Processing and Its Applications, IEEE, Vol. 1, pp. 203-206, August 2005.
[2] : K.C. Chua, V. Chandran, R. Acharya, & C.M. Lim, Application of higher order statistics/spectra in biomedical signals: a review, Medical Engineering and Physics, Vol. 32, No. 7, pp. 679-689, 2010.
[3] : A. M. Amiri, G. Armano, Heart sound analysis for diagnosis of heart diseases in newborns, APCBEE procedia, Vol.7, pp. 109-116, 2013.
[4] : R. G. Garcia, G. Valenza, C. A. Tomaz, & R. Barbieri, Instantaneous bispectral analysis of heartbeat dynamics for the assessment of major depression, in 2015 Computing in Cardiology Conference (CinC), pp. 781–784, September 2015.
[5] : S. Abdelouahed, F. Bourdji, Détection précoce d'épilepsie, Graduation project, Abou Bekr Belkaid University, Tlemcen, Algeria, 2016.
[6] : LJ. Hadjileontiadis, Continuous wavelet transform and higher-order spectrum: combinatory potentialities in breath sound analysis and electroencephalogram-based pain characterization, Philos Trans R Soc Math Phys Eng Sci, Vol. 376, No. 2126, pp. 20170249, 2018.
[7] : N. Mahmoodian, A. Boese, M. Friebe, & J. Haddadnia, Epileptic seizure detection using cross-bispectrum of electroencephalogram signal. Seizure, Vol. *66*, pp. 4-11, 2019.
[8] : I. Debbal, H. Boudis, Y.N.E.H. Baakek, & S.M. Debbal, Phonocardiograms Signals Analysis using the Graphical Bispectral Technique. Ann. Clin. Cases, Vol. 1, No. 2, pp. 1009, 2020.
[9] : S.A. Berraih, S.M.E.A. Debbal, Pathological discrimination of the phonocardiogram signal using the bispectral technique. Physical and Engineering Sciences in Medicine, Vol. 43, No. 4, pp. 1371-1385, 2020.
[10] : S.A. Berraih, S.M.E.A. Debbal, Severity cardiac analysis using the Higher-order spectra. Applied Mathematics and Computation, Vol. 409, pp. 126389, 2021.
[11] : I. Debbal, H. Boudis, Y.N.E.H. Baakek, and S.M. Debbal, Cardiac Pathologies Analysis on the Phonocardiogram Signals Using the Bispectral Technic, International Journal of Advanced Science and Technology, Vol. 29, No. 3, pp. 6764 – 6784, 2020.

[12] : S.A. Berraih, Y.N.E.H. Baakek, & S.M.E.A. Debbal, Preliminary study in the analysis of the severity of cardiac pathologies using the higher-order spectra on the heart-beats signals. Polish Journal of Medical Physics and Engineering, Vol. 27, No. 1, pp. 73-85, 2021.

[13] : Y.N.E.H. Baakek, I. Debbal, H. Boudis, & S.M. Debbal, Study of the impact of clicks and murmurs on cardiac sounds S1 and S2 through bispectral analysis. Polish Journal of Medical Physics and Engineering, Vol. 27, No. 1, pp. 63-72, 2021.

[14] : J.F. Bercher ,Signaux Aléatoires, École Supérieure d'Ingénieurs en Électrotechnique et Électronique, Educational handout, November 2001.

[15] : C. Ahlström, Processing of the Phonocardiographic Signal −Methods for the Intelligent Stethoscope, Linköping University, Sweden, 2006.

[16] : E. Bou Assi, L. Gagliano, S. Rihana, et al., Bispectrum Features and Multilayer Perceptron Classifier to Enhance Seizure Prediction, Sci Rep, Vol. 8, pp. 15491, 2018.

[17] : Y.N.E.H. Baakek, Parametric and non-parametric modeling for cardiac system identification, PhD thesis, Abou Bekr Belkaid University Tlemcen, Algeria, 2015.

[18] : G.R. Andrzejak, K. Lehnertz, F. Mormann, et al., Indications of nonlinear deterministic and finite-dimensional structures in time-series of brain electrical activity:Dependence on recording region and brain state, Physical Review, The American Physical Society, Vol. 64, pp.061907, 2001.

[19] : A. Goshvarpour, A. Goshvarpour, S Rahati, et al., Bispectrum estimation of electroencephalogram signal during meditation, Iran J Psychiatry BehavSci, Vol 6, No. 2, pp. 48-54, 2012.

[20] : C.L. Nikias, M.R. Raghuveer, Bispectrum estimation: a digital signal processing framework. Proc IEEE, Vol. 75, No. 7, pp. 869-91, 1987.

[21] : D. Kumar, R. Jadeja, & S. Pande, Wavelet bispectrum-based nonlinear features for cardiac murmur identification, Cogent Engineering, vol. 5, No 1, pp. 150290, 2018.

[22] : D.R. Brillinger, Time Series, Data Analysis and Theory, Holden-Day, 1981.

[23] : C.K Chua, Analysis of cardiac and epileptic signals using higher order spectra, Ph.D. thesis, Queensland University of Technology, Australia, 2010.

[24] : C. Strobl, A.L. Boulesteix, A. Zeileis, Bias in random forest variable importance measures: Illustrations, sources and a solution, BMC Bioinform, Vol. *8*, No. 25, 2007.

[25] : L.N. Rani, S. Defit, Determination of Student Subjects in Higher Education Using Hybrid Data Mining Method with the K-Means Algorithm and FP Growth. Int. J. Artif. Intell. Res., Vol. *5*, pp. 91–101, 2021.

[26] : W. Shang, H. Dong, and H. Dong, A Novel Feature selection algorithm for text categorization, Expert Syst. Appl., Vol. 33, pp. 1–5, 2007.

[27] : E.A. Algehyne, M.L. Jibril, N.A. Algehainy, et al., Fuzzy Neural Network Expert System with an Improved Gini Index Random Forest-Based Feature Importance Measure Algorithm for Early Diagnosis of Breast Cancer in Saudi Arabia. *Big Data Cogn. Comput. Vol. 6,* pp.13, 2022.

[28] : R. Genuer, J.-M. Poggi, and C. Tuleau-Malot, Variable selection using random forests, Pattern Recogn. Lett. Vo. 31, No. 14, pp. 2225-2236, 2010.

[29] : J. Brownlee, How to choose a feature selection method for machine learning. Mach. Learn. Mastery, Vol. 10, 2019.

[30] : A. Almadhor, G.A. Sampedro, M. Abisado, et al. Efficient feature-selection-based stacking model for stress detection based on chest electrodermal activity. Sensors, Vol. 23, No. 15, pp. 6664, 2023.

Chap V:

[1] : H. Jeon, S. Oh, Hybrid-Recursive Feature Elimination for Efficient Feature Selection. Appl. Sci., Vol.10, pp. 3211, 2020.

[2] : Khan Mamun, M. M. R., & Elfouly, T., Detection of Cardiovascular Disease from Clinical Parameters Using a One-Dimensional Convolutional Neural Network. Bioengineering, Vol.10, No.7, pp-796, 2023.

[3] : E.A. Algehyne, M.L. Jibril, N.A Algehainy, et al., Fuzzy Neural Network Expert System with an Improved Gini Index Random Forest-Based Feature Importance Measure Algorithm for Early Diagnosis of Breast Cancer in Saudi Arabia. Big Data Cogn. Comput. Vol. 6, pp.13, 2022.

[4] : A. Almadhor, G.A. Sampedro, & M. Abisado, et al. Efficient feature-selection-based stacking model for stress detection based on chest electrodermal activity. Sensors, Vol. 23, No. 15, pp. 6664, 2023.

[5] : J. Liang, L. Hou, Z. Luan, & W. Huang, Feature Selection with Conditional Mutual Information Considering Feature Interaction. Symmetry, Vol.11, pp.858, 2019.

[6] : N. Pudjihartono, T. Fadason, A.W. Kempa-Liehr, & J.M. O'Sullivan, A review of feature selection methods for machine learning-based disease risk prediction. Frontiers in Bioinformatics, Vol.2, pp.927312, 2022.

[7] : C. Shannon, A mathematical theory of communication, Bell Syst. Tech. J. Vol.27, pp.379–423, 1948.

[8] : K. Iskarous, C. Mooshammer, P. Hoole, et al, The coarticulation/invariance scale: Mutual information as a measure of coarticulation resistance, motor synergy, and articulatory invariance. The Journal of he acoustical society of America, Vol.134, No.2, pp.1271-1282, 2013.

[9] : A. Y. W. Prasetyo, N. H. Murpratama, & M. D. Prasetyo, Penggunaan Alat Candling Otomatis Berbasis Aplikasi Matlab, Politeknik Pembangunan Pertanian Yogyakarta – Magelang, 2020.

[10] : Y.S. Ambarwati, S. Uyun, Feature selection on magelang duck egg candling image using variance threshold method. In 2020 3rd International Seminar on Research of Information Technology and Intelligent Systems (ISRITI), IEEE, pp. 694-699, December 2020.

[11] : I. Kononenko, Estimating attributes: Analysis and extensions of RELIEF, In European conference on machine learning, Berlin, Heidelberg: Springer Berlin Heidelberg, pp. 171-182, April 1994.

[12] : Y. Saeys, I. Inza, P. Larrañaga, A review of feature selection techniques in bioinformatics. Bioinformatics, Vol.23, pp. 2507–2517, 2007.

[13] : H. Liu, H. Motoda, Computational Methods of Feature Selection; Chapman and Hall/CRC: New York, NY, USA, 2007.

[14] : CX. Feng, Z. Yu, U. Kingi, & M.P. Baig, Threefold vs. fivefold cross validation in one-hidden-layer and two-hidden-layer predictive neural network modeling of machining surface roughness data, Journal of Manufacturing Systems, Vol. 24, No.2, pp. 93–107, 2005.

[15] : R. Picard, D. Cook, Cross-validation of regression models, Journal of the American Statistical Association, Vol.79, No.387, pp. 575–83, 1984.

[16] : C. Shao, K. Paynabar, T.H. Kim, et al., Feature selection for manufacturing process monitoring using cross-validation, Journal of Manufacturing Systems, Vol.32, No.4, pp.550-555, 2013.

[17] : S. Hochreiter, J. Schmidhuber, Long Short-Term Memory, Neural Computation, Vol.9, No.8, pp.1735-1780, 1997.

[18] : E. Kang, [Internet], Long Short-Term Memory (LSTM): Concept, [updated 2017 September; cited 2024 December 24], Available from: https://medium.com/@kangeugine/long-short-term-memory-lstmconcept-cb3283934359

[19] : F.A. Khan, A. Abid, & M.S. Khan, Automatic heart sound classification from segmented/unsegmented phonocardiogram signals using time and frequency features, Physiological measurement, Vol.41, No.5, pp. 055006, 2020.

[20] : D. S. B. Sundaram, D. N. Damani, A. Kapoor, et al., Deep learning based discrimination of phonocardiogram signal with normal heart sounds and murmur: Feasiblity study. Biomedical Sciences Instrumentation, vol.57, no.2, 2021.

[21] : D. Imane, H.C. Lotfi, and B. Y. N. El Houda, Entropy parameter of cardiac degree severity analysis. Journal of Mechanics in Medicine and Biology, Vol. 24, No. 3 (2024), pp. 2350046, 2023.

[22] : I. Debbal, L. Hamza Cherif, and Y.N.E.H. Baakek, A new approach to phonocardiogram severity analysis, Journal of Medical Engineering & Technology, vol. 47, no 5, pp. 265-276, 2023.

[23] : I. Debbal, H. Boudis, Paramètres de discrimination pathologique des bruits cardiaques, Graduation project, Abou Bekr Belkaid University, Tlemcen, Algeria, 2020.

[24] : I. Debbal, L. Hamza Cherif, and Y.N.E.H. Baakek, Comparison study between the Discrete Wavelet Transform DWT and the Bispectral Analysis for the cardiac severity assessment, Les Journées Scientifiques du Salon International de la Santé (SIMEM 2024) : Symposium on Innovative Research in Biomedical Engineering (SIRBE'2024), Oran,Algeria, 2024.

[25] : YASEEN, G.Y.SON, & S. KWON, Classification of heart sound signal using multiple features. Applied Sciences, Vol. 8, No 12, pp. 2344, 2018.

[26] : A. Raza, A. Mehmood, S. Ullah, et al., Heartbeat sound signal classification using deep learning. Sensors, Vol. 19, No 21, pp. 4819, 2019.

[27] : S. Aziz, M.U. Khan, M. Alhaisoni, et al., Phonocardiogram signal processing for automatic diagnosis of congenital heart disorders through fusion of temporal and cepstral features. Sensors, Vol. 20, No 13, pp. 3790, 2020.

[28] : B. Ahmad, F. Khan, K. Ahmad, N. Kaleem, et al. Automatic classification of heart sounds using long short-term memory. In : 2021 15th International Conference on Open Source Systems and Technologies (ICOSST). IEEE, pp. 1-6, 2021.

[29] : A. Özkan, K. Mustafa, Effect of Hilbert-Huang transform on classification of PCG signals using machine learning. Journal of King Saud University-Computer and Information Sciences, Vol. 34, No 10, pp. 9915-9925, 2022.

General conclusion

General Conclusion

The science of health has been constantly evolving since the dawn of time, and the research published and the discoveries made to date bear witness to the great efforts and immense knowledge that has been passed down from generation to generation. The same is true in the field of biomedical electronics, where scientific research has produced important and interesting results thanks to the enormous progress made in recent years. With the help of new applied technologies and the use of computer tools, an optimal approach has been achieved in the complex study of the functioning of the organs of the human body, such as the heart: the essential motor and source of life for everyone.

Since the invention of the stethoscope, cardiac auscultation has become a key diagnostic method, with doctors referring to heart sounds to detect anomalies, screen for cardiac pathologies and establish the most reliable diagnoses. In addition, with the advent of phonocardiography, this task has become increasingly easier for doctors, since the phonocardiogram (PCG) signal translates cardiac activity with greater precision.

To this end, several digital analysis methods have emerged to help the cardiologists make a more reliable diagnosis of his patient, since these methods allow better characterisation and bring out all the information useful for the diagnosis.

It is in this same context that we carried out this Ph.D. thesis in which we applied frequency and time-frequency analysis techniques (Fast Fourier Transform (FFT), Short Time Fourier Transform (STFT), Discrete Wavelet Transform (DWT), HOSA-Bispectral) to a database dedicated to studying the cardiac severity of phonocardiogram (PCG) signals to arrive at a possible and satisfactory discrimination between three different severity levels:

-Light
-Moderate
-Severe

To validate our results, we employed machine learning and neuronal networks classifiers as the K-Nearest Neighbor (KNN), One-vs-All Support Vector Machine (OVA-SVM), and the Long Short Time Memory (LSTM). The chosen techniques have been studied individually to test the efficiency of each one of them and its features before embarking on the main phase of this study, namely the selection of the optimal technique for cardiac severity assessment through a complex comparison workflow.

The selected features from the complex comparison workflow led to an unexpected conclusion. Rather than choosing a unique optimal technique, the workflow highlighted that the majority of severity information

is in the frequency domain and that entropy holds an important role in cardiac severity assessment. Thus, the final selection included a high number of frequency features and both spectral and time-frequency entropies. On the other hand, even though the bispectral features displayed great results when studied individually, their efficiency does not compare with the frequency and time-frequency features.

To conclude, we recommend prioritising features that could quantify information like entropy and are related to the signals' frequencies when studying cardiac severity assessment. In our case, the FFT, STFT, and DWT delivered such features.

The obtained results open to us other research perspectives:

- Explore heart sounds for cardiac severity study using the recommended features.
-Work on an automatic severity-ranking algorithm using the selected features and the medical information mentioned in chapter II.
-Adapt the algorithms in order to materialise these results for use in real-life situations.

We hope that our modest research work in phonocardiogram signal processing will be just one of the many milestones achieved by the research members of the Génie Biomedical Laboratory and especially the 'traitement des signaux sonores et ultrasonores' Research Team over the last few years.

Appendices

Journal of Theoretical and Applied Information Technology
31st May 2023. Vol.101. No 10

ISSN: 1992-8645 www.jatit.org E-ISSN: 1817-3195

PATHOLOGY CARDIAC MONITORING STUDY OF THE PHONOCARDIOGRAM SIGNAL

DEBBAL IMANE[1], HAMZA CHERIF LOTFI[2], BAAKEK YETTOU NOUR EL HOUDA[3]

[1,2,3] *Genie* Biomedical Laboratory (GBM), Faculty of Technology, University Abou Bakr Belkaid Tlemcen, Genie Biomedical department, Algeria

E-mail: [1]Imane.debbal@univ-tlemcen.dz, [2]Lotfi.hamzacherif@univ-tlemcen.dz, [3]nourelhouda.baakekyettou@univ-tlemcen.dz

ABSTRACT

In this paper, we will discuss the efficiency of the Fast Fourier transform (FFT) and the Short-Time Fourier Transform (STFT) to distinguish cardiac pathological signals, along with following the severity evolution of diverse diseases through three selected features. The cardiac signals analysed and previously classified via some clinical data will be arranged into three main classes or groups: a group of signals containing neither clicks nor murmurs and having a similar morphology, a second group of signals containing only clicks (reduced murmurs), and a third group of signals with a significant murmur. The features that we are going to define from each technic will help us in this sense to classify the different signals analysed in one of the mentioned groups. We will then extract the same features from a fourth group of phonocardiogram (PCG) signals suffering from murmur with different severity levels. In the end, we will discuss the accuracy of these features with the Energetic Ratio (ER) parameter and a K-Nearest Neighbor classifier in terms of classifying phonocardiogram (PCG) signals according to their pathological origin and cardiac severity level. An accuracy of 99.2% is achieved when using a combination of time and spectral features (frequency band (FB), frequency extent (ΔF), time extent (ΔT)) to classify the PCG signals in the three main groups and a 98.9% accuracy when ranking signals according to their severity level (Light, Moderate, Severe).

The main aim of this paper is to proceed with the use of the FFT and the STFT technics to obtain information likely not only to discriminate the three groups' cases but also to detect the level (or degree) of severity in the same studied pathology as well. Thus, the intent of this study on phonocardiogram (PCG) signals is to follow the evolution of the pathology at different levels and identify each severity degree via the extracted features, which makes the originality of this paper. These results can only help the clinician to make his decision with serenity.

Keywords: *Phonocardiogram, Normal, Pathological, Classification, Discrimination, Severity, FFT, STFT, Spectral, Time Extency, Frequency Extency.*

1. INTRODUCTION

A phonocardiogram (PCG) is a scheme for emulating high precision copy of the sounds made by the heart along with the murmurs made during the procedure of pumping blood [1]. The cardiac signals recorded via a phonocardiograph may reflect divers' pathological conditions of cardiovascular system that being the case for why several researchers focus on heart sounds analysis (acquisition, signal processing, segmentation and feature extraction from different PCG cycles).

Under normal conditions, two heart sounds can be distinguish on the graphic representation of the recorded phonocardiogram (PCG). The first heart sound known also as heartbeat S1, corresponding to the beginning of ventricular systole, is the result of the closure of the mitral and tricuspid valves [2]. While the second heartbeat S2, referring to the end of the ventricular systole and marking the beginning of the diastole, is associated with the closure of the aortic and pulmonic valves [2]. Other than S1 and S2, murmurs and short murmurs (clicks) appears indicating abnormal heart condition. Murmurs are sounds resulting from certain cardiovascular diseases that are audible during the systole, the diastole, or both [3][4].

Stenosis and regurgitation are the two ailments who relate to the opening and the closing of the valves detected by analysing the PCG signal [1]. Therefore the algorithms used for cardiac signals processing is more on a quantitative, precise and objective

interpretation of heart sounds [5], improving the process of cardiovascular diagnosis. Beyond this, computer-assisted auscultation allows the detection of pathologies who are unrecognized through a conventional auscultation [6].

Hence, researchers used numerous signal-processing tools on PCG recordings for various purposes. Many denoising algorithms have been proposed such as parameter extraction using Discrete Wavelet Transform (DWT) [7], DWT decomposition level exploitation [8-10], Empirical Mode Decomposition [11].

In another study, Baakek et al. conducted a comparative study to highlight the impact of clicks and murmurs on heart sound using an STFT spectrogram [12]. The power spectrum was obtained using FFT analysis, later employed as a feature to classify and discriminate the PCG signals database [13]. In [14], the authors applied an FFT and STFT algorithm on divers PCG signals and used the FFT spectrum to identify the heart sound component as a first step, then extracted the frequency extent of both heart sound 1 (S1) and heart sound 2 (S2). To affirm which of the heart sounds is concerned by the pathology and which of their component is directly affected. The frequency extend values extracted from the STFT spectrogram, discriminated between diastolic and systolic murmur of the studied cardiac pathologies. Hence, these murmurs did not considerably affect the time-frequency content of the sounds S1 and S2.

In this paper, we are focusing on the efficiency of the frequency feature of the Fast Fourier Transform (FFT) and the time-frequency characteristics of the Short-Time Fourier Transform (STFT) to classify different cardiac signals, in one of three pre-established phonocardiogram groups and then study the ability of these characteristics to follow the evolution of the pathology. Therefore, our database classified via some clinical data will be arranged into three main classes or groups: a group of signals containing neither clicks nor murmurs and having a similar morphology, a second group of signals containing only clicks (reduced murmurs), and a third group containing signals with large murmurs. The first step of this work will be to analyse the PCG signals with the FFT and STFT technics. Then, follow with feature extraction (frequency band, time extent, frequency extent) and an Energetic Ratio (ER) parameter comparison / K-Nearest Neighbor (KNN) classification process.

We will proceed with the same analysis on a fourth group containing PCG signals with different severity levels of the same pathology. The obtained results will be used in a KNN classifier to classify the fourth group signals into three classes according to their severity level. Plus, an ER parameter comparison to appreciate the features' variation and evolution.

One of the limitations of this analysis is the possibility of the extracted features to classify the pathological signals of the first group in the second group. Since some of the first group signals are morphology similar to a healthy PCG signal. Yet, their frequency information may be affected by the pathology. The second limitation is the inability of these features to separate close severity levels, which may lead to an incorrect classification and a rather affected accuracy value.

In the end, the correlation of these features with the ER parameter helps us find a plausible medical explanation for the features' variation and evolution.

2. MATERIALS AND METHODS

2. 1 PCG signals database

Based on clinical data, we can classify the PCG signals into four distinct groups (Table1):

- Group 1 (G1): PCG signals having neither click (reduced murmur) nor significant murmur.
- Group 2 (G2): PCG signals with clicks.
- Group 3 (G3): PCG signals with clicks or murmurs.
- Group 4 (G4): PCG signals with murmurs including different severity levels.

We aim through this study to obtain relevant parameters able to classify our signals into the three main groups and follow the evolution of the cardiac pathology concerned.

The diagram below (Figure 1) illustrates how we proceeded with this study. The relevant parameters calculated during the features extraction step will be introduced into a KNN classifier for a multi-class classification. In addition to that, we used the energy rate parameter (or energetic ratio) ER, since recognised by researchers as a predominant element for pathology monitoring, to compare our results with. We implemented the same program mentioned by previous papers using this parameter for similar research purposes.

We also checked the accuracy of the ER parameter with a KNN classifier to see if it is efficient for this paper' purposes. The classification process consists of classifying the PCG signals into the three main groups as a first step and then classifying the fourth

group of PCG signals into three classes according to their severity level (light, moderate, severe).

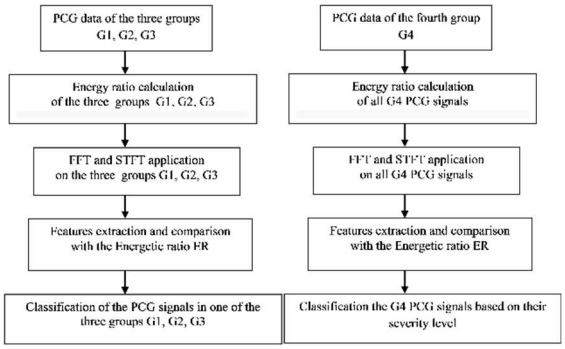

Figure1. Flow Diagram of features extraction on PCG signals and comparison of pathological severity using the FFT and STFT technic

The table 1 below defines the PCG signals of the four groups (G1, G2, G3 and G4) used for detecting cardiac pathological differences.

Table1 PCG signals used for the four groups

PCG signals Group1 (G1)	Abbreviation	**PCG signals Group2 (G2)**	Abbreviation
Normal heartbeat cardiac sound	N	Ejection click	EC
Innocent murmur	IM	Early aortic stenosis	Eas
Coarctation of the aorta	Coa	Late systolic	LS
		Aortic gallop	AG
PCG signals Group3 (G3)	Abbreviation	**PCG signals Group4 (G4)**	Abbreviation
Systolic pulmonary Stenosis	PS	Aortic stenosis	As1,As2, As3,As4
Aortic regurgitation	Ar	Mitral stenosis	Ms1,Ms2 ,Ms3,Ms4
Tricuspid regurgitation	Tr	Mitral regurgitation	Mr1,Mr2, Mr3,Mr4

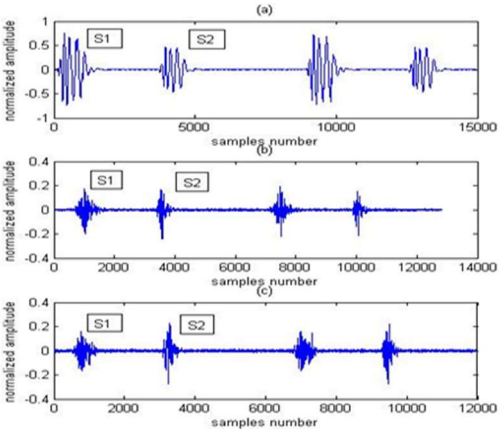

Figure2. Time representation of a two cycles PCG signals of the group1 (a) the normal signal (N), (b) the innocents murmur signal (IM),(c) the coarctation of the aorta signal (coa).

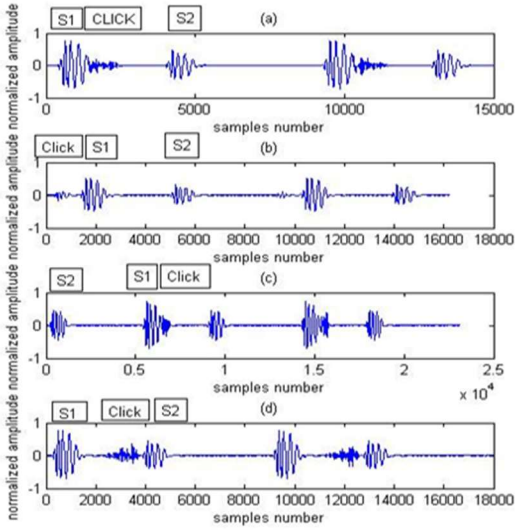

Figure3. Time representation of a two cycles PCG signals of the group2 (a) the early aortic stenosis signal (Eas),
(b) the aortic gallop signal (AG),
(c) the ejection click signal (EC),
(d) the late systole signal(LS).

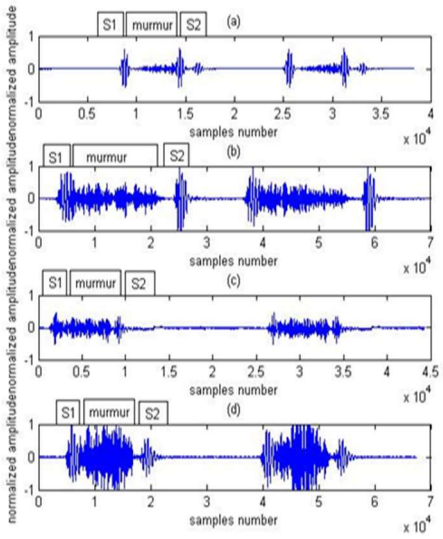

Figure4. Time representation of a two cycles PCG signals of the group3. (a) the systolic pulmonary stenosis signal (PS), b) the aortic regurgitation signal (Ar), (c) the tricuspid regurgitation signal (Tr), (d) the aortic stenosis signal(As).

2.2 Theoretical background

2.2.1 Fast Fourier Transform (FFT)

In 1882, Joseph Fourier discovered that we could represent any periodic function as an infinite sum of periodic complex exponential functions [15]. Later then extended it to any discrete time function. The FT is widely used and usually implemented in the form of FFT algorithm (fast Fourier transform)[16]. The mathematical definition of the FT is given below.

$$X(f) = \int x(t)\, e^{-j2\Pi ft}\, dt \qquad (1)$$

Where t and f are respectively the time and frequency parameters. It defines the spectrum of s(t) which consists of components at all frequencies over the range for which it is non zero [17].

The Fourier Transform (FT) is the most famous and oldest of the transformations used in signal processing fields. During this transformation, the signal is decomposed into a set of basic functions, which are the cosine, the sine, or the imaginary exponential.

The so-called Fourier series decomposition method, consist in decomposing the signal into a sum of sinusoidal function of different frequencies.

The Fourier series is the most used tool to transit from the time domain to the frequency domain. Moreover, a temporal analysis of a signal is often followed by frequency analysis. Since the first representation informs us about the signal's duration and its discontinuities, the second presents the periodicity of the signal.

For the Fourier Transform to exist, the signal must be square summable, i.e of finite energy. For real signals, this condition is always satisfied since the measurement is made over a finite time.

Fourier analysis implicitly assumes that the signal is identical to itself outside the measurement interval. The function (w) being periodic of period T, it is usual to limits its definition to [-T/2, T/2].

Here is one of the properties of the Fourier transform [18], called Parseval identity (conservation of energy independent of any time or frequency variation).

$$\int_{-\infty}^{+\infty} |s(t)|^2 dt = \frac{1}{2\Pi} \int_{-\infty}^{+\infty} |\hat{s}(w)|^2 dw \qquad (1)$$

In general, we can define the Fourier Transform as a linear application which associates N values s(0),…,s(k),…,s(N-1), N other values

$$\hat{S}_0, \ldots\ldots, \hat{S}_n, \ldots\ldots, \hat{S}_{N-1}$$

Defined by:

$$\hat{s}_n = \sum_{k=0}^{N-1} s(k) e^{-j2\Pi kn/N} \qquad (2)$$

$$n \in \{0, \ldots, N-1\}$$

Where N represents the minimum number of samples to be taken to reconstruct the signal s(t). In this case, we will name this transform, discrete Fourier transform. The inverse discrete Fourier transform is written:

$$s(k) = \frac{1}{N} \sum_{n=0}^{N-1} s_n e^{j2\Pi kn/N}, k \in \{0, \ldots, N-1\} \qquad (3)$$

Sampling

By definition, a signal s(t) of finite energy whose Fourier transform has bounded support [-B, B], is entirely defined by its samples s(kTe) taken at the sampling frequency fe $\geq 2B$. The sampling process consists in multiplying the signal s(t) by the sampling function e(t).

$$\tilde{s}(t) = s(t)e(t) = \sum_{k=-\infty}^{+\infty} s(kTe)\delta(t - kTe) \qquad (4)$$

With $\tilde{s}(t)$ is the sampled signal.

The Fourier Transform is then written as the following

$$\tilde{\hat{s}}(f) = \frac{1}{Te}\sum_{n=-\infty}^{+\infty} s\left[f - \frac{n}{Te}\right] \quad (5)$$

To prevent the spectrum from folding up to the axes of symmetry, the signal must not contain any frequency higher than fe/2.

N.B;

The Fast Fourier Transform (FFT) is an algorithm, which makes it possible to calculate Discrete Fourier Transforms DFT. The DFT appears in many applications in signal processing because of its aptitude to determine the weighting between different discrete frequencies. Therefore, the discrete data taken as input is often called a ***signal,*** and in this case, it is defined in the time domain. The output values are then called the ***spectrum*** and are defined in the frequency domain.

2.2.2 Short-time Fourier transforms (STFT)

The STFT consist on calculating the Fourier transform of a sliding windowed version of the time signal s(t). The location of the sliding window adds a time dimension and one gets a time-varying frequency analysis.

The mathematical representation of STFT is:

$$S(t,f) = \int_{-\infty}^{+\infty} s(\tau)w(\tau - t)e^{-j2\pi \ ft}d\tau \quad (6)$$

Where $w(\tau - t)$ it is the sliding window applied to the signal $s(t)$, f is the frequency and t is the time.

The length of the window is chosen so that to maintain signal stationary in order to calculate the Fourier transform. To reduce the effect of leakage (the effect of having finite duration), each sub-record is then multiplied
by an appropriate window and then the Fourier transform is applied to each sub-record. As long as each sub-record does not contain rapid changes the spectrogram will give an excellent idea of how the spectral composition of the signal has changed during the whole time record.[16]

2.3 Parameters study and analysing

2.3.1Frequency Band

It is the frequency range occupied by one cycle of a PCG signal (Figure 5)

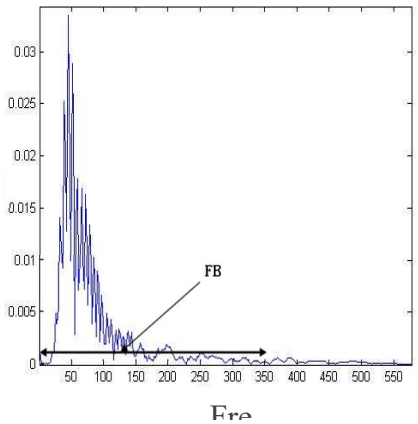

Figure 5: Illustrate the FB feature of a normal PCG case on an FFT spectral representation.

2.3.2 Temporal extent (Δ*T*) and frequency extent (Δ*F*)

The Figure 6 down below illustrate de definition of these two features.

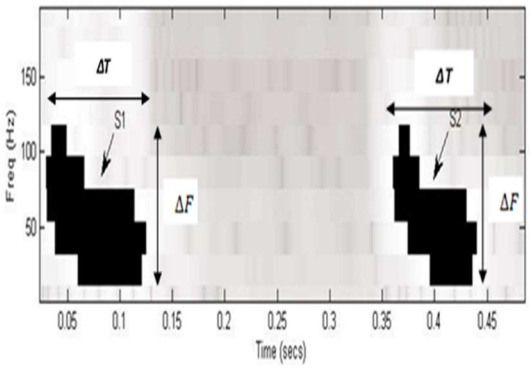

Figure 6: Illustrate the ΔT and ΔF features on an STFT representation for a normal PCG case

2.3.3 Energetic Ratio (ER)

Used in this study, as a reference feature to compare the results obtained by using FFT and STFT technic with. Previous research mentioned that the ER is very efficient for tracking cardiac disease severity [12, 19][20-27].

The ER provides an idea of the relative energy of cardiac murmurs relative to other heart sounds S1 and S2 [24], which make him important indicators on estimating the degree of heart severity. It is defined as in the equation below [19]

$$ER = \frac{E_2}{E_1 + E_2} \times 100 \quad (7)$$

Where E2 is the heart murmur energy, E1 is the energy of S1 + S2 and (E1 + E2) is the total energy. In case ER equals to 100%, we have a complete dominance of the clicks or murmur over the two heart sounds (S1 and S2).

2.4 Machine learning method

2.4.1 K-nearest neighbor

The main principle of nearest neighbor methods is to find the nearest predetermined number of training samples to the new point and estimate the class. The number of samples -K- is a user-defined constant (k-nearest neighbor learning) or a variable depending on the local density of points [28]. Distance can generally be any metric measure: for example, the standard Euclidean distance is the most common choice. Neighbor-based methods are known as non-generalized machine learning methods and classification is sample-based learning. The classification is calculated by a simple majority vote of each point's nearest neighbors, and a query point is assigned the data class with the most representative among the point's nearest neighbors. [29-31]

The parameter setting of KNN model is shown in Table

Table 2: K-Nearest Neighbor parameter setting

KNN parameter	Value
Learning rate	1e-4
Number of epoch	200
Neighbours number	3
Distance	Euclidian

3. RESULTS

Just like illustrated in the diagram (figure1) this work is divided into two parts. The first one is about a classification of pathological severity between the three groups G1, G2, G3, when the seconds aim is to classify the G4 PCG signals based on their severity level.

3.1 Analysis results of the PCG signals of the four groups (G1, G2, G3 and G4) by using the FFT technique.

All the tables include the results obtained when implementing the energetic ratio ER program.

Table 3 and table 4 give the results obtained by applying the FFT technique to the four groups (G1, G2, G3 and G4).

The figure 7 represent the FFTs' frequency spectrum of one PCG signal from each group, which we used to extract the frequency band (FB) feature.

Figure 8 holds the obtain results of the frequency band for the three groups of signals.

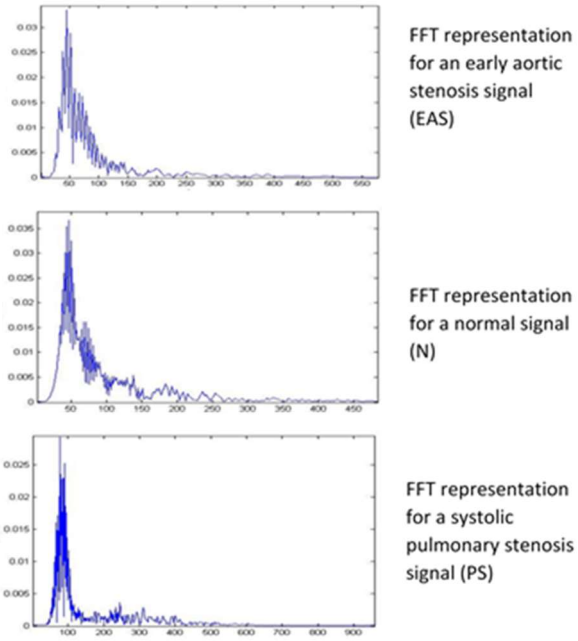

Figure 7: FFTs' frequency spectrum of one PCG signal from each of the three groups.

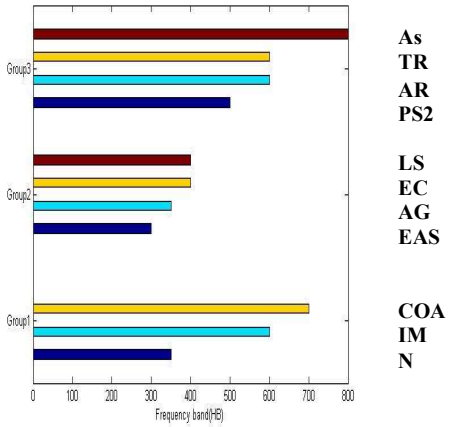

Figure 8: variation of frequency Band (FB) feature for the three groups (G1, G2 and G3) PCG signals.

3.2 Analysis results of the PCG signals of the four groups (G1, G2, G3 and G4) by using the STFT technique.

Table 6 and table 7 give the results obtained by applying the STFT technic to the four groups (G1, G2, G3 and G4).

Figure 9 and figure 10 give an overview on the application of the STFT technic on the PCG signals (G1 and G4)

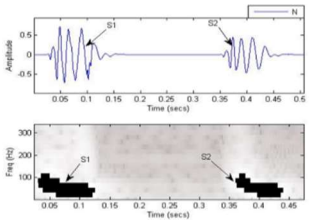

STFTrepresentation for a normal signal (N)

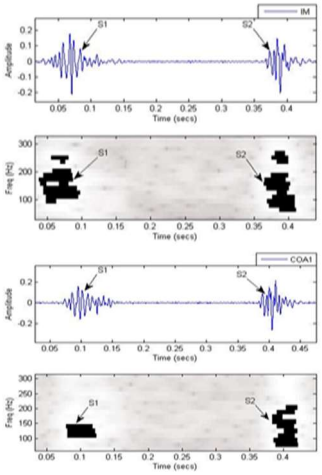

STFT representation for an innocent murmur signal (IM)

STFT representation for a coarctation of the aorta signal (COA)

Figure 9: STFT representation for group 1 PCG signals

Table 3: variation of frequency band (FB) and energetic ratio (ER) features for the three group PCG signals

Features / signals	One PCG cycle	
	Energetic Ratio (ER)(%)	Frequency Band (FB) (Hz)
PCG signals without clicks nor murmurs		
N	0	0 - 350
IM	0	0 - 600
Coa1	0	0 - 700
PCG signals with clicks		
EAS	2.5	0 - 300
AG	2.8	0 - 350
EC	3.9	0 - 400
LS	4.1	0 - 400
PCG signals with murmurs		
PS2	5.3	0 - 500
AR	38.3	0 - 600
TR	57.8	0 - 600
AS	85.4	0 - 800

Table 4: variation of ΔT, ΔF and the energetic ratio ER features within the three groups

Journal of Theoretical and Applied Information Technology
31st May 2023. Vol.101. No 10

ISSN: 1992-8645 www.jatit.org E-ISSN: 1817-3195

Features / signals	Energetic ratio (ER)	S1		S2		Murmurs		Click	
		Temporal Extent Δt (sec)	Frequency Extent Δf (Hz)	Δt (sec)	Δf (Hz)	Δt (sec)	Δf (Hz)	Δt (sec)	Δf (Hz)
PCG signals without clicks nor murmurs									
N	0	0.11	130	0.09	130				
IM	0	0.08	129	0.05	144				
Coa1	0	0.04	67	0.04	159				
PCG signals with clicks									
EAS	2.5	0.15	145	0.14	130			0.02	65
AG	2.8	0.11	141	0.12	128			0.08	85
EC	3.9	0.10	135	0.12	126			0.08	160
LS	4.1	0.10	129	0.12	110			0.1	200
PCG signals with murmurs									
PS2	5.3	0.07	140	0.08	136	0.22	215		
AR	38.3	0.07	235	0.06	136	0.27	301		
TR	57.8	0.06	287	0.05	287	0.30	345		
AS	85.4	0.05	416	0.04	374	0.35	517		

Table 5: Variation of FB and ER features within the fourth group of signals

Features / signals	One PCG Cycle	
	Energetic Ratio (ER) (%)	Frequency Band FB (Hz)
PCG signals with diastolic murmurs		
Mitral Stenosis		
MS1	12	0 - 600
MS2	40	0 - 550
MS3	76	0 - 500
MS4	85	0 - 450
PCG signals with systolic murmurs		
Aortic Stenosis		
AS1	55	0 - 550
AS2	93	0 - 450
AS3	94	0 - 400
AS4	95	0 - 300
Mitral Regurgitation		
MR1	14	0 – 1300
MR2	24	0 – 1200
MR3	56	0 – 950
MR4	75	0 – 950

Journal of Theoretical and Applied Information Technology
31st May 2023. Vol.101. No 10

ISSN: 1992-8645 www.jatit.org E-ISSN: 1817-3195

Table 6: Variation of ΔT, ΔF and ER features within the fourth group signals (Mitral stenosis (MS) aortic stenosis (AS and mitral regurgitation (MR)).

Features / Signals	Energetic ratio (ER)	S1		S2		murmurs	
		Temporal extent Δt (sec)	Frequency extent Δf (Hz)	Δt (sec)	Δf (Hz)	Δt (sec)	Δf (Hz)
PCG signals with diastolic murmurs							
Mitral Stenosis							
Ms1	12	0.04	131	0.15	480	0.16	411
Ms2	40	0.08	285	0.13	431	0.30	110
Ms3	76	0.08	285	0.08	256	0.22	90
Ms4	85	0.09	215	0.08	225	0.05	87
PCG signals with systolic murmurs							
Aortic Stenosis							
As1	55	0.01	140	0.02	250	0.25	600
As2	93	0.04	258	0.03	275	0.26	480
As3	94	0.07	330	0.03	300	0.26	460
As4	95	0.07	340	0.05	310	0.28	300
Mitral regurgitation							
Mr1	14	0.09	105	0.06	128	0.28	160
Mr2	24	0.09	107	0.06	111	0.28	323
Mr3	56	0.07	135	0.05	110	0.17	352
Mr4	75	0.07	172	0.05	86	0.17	452

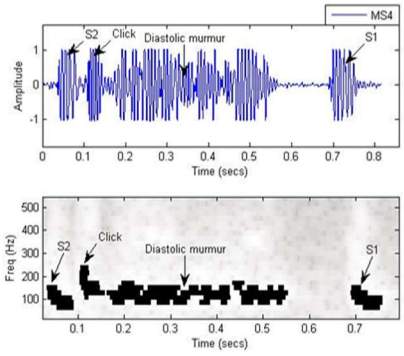

Temporal and STFT representation for the MS4 signal

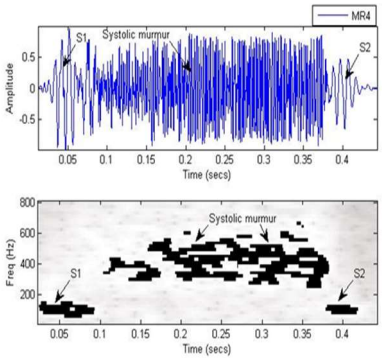

Temporal and STFT representation for the MR4 signal

Figure 10: Temporal and STFT representation for one of the MS (Mitral Stenosis) and MR (Mitral Regurgitation) signals.

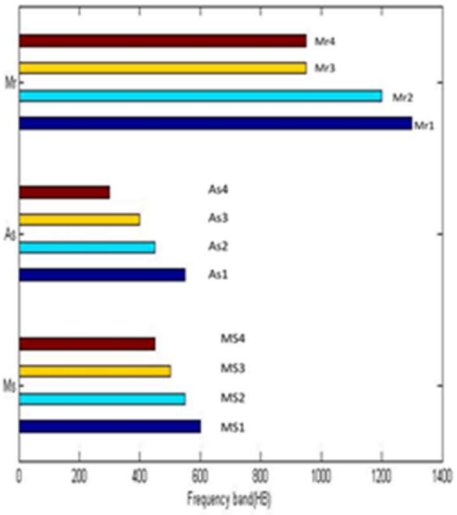

Figure 11: variation of the frequency band (FB) feature for the fourth group PCG signals: mitral stenosis (MS), aortic stenosis (AS), mitral regurgitation (MR);

3.3 Machine learning results

This classification will help us check the efficiency of the FFT and the STFT features to classify the database into the three main groups previously rearranged according to clinical data:

- Group 1 (G1): PCG signals having neither click (reduced murmur) nor significant murmur.
- Group 2 (G2): PCG signals with clicks.
- Group 3 (G3): PCG signals with clicks or murmurs.

Table 7 summarizes the performances of the KNN classifier to rearrange the database signals into the three groups using frequency and time-frequency features.

Table 7: performance table of the KNN classifier into the three main group

Performance	Accuracy	Sensitivity	specificity
Values	99.2%	98.2%	99.4%

We also proceeded with a new KNN classification for the fourth group PCG signals. This time, the classification consisted on ranking the fourth group signals into three classes according to their severity level (light, moderate, severe).

Table 8: performance table of the KNN classifier into three severity levels

Performance	Accuracy	Sensitivity	specificity
Values	98.9%	97.9%	99.1%

To evaluate the accuracy of the Energetic ratio ER parameter for this paper' purposes, we proceeded with the same classification process than the FFT and STFT, but with the ER values as a classification feature.

Table 9 : performance table of the KNN classifier in the three main groups using the energetic ratio ER.

Performance	Accuracy	Sensitivity	specificity
Values	99.5%	98.5%	99.7%

Table 10: performance table of the KNN classifier into three severity levels using the energetic ratio ER.

Performance	Accuracy	Sensitivity	specificity
Values	98.8%	97.8%	99%

4. DISCUSSION

4.1 Comparison of pathological severity between the three groups (G1, G2 and G3)

We applied the Fast Fourier Transform (FFT), the Short-Time Fourier Transform (STFT) and the Energetic Ratio (ER) algorithms on the three groups of PCG signals. In this section, we will compare these results with the energetic ratio ER for plausible medical explanations.

4.1.1 The FFT analysis of the three groups

The figure 7 represent the FFTs' frequency spectrum of one PCG signal from each group, which we used to extract the frequency band (FB) feature.

The table 3 and Figure 8 holds the obtain results of the three groups signals. According to these results, the three groups' frequency band feature is proportional to the ER parameter evolution. In the first group of signals (PCG signals without clicks and murmurs), the IM and COA signals occupy a larger frequency band than the normal case 'N'. At the same time, the COA case FBs' is wider than the IMs'. In other words, the case of an aortic coarctation 'COA' is more intense than a mitral insufficiency 'IM'.

The second and third group of signals (PCG signals with clicks and murmurs) present the

Journal of Theoretical and Applied Information Technology
31st May 2023. Vol.101. No 10

ISSN: 1992-8645 www.jatit.org E-ISSN: 1817-3195

same results concerning the FB feature (acceleration of the FB with the increase of the energetic ratio ER). We can also note that the frequency band of pathological cases is greater than of the normal cases [FB of the 3rd group reaches up to 1300 Hz].

4.1.2 The STFT analysis of the three groups

4.1.2.1 Temporal extent feature: ΔT

Figure 9 illustrates de STFT graphic results for the first group of PCG signals. We noted that their temporal representations are similar, whereas the STFT shows differences. Indeed, the temporal extent ΔT of the second heart sound (S2) is greater than that of the first heart sound (S1) for the three cases (N, IM, and COA) (figure 12, table 4), which we can interpret by the semi-lunar shape of the aortic valves and rapidly closing lungs [32]. We also noticed that the temporal extent of (S1) and (S2) is proportional to the signals' energy of group 1.

The PCG signals of group 2 (PCG signals with clicks) present a direct proportionality of the click segments' temporal extent ΔT to the energetic ratio (ER) and an inverse one for the heart sounds S1 and S2. The same observation is made for group 3 (PCG signals comprising significant murmurs).

4.1.2.2 Frequency extent feature: ΔF

The first group show a slight decrease in the frequency extent (ΔF) of the first heart sound (S1) and an increase in the second heart sound (S2). Still, the three cases of the first group (N, IM, and CAO) manifest a greater frequency extent of S2 than S1 (table 4 and figure 13).

Regarding the PCG signals of the second group, we note that the presence of clicks affect the heart sounds S1 and S2, where we find a decrease in their frequency extent with an increase in the clicks' ΔF. Yet, both results remain correlated to the energetic ratio ER. From the degree of severity perspective, we could say that the more the frequency extent of the clicks increases, the more the pathological severity evolves.

The presence of murmurs in the thirds group of PCG signals leads to an increase in the frequency extent of both the heart sounds (S1 and S2) and the murmur with a proportional correlation to the energetic ratio evolution. Therefore, the more the frequency extent of the murmurs increases, the more the degree of pathological severity develops.

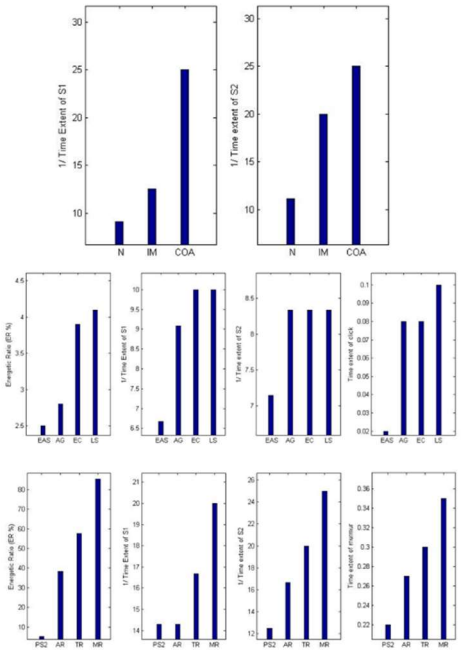

Figure 12: variation of temporal extent ΔT in function of : first heart sound (S1), second heart sound (S2), clicks and murmurs for Group 1,Group 2 and Group 3 PCG signals.

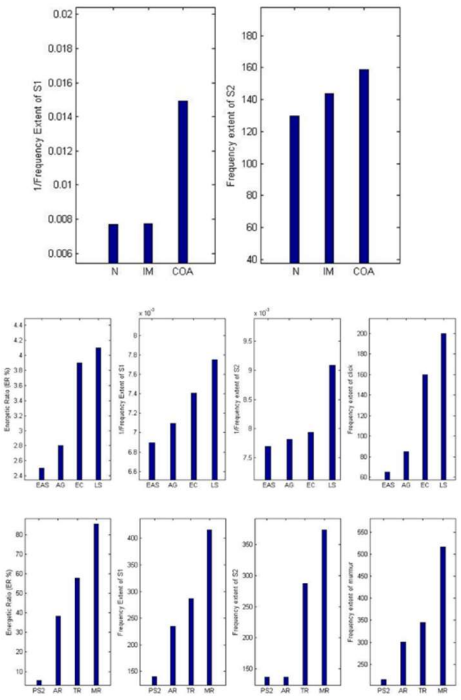

Figure 13: variation of frequency extent ΔF in function of : first heart sound (S1), second heart sound (S2), clicks and murmurs for Group 1,Group 2 and Group 3 PCG signals.

4.2 Comparison of the level of severity between the PCG signals of the same pathology (group G4)

Just like for part 1, we analysed the group 4 of PCG signals as mention in table 1 with the FFT and STFT algorithms, we then extracted their relative features and used them to classify our signals from the least sever to the most, afterwards, compared the obtained results to the energetic ratio (ER) evolution.

According to figure 11 and table 5, the frequency band feature (FB) extracted from the FFT analysis shows its ability to monitor the evolution of pathological severity degree. It presents a decrease in values correlated with the increase in energetic ratio ER within the three pathologies (for example: for PCG signals of mitral stenosis (MS), the frequency domain decreases from the case of 'MS1' to the case 'MS4').
The figure 10 represented in the results section illustrates the STFT graphic results for one of the MS (Mitral Stenosis) and MR (Mitral Regurgitation) signals, later found to be the most severe in their signal group.

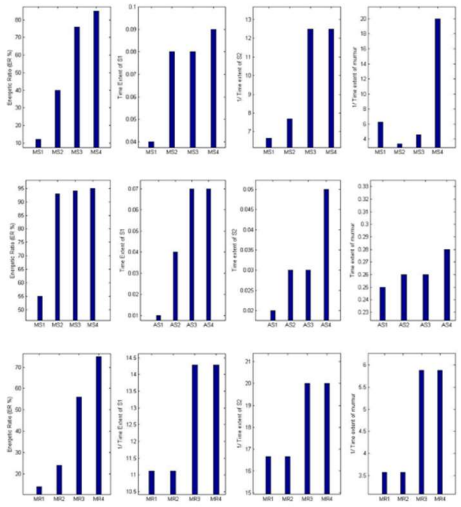

Figure 14 : variation of temporal extent ΔT in function of cardiac sound S1 : (a) mitral stenosis (MS),(d) aortic stenosis (AS), (g) mitral regurgitation (MR);of cardiac sound S2: (b) mitral stenosis (MS),(e) aortic stenosis (AS), (h) mitral regurgitation (MR); and murmurs (c) mitral stenosis (MS),(f) aortic stenosis (AS), (i) mitral regurgitation (MR);

4.2.1 Temporal extent feature: ΔT

According to the results (figure 14, table 6), the ΔT of S1 is correlated with the energetic ratio either in an ascending way as for the aortic stenosis and the mitral stenosis signals; Or descending as for the mitral regurgitation signals. On the other hand, the temporal extent of S2 is also correlated to the energetic ratio (ER) either upwards or downwards for the PCG signals of the three pathologies.

The PCG signal murmurs of aortic stenosis show an increase in their ΔT under the increase of the ER, where this development is a direct indicator of the degree of severity within this pathology [33] (the more ΔT of the murmurs increases the more the pathological severity of the aortic stenosis develops). Moreover the ΔT of the mitral stenosis PCG signals (except MS1) and the mitral regurgitation decreases with ER evolution.

4.2.2 Frequency extent feature: ΔF

The frequency extent (ΔF) of the S1 sound increases for the three cardiac pathologies (figure 15).
In the mitral stenosis case (MS): the first heart sound S1 increased proportionally to the ER evolution, this may be the result of severe mitral stenosis, which includes a loud S1 sound caused by the leaflets of a stenotic mitral valve closing abruptly [34], so we can say that the more the mitral stenosis evolves, the more the S1 increases. However, the frequency extent of S2 and murmurs is inversely correlated to ER (these murmurs can decrease or even disappear when blood flow decreases through the mitral valve [35]).

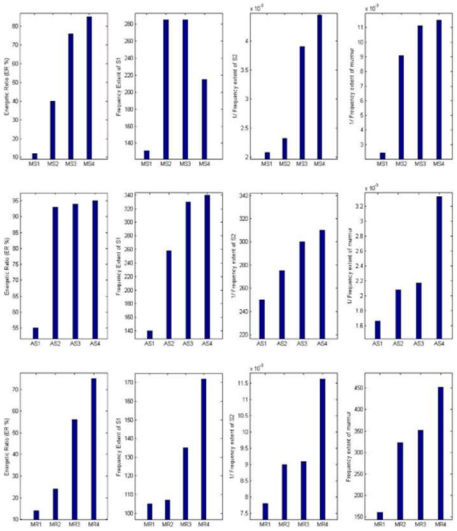

Figure 15 : variation of frequency extent Δf in function of cardiac sound S1 : (a) mitral stenosis (MS), (d) aortic stenosis (AS), (g) mitral regurgitation (MR); of cardiac sound S2: (b) mitral stenosis (MS), (e) aortic stenosis (AS), (h) mitral regurgitation (MR); and murmurs (c) mitral stenosis (MS), (f) aortic stenosis (AS), (i) mitral regurgitation (MR);

Concerning the AS group (aortic stenosis), both heart sound S1 and S2 evolve proportionally of the energy ratio. Regarding murmurs, it is the opposite (ΔF decreases with the RE evolution); which may be due to the decrease in murmur intensity when heart failure develops due to aortic stenosis [33]. .

Regarding the PCG signals of mitral regurgitation (MR), we found that the first heart sound (S1) and the murmurs show an increase in the frequency extent with the evolution of the energetic ratio (ER), while the second heart sound decreases with this evolution.

Hence, all results discussed above remain correlated to the energetic ratio evolution and have a proper medical explanation. Therefore, this comparison of our results with the ER helped us appreciate the features' variation and link it to a plausible medical reason.

Which is the main positive point of these analyses besides there simplicity and speed in term of feature calculation when implemented into more developed signal processing programs.

4.3 Machine learning results discussion

As seen in table 7, 99.2% accuracy is achieved when using a combination of spectral and time features (frequency band (FB), frequency extent (ΔF), time extent (ΔT)) to classify the PCG signals in the three main groups.

As we assumed in the introduction, the FFT and STFT technics considered pathological signal morphology similar to a normal (healthy) PCG signal as an unhealthy signal; however, the values of the features somehow remained close to the first group signals. Which, led to a correct classification and a high accuracy value.

When ranking signals according to their severity level (table 8), we achieved a bit lower accuracy (98.9%) than the first.

The problem occurs for signals with a severity level close to the next level. Which may have rather affected the classification process and the accuracy value.

Hence, the classification results shows the efficiency of the STFT and FFT for the phonocardiogram signals classification and that for healthy/clicks/murmurs or severity level discrimination.

To confirm that our comparison to the ER is efficient and consistent, we tested the ability of this feature to classify our database in the two mentioned ways.

Table 9 and 10 results also proves this ability of the energetic ratio parameter (ER) to establish similar classification of the database to a machine learning process with an accuracy of 99.5% and 98.8%. Which is coherent, since the energetic ratio, as mentioned before, refer to the intensity of heart sounds S1, S2 and added sounds (click and murmur) to highlight the dominance of added sounds over heart sounds and to classify the PCG signals according to this dominance. Where [36]

- RE <30% , refers to Light severity level.
- 30% <RE<70%, Moderate severity level.
- RE> 70%, Severe severity level.

As mentioned in the introduction, many research focused on exploiting the FFT and STFT technics for various purposed, like cardiac components identification, pathology discrimination, binary classification etc…. However, with this work, we managed to use the capacities of these technics to classify our PCG signals in two ways:

- According to their pathological origin (normal/morphologically similar, click or murmur).
- According to their severity level (Light, Moderate, and Severe).

Using two approaches:

- The energetic ratio (ER) as a reference parameter, previously used in numerous works [12,19][20-27].
- A machine learning classifier (KNN).

One of the similarities with some of these previous works is the use of the Energetic Ratio ER as a reference feature to compare our results with. Hence, in this work, we started by proving it accuracy before using it for comparison. Which affirms the consistency of our comparison and the previous works using it as a reference feature for PCG signal classification. [12,19][20-27].

Finally, besides ranking a part of our database into the three pre-established groups, the ability of this work to identify the level of severity from a PCG recording and classify it into one of the three named classes using a machine learning process makes the novelty of this paper.

5. CONCLUSION:

In closing, Very promising results were obtained in this paper using only two basic methods of signal processing (FFT and STFT) to achieve the assigned objectives, namely the analysis of the pathological severity between different cardiac signals ranked in three pre-established groups, as well as, the severity level evolution of the same pathology (mitral stenosis, aortic stenosis, and mitral regurgitation).

Both approaches used to affirm the obtained results (K-Nearest Neighbours classifier with FFT/STFT features and Energetic Ratio parameter) allowed us to rearrange a part of our database into three main groups:

- Group 1 (G1): PCG signals having neither click (reduced murmur) nor significant murmur.
- Group 2 (G2): PCG signals with clicks.
- Group 3 (G3): PCG signals with clicks or murmurs.

And successfully classify the remaining database into three classes based on the pathology' severity levels (light, moderate, severe) with high accuracies, 99.2%, 98.9% for the K-Nearest Neighbours classifier with FFT/STFT features and 99.5%, 98.8% for the Energetic Ratio parameter.

Therefore, the energetic ratio ER parameter proved it efficiency for PCG signal classification, which made it a great way to quickly confirm the consistency of an analysis before proceeding with a machine learning classification.

In the end, this study paved the way towards using simple, yet effective, features in cardiac pathologies identification and classification to assist clinicians in critical decision making.

Acknowledgements

The authors would like to thank the Directorate-General of Scientific Research and Technological Development (Direction Générale de la Recherche Scientifique et du Développement Technologique, DGRSDT, URL:www.dgrsdt.dz, Algeria) for the financial assistance towards this research.

"Compliance with Ethical Standards"

- No, I have nothing to report
- This study was not funded by any party: it is an academic PhD study
- No conflict of interest
- No animal or other used in this study

REFERENCES

[1]: Shivam Varshney, Satyendra Singh, Computation of Biological Murmurs In Phonocardiogram Signals Using Fast Fourier & Discrete Wavelet Transform, International Conference on Computation, Automation and Knowledge Management (ICCAKM) Amity University, 2020

[2]: Li X et al , Synchronization control of pulsatile ventricular assist devices by combination usage of different physiological signals, Comput Assist Surg 24(sup1):105–112. 2019.

[3]: S. A. Taplidou and L. J. Hadjileontiadis, 'Nonlinear analysis of heart murmurs using wavelet-based higher-order spectral parameters', in *2006 International Conference of the IEEE Engineering in Medicine and Biology Society*, pp. 4502–4505, 2006.

[4]: Ahmad MS, Mir J, Ullah MO, Shahid MLUR, Syed MA, An efficient heart murmur recognition and cardiovascular disorders classification system. Australas Phys Eng Sci Med
42(3):733–743. 2019.

[5]: Watrous R L , Computer-aided auscultation of the heart: from anatomy and physiology to diagnostic decision support Proc. 28th Ann. Int. Conf. IEEE-EMBS 1 140, 2006.

[6]: Akay M, Semmlow J L, Welkowitz W, Bauer M D and Kostis J B , Noninvasive detection of coronary stenoses before and after

angioplasty using eigenvector methods , IEEE Trans. Bio-Med, Eng. 37 1095–104, 1990.

[7]: POTDAR, Ravindra Manohar, *et al,* Optimal Parameter Selection for DWT based PCG Denoising *Turkish Journal of Computer and Mathematics Education (TURCOMAT)*, vol. 12, no 9, p. 3207-3219.2021.

[8]: S.M Debbal and F. Bereksi-Reguig. Second cardiac sound , analysis techniques and performance comparison , Journal of Mechanics in Medicine and Biology (JMMB); ISSN : 0219-5194; 5 (3), September2005.

[9]: T .Omari. Study of aortique stenosis pathological severity degree, magister theses, Tlemcen University, pp 51, 2009.

[10]: R. R.Coifman, Y.Meyer, M. V. Wickerhauser, Wavelet analysis and signal processing. In Wavelets and their applications , Jones and Bartlett, Boston, MA, USA, pp 153-178.1992.

[11]: FATMAWATI, T. Y., YULIANI, A., AFANDI, M. A., *et al,* Comparative Analysis of the Phonocardiogram Denoising System Based-on Empirical Mode Decomposition (EMD) and Double-Density Discrete Wavelet Transform (DDDWT), In : *Proceedings of the 1st International Conference on Electronics, Biomedical Engineering, and Health Informatics*. Springer, Singapore, p. 593-604.2021.

[12]: Baakek, Y. N. E. H., Debbal, I., Boudis, H., & Debbal, S. M. E. A. Study of the impact of clicks and murmurs on cardiac sounds S1 and S2 through bispectral analysis. Polish Journal of Medical Physics and Engineering2021. 27(1), 63-72.

[13]: Sundaram, D. S. B., Damani, D. N., Kapoor, A., Shivaram, S., & Arunachalam, S. P. Deep learning based discrimination of phonocardiogram signal with normal heart sounds and murmur: Feasiblity study. Biomedical Sciences Instrumentation. 2021. 57, 2.

[14]:DEBBAL S.M, Hamza Ch. Pathologies cardiac discrimination using the Fast Fourir Transform (FFT) The short time Fourier transforms (STFT) and the Wigner distribution. J Cardiology Interventions. 2021. 1(1);

[15] S Debbal, F Bereksi-Reguig.,*Spectral analysis of the PCG signals*, The Internet Journal of Medical Technology. Vol 4 N°1.2006.

[16] DEBBAL, S. M., & BEREKSI-REGUIG, F., CARDIAC MURMUR ANALYSIS USING THE SHORT-TIME FOURIER TRANSFORM, Journal of Mechanics in Medicine and Biology, 06(03), 273–284.2006.

[17] S. M DEBBAL- F BEREKSI REGUIG , *The fast Fourier transform and the continuous wavelet transform analysis of the normal and the pathological phonocardiogram"* ; Sciences et Technologies ; ISSN : 1111-5041 , Vol. 17 , pp 81-86.2002.

[18] Abrams,J, Current Concepts of the genesis of heart sounds.I.First and second sounds. ,JAMA, 239-2787. 1978.

[19] Meziani F, Debbal SM, Atbi A, Analysis of phonocardiogram signals using wavelet transform. ,J Med Eng Technol. 2012. 36(6), 283.

[20] Cherif LH, Debbal SM , Adaptive filtering algorithm based on a wavelet packet tree for heart sound signal analysis, Int. J.Med. Eng. Inform. 2018. 10(2), 150

[21] Debbal SM, Hamza C. Heart sounds analysis using the three wavelet transform versions the continuous wavelet transform (CWT) the discrete wavelet transform (DWT) and the wavelet packet transforms (PWT). Journal of Cardiology Interventions. 2021. vol. 1, no 1.

[22] Ahmad TJ, Ali H, Khan SA. Classification of Phonocardiogram using an Adaptive Fuzzy Inference System. In Proc. Int. Conf. Image Process. Comput Vis Pattern Recognit., IPCV 2009, Las Vegas, Nevada, USA, July 13-16, 2009.

[23] Baakek YNEH, Debbal I, Boudis H, Debbal, SMEA. Study of the impact of clicks and murmurs on cardiac sounds S1 and S2 through bispectral analysis. Polish Journal of Medical Physics and Engineering. 2021.27(1) : 63-72.

[24] Berraih SA, Baakek YNEH, Debbal SMEA. Pathological discrimination of the phonocardiogram signal using the bispectral technique. Physical and Engineering Sciences in Medicine. 2020. 43(4), 1371.

[25] Berraih SA, Baakek YNEH, Debbal SMEA. Severity cardiac analysis using the Higher-order spectra. Applied Mathematics and Computation.2021. 409, 126389.

[26] Debbal I, Boudis H, BAAKEK YNEH, Debbal SMEA. Cardiac Pathologies Analysis on the Phonocardiogram Signals Using the Bispectral Technic. International Journal of Advanced Science and Technology. 2020. 29(3), 6764 - 6784.

[27] Berraih SA, Baakek YNEH, Debbal SMEA. Preliminary study in the analysis of the severity of cardiac pathologies using the

higher-order spectra on the heart-beats signals. Polish Journal of Medical Physics and Engineering.2021. 27(1), 73-85.

[28] P.M. Narendra. A branch and bound algorithm for computing k-nearest. IEEE Trans. Comput., 100 (7) (1975), pp. 750-753

[29] Laaksonen, J., Oja, E., 1996. Classification with learning k-nearest neighbors. in: Proceedings of International Conference on Neural Networks (ICNN'96), IEEE, 1996, pp.1480–1483.

[30] Kramer, O., 2013. K-nearest neighbors, . pp.13–23

[31] ARSLAN, Özkan et KARHAN, Mustafa. Effect of Hilbert-Huang transform on classification of PCG signals using machine learning. *Journal of King Saud University-Computer and Information Sciences*, 2022, vol. 34, no 10, p. 9915-9925.

[32] LAMRAOUI H. Characterisation of the phonocardiogram signal. Hadj Lakhdar University. Batna 2. Algeria. 2016.

[33] Xiushui, MD [Internet]. What is the relationship between the systolic murmur and severity of aortic stenosis (AS)?, Medscape [updated 2019 May 7; cited 2023 Jan 19]. Available from: https://www.medscape.com/answers/150638-44363/what-is-the-relationship-between-the-systolic-murmur-and-severity-of-aortic-stenosis-as .

[34] Healio.com [Internet]. Mitral Stenosis - Physical Examination-Topic Reviews [cited 2023 Jan 19]. Available from: https://www.healio.com/cardiology/learn-the-heart/cardiology-review/topic-reviews/mitral-stenosis/physical-examination

[35] Guy P. Armstrong , MD [Internet]. Waitemata Cardiology, Auckland Valvular Disorders, MSDManuals [updated 2022 sep ; cited 2023 Jan 19]. Available from: https://www.msdmanuals.com/professional/cardiovascular-disorders/valvular-disorders/mitral-stenosis.

[36] Debbal S, Bereksi-Reguig F. Analyse spectro-temporelle des bruits cardiaques par les transformees discrete et continue d'ondelettes. Sciences & Technologie. B, Sciences De l'ingénieur. 2005(23):5-15.

1st International Conference on Scientific and Academic Research

ICSAR

https://www.icsarconf.com/

December 10-13, 2022, Konya, Turkey

Pathological cardiac severity discrimination using a spectral entropy

DEBBAL Imane*, HAMZA CHERIF Lotfi [2] BAAKEK Yettou Nour El Houda [3]

[1] *Genie Biomedical department/ Genie Biomedical Laboratory (GBM),University Abou Bakr Belkaid Tlemcen , Algeria*
[2] *Genie Biomedical department/ Genie Biomedical Laboratory (GBM),University Abou Bakr Belkaid Tlemcen , Algeria*
[3] *Genie Biomedical department/ Genie Biomedical Laboratory (GBM),University Abou Bakr Belkaid Tlemcen , Algeria*

*imane.debbal@univ-tlemcen.dz,
[2]lotfi.hamzacherif@univ-tlemcen.dz, [3]nourelhouda.baakekyettou@univ-tlemcen.dz

Abstract **–** The Phonocardiogram (PCG) reflects non-stationary acoustic signals generated by cardiac activity (normal and pathological) [1]. This signal is sometimes affected by added parameters that reflect the presence of a specific pathology. The frequency analysis of phonocardiogram signals previously helped identify the heart's frequency components or discriminate and diagnose cardiac pathologies using features extracted from the spectrum. This research is oriented toward identifying and discriminating the cardiac severity level within the same pathology using spectral entropy. Sixteen phonocardiogram recordings from two cardiac pathologies were studied. The spectral entropy presented a proportional correlation with the cardiac severity evolution which reflects the aptitude of the frequency analysis to assess the pathology' development and display it in the spectrum. Therefore, we could say that spectral entropy is a valid indicator for pathological cardiac severity assessment.

Keywords – frequency analysis, spectral entropy, phonocardiogram signal, cardiac severity evolution, level discrimination.

I. INTRODUCTION

A phonocardiogram (PCG) is a scheme for emulating high precision copy of the sounds made by the heart along with the murmurs made during the procedure of pumping blood [2]. The cardiac signals recorded via a phonocardiograph may reflect divers' pathological conditions of cardiovascular system the reason for why several researchers study the heart sounds (acquisition, segmentation and feature extraction, signal processing).

Under normal conditions, two heart sounds can be distinguish on the graphic representation of the recorded phonocardiogram (PCG). The first heart sound known also as heartbeat S1, corresponding to the beginning of ventricular systole, is the result of the closure of the mitral and tricuspid valves [3]. While the second heartbeat S2, referring to the end of the ventricular systole and marking the beginning of the diastole, is associated with the closure of the aortic and pulmonic valves [3]. Other than S1 and S2, murmurs and short murmurs (clicks) appears indicating abnormal heart condition. Murmurs are sounds resulting from certain cardiovascular diseases that are audible during the systole, the diastole, or both [4][5].

Stenosis and regurgitation are the two ailments who relate to the opening and the closing of the valves detected by analysing the PCG signal [2]. Therefore the algorithms used for cardiac signals processing is more on a quantitative, precise and objective interpretation of heart sounds [6], improving the process of cardiovascular diagnosis. Beyond this, computer-assisted auscultation allows the detection of pathologies who are unrecognized through a conventional auscultation [7].

Hence, researchers used numerous signal-processing tools on PCG recordings for various purposes. Many denoising algorithms have been proposed for cardiac pathologies discrimination, denoising, and classification using Discrete Wavelet Transform (DWT) [8]-[12], DWT decomposition

level exploitation [13]-[15], Empirical Mode Decomposition [16][17].

In another study, Debbal et al. [18] used the continuous wavelet transform (CWT) to analyse cardiac sounds and murmurs, which leaded to suitable information about frequency content. The discrete wavelet transform (DWT) technique happens to be a very useful tool for discrimination between various heart sounds signals [2][19]. Cherif. L et al. proposed a wavelet packet tree based algorithm to distinguish between the severities of pathological cases for different heart sound signals [20]. Jian-bo WU et al. showed that the Entropy Power Spectrum is a valid indicator to analysis the abnormal PCG [21].

In this paper, we focused on quantifying the information of the spectrum to see if it follows the pathology' evolution and concluded that spectral entropy is a valid indicator for pathological cardiac severity assessment.

II. Materials and Method

Many studies conducted on phonocardiogram signals using a frequency analysis focused on extracting parameters from the spectrum as the higher frequency, maximum amplitude, or other mathematical features like the mean, and stander deviation, and furthermore to classify the signals. However, the spectrum's ability to separate and discriminate each cardiac severity level from the other was not fully exploited. Therefore, the purpose of this work.

In this paper, we used an open phonocardiogram signal database from github [22], eight PCG signals were selected from each pathology (Aortic Stenosis (AS) and Mitral Stenosis (MS)). Figure 1 and Figure 2 illustrate the temporal representation of the phonocardiogram signals used for this study.

First, we ranked the PCG signals from the least to most severe using the energetic ratio (ER), and then applied a frequency analysis on the sixteen selected signals; the spectral entropy was later measured on the frequency spectrum using the equation mentioned below.

A. *Frequency analysis*

Power Spectral Density (PSD) or "the spectrum of a signal", reveals the existence or the absence of the frequency of a signal which is very important in physiological signal processing in order to reliably discriminate between normal and pathological cases.

The equation below is the one implemented to apply the frequency analysis on the selected signals.

$$X(f) = \sum_{n=1}^{N} x(n) e^{-j2\pi fn} \qquad (1)$$

Where: X(f) : the spectrum of the signal, x(n) :the temporal signal, N : samples number, f : the frequency.

B. *Energetic ratio*

Used in this study, as a reference feature to affirm the results obtained using a frequency analysis. ER is very efficient for tracking the severity of cardiac diseases [19][23]-[29].

$$ER = \frac{E_2}{E_1 + E_2} \times 100 \qquad (2)$$

Where E2 is the heart murmur or click energy, E1 is the energy of S1 + S2 and (E1 + E2) is the total energy. The above equation give ER values as a percentage. In case the ER equals to 100%, we have a complete dominance of murmurs over cardiac sounds (S1, S2).

C. *The spectral entropy*

In this paper, entropy defines a measure of information quantity contained in the phonocardiogram spectrum.

$$SEnt[X] = -\int P(X) Log\, P(X) d(X) \qquad (3)$$

Where (X): the selected part from the frequency spectrum. P(X) : a probability density.

The spectral entropy (SEnt) of a signal is a measure of its spectral power distribution.

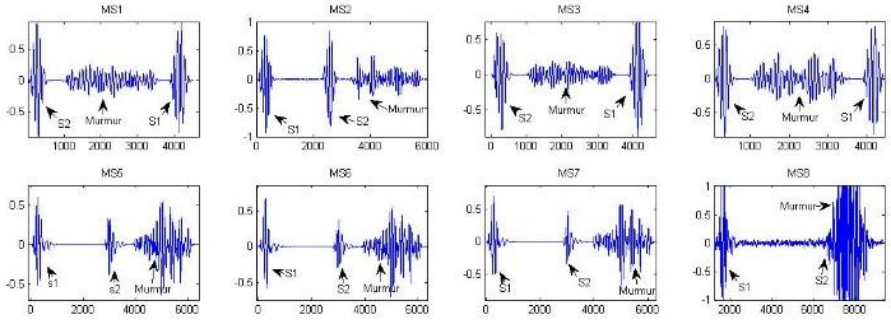

Fig. 1 Temporal representation of the eight selected mitral stenosis cases with different cardiac severity level (MS1, MS2, MS3, MS4, MS5, MS6, MS7, MS8).

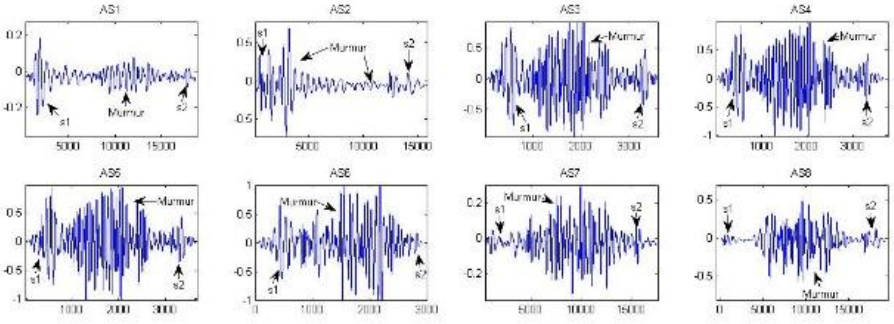

Fig. 2 Temporal representation of the eight selected aortic stenosis cases with different cardiac severity level (AS1, AS2, AS3, AS4, AS5, AS6, AS7, AS8).

III. RESULTS

After applying our algorithm on the phonocardiogram (PCG) database and extracted the spectral entropy (Sent) from the spectrum of each PCG signal, we obtained the following results:

Figure 3 illustrate the spectrum resulting from the frequency analysis of the least and the most severe case of the studied mitral stenosis (MS) signals.

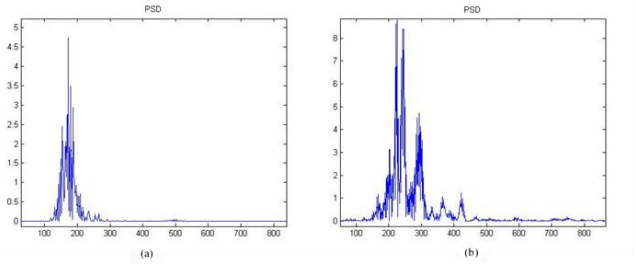

Fig. 3 (a) least severe case of mitral stenosis MS1, (b) most severe case of the mitral stenosis MS8

Table 1 and Table2 list the resulting values of the spectral entropy (SEnt) for the sixteen studied phonocardiogram signals.

Table 1.Results of the spectral entropy for the mitral stenosis cases.

PCG Signal	ER (%)	Spectral Entropy (SEnt)
Ms1	15	20.174
Ms2	20	20.200
Ms3	21	21.537
Ms4	27	29.919
Ms5	68	31.884
Ms6	70	31.903
Ms7	75	32.065
Ms8	86	65.960

Table 2. Results of the spectral entropy for the aortic stenosis cases.

PCG Signal	ER (%)	Spectral Entropy (SEnt)
As1	47	10.400
As2	65	17.882
As3	77	21.197
As4	81	29.074
As5	85	30.049
As6	87	39.376
As7	93	48.566
As8	96	50.768

Figure 4 highlight the correlation between the energetic ratio (ER) and the spectral entropy (SEnt).

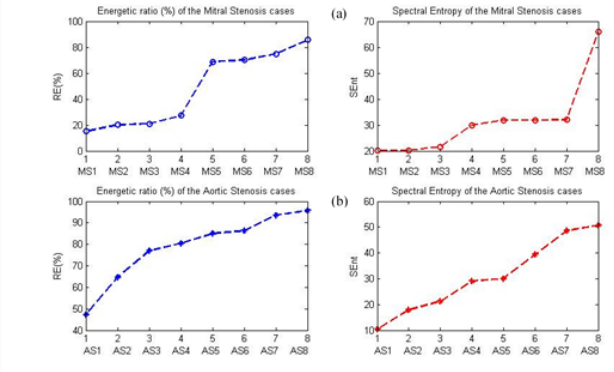

Fig. 4 graphic representation of the Energetic Ratio (ER) and the spectral Entropy (SEnt) results for : (a) the eight severity levels of the mitral stenosis (MS1, MS2, MS3, MS4, MS5, MS6, MS7, MS8), (b) the eight severity levels of the aortic stenosis (AS1, AS2, AS3, AS4, AS5, AS6, AS7, AS8)

IV. DISCUSSION

In this paper, we focused on studying the variation of frequency information between each pathological cardiac severity level using a spectral entropy, and compare it evolution with the energetic ratio evolution to highlight the aptitude of the spectrum to identify frequency information about the pathological cardiac severity.

First, the Energetic Ratio (ER) values helped us ranking our pathological signals from the least severe to the most, for both the aortic stenosis (AS) signals and the mitral stenosis (MS). The Energetic Ratio highlight the importance of the murmurs energy and their dominance over heart sounds. Therefore, we used his ranking order of the signals to evaluate the efficiency of our calculated feature. [19] [23]-[29]

The frequency spectrums obtained (Figure 3) graphically discriminated between the least and the most severe case of the mitral stenosis cases. Which comforts our current research scope, and that frequency analysis is capable of discriminating the pathological cardiac severity level. The spectral entropy confirmed this ability with results presenting an ascending evolution with the cardiac severity development (Figure 4).

The obtained results are coherent with the medical explanation of the two chosen pathologies. In a mitral stenosis, hemodynamic abnormality defines an obstruction of the left ventricular inflow at the mitral valve level caused by restricted valve opening due to an abnormal mitral valve apparatus. Which needs an increasing of pressure gradient to propel the blood forward from left atrium to the left ventricular. While in an aortic stenosis the dysfunctions leads to an augmentation of the left ventricular outflow and afterload [30]. Hence, the ascending evolution obtained for both the spectral entropy and the energetic ratio in the sixteen studied severity cases.

Lastly, these results showed that phonocardiogram' spectrums does not limit to frequency information about it component, heart sounds (S1, S2) and added sounds (murmur, click), but discriminate the cardiac severity level and follows it evolution. The spectral entropy helped us highlighting the quantity of information present in a phonocardiogram' spectrum regardless the previously used features for phonocardiogram signal classification.

V. CONCLUSION

In closure, our algorithm based on a frequency analysis and a spectral entropy extraction from the phonocardiogram spectrum identified and separated cardiac severity levels for the sixteen studied cases.

The spectrum in itself presented discriminative results between the cases, which means that cardiac severity information are present in the frequency domain. The spectral entropy was the feature who helped us quantifying this severity information from the frequency spectrum.

The proportional correlation between the spectral entropy and the pathological cardiac severity evolution accordingly to the medical explanation of the pathology proves the efficiency of our algorithm for cardiac severity level discriminating and assessing.

These results could be the object of future works for the aim of early identification and diagnosis of cardiac severity levels, which may help in treatment options and impact directly the life expectancy of the population and in particular highers the patient's chances of recovery.

Arriving to promising results in term of pathological cardiac severity level discrimination and monitoring with direct impact future works using simple algorithms helps us promote more economical healthcare and health research.

ACKNOWLEDGMENT

The authors would like to thank the Directorate-General of Scientific Research and Technological Development (Direction Générale de la Recherche Scientifique et du Développement Technologique,

DGRSDT, URL:www.dgrsdt.dz , Algeria) for the financial assistance towards this research.

"**Compliance with Ethical Standards**"

- No, I have nothing to report
- This study was not funded by any party: it is an academic PhD study
- No conflict of interest
- No animal or other used in this study

REFERENCES

[1] Z. B. Stambouli, " Phonocardiogram signal classification based on an SNR ratio study'', M. Eng. thesis, Abou Bekr Belkaid University, Tlemcen, Algeria, 2012

[2] S. Varshney, S. Singh, "Computation of Biological Murmurs in Phonocardiogram Signals using Fast Fourier & Discrete Wavelet Transform", *In 2020 International Conference on Computation, Automation and Knowledge Management (ICCAKM)*, January 2020, pp. 234-240, IEEE.

[3] X. Li, L. Zhong, L. Luo, S. ZHU, K. Ni, Q. Zhou, B. Yang, X. Wang, "Synchronization control of pulsatile ventricular assist devices by combination usage of different physiological signals", *Computer Assisted Surgery*, vol. 24 no sup1: 105-112, 2019.

[4] SA. Taplidou, LJ. Hadjileontiadis, "Nonlinear analysis of heart murmurs using wavelet-based higher-order spectral parameters", *in Int. Conf. IEEE-EMBS*, 2006, IEEE : 4502-4505.

[5] MS. Ahmad, J. Mir, MO. Ullah, MLUR. Shahid, MA. Syed, "An efficient heart murmur recognition and cardiovascular disorders classification system", *Australas Phys Eng Sci Med.* 42(3), 733, 2019.

[6] RL. Watrous, "Computer-aided auscultation of the heart: from anatomy and physiology to diagnostic decision support" *In Proc. 28th Ann. Int. Conf. IEEE-EMBS*, 1, 140, 2006.

[7] M. Akay, J L. Semmlow, W. Welkowitz, M D. Bauer, J B. Kostis, "Noninvasive detection of coronary stenoses before and after angioplasty using eigenvector methods". *IEEE Trans. Bio-Med. Eng*, 37, 1095, 1990.

[8] RM. Potdar, "Optimal Parameter Selection for DWT based PCG Denoising", *Turkish Journal of Computer and Mathematics Education (TURCOMAT)*, 12(9), 3207,2021.

[9] A. Hossain, S. Uddin, P. Rahman, MJ. Anee, MMH. Rifat, MM. Uddin, "Wavelet and Spectral Analysis of Normal and Abnormal Heart Sound for Diagnosing Cardiac Disorders*", BioMed Research International*, 2022.

[10] Li H, Ren G, Yu X, Wang D, Wu S, "Discrimination of the diastolic murmurs in coronary heart disease and in valvular disease", *IEEE Access*, vol. 8 : 160407–160413, 2020.

[11] Li H, Ren Y, Zhang G, Wang R, Cui J, Zhang W, "Detection and classification of abnormities of first heart sound using empirical wavelet transform", *IEEE Access*, vol. 7: 139643–139652, 2019.

[12] Liu Q, Xu Y, Zhang L, Liang C, "Research on heart sound signal denoising algorithm based on variational mode decomposition and wavelet threshold", *Journal of Computer and Communications*, vol. 9, no. 10: 110–121, 2021.

[13] SM. Debbal and F. Bereksi-Reguig, "Second cardiac sound analysis techniques and performance comparison", *Journal of Mechanics in Medicine and Biology (JMMB)*, ISSN : 0219-5194; 5 (3), 2005.

[14] T. Omari, "Study of aortique stenosis pathological severity degree", M. Eng. thesis, Abou Bekr Belkaid University, Tlemcen, Algeria, 51, 2009.

[15] RR. Coifman, Y. Meyer, MV. Wickerhauser, *Wavelet analysis and signal processing, In Wavelets and their applications*, Jones and Bartlett, Ed. Boston, MA, USA, 153, 1992.

[16] TY. Fatmawati, A. Yuliani ,MA. Afandi, D. Zulherman, "Comparative Analysis of the Phonocardiogram Denoising System Based-on Empirical Mode Decomposition (EMD) and Double-Density Discrete Wavelet Transform (DDDWT)", in *Proc. of the 1st International Conference on Electronics, Biomedical Engineering, and Health Informatics. Springer, Singapore*, 2021, p. 593.

[17] M. Mishra, A. Singh, MK. Dutta, AR. Muñoz, "Automatic screening of cardiac disorders using wavelet analysis of heart sound", *in 2017 4th IEEE Uttar Pradesh Section Int. Conf. on Electrical, Computer and Electronics (UPCON), Mathura, India*, October 2017, p. 472–476.

[18] SM. Debbal, AM. Tani, "Heart sounds analysis and murmurs", *Int. J. Med. Eng. Inform*. 8(1), 49, 2015

[19] F. Meziani, SM. Debbal, A. Atbi, "Analysis of phonocardiogram signals using wavelet transform" ,*J Med Eng Technol*, 36(6), 283.2012

[20] L. H. Cherif , SM. Debbal , "Adaptive filtering algorithm based on a wavelet packet tree for heart sound signal analysis*", Int. J.Med. Eng. Inform* , 10(2), 150, 2018

[21] J. -b. Wu, S. Zhou, Z. Wu and X. -m. Wu, "Research on the method of characteristic extraction and classification of Phonocardiogram", in *2012 International Conference on Systems and Informatics (ICSAI2012)*, 2012, pp. 1732-1735.

[22] 2022 Phonocardiogram database available: https://github.com/yaseen21khan/Classification-of-Heart-Sound-Signal-Using-Multiple-Features-

[23] SM. Debbal, L. Hamza C, "Heart sounds analysis using the three wavelet transform versions the continuous wavelet transform (CWT), the discrete wavelet transform (DWT) and the wavelet packet transforms (PWT)", *Journal of Cardiology Interventions*, vol. 1, no 1, 2021.

[24] TJ. Ahmad, H. Ali, SA. Khan, "Classification of Phonocardiogram using an Adaptive Fuzzy Inference System", *in Proc. Int. Conf. Image Process. Comput Vis Pattern Recognit., IPCV 2009, Las Vegas, Nevada, USA*, July 13-16, 2009.

[25] YNEH. BAAKEK, I. Debbal, H. Boudis, SMEA. Debbal, "Study of the impact of clicks and murmurs on cardiac sounds S1 and S2 through bispectral analysis". *Polish Journal of Medical Physics and Engineering*, 27(1) : 63-72.2021.

[26] SA. Berraih, YNEH. Baakek, SMEA. Debbal, "Pathological discrimination of the phonocardiogram

signal using the bispectral technique“, *Physical and Engineering Sciences in Medicine*, 43(4), 1371, 2020.

[27] SA. Berraih, YNEH. Baakek, SMEA. Debbal, “Severity cardiac analysis using the Higher-order spectra“. *Applied Mathematics and Computation*, 409, 126389.2021.

[28] I. Debbal, H. Boudis, YNEH. BAAKEK, SMEA. Debbal, “Cardiac Pathologies Analysis on the Phonocardiogram Signals Using the Bispectral Technic“, *International Journal of Advanced Science and Technology*, 29(3), 6764 - 6784.

[29] SA. Berraih, YNEH. Baakek, SMEA. Debbal, “Preliminary study in the analysis of the severity of cardiac pathologies using the higher-order spectra on the heart-beats signals“, *Polish Journal of Medical Physics and Engineering*, 27(1), 73-85.2021.

[30] Wang, A., & Bashore, T. M. (Eds.).”Valvular heart disease”. *Springer Science & Business Media*. 2010.

Pathological cardiac discrimination and severity monitoring of the phonocardiogram signal using the Discrete Wavelet Transform (DWT)

DEBBAL Imane
Genie Biomedical department
(Genie Biomedical Laboratory (GBM))
Faculty of Technology, University
Abou Bakr Belkaid
Tlemcen, Algeria
imane.debbal@univ-tlemcen.dz

HAMZA CHERIF Lotfi
Genie Biomedical department
(Genie Biomedical Laboratory (GBM))
Faculty of Technology, University
Abou Bakr Belkaid
Tlemcen, Algeria
lotfi.hamzacherif@univ-tlemcen.dz

BAAKEK Yettou Nour El Houda
Genie Biomedical department
(Genie Biomedical Laboratory (GBM))
Faculty of Technology, University
Abou Bakr Belkaid
Tlemcen, Algeria
nourelhouda.baakekyettou@univ-tlemcen.dz

Abstract— In this paper, we'll be discussing the efficiency of the Discrete Wavelet Transform (DWT) to distinguish between pathologies with clicks and those with murmur, along with assessing the cardiac severity evolution of diver's diseases through a three selected features. The cardiac signals analysed and previously classified via the energetic ratio (ER) parameter will be arranged into two main groups: a group of cardiac pathologies suffering from reduced murmurs and a second group containing pathologies with significant murmurs. The DWT-based features will help us to discriminate between the two mentioned groups and to assess the pathological cardiac severity evolution. In the end, we'll discuss the correlation of these features with the ER parameter in term of classifying phonocardiogram (PCG) signals. These results can only help the clinician to make his decision with serenity.

Keywords— Phonocardiogram, discrimination, severity, DWT, Entropy of approximation coefficients, mean variance of details, reconstruction error.

I. INTRODUCTION

A phonocardiogram (PCG) is a scheme for emulating high precision copy of the sounds made by the heart along with the murmurs made during the procedure of pumping blood [1]. The cardiac signals recorded via a phonocardiograph may reflect divers' pathological conditions of cardiovascular system that being the case for why several researchers focus on heart sounds analysis (acquisition, signal processing, segmentation and feature extraction from different PCG cycles). Hence, researchers used numerous signal-processing tools on PCG recordings for various purposes. Many denoising algorithms have been proposed such as parameter extraction using Discrete Wavelet Transform (DWT) [2], DWT decomposition level exploitation [3-5], Empirical Mode Decomposition [6].

The discrete wavelet transform (DWT) technique happens to be a very useful tool for discrimination between various heart sounds signals [7]. Authors of [8] were able to show through the discrete wavelet transform (DWT) and the continuous wavelet transform (CWT) that there is a clear difference between the signal and images of the arterial pathologies compared to those of healthy cases. The wavelet analysis technique in this work enhanced the medical benefits of the pulse wave. In [9], the authors chose the Symlet wavelet family to analyse the signals and extract three discriminative features –the mean value, variance, and energy of DWT-all of them were able to differentiate between healthy/unhealthy phonocardiogram recordings.

In this work, we're going to study the pathological severity of our PCGs signals with the calculation of three parameters obtained from the application of the DWT namely:

- The reconstruction error (Ɛermoy).
- The mean of detail coefficients (Md).
- The entropy of approximation coefficients (EAC).

The DWT will be applied on various PCG signals of several cardiac pathologies ranked according to their energetic ratio (ER) value, and classified into two main groups scilicet:

- PCG signals with reduced (minor) murmurs (CLICKS).
- PCG signals with significant murmurs.

II. METHODOLOGY

A. PCG signals database

Table I below defines the phonocardiogram (PCG) signals of the two groups (G1 and G2) used for detecting pathological cardiac severity.

Fig. 1 give the temporal - representation of some PCG signals from each group over two cardiac cycles.

TABLE I. PCG SIGNALS NAME ABBREVIATION

PCG signals	**Abbreviation**		
Group 1		***Group 2***	
EAS	Early Aortic Stenosis	PS	Systolic Pulmonary Stenosis
EC	Ejection Click	MR	Mitral Regurgitation
LS	Late Systole	AS	Aortic Stenosis
AG	Atrial Gallop	AR	Aortic Regurgitation
OS	Open Snap	DASD	Diastolic Atrial Septal Defect
		DAI	Diastolic Aortic Insufficiency

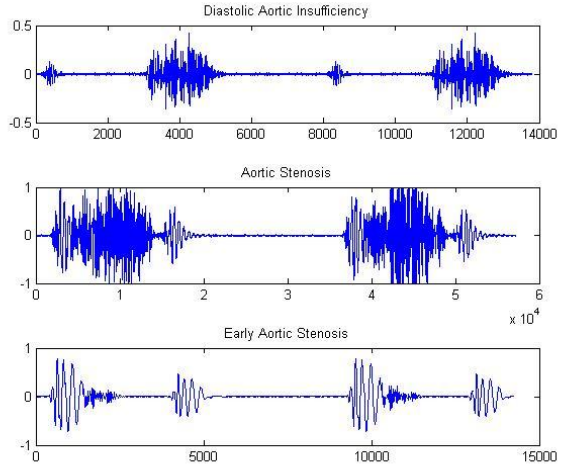

Fig. 1. Graphical representation of some PCG signals over two cycles – the diastolic aortic insufficiency (diastolic murmur), aortic stenosis (systolic murmur), early aortic stenosis (click).

B. *The discrete wavelet transform (DWT)*

The 7th level of the Daubechies wavelet (db7) will be used to decompose our PCG groups at a sampling frequency specific to each PCG signal. In addition, the 6th level of approximation (a6) gives a good approximation of the PCG signal analysed in the process of murmur filtering. [10]

The figure below represent the principle of the DWT decomposition:

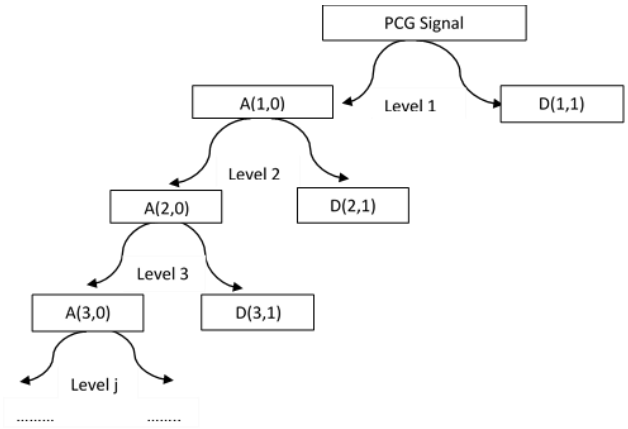

Fig. 2. Discrete Wavelet Transform' decomposition tree of the PCG signal.

The Aj approximations and the details: d1 to dj correspond to the different frequency bands obtained from a DWT.

C. *The reconstruction error parameter*

With: N=Samples number, So =Original signal, Sr = Synthesis signal: the approximation signal. [10]

$$\text{Ɛermoy} = \frac{\sum_{i=1}^{N} |S_0(i) - S_r(i)|}{N} \quad (1)$$

D. *The entropy of approximation coefficients*

In our framework, entropy defines a measure of information quantity contained in the murmur and click segments.[11]

$$E[X] = -\int P(X) Log\, P(X) d(X) \quad (2)$$

X : a continuous random variable : the approximation signal ; P(X) : a probability density.

E. *The mean of detail coefficients*

We calculate the mean of detail coefficients from the sixth level of details (d6) for the two groups of the studied PCG signals.

$$Md = \frac{\sum_1^N d_j}{N} \quad (3)$$

With d_j Detail coefficient among N of level "j".

Both EAC and MD will be calculated for murmurs and clicks only, while the reconstruction error will be for one PCG cycle.

F. *Energetic Ratio*

Used in this study, as a reference feature to affirm the results obtained using DWT technic. ER is very efficient for tracking cardiac disease severity [11].

$$ER = \frac{E_2}{E_1 + E_2} \quad (4)$$

Where E2 is the heart murmur or click energy, E1 is the energy of S1 + S2 and (E1 + E2) is the total energy.

III. Result and Disscussion

The features presented above gave satisfactory results for pathological severity tracking and discriminating.

The perfect wavelet type for our PCG database is the one with the least reconstruction error value. Therefore, we used a cardiac cycle instead of only murmurs or click segments. Yet, it proportionally followed the evolution of the energetic ratio parameter (ER) from the least severe case to the most severe one, making it a valuable parameter for pathological severity tracking (Fig. 3,4,5 and Table II).

We calculated the entropy of approximation coefficients (EAC) and the mean of details (MD) for minor and significant murmurs segments, only to have results specifically related to the medical differences between these two.

The entropy of approximation coefficients (EAC) followed the cardiac severity evolution and discriminated between PCG signals with clicks and those with murmurs. The figure below illustrates the proportional correlation of the EAC to that of the energetic ratio ER (Fig. 3 and Table II). The boxplot shows the variation range of the EAC between the minor and the significant murmurs (Fig. 6). Medical articles helped us to interpret these results; the clicks define a

dysfunction of some of the heart components like valvular aortic stenosis or left ventricle inflexibility, while murmurs are more on blood flow problems due to stenosis and regurgitations [11]. Therefore, they have two distinct graphic representations with two different frequency information.

The entropy (EAC) highlighted the quantity of information present in murmurs compared to clicks and showed that their complexity has an impact on the pathology's severity. (Fig. 4 and Table II)

To investigate the quantity of valuable information remaining in the details bands after a DWT decomposition, we decided to extract a parameter from these bands. Hence, to calculate MD, we chose the sixth level of details (d6) corresponding to the sixth level of approximation (a6) used in the reconstruction error parameter. Even though the variation of this feature is minim, still, it can follow the evolution of the cardiac severity for both clicks and murmurs (Fig. 3,4,5 and Table II). The mean of details also showed the amount of valuable information remaining in the detail bands after a DWT analysis.

Lastly, the three features showed a good correlation with the ER parameter. Therefore, they can be used in their turn for the discrimination and the monitoring of pathological cardiac severity.

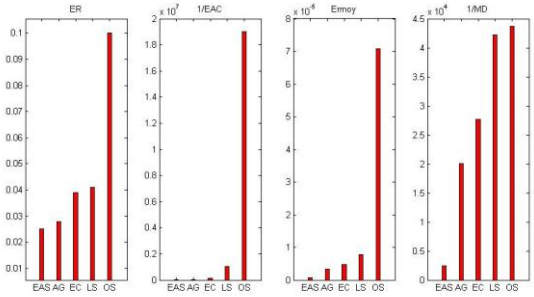

Fig. 3. histogram representation of the three studied parameters for Click PCG signals– (ER) Energetic Ratio, (ECA) Entropy of Approximation Coefficients, (Ermoy) Reconstruction Error, (MD) Mean Variance of Details.

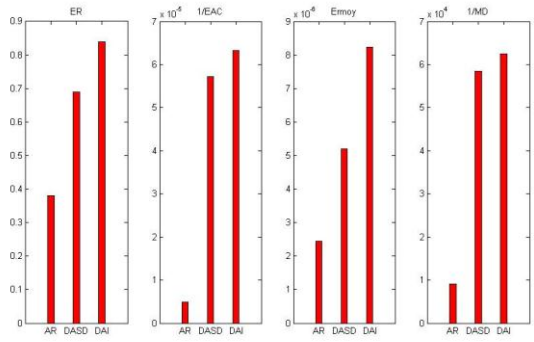

Fig. 4. histogram representation of the three studied parameters for diastolic murmur PCG signals– (ER) Energetic Ratio, (ECA) Entropy of Approximation Coefficients, (Ermoy) Reconstruction Error, (MD) Mean Variance of Details.

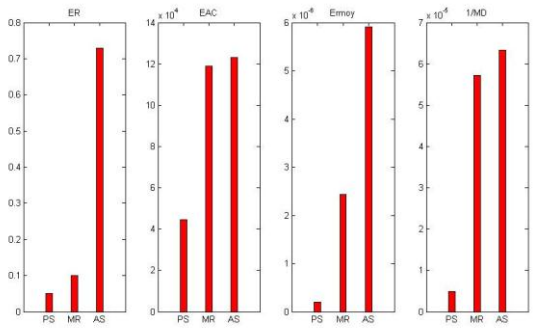

Fig. 5. histogram representation of the three studied parameters for systolic murmur PCG signals– (ER) Energetic Ratio, (ECA) Entropy of Approximation Coefficients, (Ermoy) Reconstruction Error, (MD) Mean Variance of Details.

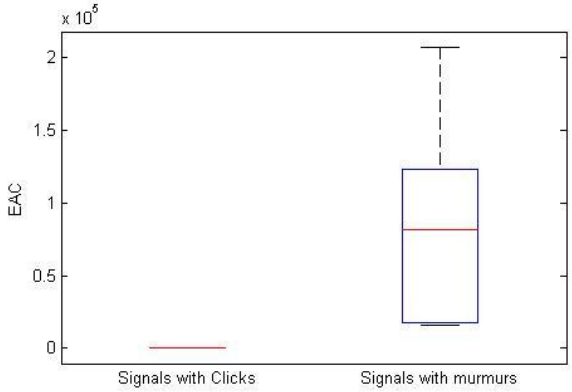

Fig. 6. Boxplot representation of the entropy of approximation coefficients (EAC) variation for PCG signals with clicks and murmurs.

TABLE II. TABLE OF THE EXTRACTED FEATURES FROM THE DISCRETE WAVELET TRANSFORM (DWT) ANALYSIS ON PHONOCARDIOGRAM SIGNALS

PCG Signals	**Extracted features**			
	Energetic Ratio (ER)	***Reconstruction Error (Ɛermoy)***	***Entropy of approximation coefficients (EAC)***	***Mean of details (MD)***
PCG signals with minor murmurs (CLICKS)				
EAS	0.02	6.07e-07	5.48e-05	4.09e-04
AG	0.03	3.32e-06	4.93e-05	4.98e-05
EC	0.04	4.67e-06	7.13e-06	3.61e-05
LS	0.05	7.77e-06	9.51e-07	2.37e-05
OS	0.10	7.08e-05	5.26e-08	2.29e-05
PCG signals with significant murmurs				
Systolic murmurs				
PS	0.05	2.06e-07	4.45e+04	2.91e-05
MR	0.10	2.43e-06	1.19e+05	4.44e-05
AS	0.73	5.91e-06	1.23e+05	5.25e-05
Diastolic murmurs				
AR	0.38	2.44e-06	2.07e+05	1.11e-04
DASD	0.70	5.19e-06	1.75e+04	1.74e-05
DAI	0.84	8.24e-06	1.58e+04	1.60e-05

IV. Conclusion

In closing, the discrete wavelet transform (DWT) technic is a valuable tool in discriminating between the pathological added sounds in a phonocardiogram signal. The three extracted features (the reconstruction error (Ɛermoy), the mean of detail coefficients (Md), and the entropy of approximation coefficients (EAC)) showed pathological discrimination between minor and significant murmurs, along with their ability to assess the pathological cardiac severity's evolution. The correlation of our extracted features with the energetic ratio (ER) used as a reference parameter proves the accuracy of our results in the pathological cardiac discrimination and severity monitoring of the phonocardiogram signal.

Acknowledgment

The authors would like to thand the Directorate-General of Scientific Research and Technological Development (Direction Générale de la Recherche Scientifique et du Développement Technologique, DGRSDT, URL;www.dgrsdt.dz, Algeria) for the financial assistance toward this research.

References

[1] Shivam Varshney, Satyendra Singh, Computation Of Biological Murmurs In Phonocardiogram Signals Using Fast Fourier & Discrete Wavelet Transform, International Conference on Computation, Automation and Knowledge Management (ICCAKM) Amity University,2020.

[2] POTDAR, Ravindra Manohar, et al. Optimal Parameter Selection for DWT based PCG Denoising. Turkish Journal of Computer and Mathematics Education (TURCOMAT), vol. 12, no 9, p. 3207-3219.2021.

[3] S.M Debbal and F. Bereksi-Reguig. Second cardiac sound : analysis techniques and performance comparison; Journal of Mechanics in Medicine and Biology (JMMB);

ISSN : 0219-5194; 5 (3), September2005.

[4] T .Omari. Study of aortique stenosis pathological severity degree, magister theses, Tlemcen University, pp 51, 2009.

[5] R. R.Coifman, Y.Meyer, M. V. Wickerhauser. Wavelet analysis and signal processing. In Wavelets and their applications , Jones and Bartlett, Boston, MA, USA, pp 153-178.1992.

[6] FATMAWATI, T. Y., YULIANI, A., AFANDI, M. A., et al. Comparative Analysis of the Phonocardiogram Denoising System Based-on Empirical Mode Decomposition (EMD) and Double-Density Discrete Wavelet Transform (DDDWT). In : Proceedings of the 1st International Conference on Electronics, Biomedical Engineering, and Health Informatics. Springer, Singapore, p. 593-604.2021.

[7] Meziani F, Debbal SM, Atbi A. Analysis of phonocardiogram signals using wavelet transform. J Med Eng Technol 36(6):283–302.2012

[8] El-Sharo, S., Al-Ghraibah, A., Al-Nabulsi, J., & Matalgah, M. M. (2022). Evaluation of the carotid artery using wavelet-based analysis of the pulse wave signal. International Journal of Electrical & Computer Engineering (2088-8708), 12(2).

[9] Hossain, A., Uddin, S., Rahman, P., Anee, M. J., Rifat, M. M. H., & Uddin, M. M. Wavelet and Spectral Analysis of Normal and Abnormal Heart Sound for Diagnosing Cardiac Disorders. BioMed Research International, 2022.

[10] DEBBAL Imane, Boudis Hidayet, Pathological discrimination parameters of heart sounds, Graduation project, Abou Bekr Belkaid University, Tlemcen, Algeria. 2020

[11] Meziani Fadia, Phonocardiogram signal severity level analysis using wavelet transform (WT), PhD thesis, Abou Bekr Belkaid University, Tlemcen, Algeria. 2013

Journal of Medical Engineering & Technology

ISSN: (Print) (Online) Journal homepage: www.tandfonline.com/journals/ijmt20

A new approach to phonocardiogram severity analysis

Debbal Imane, Hamza Cherif Lotfi & Baakek Yettou Nour El Houda

To cite this article: Debbal Imane, Hamza Cherif Lotfi & Baakek Yettou Nour El Houda (2023) A new approach to phonocardiogram severity analysis, Journal of Medical Engineering & Technology, 47:5, 265-276, DOI: 10.1080/03091902.2024.2310157

To link to this article: https://doi.org/10.1080/03091902.2024.2310157

JOURNAL OF MEDICAL ENGINEERING & TECHNOLOGY
2023, VOL. 47, NO. 5, 265–276
https://doi.org/10.1080/03091902.2024.2310157

Taylor & Francis
Taylor & Francis Group

RESEARCH ARTICLE

A new approach to phonocardiogram severity analysis

Debbal Imane , Hamza Cherif Lotfi and Baakek Yettou Nour El Houda

Genie Biomedical Laboratory (GBM), Genie Biomedical Department, Faculty of Technology, University Abou Bakr Belkaid Tlemcen, Algeria

ABSTRACT

Phonocardiogram signal (PCG) has been the subject of several signal processing studies, where researchers applied various analysis techniques and extracted numerous features for different purposes, like cardiac pathologies identification, healthy/pathologic case discrimination, and severity assessment. When talking about cardiac severity, many think directly about the intensity or energy of the signal as the most reliable parameter. However, cardiac severity is not always reflected by the intensity or energy of the signal but includes other variables as well. In this paper, we will discuss the probability of having a Discrete Wavelet Transform (DWT) parameter that discriminates, identifies, and assesses the pathological cardiac severity levels, a parameter that takes into consideration other variables and elements for the severity study. For this purpose, we studied six PCGs signals that contain reduced murmurs (clicks) and eight murmur signals with four different cardiac severity levels. We extracted the Entropy of Approximation Coefficients (EAC) from the Discrete Wavelet Transform (DWT) sub-bands as the feature to study in this novel approach. The Energetic Ratio (ER) served as a reference parameter to evaluate the EAC evolution, due to its proven efficiency in cardiac severity tracking. While the DWT-EAC algorithm results revealed that the EAC provides better results for the paper purposes, the One versus All Support Vector Machine (OVA-SVM) classifier affirmed the efficiency of the Entropy of Approximation Coefficients (EAC) for cardiac severity assessment and proved the accuracy of this novel approach.

ARTICLE HISTORY
Received 2 November 2022
Revised 19 January 2024
Accepted 20 January 2024

KEYWORDS
Phonocardiogram signal; cardiac severity; entropy of approximation coefficients; One versus All Support Vector Machine

1. Introduction

The phonocardiogram signal has inspired many researchers in their quest to study cardiac pathologies. Processing these signals using analysing techniques developed for sound and/or physiological signals has enabled the automatic detection of numerous cardiac pathologies, discrimination between pathological and healthy cases, identification/localisation of heart sounds as well as clicks and murmurs, and assessing the cardiac severity.

With the optic of phonocardiogram (PCG) signals concealing relevant information about cardiac pathologies, we carry out this study. In a healthy case, the PCG signal presents two heart sound (S1 and S2). The first one S1, results from the closure of the mitral and tricuspid valves [1]. While the second heart sound S2, refers to the closure of the aortic and pulmonic valves [1]. In pathological cases, other sounds may be present on the graphic representation of the PCG recording, murmurs and short murmurs (clicks) are the most known; however, other added sounds may appear to indicate abnormal heart condition, like splits, gallops, and third and fourth heart sounds S3, S4. Certain cardiovascular diseases produce audible sounds during the systole, the diastole or both known under the name of murmurs [2,3].

Studies like cardiac pathologies discrimination, denoising and classification using Discrete Wavelet Transform (DWT) [4–9], the Empirical Mode Decomposition [10–14] are popular among researchers. Spectral and spectro-temporal entropy were found relevant for various purposes of the PCG signal, like classification, discrimination, identification etc[15–18].

In this paper, we will study the cardiac severity. First, we will analyse click and murmur segments with the Discrete Wavelet Transform (DWT), extract the Entropy of Approximation Coefficients (EAC) then compare it to the Energetic Ratio (ER) evolution. Second, we will repeat the same process on one PCG cycle instead of the click or murmur segments. Lastly, we will introduce the extracted EAC from click/murmur and one PCG cycle into a one-vs-all Support Vector

CONTACT Debbal Imane imane.debbal@univ-tlemcen.dz Genie Biomedical Laboratory (GBM), Genie Biomedical Department, Faculty of Technology, University Abou Baki Belkaid Tlemeen, Algeria.

Machine (OVA-SVM) classifier, to check the accuracy of these features for cardiac severity assessment.

2. Methodology

To highlight the differences between the pathological cardiac severity levels, we studied our phonocardiogram (PCG) database in two ways (Figure 1).

First, we segmented manually the click and murmurs from the PCG recordings by referring to the information present in Table 1. We then processed these segments with the Discrete Wavelet Transform (DWT), extracted the Entropy of Approximation Coefficients (EAC) and compared it to the Energetic Ratio (ER) evolution.

Second, we repeated the same process on one PCG cycle instead of the click or murmur segments. This

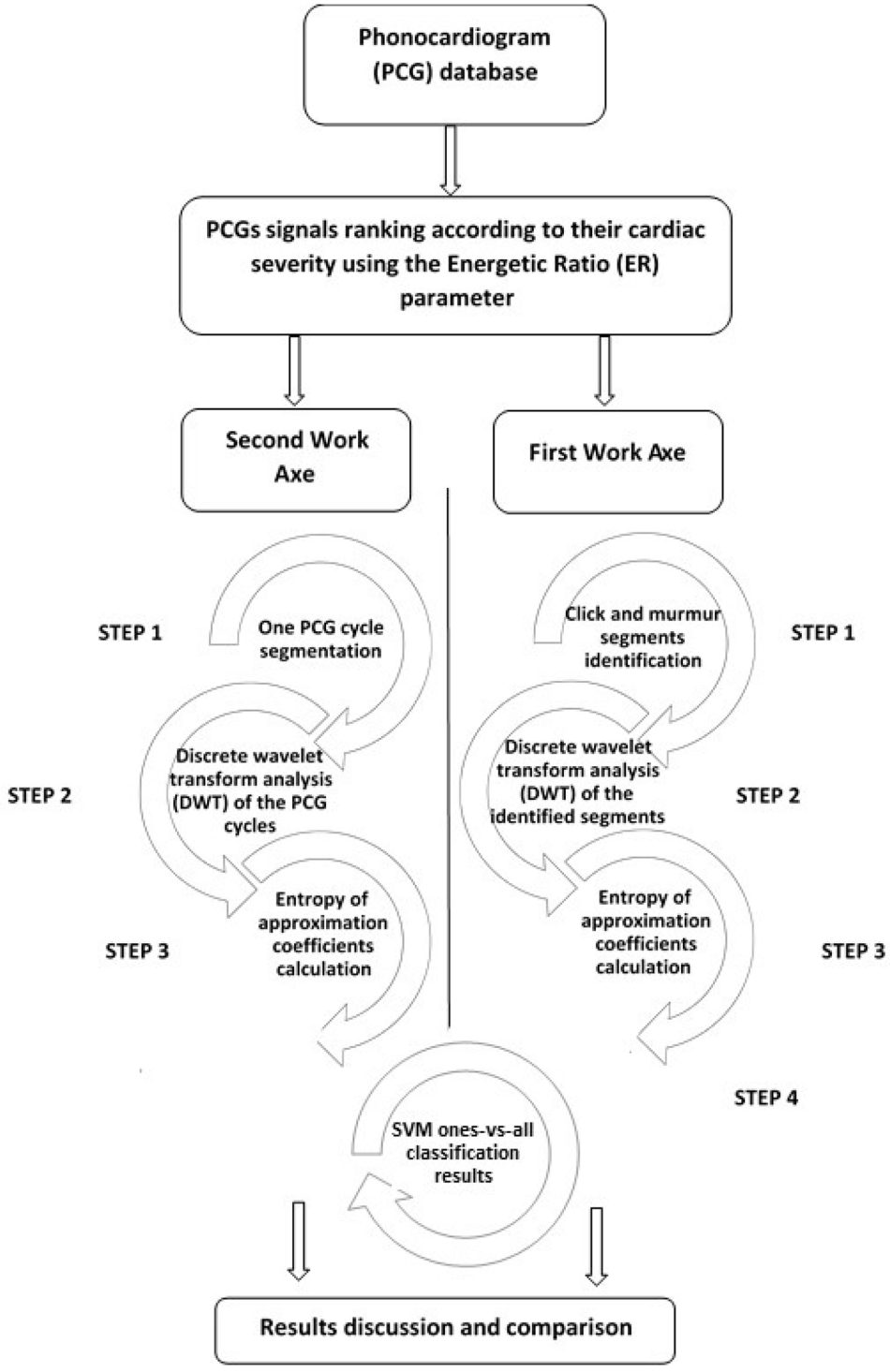

Figure 1. Discrete Wavelet Transform analysis work organogram.

Table 1. Clicks and murmurs characteristics for the studied pathologies [19].

PCG signals	Click/Murmur characteristics			
	Frequency Range	Duration / location in the cardiac cycle	Configuration	Timber
		Group 1		
Early Aortic Stenosis	100-800Hz (High pitch)	≈10-20ms, early-systolic	/	Dry
Ejection Click		early-systolic	/	Sharp
Late Systole		Late-systolic	/	/
Open Snap		Early-diastolic	/	Sharp
Atrial Gallop	15-50Hz (Low pitch, very low frequency, short and faint)	≈0.08-0.20s just before S1	/	Galloping rhythm, lilt or canter quality
Ventricular Gallop		≈0.15s after S2, early-diastolic	/	
		Group 2		
Aortic Stenosis	Up to 600 Hz (Medium to low pitch)	Mid-, late-, holo-systolic	Crescendo–decrescendo	Harsh, rasping, grunting or rough
Aortic Regurgitation	Up to 600 Hz (High or low pitch)	Early-diastolic	Decrescendo	Blowing

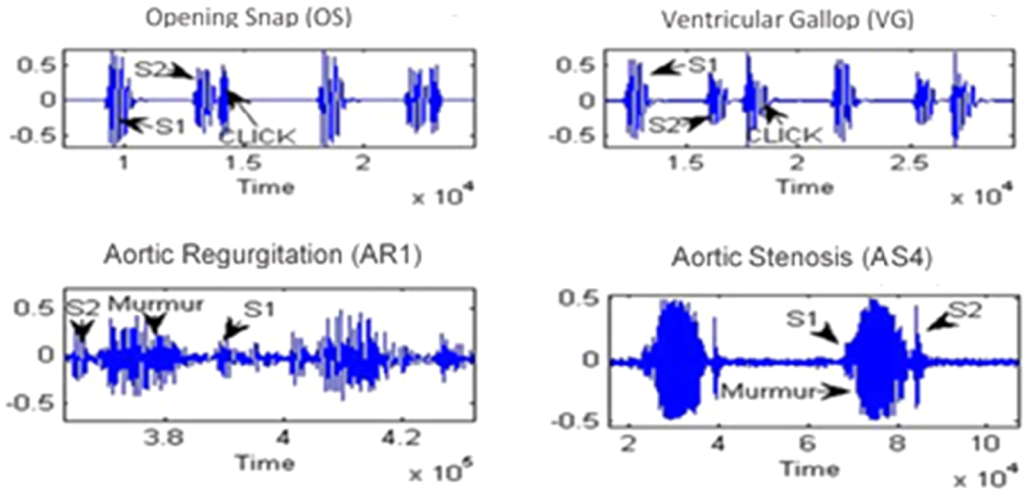

Figure 2. illustrates two PCG signals from each group: the opening snap and Ventricular gallop from group 1, and the lest severe case of the Aortic Regurgitation (AR1) and the most severe case of the Aortic Stenosis (AS4) from group 2.

approach permitted us to appreciate the presence of severity information in the heart sounds (S1 + S2).

The energy/intensity of the signal is one of the features related to the severity evolution. Hence, the comparison of our results with the Energetic Ratio (ER).

Lastly, we introduced the EAC values obtained from the two study ways into a One-vs-All Support Vector Machine (OVA-SVM) classifier, to check the accuracy of the EAC for cardiac severity assessment.

We listed all the studied phonocardiogram signals in Table 2. We divided the database into two groups (G1 and G2) for discriminating the cardiac severity levels.

Information regarding frequency range and timings in Table 1 are from [19–25].

We illustrated two PCG signals from each group mentioned in Table 1 in Figure 2.

The PCGs signals used in our study are real signals acquired from the four auscultation sites (aortic, tricuspid, mitral and pulmonary) that are publicly available online ((http://www.egeneralmedical.com, http://www.cardiosource.com/heartsounds, http://www.dundee.ac.uk/medther/Cardiology/hsmur.html, accessed on 2009) and (https://github.com/yaseen21khan/Classification-of-Heart-Sound-Signal-Using-Multiple-Features-, accessed on 2023)) for research purposes. No participants' personal information (e.g. name or address) was included in this study.

2.1. The discrete wavelet transforms (DWT)

Discrete wavelet transform (DWT) algorithms have become standard tools for processing of images and signals in several areas of biomedical applications. The Discrete Wavelet Transform (DWT) is defined as the following:

$$\Psi\ \mathrm{jk}(t) = 2^{-j/2}\,\Psi\ (2^{-jt} - k) \tag{1}$$

With j,k $\in$ Z

The discrete wavelet transforms (DWT) discretises the time-scale and time parameters. [26]

Figure 3(a) illustrates the principle of the DWT decomposition. Width varying filter banks holds the decomposed phonocardiogram signal. The decomposition level defines the width of these band-pass filter banks (Figure 3(b)).

Table 2. Phonocardiogram signals used for cardiac severity discrimination.

Phonocardiogram signals	Name Abbreviation
Group 1	
EAS	Early Aortic Stenosis
EC	Ejection Click
LS	Late Systole
OS	Open Snap
AG	Atrial Gallop
VG	Ventricular Gallop
Group 2	
AS1/AS2/AS3/AS4	Aortic Stenosis
AR1/AR2/AR3/AR4	Aortic Regurgitation

The high-pass and low-pass filters of the DWT allow as decomposing the PCG signal into approximations and details. Here, the approximation corresponds to the informative (noise-free) PCG signal, while the details to the extracted noises from the PCG signal after decomposition (Figure 3(a)).

We selected the seventh level of the DAUBECHIES wavelet (db7), as the mother wavelet, to decompose our PCG signals. Since it displays robust results in the analysis of linear time-varying biomedical signals, due to its ability to compensate for missed coefficient in the final decomposition paradigm [28], and the shape similarities with the heart sounds. We used a sampling frequency of 8 kHz, as recommended by previous researches for PCG signal processing and filtering. We extracted the Entropy of Approximation Coefficients (EAC) forms the sixth level of approximation (a6) due to it minimal reconstruction error of the original signal. The φ_3^D is the DAUBECHIES scaling function, and it is defined by the following relation [28]:

$$\varphi_3^D = \sum_{k=0}^{3} p_k \varphi(2t-k) \tag{2}$$

2.2. Energetic ratio

The energy/intensity of the signal is one of the features related to the severity evolution. The energy ratio is the energy of the murmur segment over the energy of the cardiac cycle. The equation bellow highlight the importance of the murmur. The more the murmur intensifies, the higher is the ER.

$$ER = \frac{E_2}{E_1 + E_2} \times 100 \tag{3}$$

where E2 is the click or heart murmur energy, E1 is the energy of the two heart sounds S1 + S2 and (E1 + E2) is the energy of one PCG cycle.

- ER <30%, refers to Light severity level.
- 30% <ER < 70%, Moderate severity level.
- ER> 70%, Severe severity level.

The equation of ER varies from 0-100%. If ER equals to 100%, the murmurs dominate the cardiac cycle over cardiac sounds (S1, S2). Therefore, ER is very efficient for tracking cardiac disease severity. We used it in this study as a reference feature to compare and evaluate the results obtained using the DWT analysis. [29–31].

2.3. The entropy of approximation coefficients

Entropy is the definition of the complexity, irregularity, unpredictability characteristics present in the

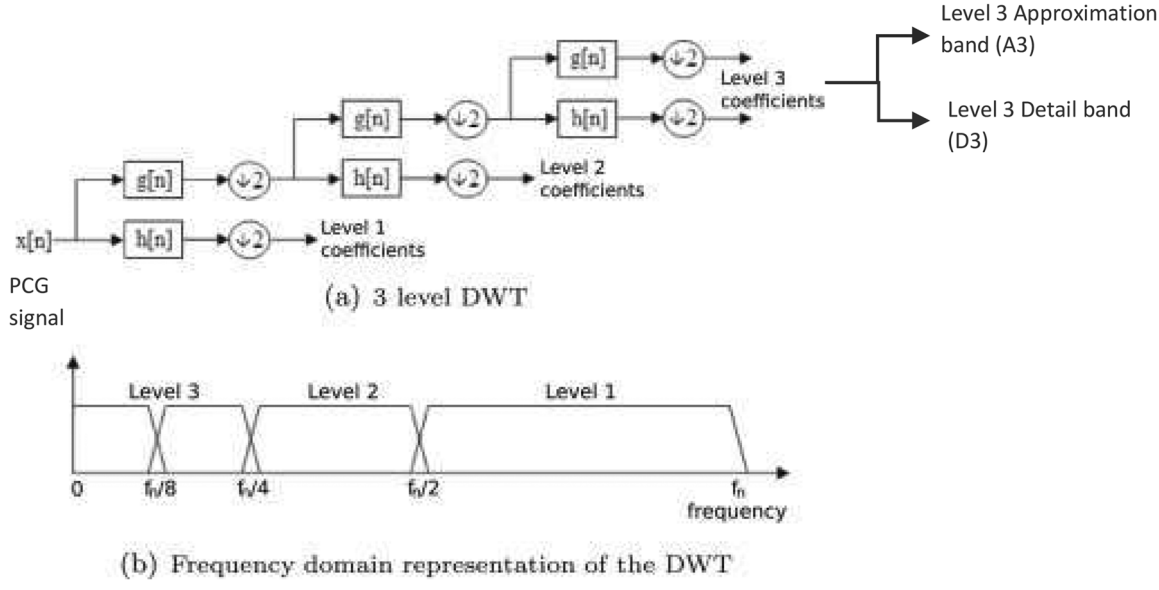

Figure 3. The principle of Discrete Wavelet Transform: (a) Discrete Wavelet Transform' decomposition tree of the PCG signal, (b) frequency domain representation of the DWT (filter banks).[27].

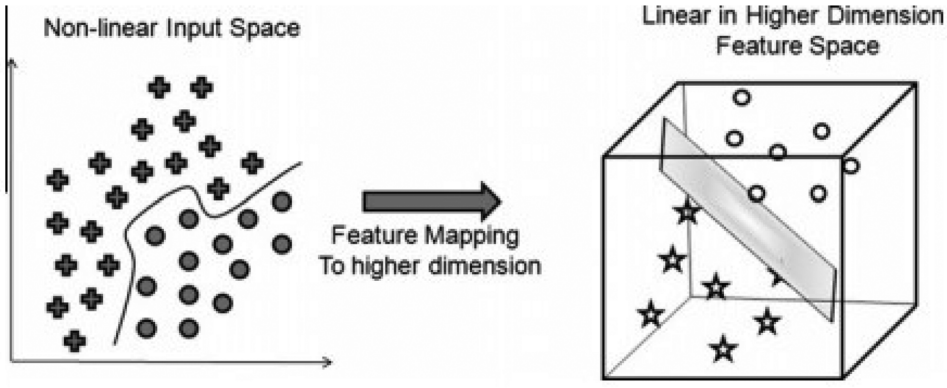

Figure 4. Non-linear to linear transformation using support vector machine SVM technique [34].

phonocardiogram signal. We implemented the standard equation of the entropy in our algorithm (Equation 4).

$$E[X] = -\int P(X)\log P(X)d(X) \quad (4)$$

X: a continuous random variable: the approximation signal (a6); P(X): a probability density.

2.4. One versus all support vector machine (OVA-SVM)

The statistical learning theory of Vapnik [32] and quadratic programming [33] are the base of the Support Vector Machine (SVM). The SVM classifier uses hyper-planes to devise between different classes in a high dimensional feature space. SVM is employed to discriminate a set of linearly separable hyper-planes, which are linear functions of the high dimensional feature space (Figure 4). The hyper-planes are placed in a way to maintain maximum distance from both classes.

It is possible to use SVM for multi-class problems. In general, the common approaches to multiclass classification are one-versus-one method and one-versus-all method [35]. For a N-class classification problem, the former approach requires N binary SVM classifiers. In this work, we used a 2-class and 3-class classifier model with two and three SVM binary classifiers, following a one-versus-all approach.[36]

3. Results and discussion

Results and figures highlight the efficiency of the Entropy of Approximation Coefficients (EAC) for cardiac severity assessment.

As mentioned before, the Energetic Ratio (ER) is effective for cardiac severity tracking. Therefore, we relayed on it to rank the group 1 (G1) and group 2 (G2) phonocardiogram signals (PCGs) from the least to the most severe case. We lately compared the obtained results with the ER to evaluate the accuracy of the EAC evolution with the cardiac severity [29–31,36–39].

Figure 1 illustrates how we proceeded with this study. In the first work axe, we segmented manually the clicks and murmurs from the PCG recordings by referring to the information present in Table 1. We then processed these segments with the Discrete Wavelet Transform (DWT), extracted the Entropy of Approximation Coefficients (EAC) and compared it to the Energetic Ratio (ER) evolution.

As shown in Figure 5(b), the entropy of approximation coefficients (EAC) presented an ascending evolution similar to that of the cardiac severity represented by the Energetic Ratio (ER) (Figure 5(a)). Which refers to the ability of the EAC to identify each pathology with minor murmurs (click) as a different cardiac severity level. The figure below illustrates the proportional correlation between the complexity, irregularity, unpredictability characteristics and the energy/intensity of the click/murmur segments through the EAC and the ER for the six studied pathologies of group 1 (Figure 5).

To test the efficiency of the EAC in assessing the severity within the same pathology, we processed eight PCGs signals, four signals from the aortic stenosis (AS1, AS2, AS3 and AS4) and four from the aortic regurgitation (AR1, AR2, AR3 and AR4), each signal had a different severity level from the other. First, we started by segmenting the murmur segments and then apply the DWT- EAC algorithm.

Figure 6(b) illustrate the increasing of the stroke volume corresponding to the severity of the aortic regurgitation [40] and the increasing of the left ventricular outflow tract obstruction in the aortic stenosis [40,41] through the ascending evolution of the EAC for the four cases of AS and AR.

Hence, through this first work axe where we studied click and murmur segments from each pathology (G1) and severity level (G2), we highlighted the

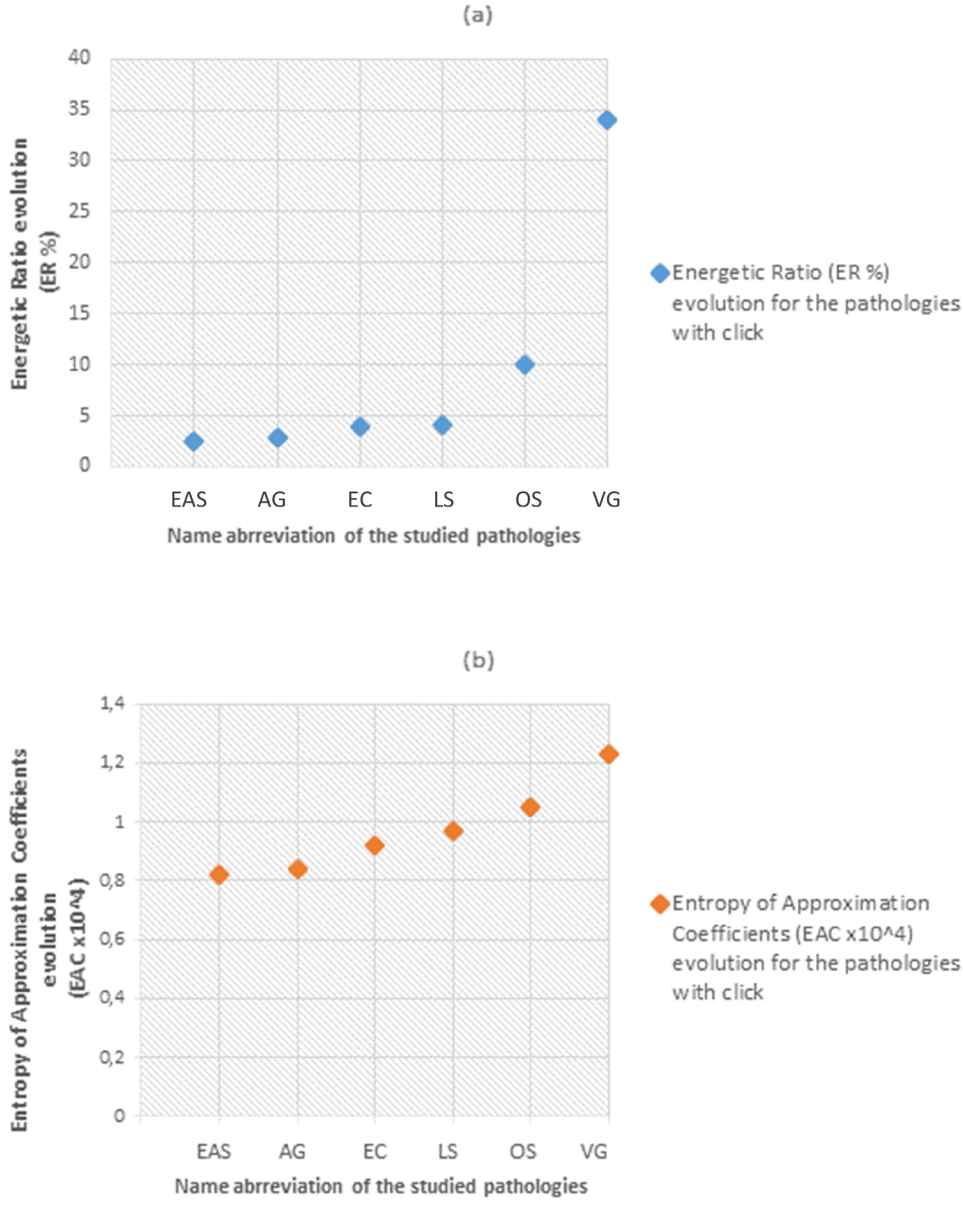

Figure 5. (a) Energetic Ratio (ER %) evolution for the pathologies with click, (b) first axe results: Entropy of Approximation Coefficients (EAC x10^4) evolution for the pathologies with click when using click segments only.

influence of clicks and murmurs complexity on the pathology's severity by the help of the entropy of approximation coefficients and the energetic ratio.

For the second work axe, we repeated the same process and algorithm on our database. However, this time we used a full PCG cycle (S1 + S2+ Added sound (click or murmur)) instead of click/murmur segments. This approach permitted us to appreciate the presence of severity information in the heart sounds (S1 + S2) along with the one in the added sounds.

Even after processing the heart sounds with the added sounds (one PCG cycle), the EAC evolution remains correlated to the severity and the Energetic Ratio (ER). Which confirms the probability that says heart sounds retains severity information that evolve proportionally to the cardiac severity even within the same pathology. Figures 7 and 8 illustrate this proportional evolution when studying the severity for pathologies of group 1 and 2. Through these results, we can claim that adding heart sounds to the analysis algorithm will not affect the EAC in the severity assessment.

Since the EAC values in this second work axe were found superior to the ones obtained in the first work axe, we calculated the difference between them as a final step for this second work axe. We then plotted the results into a graph to appreciate it evolution (Figure 9). The proportional evolution highlighted in Figure 9 for the group 1 signals and Aortic Stenosis cases confirms again the probability that says heart sounds retains severity information that evolves

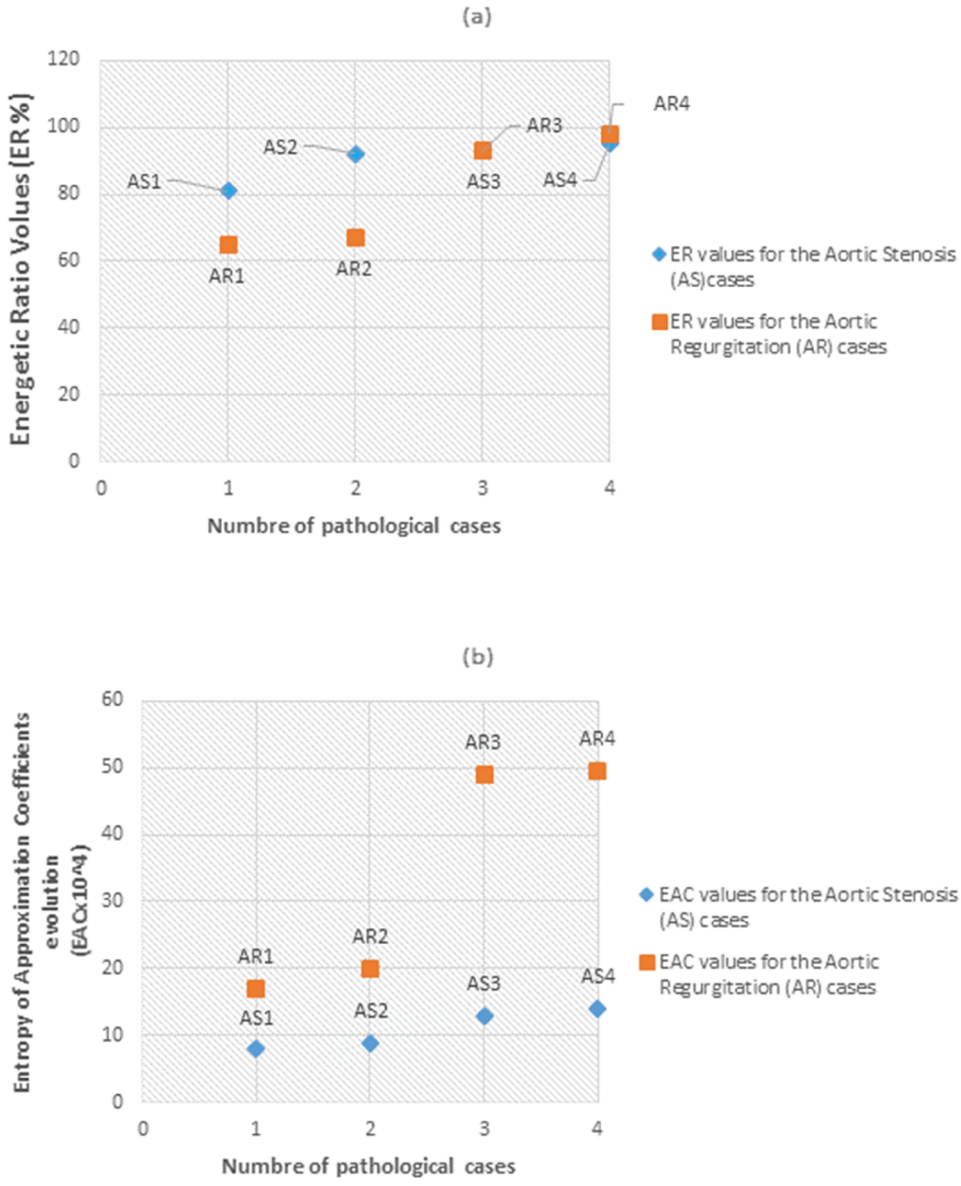

Figure 6. (a) Energetic Ratio (ER) evolution within the Aortic Stenosis (as) and the Aortic Regurgitation (AR) cases, first work axe results: (b) Entropy of Approximation Coefficients (EAC x10^4) evolution for the Aortic Stenosis (as) and the Aortic Regurgitation (AR) cases when using murmur segments only.

proportionally to the cardiac severity even within the same pathology. However, the inversely proportional evolution of the Aortic Regurgitation cases allows us to say that in some pathologies the heart sounds are not as affected by the severity as in other cardiac diseases.

In this study, the Energetic Ratio (ER) served as a reference feature to evaluate the accuracy of the obtained results using a DWT analysis [29–31,36–39] before introducing them into a one-vs-all SVM machine learning classifier.

When comparing the EAC results with the ER values, we noticed that our parameter, the Entropy of Approximation Coefficients (EAC), displayed better results in separating the different severity levels of the studied cardiac pathologies, for both added sounds (click and murmur) segments and one PCG cycle (heart sound + added sound) (Figures 5–8).

Since some pathologies tend to lose it murmur intensity when reaching severe levels (e.g. the aortic stenosis present short and soft murmur for extreme severity levels [41]), relaying only on the signal's intensity for severity study may therefore be misleading in these circumstances. Thus, the necessity to use features like the entropy (EAC) that quantifies the information present in the studied signals without focusing only on their intensity. Therefore, the Entropy of Approximation Coefficients (EAC) established in this

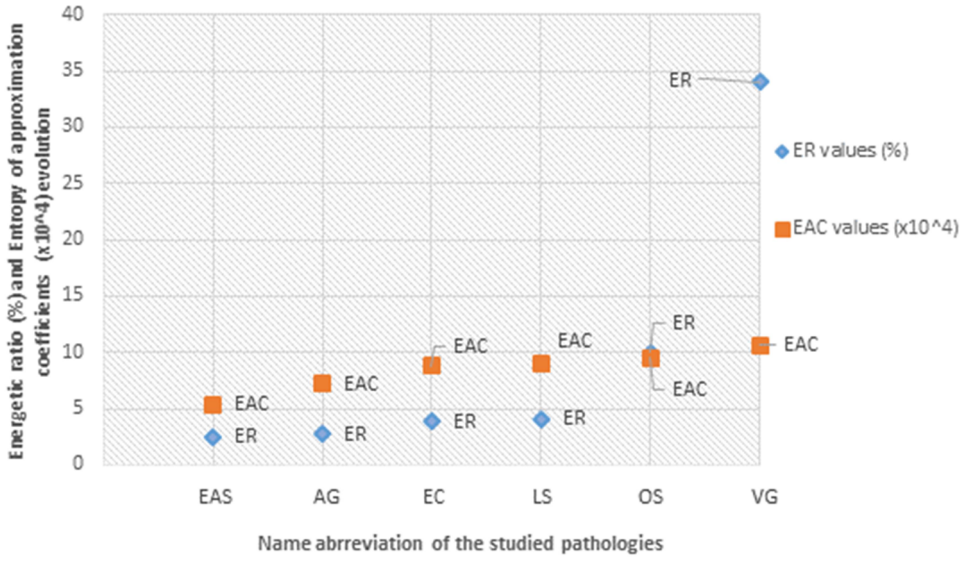

Figure 7. Second work axe: Energetic ratio (%) and Entropy of approximation coefficients (x10^4) evolution for the pathologies with click when using one PCG cycle.

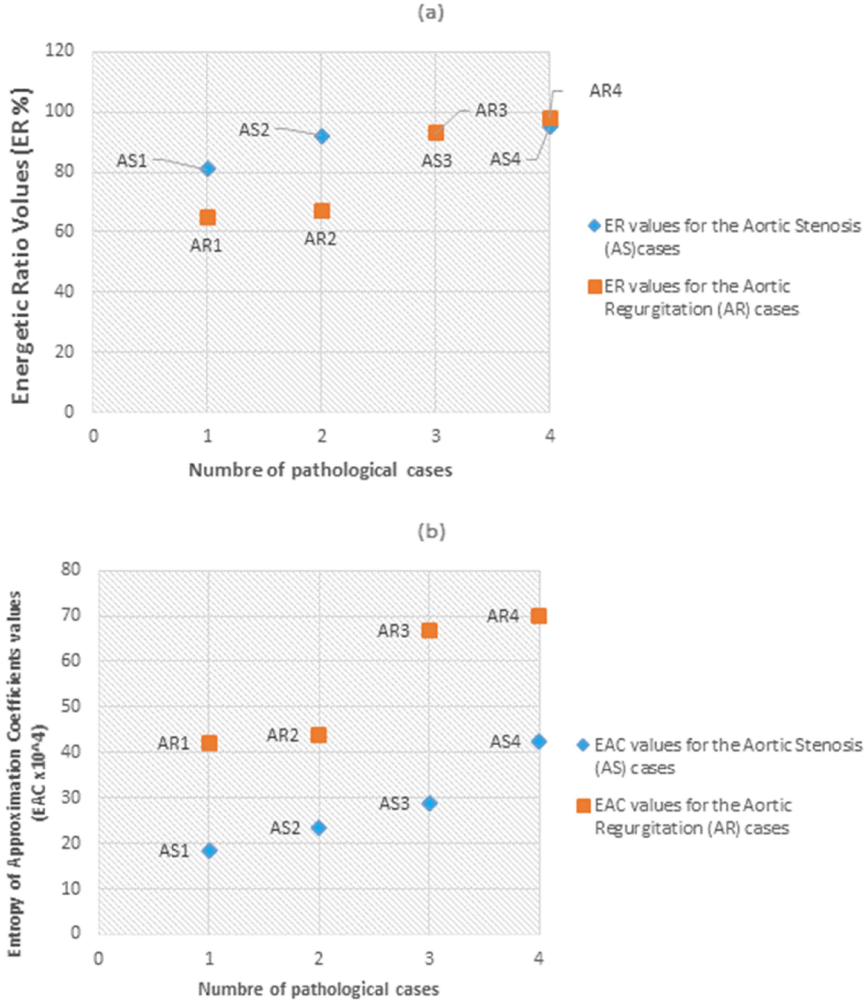

Figure 8. Energetic Ratio (ER) evolution within the Aortic Stenosis (as) and the Aortic Regurgitation (AR) cases, Second work axe results: (b) Entropy of Approximation Coefficients (EAC x10^4) evolution for the Aortic Stenosis (as) and the Aortic Regurgitation (AR) cases when using one PCG cycle.

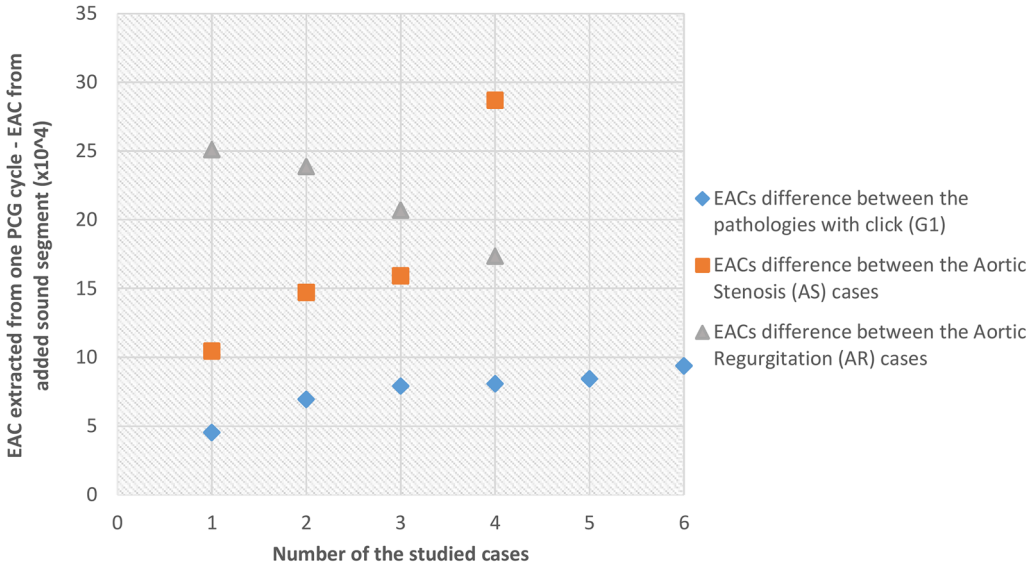

Figure 9. Displays the difference values (EAC extracted from one PCG cycle - EAC from added sound segment) for the group 1 and group 2 signals.

paper a better discrimination between the severity levels then the energetic ratio ER. Which makes normalising the use of the EAC for severity level identification and assessment a new approach to phonocardiogram severity analysis.

Figures 6(b) and 8(b) affirm this new approach, where the entropy (EAC) identifies the Aortic Stenosis and Regurgitation separately when the Energetic Ratio (ER) place them together in high severities (Figures 6(a), 8(a)). We can also notice through these two figures that the entropy (EAC) ranked the AR and AS differently in term of values importance compared to the Energetic Ratio (ER). The AR presented EAC values superior to that of the AS which means that the signals' intensity is clearly not the only parameter directly related to the cardiac severity since information like the complexity, irregularity, unpredictability characteristics of the signal established a better separation between cardiac pathologies. The same observation could be made for the pathologies with a minor murmur. The ER clearly discriminates between pathologies with high energy (e.g., Ventricular Gallop (VG) and Open Snap (OS)) however presents a kind of steady evolution for low-energy pathologies (Figures 5(a), 7(a)). On the other hand, the entropy of approximation coefficient (EAC) presented a significant discrimination and separation between all the pathologies (Figures 5(b), 7(b)).

Finally, yet importantly, we introduced the EAC values obtained from the two work axes into a machine learning (one-vs-all SVM) classifier to test the accuracy of these features for click/murmur discrimination and cardiac severity assessment.

First, we tested the ability of the EACs to discriminate between the two pre-established groups of PCGs signals (G1 and G2). As noticed from Figure 10, the EACs successfully classified the database in two distinct classes that correspond respectively to the group 1 and group 2 of PCGs signals. We can easily distinguish the Aortic Stenosis cases (AS1, AS2, AS3 and AS4) from the Aortic Regurgitation severity (AR1, AR2, AR3 and AR4) in the blue zone that refers to the PCG signal with murmurs.

Second, we divided the database into three classes:

- Class 1 for the pathologies with minor murmurs (EAS, AG, LS, EC, OS, VG).
- Class 2 for the Aortic Stenosis severity cases (AS1, AS2, AS3, and AS4).
- Class 3 for the Aortic Regurgitation severity cases (AR1, AR2, AR3, and AR4).

Figure 11 highlights the aptitude of the EACs (EAC extracted from added sound segment + EAC from one PCG cycle) to distinguish between the three classes. The SVM classifier classified the PCGs signals into three colourful zones where each zone represents a particular class. One can notice from the Figure 11, that the SVM classifier respected the severity levels of the phonocardiogram signals since each zone display an evolution similar to the ones obtained in Figures 5–8.

Lastly, this application of introducing the EACs values into a machine learning classifier affirms the Entropy of Approximation Coefficients (EAC) efficiency

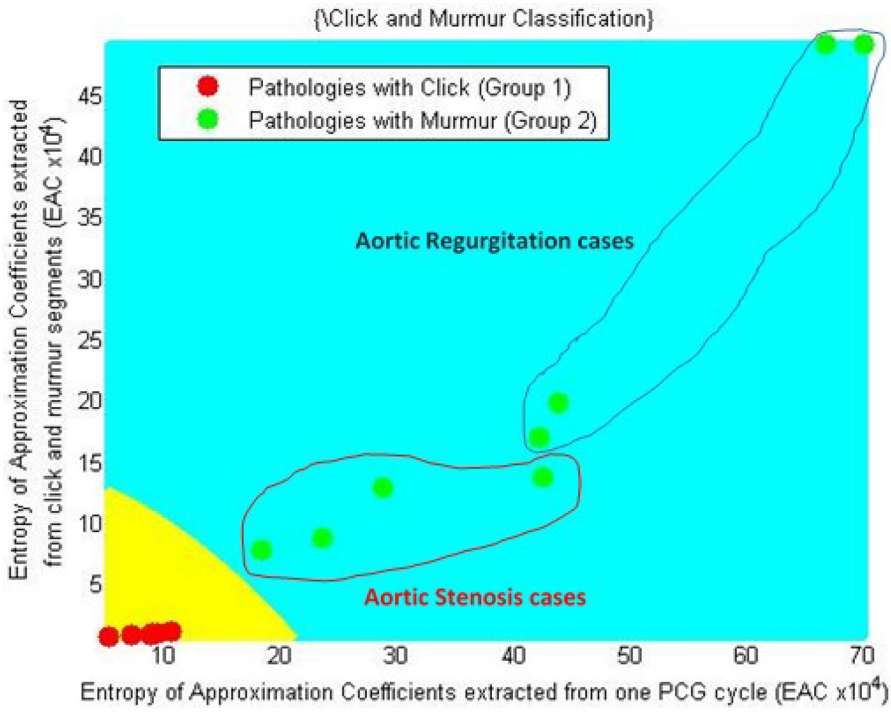

Figure 10. One versus all Support Vector Machine (OVA-SVM) classification results for a two-class classification (click pathologies – murmur pathologies): the yellow zone refers to the pathologies with click and the blue one classifies the eight cases of the aortic stenosis and the aortic regurgitation cases.

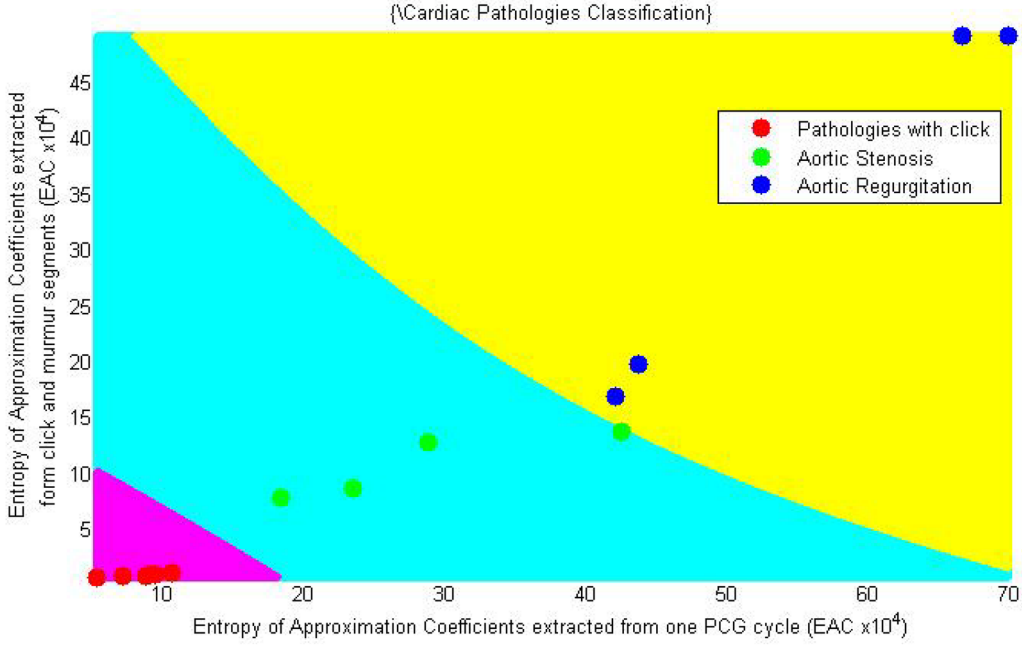

Figure 11. One versus all Support Vector Machine (OVA-SVM) classification results for a three-class classification (click pathologies – Aortic Stenosis – Aortic Regurgitation): the purple zone refers the pathologies with click, the blue one classifies the four cases of the aortic stenosis, and the yellow zone correspond to the aortic regurgitation cases.

for cardiac severity assessment and prove the accuracy of this novel approach.

Conclusion

In conclusion, the discrete wavelet transform (DWT) in itself is a valuable tool in discriminating between pathological phonocardiogram signals, let al.one extracting features like the entropy of approximation coefficients (EAC) from it sub-bands.

In this work, we exploited the efficiency of the DWT and the EAC to assess the cardiac severity. We analysed click and murmur segments as a first step, then a whole PCG cycle. We then compared our results to the Energetic Ratio (ER) evolution. Lastly, we introduced the EACs (EAC extracted from added sound segment+EAC from one PCG cycle) into a one-vs-all Support Vector Machine (SVM) classifier, to check the accuracy of these features for cardiac severity assessment.

Through this work, we found that the EACs values are discriminative enough to separate clicks from murmurs, to assess the cardiac severity and identify each severity level separately. The entropy of approximation coefficients excelled where the energetic ratio could not, even though it was the reference feature for this work. Which makes the EAC a better cardiac severity discriminative, and assessing tool.

In the end, the main aim behind this work is to demonstrate that relaying completely on the signal energy/intensity when studying the cardiac severity could be misleading. However, use features like our novel approach "the entropy of approximation coefficients EAC" that quantifies different relevant severity elements and information from the signal.

"Compliance with ethical standards"

- No, I have nothing to report
- This study was not funded by any party: it is an academic PhD study
- No conflict of interest
- No animal or other used in this study

Acknowledgements

The authors would like to thank the Directorate-General of Scientific Research and Technological Development (Direction Générale de la Recherche Scientifique et du Développement Technologique, DGRSDT, URL:www.dgrsdt.dz, Algeria) for the financial assistance towards this research.

Disclosure statement

No potential conflict of interest was reported by the author(s).

Funding

The author(s) reported there is no funding associated with the work featured in this article.

References

[1] Li X, Zhong L, Luo L, et al. Synchronization control of pulsatile ventricular assist devices by combination usage of different physiological signals. Comput Assist Surg (Abingdon). 2019;24(sup1):105–112. doi: 10.1080/24699322.2018.1560089.

[2] Taplidou SA, Hadjileontiadis LJ. Nonlinear analysis of heart murmurs using wavelet-based higher-order spectral parameters. in 2006 International Conference of the IEEE Engineering in Medicine and Biology Society, pp. 4502–4505, 2006. doi: 10.1109/IEMBS.2006.259619.

[3] Ahmad MS, Mir J, Ullah MO, et al. An efficient heart murmur recognition and cardiovascular disorders classification system. Australas Phys Eng Sci Med. 2019;42(3):733–743. doi: 10.1007/s13246-019-00778-x.

[4] Chowdhury TH, Poudel KN, Hu Y. Time-Frequency analysis, denoising, compression, segmentation, and classification of PCG signals," in. IEEE Access. 2020;8:160882–160890. doi: 10.1109/ACCESS.2020.3020806.

[5] Hossain A, Uddin S, Rahman P, et al. Wavelet and spectral analysis of normal and abnormal heart sound for diagnosing cardiac disorders. Biomed Res Int. 2022;2022:9092316–9092346. doi: 10.1155/2022/9092346.

[6] Li H, Ren G, Yu X, et al. Discrimination of the diastolic murmurs in coronary heart disease and in valvular disease. IEEE Access. 2020;8:160407–160413. doi: 10.1109/ACCESS.2020.3021093.

[7] Ghosh SK, Tripathy RK, R N P. Evaluation of performance metrics and denoising of PCG signal using wavelet based decomposition. 2020 IEEE 17th India Council International Conference (INDICON), New Delhi, India, pp. 1–6, 2020 doi: 10.1109/INDICON49873.2020.9342464.

[8] Touahria R, Hacine-Gharbi A, Ravier P. Discrete Wavelet based Features for PCG Signal Classification using Hidden Markov Models. In: ICPRAM. p. 334-340. 2021

[9] Liu Q, Xu Y, Zhang L, et al. Research on heart sound signal denoising algorithm based on variational mode decomposition and wavelet threshold. JCC. 2021;09(10):110–121. doi: 10.4236/jcc.2021.910007.

[10] Talal M, Aziz S, Khan MU, et al. Machine learning-based classification of multiple heart disorders from PCG signals. Expert Syst. 2023;40(10):e13411. doi: 10.1111/exsy.13411.

[11] Fatmawati TY, Yuliani A, Afandi MA, et al. Comparative analysis of the phonocardiogram denoising system based-on empirical mode decomposition (EMD) and Double-Density discrete wavelet transform (DDDWT). In Proceedings of the 1st international conference on electronics, biomedical engineering, and health informatics. Springer, Singapore, p. 593–604. 2021.

[12] Qi P, Xu H, Zhang H, et al. Residual neural networks based on empirical mode decomposition for mitral regurgitation prediction. Biomed Signal Process Control. 2023;86:105265. doi: 10.1016/j.bspc.2023.105265.

[13] Yang L, Li S, Zhang Z, et al. Classification of phonocardiogram signals based on envelope optimization model

and support vector machine. J Mech Med Biol. 2020;20(01):1950062. doi: 10.1142/S0219519419500623.
[14] Arslan Ö. Automated detection of heart valve disorders with time-frequency and deep features on PCG signals. Biomed Signal Process Control. 2022;78:103929. 2022. doi: 10.1016/j.bspc.2022.103929.
[15] Rizal A e, Wijayanto I. Phonocardiogram classification using multilevel wavelet packet entropy and random Forest. In 2020 6th International Conference on Science and Technology (ICST). IEEE, p. 1–4, 2020. doi: 10.1109/ICST50505.2020.9732841.
[16] Safara F, Doraisamy S, Azman A, et al. Wavelet packet entropy for heart murmurs classification. Adv Bioinformatics. 2012;2012:327266–327269. doi: 10.1155/2012/327269.
[17] Zhang H, Wang X, Liu C, et al. Discrimination of patients with varying degrees of coronary artery stenosis by ECG and PCG signals based on entropy. Entropy. 2021;23(7):823. doi: 10.3390/e23070823.
[18] Karan B, Padhi T. Hilbert domain characterizations of wavelet packets for automated heart sound abnormality detection. Biomed Signal Process Control. 2024;90:105793. doi: 10.1016/j.bspc.2023.105793.
[19] :Dwivedi AK, Imtiaz SA, Rodriguez-Villegas E. Algorithms for automatic analysis and classification of heart sounds–a systematic review. IEEE Access. 2019;7:8316–8345. doi: 10.1109/ACCESS.2018.2889437.
[20] Liu C, Springer D, Li Q, et al. An open access database for the evaluation of heart sound algorithms. Physiol Meas. 2016;37(12):2181–2213. doi: 10.1088/0967-3334/37/12/2181.
[21] Mason D. Listening to the heart: a comprehensive collection of heart sounds and murmurs., 2nd ed. Philadelphia, Hahnemann University, School of Medicine, 2000.
[22] Thoms L, Colicchia G, Girwidz R. Phonocardiography with a smartphone. Phys Educ. 2017;52(2):023004. no. 023004, doi: 10.1088/1361-6552/aa51ec.
[23] Naseri H, Homaeinezhad MR. Detection and boundary identification of phonocardiogram sounds using an expert frequency-energy based metric. Ann Biomed Eng. 2013;41(2):279–292. doi: 10.1007/s10439-012-0645-x.
[24] Noponen A-L, Lukkarinen S, Angerla A, et al. Phono-spectrographic analysis of heart murmur in children. BMC Pediatr. 2007;7(1):23. doi: 10.1186/1471-2431-7-23.
[25] Grayzel J. Gallop rhythm of the heart. Am J Med. 1960;28(4):578–592. doi: 10.1016/0002-9343(60)90152-2.
[26] Debbal SM, Et Hamza C. Heart sounds analysis using the three wavelet transform versions the continuous wavelet transform (CWT), the discrete wavelet transform (DWT) and the wavelet packet transforms (PWT). J Cardiol Intervent. 2021;1(1):3.
[27] : Wimmer G, Tamaki T, Tischendorf JJW, et al. Directional wavelet based features for colonic polyp classification. Med Image Anal. 2016;31:16. doi: 10.1016/j.media.2016.02.001.
[28] Abbas AK, Et Bassam R. Phonocardiography signal processing. Switzerland: Springer Nature; 2009. p. 77.
[29] Meziani F. " phonocardiogram signal severity level analysis using wavelet transform (WT)".pp 64-67, PhD Thesis, Abou Bekr Belkaid University, Tlemcen. 2013.
[30] : Ahmad TJ, Ali H, Khan SA. Classification of Phonocardiogram using an Adaptive Fuzzy Inference System. Proc. Int. Conf. Image Process. Comput Vis Pattern Recognit. Proceedings of the 2009 International Conference on Image Processing, Computer Vision, & Pattern Recognition, IPCV 2009, Las Vegas, Nevada, USA, July 13-16,2009.
[31] Debbal I, Hamza Cherif L, Baakek YNEH. Pathology cardiac monitoring study of the phonocardiogram signal. Journal of Theoretical and Applied Information Technology. 2023;101(10):3–18.
[32] Vapnik V. The nature of statistical learning theory., Springer Verlag: New York, 1995.
[33] Nello C, John S-T. An introduction to support vector machines and other kernel-based learning methods. Cambridge: Cambridge University Press; 2000. p. 173–186.
[34] Manikandan J, Venkataramani B. Design of a real time automatic speech recognition system using modified one against all SVM classifier. Microprocess Microsyst. 2011;35(6):568–578. doi: 10.1016/j.micpro.2011.06.002.
[35] Rocha A, Goldenstein SK. Multiclass from binary: expanding one-versus-all, one-versus-one and ECOC-based approaches. IEEE Trans Neural Netw Learn Syst. 2013;25(2):289–302. doi: 10.1109/TNNLS.2013.2274735.
[36] Deepak S, Ameer PM. Automated categorization of brain tumor from MRI using CNN features and SVM. J Ambient Intell Human Comput. 2020;12(8):8357–8369. doi: 10.1007/s12652-020-02568-w.
[37] Baakek YNEH, Debbal I, Boudis H, et al. Study of the impact of clicks and murmurs on cardiac sounds S1 and S2 through bispectral analysis. Polish J Med Phys Eng. 2021;27(1):63–72. doi: 10.2478/pjmpe-2021-0009.
[38] Berraih SA, Baakek YNE, Debbal SMEA. Pathological discrimination of the phonocardiogram signal using the bispectral technique. Phys Eng Sci Med. 2020;43(4):1371–1385. doi: 10.1007/s13246-020-00943-7.
[39] Berraih SA, Debbal SMEA, Yettou NeB Severity cardiac analysis using the higher-order spectra. Appl Math Comput. 2021;409:126389. doi: 10.1016/j.amc.2021.126389.
[40] Berraih SA, Baakek YNE, Debbal SMEA. Preliminary study in the analysis of the severity of cardiac pathologies using the higher-order spectra on the heart-beats signals. Polish J Med Phys Eng. 2021;27(1):73–85. doi: 10.2478/pjmpe-2021-0010.
[41] Wang A, Bashore TM, editors . Valvular heart disease. 1st ed. New York: Humana press; 2009.
[42] Armstrong GP. MD [Internet]. Waitemata Cardiology, Auckland Valvular Disorders, MSD Manuals [updated 2023 April; cited 2024 January 03]. Available from: https://www.msdmanuals.com/professional/cardiovascular-disorders/valvular-disorders/aortic-stenosis.

Journal of Mechanics in Medicine and Biology
Vol. 24, No. 3 (2024) 2350046 (19 pages)

DOI: 10.1142/S021951942350046X

World Scientific
www.worldscientific.com

ENTROPY PARAMETER OF CARDIAC DEGREE SEVERITY ANALYSIS

DEBBAL IMANE*, HAMZA CHERIF LOTFI† and BAAKEK YETTOU NOUR EL HOUDA‡

Genie Biomedical Laboratory (GBM)
Genie Biomedical Department
Faculty of Technology
University Abou Bakr Belkaid Tlemcen, Algeria
**imane.debbal@univ-tlemcen.dz*
†*lotfi.hamzacherif@univ-tlemcen.dz*
‡*nourelhouda.baakekyettou@univ-tlemcen.dz*

Received 24 March 2023
Revised 11 April 2023
Accepted 17 April 2023
Published 25 July 2023

The phonocardiogram (PCG) signal is sometimes affected by added parameters that reflect the presence of a specific pathology. The intensity or the energy of the signal is one of the most reliable parameters when studying cardiac severity. Yet, in a pathological electrophysiological and audio signal, the severity information does not fully remain in the intensity or energy, but in other variables. In this paper, we will discuss the ability of a time-frequency parameter to discriminate, separate, and monitor the pathological cardiac severity levels. We studied 14 PCG signal from eight pathologies, six of them contain clicks (reduce murmurs), and eight murmur PCG signals with four different cardiac severity levels. We then calculated the entropy of approximation coefficients (EAC) from a discrete wavelet transform (DWT) analysis, to differentiate the PCG signals with clicks from those with murmurs and to assess the cardiac severity evolution. Since the entropy EAC is also related to the signal's intensity (energy), we compared it to the energetic ratio (ER) evolution, a parameter widely used for PCG signals discrimination and classification, which revealed that the EAC provied better results for the paper' purposes.

Keywords: Phonocardiogram; discrimination; severity; discrete wavelet transform; entropy of approximation coefficients.

1. Introduction

Health science has been evolving since the dawn of time. The research done and published, along with the discoveries made until today, reveal that great efforts have been made and significant knowledge has been acquired through several generations.

*Corresponding author.

In the biomedical field, scientific research has led to enormous progress in recent years. Thus, with the help of new applied technologies and the use of computer tools, the perfect approach possible has been obtained in the complex study of the humans' body organs functioning, such as the brain, kidney, liver, stomach, and above all, the heart: everyone's essential motor and source of life.[1]

In some cases, cardiac pathologies cannot be detected due to the lack of any symptom governing such a diagnosis or just not perceived by the doctor's ear during auscultation due to its low intensity. However, phonocardiography solved part of this problem concerning the different heart sounds, murmurs, and clicks (reduced murmurs) analysis. Still, for some pathologies, the information is in the frequency and time domain.

With this optic, we carry out this work. It is known that electrophysiological signals, in our case phonocardiogram (PCG) signals, conceal and group information of very high value for reliable and effective diagnosis of cardiac pathologies. In addition, the PCG signal reflects nonstationary acoustic signals generated by cardiac activity (normal and pathological), emitted by the heart, converted into an electrical signal, and then recorded.[1]

Under normal conditions, two heart sounds can be distinguished on the graphic representation of the recorded PCG.

The first heart sound known also as heartbeat S_1, corresponding to the beginning of ventricular systole, is the result of the closure of the mitral and tricuspid valves.[2] While the second heartbeat S_2, referring to the end of the ventricular systole and marking the beginning of the diastole, is associated with the closure of the aortic and pulmonic valves.[2] Other than S_1 and S_2, murmurs and short murmurs (clicks) appear indicating abnormal heart condition. Murmurs are sounds resulting from certain cardiovascular diseases that are audible during the systole, the diastole, or both.[3,4]

Hence, researchers used several signal-processing tools on the PCG recordings for different purposes. They proposed many algorithms such as for cardiac pathologies discrimination, denoising, and classification using discrete wavelet transform (DWT),[5–10] empirical mode decomposition.[11–17] The DWT technique proved its ability for discrimination between various heart sounds.[18,19] Cherif and Debbal suggested a wavelet packet tree-based algorithm to differentiate between the severities of pathological cases for different heart sound signals.[20] The automatic detection of heart sounds or cardiac pathologies using PCG signal is one of the current research axes, various algorithms were studied using different signal-processing tools and machine learning methods.[21–23]

Numerous research works used spectral and spectro-temporal entropy for various purposes of the PCG signal, like classification, discrimination, identification, etc.[24–27] In this paper, we will use a DWT-based entropy to discriminate cardiac clicks from murmurs and to assess the evolution of the cardiac severity in the same pathology (i.e., identify each severity level separately).

This paper is arranged as follows. The methodology presented in Sec. 2 explains the process followed for this work. In Sec. 3, we discuss the obtained results, and finally, Sec. 4 concluded the purpose behind this paper.

2. Methodology

To appreciate better the ability of our time-frequency feature for cardiac severity levels' study, we divided this work into two parts (Fig. 1). The first part consists on analyzing click and murmur segments to have results specifically related to the medical differences between these two. While, in the second part, we process a complete PCG cycle ($S_1 + S_2 +$ Murmur/Click), which allows us to see the impact of the cardiac severity on the heart sounds (S_1 and S_2) and added sounds (clicks and murmurs).

In both parts, we used the DWT to analyze our signals and extract the entropy of approximation coefficients (EAC), which is the parameter we used to differentiate between the pathological cardiac severity levels.

The intensity (energy) of a pathological signal is directly proportional to the severity of the pathology. Therefore, we compared our results to the energetic ratio (ER), a reference parameter for this work.

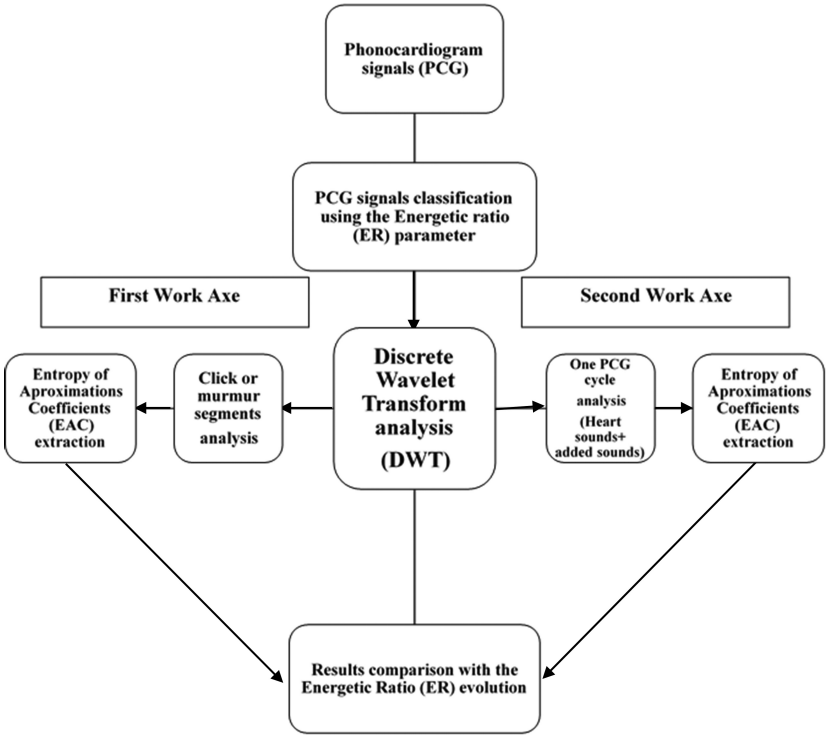

Fig. 1. DWT analysis work organogram.

Table 1. PCG signals used for cardiac severity discrimination.

PCG signals	Abbreviation
Group 1	
EAS	Early aortic stenosis
EC	Ejection click
LS	Late systole
AG	Atrial gallop
OS	Open snap
VG	Ventricular gallop
Group 2	
AS1/AS2/AS3/AS4	Aortic stenosis
AR1/AR2/AR3/AR4	Aortic regurgitation

Table 1 defines the PCG signals of the two groups (G_1 and G_2) used for discriminating the cardiac severity levels.

Figure 2 gives the temporal representation of two PCG signals from the pathologies mentioned in Table 1.

2.1. *The discrete wavelet transforms*

A common definition of the DWT equation is

$$\Psi jk(t) = 2^{-j/2}\Psi \quad (2^{-jt} - k), \tag{1}$$

with j, $k \in Z$.

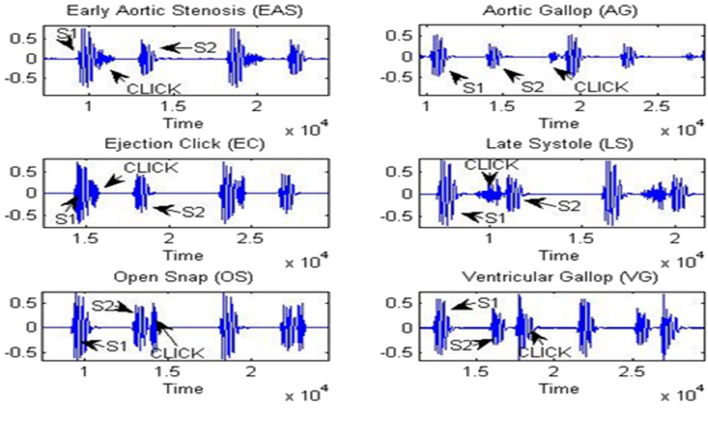

(a)

Fig. 2. Temporal representation of the studied PCG signals: (a) temporal representation of the group 1 PCG signals over two cycle (early AS (EAS), ejection click (EC), late systole (LS), atrial gallop (AG), OS, VG); (b) temporal representation of the AS PCG signals (AS1/AS2/AS3/AS4); (c) temporal representation of the AR PCG signals (AR/AR2/AR3/AR4).

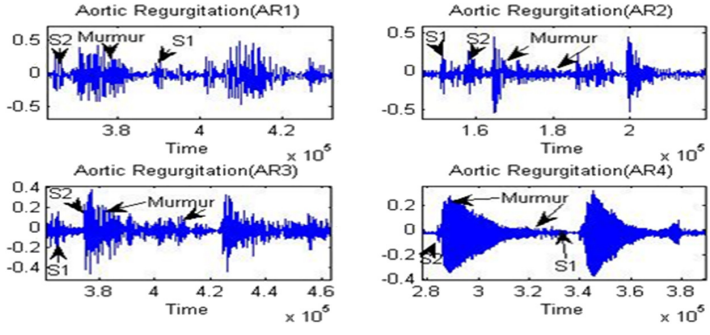

(b)

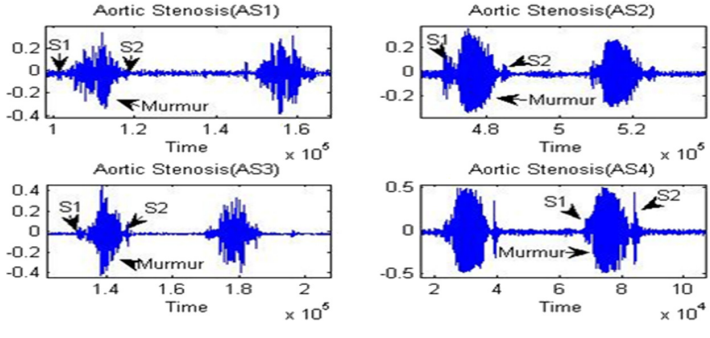

(c)

Fig. 2. (*Continued*)

In the DWTs, we discretize both the time and time-scale parameters. The algorithm chosen for the wavelet transformation partially defines the discretization process.[28]

Figure 3 represents the principle of the DWT decomposition process.

It decomposes the PCG signal in width varying filter banks (Fig. 4), the width of the filter banks band-pass depends of the decomposition level.

The A_j approximations and the details: d_1 to d_j correspond to the different frequency bands obtained from a DWT while using two filters (Fig. 5), high-pass and low-pass filters.

The approximation bands retain the informative (noise-free) PCG signal, while the details bands contain the extracted noises from the PCG signal once decomposed.

Therefore, to perform a reliable and effective DWT analysis, we used the seventh level of the Daubechies wavelet (db7) to decompose our PCG signals because of the shape similarities between the wavelet and the heart sounds, at a sampling frequency equaling to 8 kHz, previously found adequate for PCG signal filtering and processing. We utilized the sixth level of approximation ($a6$) for time-frequency entropy extraction since it induces a minimal reconstruction error of the original signal.

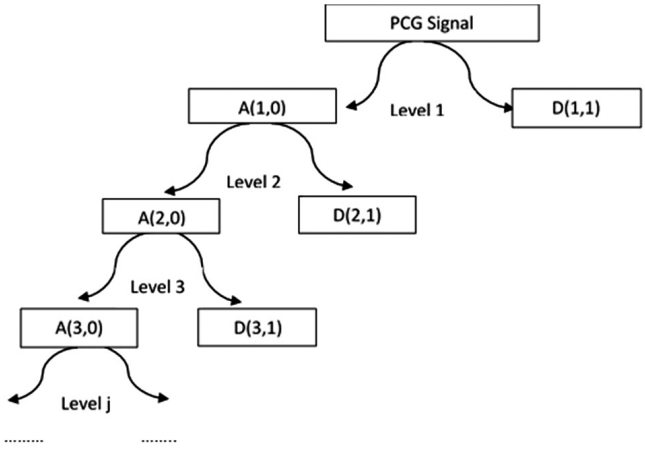

Fig. 3. DWT decomposition tree of the PCG signal.

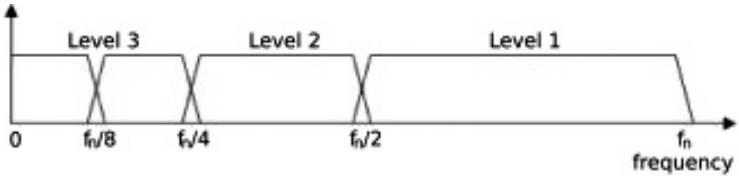

Fig. 4. Frequency domain representation of the DWT (filter banks).

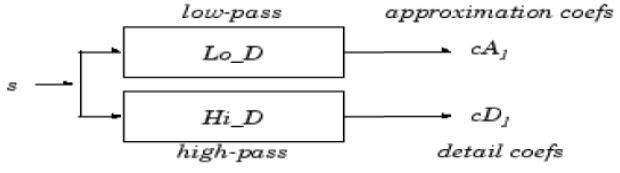

Fig. 5. The principle of DWT.

We calculated two parameters for this work, the ER and the EAC.

2.2. *Energetic ratio*

It is used in this study as a reference feature to affirm the results obtained using DWT analysis. ER is very efficient for tracking cardiac disease severity.[29–31]

$$\mathrm{ER} = \frac{E_2}{E_1 + E_2} \times 100, \tag{2}$$

where E_2 is the heart murmur or click energy, E_1 is the energy of $S_1 + S_2$ and $(E_1 + E_2)$ is the total energy. The above equation gives ER values as a percentage.

In case the ER equals to 100%, we have a complete dominance of murmurs over cardiac sounds (S_1, S_2).

2.3. *The entropy of approximation coefficients*

In this paper, entropy defines a measure of information quantity contained in the PCG segments. For example, intensity, randomness, perturbation, similarities, etc.

$$E[X] = -\int P(X)\mathrm{Log}P(X)d(X), \tag{3}$$

where X is a continuous random variable denoting the approximation signal ($a6$); $P(X)$ is a probability density.

3. Results and Discussion

Numerical results presented in tables and figures show statically the efficiency of the DWT feature for cardiac pathologies discrimination and severity monitoring. Yet, as biomedical scientists, we must find a correlation between these results and the medical field to help clinicians with their diagnostic decisions.

First, the ER values helped us ranking our pathological signals from the least severe to the most, for both clicks and murmur. Medically speaking, the ER highlights the importance of the murmurs and clicks energy and their dominance over heart sounds. Thus, we used his ranking order of the signals to evaluate the efficiency of our calculated feature.[29–37]

This section is divided into two results and discussion parts according to the paper's work axes.

3.1. *Phonocardiogram analysis using click and murmur segments only*

In this first part, we segmented the clicks and murmurs from one PCG cycle, then, applied our algorithm on these segments and extracted the Entropy from the DWT sixth level of approximation ($a6$).

Through Fig. 6, we illustrate the proportional correlation of the EAC to that of the ER for the eight studied pathologies (Fig. 6 and Table 2). In addition to the EAC ability to follow the cardiac severity in the same pathology (aortic stenosis (AS) and aortic regurgitation (AR)), it identified each pathology as a severity level, which helped us discriminate between the click pathologies.

Figure 7 shows three discriminated variation extents of both clicks and murmurs segments when using the entropy (EAC) parameter. Each boxplot (extent) identifies a category. As you can see, the first extent, which refers to the click pathologies, has a minimal variation in comparison to the pathologies with murmurs (second and third extent). Probably, due to the differences in their medical origins, where the clicks and gallops define a dysfunction of some of the heart components like early valvular AS or

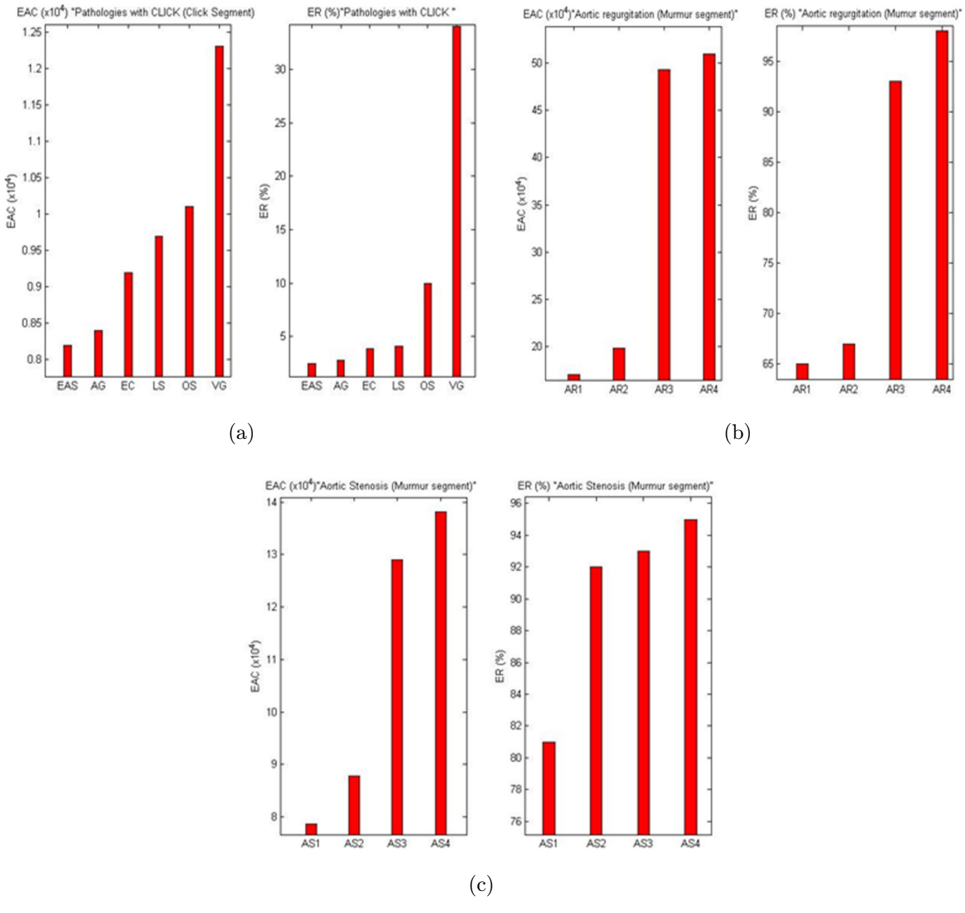

Fig. 6. Histogram representation of the DWT EAC and the ER for click and murmur segment only: (a) click segment from (EAS, AG, EC, LS, OS, VG); (b) murmur segments from four AS cases (AS1, AS2, AS3, AS4); (c) murmur segments from four AR cases (AR1, AR2, AR3, AR4).

left ventricle inflexibility, while murmurs are more on blood flow problems due to stenosis and regurgitations.[29]

Therefore, they have two distinct graphic representations with two different time-frequency information (Fig. 8). Moreover, the duration of the click is generally shorter than that of the murmur, which creates a difference (discrimination) in the frequency, energy content (ER parameter), and quantity of information between the two events. Therefore, the obtained discrimination results when using the entropy EAC.

In another hand, the second extent and third extent illustrate the variation of the AS and AR, respectively, between the least severe case and the most severe case, where the AS presents a more important severity evolution rate than the AR leading

Table 2. The DWT parameter values for click and murmur segments analysis.

Signals \ Parameters	ER (%)	EAC (for clicks and murmurs only) ($\times 10^4$)
Group 1: PCG signals with clicks		
EAS	2.5	0.82
AG	2.8	0.84
EC	3.9	0.92
LS	4.1	0.97
OS	10	1.05
VG	34	1.23
Group 2: PCG signals with murmurs		
	AS	
AS1	81	7.86
AS2	92	8.78
AS3	93	12.90
AS4	95	13.81
	AR	
AR2	65	17.01
AR1	67	19.86
AR3	93	49.29
AR4	98	49.32

us to a clear discrimination between these two cardiac pathologies using the entropy EAC.

To investigate even deeper the ability of the entropy (EAC) in assessing the pathologies evolution, we used four different cardiac severity levels within the same

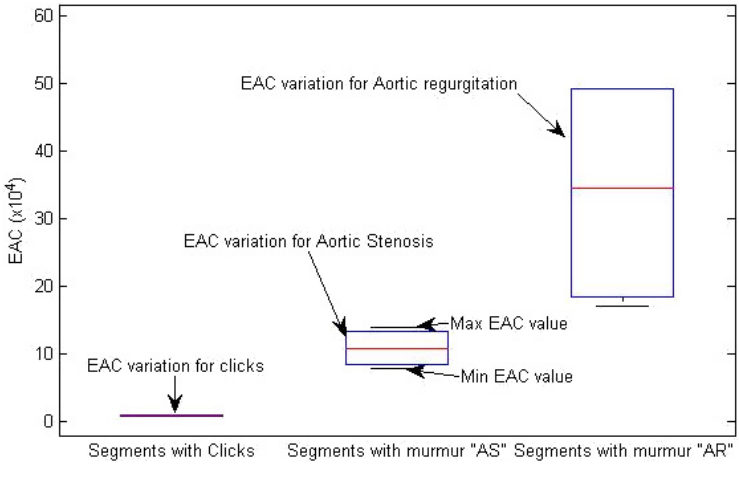

Fig. 7. Boxplot representation of the EAC variation between click and murmur segments for the 14 studied PCG signals.

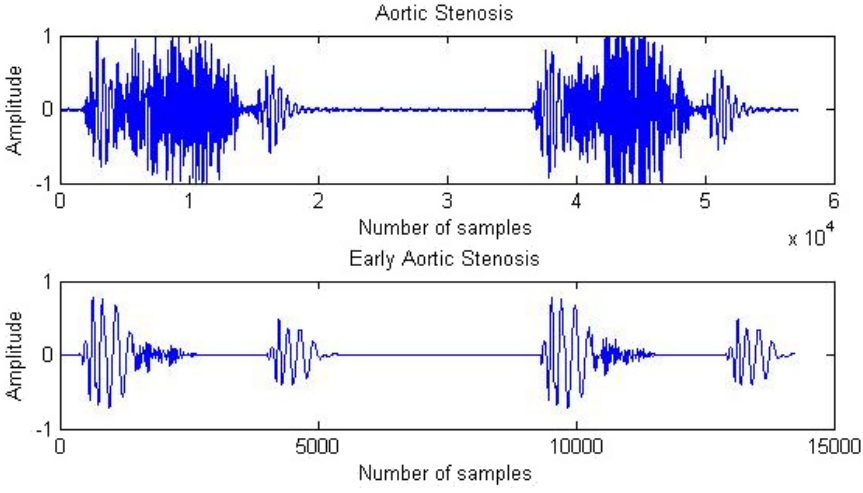

Fig. 8. Graphic difference between click and murmur: EAS (click pathology) and AS (murmur pathology).

pathology. To do so, we studied four murmur segments of the AS (AS1, AS2, AS3, AS4) and four of the AR (AR1, AR2, AR3, AR4).

As a result, both parameters, EAC and ER, presented an ascending evolution for the AS (Fig. 9), i.e., a proportional correlation to the pathology's severity evolution, which could be due to the increasing of the left ventricular outflow tract obstruction in this pathology, leading to high-intensity crescendo–decrescendo murmurs type.[38,39]

To maintain a normal cardiac output in an AR, it is necessary to increase the stroke volume corresponding to the severity of the regurgitation by increasing the

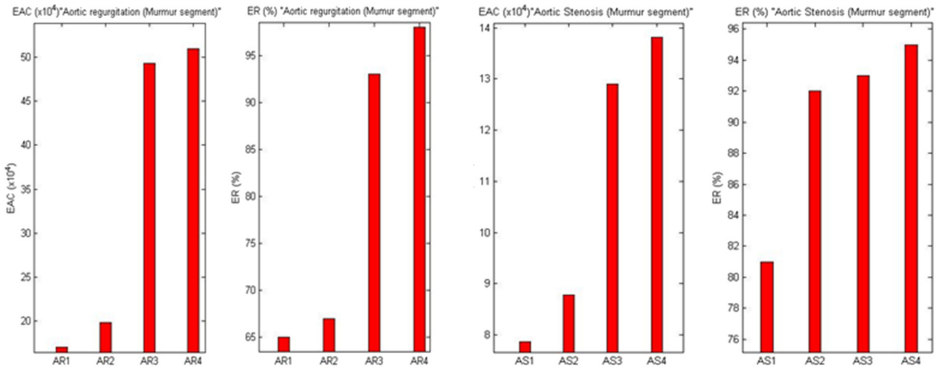

(a) (b)

Fig. 9. EAC results for (a) AR murmur segments (AR1, AR2, AR3, AR4); (b) AS murmur segments (AS1, AS2, AS3, AS4).

end-diastolic, end-systolic volumes, and the left ventricular afterload. Hence, the arising evolution of the EAC and ER, assessing the AR cardiac severity (Fig. 9).[39]

To summarize the first work axe, the entropy EAC and the ER highlighted the proportional correlation between the clicks and murmurs complexity and the pathology's severity (Table 2), where we established a click/murmur discrimination and a severity level identification using the quantity of information as a parameter and an energy-based reference feature over click and murmur segments only.

3.2. *Phonocardiogram signal analysis using one PCG cycle*

For the second work axe, many conducted studies on PCG signals found that heart sounds are also affected by the pathology. Therefore, to see the severity' quantity of information present in heart sounds (S_1, S_2) and its influence on the cardiac cycle, we analyzed one PCG cycle instead of click or murmur segments.

The EAC gave satisfactory results for this papers' purpose. We discriminated between PCG cycles with clicks from those with murmurs using the entropy's values (Table 3 and Fig. 10(a)). The AS and regurgitation murmurs showed high-energy characteristics (Fig. 10(b)) and important quantity of information compared to the click pathologies (Table 3 and Fig. 10(a)), probably due to the left ventricular outflow and afterload increment in AS and AR.[39]

In addition to the obtained results for click and murmur segments, the entropy (EAC) proved yet another time, its discriminative and cardiac severity assessing abilities when using a complete PCG cycle by displaying a proportional relationship

Table 3. The DWT parameter values for one PCG cycle analysis.

Parameters / Signals	ER (%)	ECA (for one cardiac cycle) ($\times 10^4$)
Group 1: PCG signals with clicks		
EAS	2.5	5.37
AG	2.8	7.18
EC	3.9	8.84
LS	4.1	9.05
OS	10	9.50
VG	34	10.63
Group 2: PCG signals with murmurs		
	AS	
AS1	81	18.32
AS2	92	23.50
AS3	93	28.81
AS4	95	42.50
	AR	
AR1	65	42.10
AR2	67	43.72
AR3	93	66.63
AR4	98	70.00

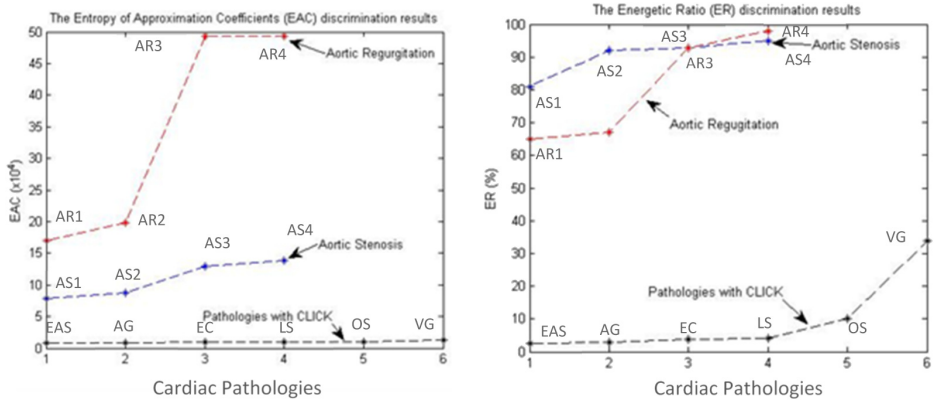

Fig. 10. Plot representation of the obtained values for the entropy (EAC) and ER for one PCG cycle DWT analysis: (a) EAC results representation for both click pathologies (EAS, AG, EC, LS, OS, VG); and murmur pathologies (four AS cases (AS1, AS2, AS3, AS4); four AR cases (AR1, AR2, AR3, AR4)).

between the PCG cycle's energy, quantity of information, and the pathological cardiac severity evolution for the eight selected pathologies (Fig. 11). Medical scientist stated that in a severe AR case, both preload and afterload are elevated. So, the maximal value is obtained for AR4.[39]

After comparing the obtained the two work axes, we noticed an augmentation in the entropy (EAC) values when using a complete PCG cycle instead of added sounds segments (Tables 2 and 3). The obtained augmentation is proportional to the pathological cardiac severity evolution, which confirms that severity information are indeed present in heart sounds and affect the cardiac cycle accordingly to the severity level evolution.

In this paper, we used the ER as a reference feature to affirm the accuracy of the obtained results using DWT analysis[29–37] since the entropy EAC is also related to the signal' intensity (energy). The results showed that our calculated parameter is as efficient, yet even better than the ER for assessing, monitoring, and discriminating the pathological cardiac severity levels.

As highlighted with black color in Fig. 12, the EAC follows the severity evolution, i.e., identify each severity level on its own. Especially for the AS and regurgitation cases. When studying the severity in one pathology, it is hard to see a clear difference between the cases. Yet, the EAC allows this discrimination between each level.

Through Fig. 13, we demonstrate the influence of the click and murmur energy (intensity) on the discrimination results, where the entropy (EAC) distinctly showed the difference between AS and regurgitation when the ER barely did (Fig. 13). If noticed, the entropy (EAC) has a different discriminative order of the AR and AS compared to the ER, which means that the signals' intensity is probably not the only

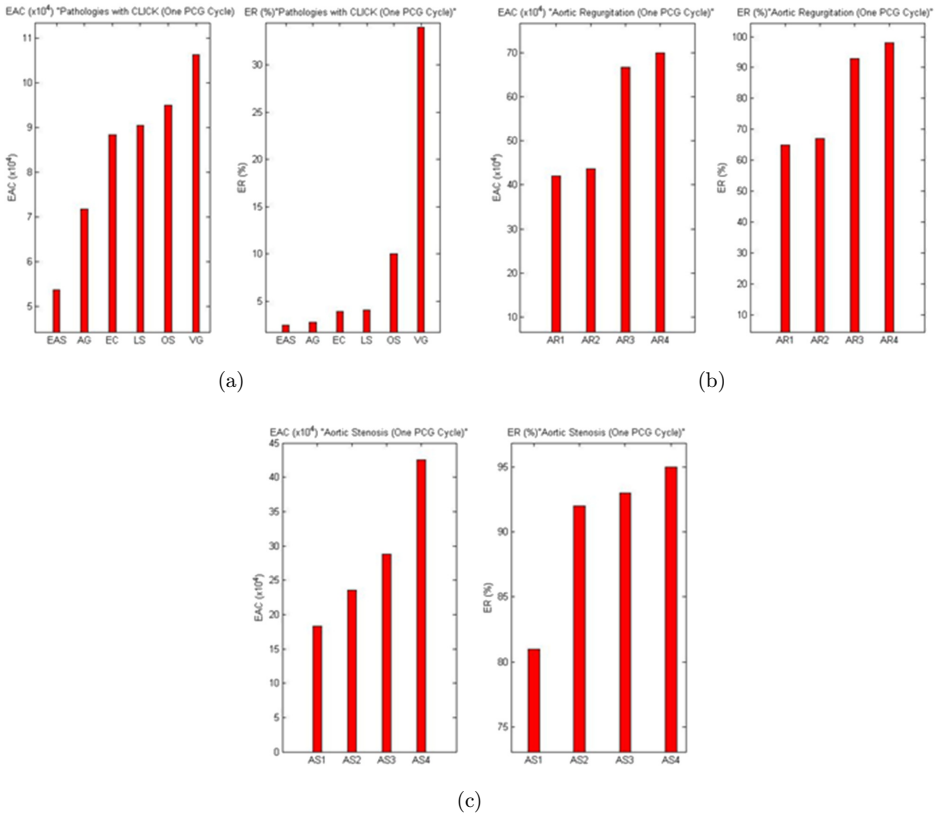

Fig. 11. Histogram representation of the DWT EAC and the ER for one PCG cycle: (a) PCG cycle from (EAS, AG, EC, LS, OS, VG); (b) PCG cycle from four AS cases (AS1, AS2, AS3, AS4); (c) PCG cycle from four AR cases (AR1, AR2, AR3, AR4).

element directly related to the cardiac severity since the quantity of information separated each pathology for the other.

The same observation was made for the pathologies with a click. The ER allowed significant discrimination only for pathologies with potential high energy (ex: open snap (OS) and ventricular gallop (VG)). Yet, the entropy (EAC) is discriminated and separated between all the pathologies (Fig. 14).

To summarize this second work axe, the EAC extracted from a complete PCG cycle (heart sound + added sounds) allowed a discrimination between the pathologies with clicks from those with murmur, identified each severity level in the same pathology, and discriminated between the AS and the AR. Hence, the three different variation areas are illustrated in Figs. 10(a), 10(b) and 13.

Murmur pathologies occupy the upper part of the figures since they are more complex and reflect higher entropy values than the pathologies suffering from clicks. The results obtained in this axe highlight the presence of significant severity information in cardiac sounds (S_1 and S_2).

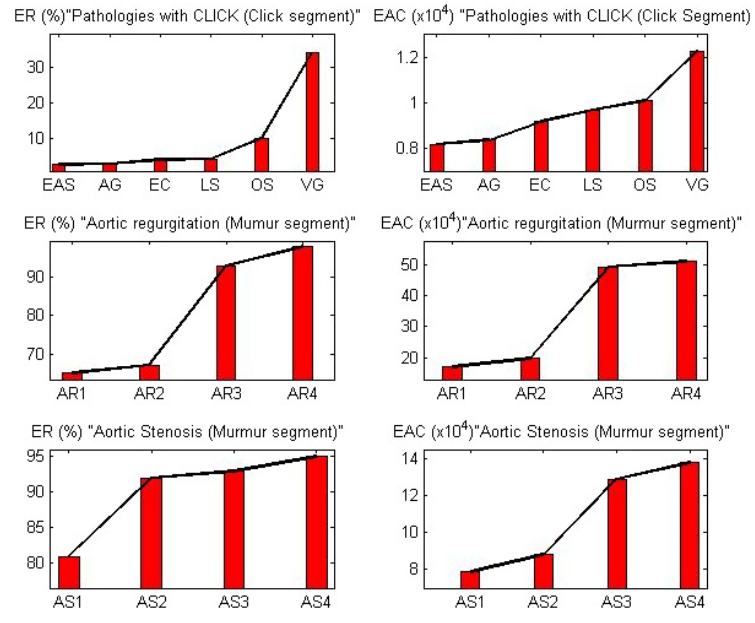

(a)

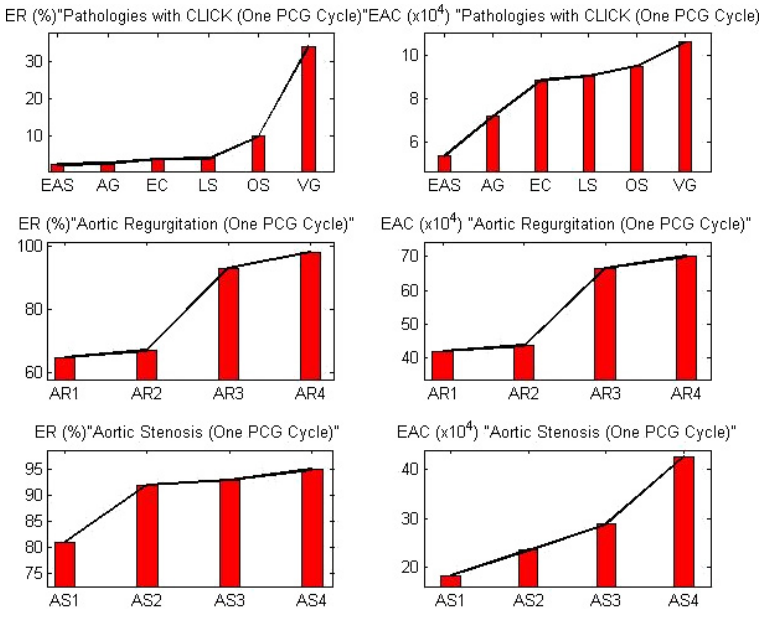

(b)

Fig. 12. Discrimination results comparison between the ER and the EAC of the eight studied pathologies: (a) when using one PCG cycle and (b) when using click and murmur segments.

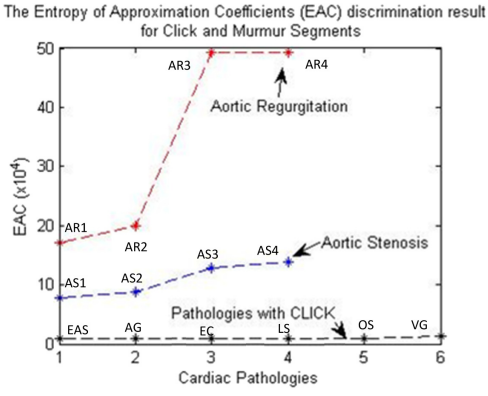

(a)

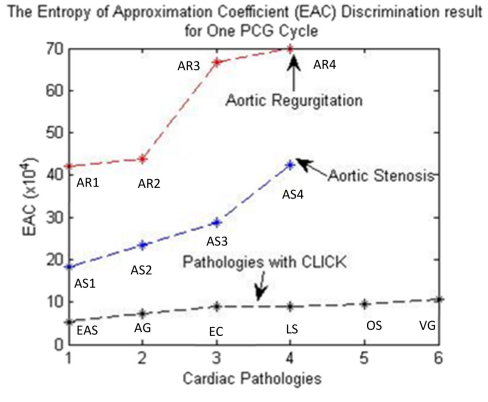

(b)

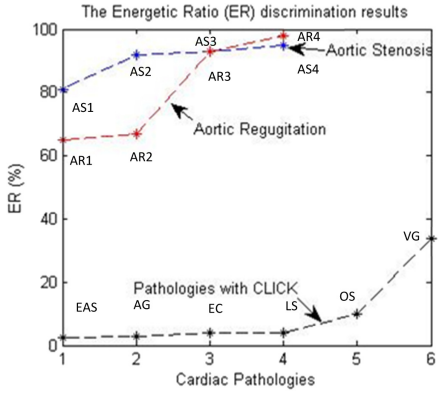

(c)

Fig. 13. Discrimination results for (a) the EAC of the eight cardiac pathologies (for click and murmur segment), (b) the EAC of the eight cardiac pathologies (for one PCG cycle) and (c) the ER of the eight cardiac pathologies.

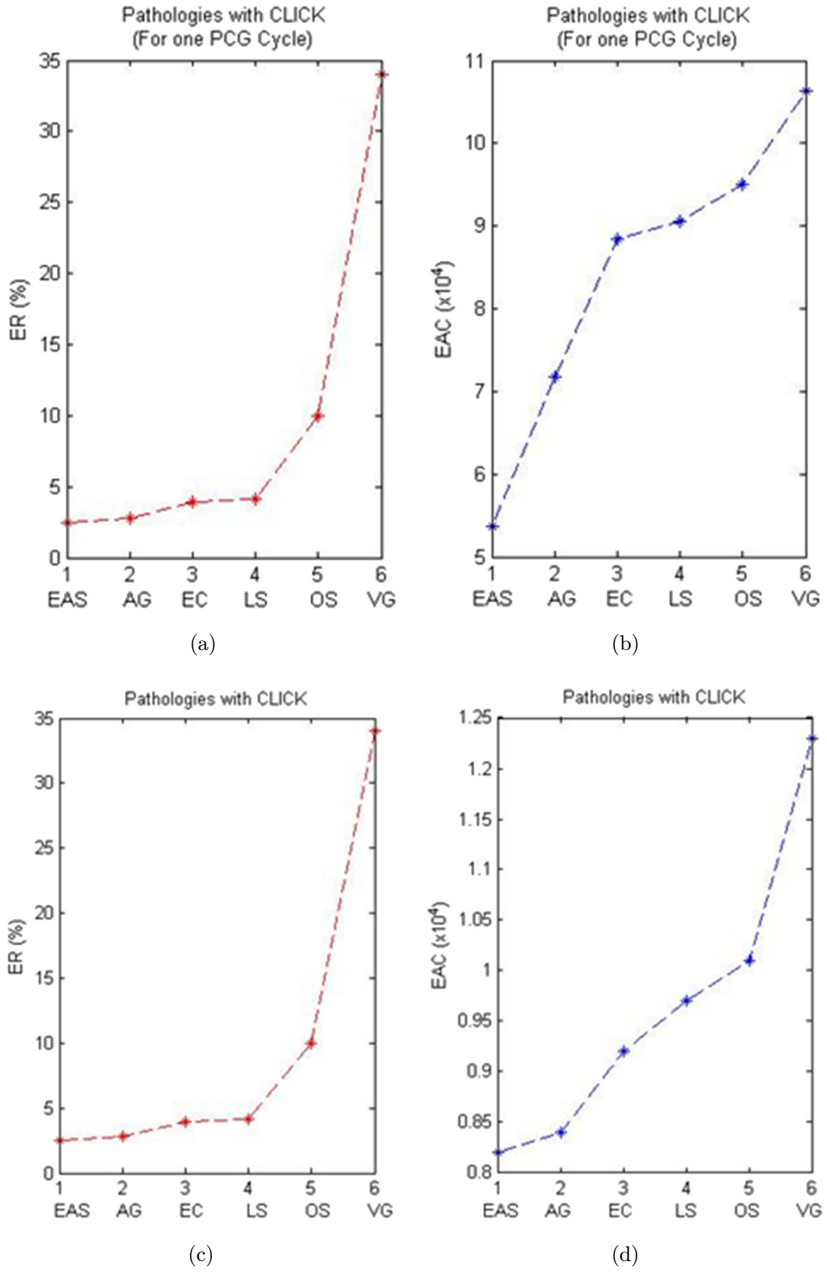

Fig. 14. Discriminative results for (a) ER for pathologies with click (one PCG cycle), (b) the EAC for pathologies with click (one PCG cycle), (c) ER for pathologies with click (click segment) and (d) the EAC for pathologies with click (click segment).

4. Conclusion

In closing, the entropy is well known for quantifying information. In this work, through a DWT parameter, we combined the statistical and medical fields to discriminate between the clicks and murmurs pathologies and assess the cardiac severity evolution using a signal-processing tool.

The EAC filed the purpose of this work, here it discriminated between cardiac pathologies, assessed the cardiac severity evolution accordingly to the pathologies' medical explanation, and proved it ability to be a better pathological cardiac severity discriminative, monitoring, and assessing tool, than the ER, which we used as a reference parameter to prove the accuracy of our results.

In the end, the entropy (EAC) could be the object of future works, like PCG severity level-based classification using the entropy EAC as a feature for machine learning algorithms. After comparing the two work axes, we can say that it is better to analyze a complete PCG cycle than just click or murmur segments when studying the cardiac severity since the severity information are present in heart sounds and affect the cardiac cycle accordingly to the severity level evolution.

The main aim of this paper was to proceed with the use of a DWT-derived parameter to obtain information likely not only to discriminate between murmurs and clicks pathologies but also, to follow the severity evolution in the same studied pathology, without focusing only on the signal' energy, which was fully fulfilled.

Acknowledgments

The authors would like to thank the Directorate-General of Scientific Research and Technological Development (Direction Générale de la Recherche Scientifique et du Développement Technologique, DGRSDT, URL:www.dgrsdt.dz, Algeria) for the financial assistance toward this research.

ORCID

Debbal Imane https://orcid.org/0000-0002-0738-7944

References

1. Stambouli B, Zineb, Classification des Signaux Phonocardiogrammes sur la Base de L'étude du Rapport SNR, introduction& pp4, Mémoire de magistère, Université de Tlemcen, 2012.
2. Li X *et al.*, Synchronization control of pulsatile ventricular assist devices by combination usage of different physiological signals, *Comput Assist Surg* **24**(sup1):105–112, 2019.
3. Taplidou SA, Hadjileontiadis LJ, Nonlinear analysis of heart murmurs using wavelet-based higher-order spectral parameters, *2006 Int Conf IEEE Engineering in Medicine and Biology Society*, New York, NY, USA, pp. 4502–4505, 2006.
4. Ahmad MS, Mir J, Ullah MO, Shahid MLUR, Syed MA, An efficient heart murmur recognition and cardiovascular disorders classification system, *Australas Phys Eng Sci Med* **42**(3):733–743, 2019.

5. Potdar RM *et al.*, Optimal parameter selection for DWT based PCG denoising, *Turk J Comput Math Educ* **12**(9):3207–3219, 2021.
6. Hossain A, Uddin S, Rahman P, Anee MJ, Rifat MMH, Uddin MM, Wavelet and spectral analysis of normal and abnormal heart sound for diagnosing cardiac disorders, *BioMed Res Int* **2022**:9092346, 2022.
7. Li H, Ren G, Yu X, Wang D, Wu S, Discrimination of the diastolic murmurs in coronary heart disease and in valvular disease, *IEEE Access* **8**:160407–160413, 2020.
8. Li H, Ren Y, Zhang G, Wang R, Cui J, Zhang W, Detection and classification of abnormities of first heart sound using empirical wavelet transform, *IEEE Access* **7**:139643–139652, 2019.
9. Liu Q, Xu Y, Zhang L, Liang C, Research on heart sound signal denoising algorithm based on variational mode decomposition and wavelet threshold, *J Comput Commun* **9**(10):110–121, 2021.
10. Ghosh SK, Ponnalagu RN, Investigation of discrete wavelet transform domain optimal parametric approach for denoising of phonocardiogram signal, *J Mech Med Biol* **22**(3):2250046, 2022.
11. Fatmawati TY *et al.*, Comparative analysis of the phonocardiogram denoising system based-on empirical mode decomposition (EMD) and double-density discrete wavelet transform (DDDWT), *Proc 1st Int Conf Electronics, Biomedical Engineering, and Health Informatics*, Springer, Singapore, pp. 593–604, 2021.
12. Mishra M, Singh A, Dutta MK, Muñoz AR, Automatic screening of cardiac disorders using wavelet analysis of heart sound, *2017 4th IEEE Uttar Pradesh Section Int Conf Electrical, Computer and Electronics (UPCON)*, Mathura, India, pp. 472–476, October 2017.
13. Jatia N, Veer K, Performance comparison of denoising methods for fetal phonocardiography using Fir filter and empirical mode decomposition (EMD), in *Optimization Methods for Engineering Problems*, Apple Academic Press, pp. 171–183, 2023.
14. Hilman F, Achmad R, Mazaya A, Alvin O, Ziani S, Classification of normal and abnormal heart sounds using empirical mode decomposition and first order statistic, *J Electron Electromed Eng Med Inform* **5**(2):82-88, 2023.
15. Ladrova M *et al.*, Elimination of interference in phonocardiogram signal based on wavelet transform and empirical mode decomposition, *IFAC-PapersOnLine* **52**(27):440–445, 2019.
16. Arslan Ö, Automated detection of heart valve disorders with time-frequency and deep features on PCG signals, *Biomed Signal Process Control* **78**:103929, 2022.
17. Wu Q *et al.*, Heart sound classification method based on complete empirical mode decomposition with adaptive noise permutation entropy, *J Phys Conf Ser* **2173**:012018, 2022.
18. Varshney S, Singh S, Computation of biological murmurs in phonocardiogram signals using fast Fourier & discrete wavelet transform, *2020 Int Conf Computation, Automation and Knowledge Management (ICCAKM)*, Dubai, United Arab Emirates, pp. 234–240, 2020.
19. Meziani F, Debbal SM, Atbi A, Analysis of phonocardiogram signals using wavelet transform, *J Med Eng Technol* **36**(6):283–302, 2021.
20. Cherif LH, Debbal SM, Adaptive filtering algorithm based on a wavelet packet tree for heart sound signal analysis, *Int J Med Eng Inform* **10**(2):150–163, 2018.
21. Ghosh SK, Ponnalagu RN, Tripathy RK, Panda G, Pachori RB, Automated heart sound activity detection from PCG signal using time–frequency-domain deep neural network, in *IEEE Trans Instrum Measure* **71**:1–10, 2022.

22. Karhade J *et al.*, Time–frequency-domain deep learning framework for the automated detection of heart valve disorders using PCG signals, *IEEE Trans Instrum Meas* **71**:1–11, 2022.
23. Zeng W *et al.*, Automatic detection of heart valve disorders using Teager–Kaiser energy operator, rational-dilation wavelet transform and convolutional neural networks with PCG signals, *Artif Intell Rev* **56**(1):781–806, 2023.
24. Varshney S, Singh S, Murmur detection in PCG signals using DWT entropy and feature clustering, *2020 IEEE Int Conf Electronics, Computing and Communication Technologies (CONECCT)*, IEEE, pp. 1–6, 2020.
25. Zhang H *et al.*, Discrimination of patients with varying degrees of coronary artery stenosis by ECG and PCG signals based on entropy, *Entropy* **23**(7):823, 2021.
26. Rizal A, Wijayanto I, Phonocardiogram classification using multilevel wavelet packet entropy and random forest, *2020 6th Int Conf Science and Technology (ICST)*, IEEE, pp. 1–4, 2020.
27. Safara F *et al.*, Wavelet packet entropy for heart murmurs classification, *Adv Bioinform* **2012**:327269, 2012.
28. Debbal SM, Hamza C, Heart sounds analysis using the three wavelet transform versions the continuous wavelet transform (CWT), the discrete wavelet transform (DWT) and the wavelet packet transforms (PWT), *J Cardiol Interv* **1**(1):1–9, 2021.
29. Meziani F, Phonocardiogram signal severity level analysis using wavelet transform (WT), PhD thesis, Abou Bekr Belkaid University Tlemcen, 2013.
30. Ahmad TJ, Ali H, Khan SA, Classification of phonocardiogram using an adaptive fuzzy inference system, *Proc 2009 Int Conf Image Processing, Computer Vision, & Pattern Recognition, IPCV 2009*, Las Vegas, Nevada, USA, July 13–16, 2009.
31. Meziani F, Debbal SM, Atbi A, Analysis of the pathological severity degree of aortic stenosis (AS) and mitral stenosis (MS) using the discrete wavelet transform (DWT), *J Med Eng Technol* **37**:61–74, 2013.
32. Baakek YNEH, Debbal I, Boudis H, Debbal SMEA, Study of the impact of clicks and murmurs on cardiac sounds S1 and S2 through bispectral analysis, *Pol J Med Phys Eng* **27**(1):63–72, 2021.
33. Berraih SA, Debbal SMEA, Pathological discrimination of the phonocardiogram signal using the bispectral technique, *Phys Eng Sci Med* **43**(4):1371–1385, 2020.
34. Berraih SA, Debbal SMEA, Severity cardiac analysis using the higher-order spectra, *Appl Math Comput* **409**:126389, 2021.
35. Imane D, Hidayat B, Houda BYNE, Amine DSME, Cardiac pathologies analysis on the phonocardiogram signals using the bispectral technic, *Int J Adv Sci Technol* **29**(3):6764–6784, 2020, http://sersc.org/journals/index.php/IJAST/article/view/7328.2020.
36. Berraih SA, Baakek YNE, Debbal SMEA, Preliminary study in the analysis of the severity of cardiac pathologies using the higher-order spectra on the heart-beats signals, *Pol J Med Phys Eng* **27**(1):73–85, 2021.
37. Imane D, Hidayat B, El Houda BYN, El Amine DSM. Phonocardiograms signals analysis using the graphical bispectral technique. *Ann Clin Cases* **1**(2):1009, 2020.
38. Djebbari A, Synthesis of temporal, spectral and spectro-temporal analysis methods of the phonocardiogram signal, Electronic magister thesis of signals and systems, Department of Electronics, Faculty of Science Engineering, University Abou Bekr Belkaid Tlemcen, Algeria, 1999.
39. Wang A, Bashore TM (eds.), *Valvular Heart Disease*, Springer Science & Business Media, 2010.